Functional contribution of the mesencephalic locomotor region to locomotion

Thèse

Nicolas Josset

Doctorat en neurobiologie
Philosophiae Doctor (Ph.D.)

Québec, Canada

Functional contribution of the mesencephalic locomotor region to locomotion

Thèse

Nicolas Josset

Sous la direction de :

Frederic Bretzner, directeur de recherche

Résumé

Parce qu'il est naturel et facile de marcher, il peut sembler que cet acte soit produit aussi facilement qu'il est accompli. Au contraire, la locomotion nécessite une interaction neurale complexe entre les neurones supraspinaux, spinaux et périphériques pour obtenir une locomotion fluide et adaptée à l'environnement.

La région locomotrice mésencéphalique (MLR) est un centre locomoteur supraspinal situé dans le tronc cérébral qui a notamment pour rôle d'initier la locomotion et d'induire une transition entre les allures locomotrices. Cependant, bien que cette région ait initialement été identifiée comme le noyau cunéiforme (CnF), un groupe de neurones glutamatergiques, et le noyau pédonculopontin (PPN), un groupe de neurones glutamatergiques et cholinergiques, son corrélat anatomique est encore un sujet de débat. Et alors qu'il a été prouvé que, que ce soit lors d'une stimulation de la MLR ou pour augmenter la vitesse locomotrice, la plupart des quadrupèdes présentent un large éventail d'allures locomotrices allant de la marche, au trot, jusqu'au galop, la gamme exacte des allures locomotrices chez la souris est encore inconnue.

Ici, en utilisant l'analyse cinématique, nous avons d'abord décidé d'identifier d'évaluer les allures locomotrices des souris C57BL / 6. Sur la base de la symétrie de la démarche et du couplage inter-membres, nous avons identifié et caractérisé 8 allures utilisées à travers un continuum de fréquences locomotrices allant de la marche au trot puis galopant avec différents sous-types d'allures allant du plus lent au plus rapide. Certaines allures sont apparues comme attractrices d'autres sont apparues comme transitionnelles. En utilisant une analyse graphique, nous avons également démontré que les transitions entre les allures n'étaient pas aléatoires mais entièrement prévisibles.

Nous avons ensuite décidé d'analyser et de caractériser les contributions fonctionnelles des populations neuronales de CnF et PPN au contrôle locomoteur. En utilisant des souris transgéniques exprimant une opsine répondant à la lumière dans les neurones glutamatergiques (Glut) ou cholinergiques (CHAT), nous avons photostimulé (ou photo-inhibé) les neurones glutamatergiques du CnF ou du PPN ou les neurones cholinergiques du PPN. Nous avons découvert que les neurones glutamatergiques du CnF initient et modulent l'allure locomotrice et accélèrent le rythme, tandis que les neurones

glutamatergiques et cholinergiques du PPN le ralentissent. En initiant, modulant et en accélérant la locomotion, notre étude identifie et caractérise des populations neuronales distinctes de la MLR.

Définir et décrire en profondeur la MLR semble d'autant plus urgent qu'elle est devenue récemment une cible pour traiter les symptômes survenant après une lésion de la moelle épinière ou liés à la maladie de Parkinson.

Abstract

Because it is natural and easy to walk, it could seem that this act is produced as easily as it is accomplished. On the contrary, locomotion requires an intricate and complex neural interaction between the supraspinal, spinal and peripheric neurons to obtain a locomotion that is smooth and adapted to the environment.

The Mesencephalic Locomotor Region (MLR) is a supraspinal brainstem locomotor center that has the particular role of initiating locomotion and inducing a transition between locomotor gaits. However, although this region was initially identified as the cuneiform nucleus (CnF), a cluster of glutamatergic neurons, and the pedunculopontine nucleus (PPN), a cluster of glutamatergic and cholinergic neurons, its anatomical correlate is still a matter of debate. And while it is proven that, either under MLR stimulation or in order to increase locomotor speed, most quadrupeds exhibit a wide range of locomotor gaits from walk, to trot, to gallop, the exact range of locomotor gaits in the mouse is still unknown.

Here, using kinematic analysis we first decided to identify to assess locomotor gaits C57BL/6 mice. Based on the symmetry of the gait and the inter-limb coupling, we identified and characterized 8 gaits during locomotion displayed through a continuum of locomotor frequencies, ranging from walk to trot and then to gallop with various sub-types of gaits at the slowest and highest speeds that appeared as attractors or transitional gaits. Using graph analysis, we also demonstrated that transitions between gaits were not random but entirely predictable.

Then we decided to analyze and characterize the functional contributions of the CnF and PPN's neuronal populations to locomotor control. Using transgenic mice expressing opsin in either glutamatergic (Glut) or cholinergic (CHAT) neurons, we photostimulated (or photoinhibited) glutamatergic neurons of the CnF or PPN or cholinergic neurons of the PPN. We discovered that glutamatergic CnF neurons initiate and modulate the locomotor pattern, and accelerate the rhythm, while glutamatergic and cholinergic PPN neurons decelerate it. By initiating, modulating, and accelerating locomotion, our study identifies and characterizes distinct neuronal populations of the MLR.

Describing and defining thoroughly the MLR seems all the more urgent since it has recently become a target for spinal cord injury and Parkinson's disease treatment.

Table of contents

List of tables

List of Figures

Abbreviations

5HT: Serotonin

AAV: Adeno-Associated Virus

BC: Brachium Conjonctivum

BG: Basal Ganglia

BSN: Nrainstem Nuclei

ChAT: Choline Acetyl-Transferase

ChR2 : Channel Rhodopsin

CIN : Comissural Interneurons

CLR: Cerebellar Locomotor Region

CnF: Cuneiform Nucleus

CPG: Central Pattern Generator

DBS: Deep Brain Stimulation

DCC: Deleted in Colorectal Cancer

DLR: Diencephalic Locomotor Region

DSCAM: Down Syndrome Cell Adhesion Molecule

FB: Full Bound

fMRI: Functional Magnetic Resonance Imaging

FOG: Freezing Of Gait

GABA: Gamma-Aminobutyric Acid

GL or LG: Gastrocnemius Nateralis

GP: Globus Pallidus

GRN: Gigantocellular Reticular Nucleus

HB: Half-Bound

IC: Inferior Colliculus

IG: Imagery of Gait

IOM: Imagery of Object Moving

IP: Iliopsoas

LDT: Latero Dorsal Tegmentum

LF: Left Forelimb

LH: Left Hindlimb

LL: Lateral Lemniscus

LPGi: Lateral ParaGigantocellular nucleus

LPN: Long Propriospinal Neurons

LW: Lateral Walk

MdV: Ventral Medullary formation

Mg: Magnocellular nucleus

MG: Medial Gastrocnemius

MLR: Mesencephalic Locomotor Region

MRN: Midbrain Reticular Nucleus

MTP: Meta-Tarso Phalangeal

NPHR3: Halorhodopsin

NRPo: Nucleus Reticularis Pontis oralis

OPW: Out-of-Phase Walk

PAG: PeriAqueductal Gray matter

PB: Posterior Biceps or Parabrachial Nucleus

PMLS: PontoMedullary Locomotor Strip

pPCtx: Posterior parietal cortex

PPN: Pedunculopontine nucleus

PPR: ParaPyramidal Region

PPTg: pedunculopontine tegmental nucleus

REM: Rapid Eye Movement

RF: Rectus femoris

RF: Reticular formation

RF: Right Forelimb

RG: Rhythm Generator

RG: Rotary Gallop

RH: Right Hindlimb

RM: Raphe Magnus

RN: Retrorubral field Nucleus

RS: ReticuloSpinal

Sartm/a: medial/anterior sartorius

SC: Superior Colliculus

SCI: Spinal Cord Injury

SLR: Subthalamic Locomotor Region

SN: Substantia nigra

SOL: Soleus

SSRi : Selective Serotonin Reuptake Inhibitors

ST: Semitendinosus

STN: Sub-Thalamic Nucleus

STN: Subthalamic nucleus

T: Trot

TA: Tibialis anterior

TG: Transverse Gallop

VCtx: Visual cortex

VGluT2: Vesicular Glutamatergic Transporter 2

VL/M/I: Vastus lateralis/ medialis/intermedialis

VTA: Ventral Tegmental Area

Dedicace

Puisque c'est une douleur vive,

Que nos vies tellement fugitives,

Se dire que jamais rien ne presse.

Laurent Voulzy/

I’ll let you be in my dreams if I can be in yours

Bob Dylan

Acknowledgments/Remerciements

Je voudrais commencer par remercier mon directeur de thèse, Fréderic Bretzner, qui m'a accueilli dans son laboratoire, qui m'a permis de participer à de très nombreux congrès scientifiques internationaux et avec qui j'ai appris l'élaboration d'un projet de recherche et la persévérance.

Je remercie les très nombreux stagiaires du laboratoire que j'ai encadré, vous m'avez de nombreuses fois sorti de mon quotidien chargé pour me rappeler que la recherche que nous faisions était particulièrement excitante. Un énorme merci particulier à Cloé Brindamour qui a été indispensable à toutes les analyses présentées ici ! Merci à l'équipe, en particulier à Marie et Louise pour le soutien durant les périodes difficiles.

Melody, ta présence dans ma vie m'a permis de ne pas passer mes journées et mes nuits au labo, de ne pas (trop) déprimer et de profiter du temps que nous avons passé à Québec. Même si nous partons élever des poules dans un endroit ou un doctorat en neurosciences ne me sera d'aucune utilité, je ne serais définitivement pas venu à Québec pour rien. Merci pour de m'avoir supporté, merci pour ta bonne humeur, et pour ton support inconditionnel.

Je vais me restreindre à une expression ou souvenir par personne qui me rappellent les bons moments que nous avons passé ensemble et dont je me souviendrais longtemps ! merci à tous, et merci au temps partiel !

Anto parce qu'on est varois tous les deux, que tu le veuilles ou non ;) et pour le fameux taille-crayon.
Julia pour toutes les photos de salomé et ta joie de vivre communicative.
Maud pour m'avoir fait connaitre (et presque apprecier) Claude François et Joe Dassin, pour ta manière de dire : c'est terrible ! et pour la quantité énorme de souvenirs que nous avons créés ensemble.
Mathilde pour tes expressions (y'a baleine sous gravier) et ta (très majoritairement) bonne humeur qui nous as fait du bien à tous au labo !
Léa, parce qu'en fait c'est toi qui a une petite tête !
Anne parce que tu es toi ;) et Laura parceque j'ai souvent lu dans ton regard exactement ce que j'étais en train de penser et que ça fait du bien de pas se sentir seul .

Merci à toute ma famille pour le soutien moral (et financier), un merci particulier à Caroline et Fabrice, on ne s'est pas vu souvent durant ces 4 ans et demi mais à chaque fois ça a été extrêmement reposant et agréable. Merci à Chantal et Pierre pour ce séjour au ski mais aussi pour le soutient pendant ma période de doute et de recherche de thèse. Merci à mes parents de m'avoir permis de revenir me ressourcer en France durant cette période exigeante, d'avoir traversé l'atlantique pour me voir et pour le soutien malgré les incertitudes.

Foreword

The first chapter of this thesis reviews the scientific work that led to my PhD. The second and third chapters are the work that I have been doing in Dr Bretzner's Laboratory for the past four years, they are presented as articles. Please remember that the figure numbering was modified to fit this manuscript's order and that supplementary videos are made available in separate files.

Chapter 2: Speed-Dependent Modulation of the Locomotor Behavior in Adult Mice Reveals Attractor and Transitional Gaits

In this chapter are presented the results of the study of locomotor gaits of the wild-type C57Bl6/J that we did in the lab.

This work was in published in the journal Frontiers in neuroscience in 2016 and the authors are listed as follows: Lemieux M*, Josset N*, Roussel M, Couraud S, Bretzner F.

* authors contributed equally.

Maxime Lemieux, myself, and Frederic Bretzner conceived and designed experiments. I collected almost all the data by testing mice on a treadmill and recording their locomotion with kinematic markers on the limbs. I also spent many hours analyzing the data to obtain files that could be processed in Matlab. Marie Roussel collected the fastidious low speed datas and also collected data and aged mice that was not included in the final manuscript. Sebastien Couraud helped with the analysis. Maxime Lemieux designed the Matlab scripts and analyzed and designed 2 thirds of the figures while I designed the other third. Maxime Lemieux, Frederic Bretzner and myself drafted the manuscript.

Chapter 3: Distinct contributions of mesencephalic locomotor region nuclei to locomotor control in the freely behaving mouse.

In this chapter, I present the results of the study that occupied most of my PhD, the study of the contribution of the MLR nuclei to locomotion using optogenetics.

This work was published in the journal Current Biology in 2018, the authors are listed as follows:

Nicolas Josset*, Marie Roussel*, Maxime Lemieux, David Lafrance-Zoubga, Ali Rastqar, Frederic Bretzner. * authors contributed equally.

The work was conceptualized by Frederic Bretzner. The amount of work including implantation of animals and their subsequent testing was approximately divided 60% for me (glutamatergic populations) and 40% for Marie Roussel (cholinergic population). Post hoc analysis was done mostly by me, then in order of importance: Marie Roussel, David Lafrance-Zoubga and Ali Rastqar. Maxime Lemieux tested the neuronal responses to photostimulation, analysed and designed the second half of figure 1. I wrote most of the matlab scripts with help from my supervisor and designed all the figures with the help of Marie Roussel. All the immunochemistry and subsequent quantification and canula localization was done by me, on tissue that was cut by Miss Cloé Brindamour. The draft was mostly written by Frederic Bretzner, myself and Marie Roussel.

The fourth and last chapter contains a discussion on the work that was done and possible studies to answer remaining questions.

Chapter 1: Introduction

1.1 Brief introduction to locomotion

The act of walking, seemingly effortless and automatized, is the result of the recruitment of an incredibly complex pool of interacting neurons and muscles. Its delicate timing is crucial to obtain propulsion, balance and adaptation to the environment. Overground locomotion is generally defined as a succession of step cycles that contain a swing phase, when the foot is off the ground, and a stance phase, when the foot is in contact with the ground (Fig 1.A). Each phase is delimited by the foot contacting on and lifting off the ground and is divided into sub-phases: the flexion (F) and extension (E_1) during the swing phase and extension ($E_{2\text{-}3}$) during the stance phase (Grillner, 1975). These phases are the result of muscle contractions (Fig 1.B). To describe each limb muscle's instrumental part in locomotion, we will start from the most proximal to the more distal. To initiate the swing phase several flexor muscles need to be engaged for each joint, for example, i*liopsoas* (IP) for the hip, *semitendinosus* (ST) for the knee and *tibialis anterior* (TA) for the ankle. Then, the extensor muscles come into play and are, to name only one per joint, the *semimembranosus* for the hip, the *vastus lateralis* (VL) for the knee, and the *gastrocnemius lateralis* (LG) for the ankle (Engberg and Lundberg, 1969). The sequence in which these muscles and limbs are coordinated is controlled by motor neurons located in the ventral horn of the spinal cord, which are themselves driven by a network of interneurons known as the central pattern generators (CPGs). Although they are still a conceptual theory, it is thought that each limb has its own CPG that will interact with others to produce alternation between flexor and extensor, between sides of the body, and finally between forelimb and hindlimb (McCrea and Rybak, 2008; Rybak et al., 2015). While studies have shown that the spinal cord is able to produce a rhythmic and patterned output on its own (Grillner and Wallén, 1985), inputs from the periphery and from the brain are necessary to adapt and fine-tune locomotion to the environment.

The first section of this thesis will focus on the precise coordination between limbs that generates locomotor gaits. We will then move on to describe the complex supraspinal control of spinal networks and their role in the initiation of locomotion, finishing with a focus on the main locomotion initiating region: the MLR.

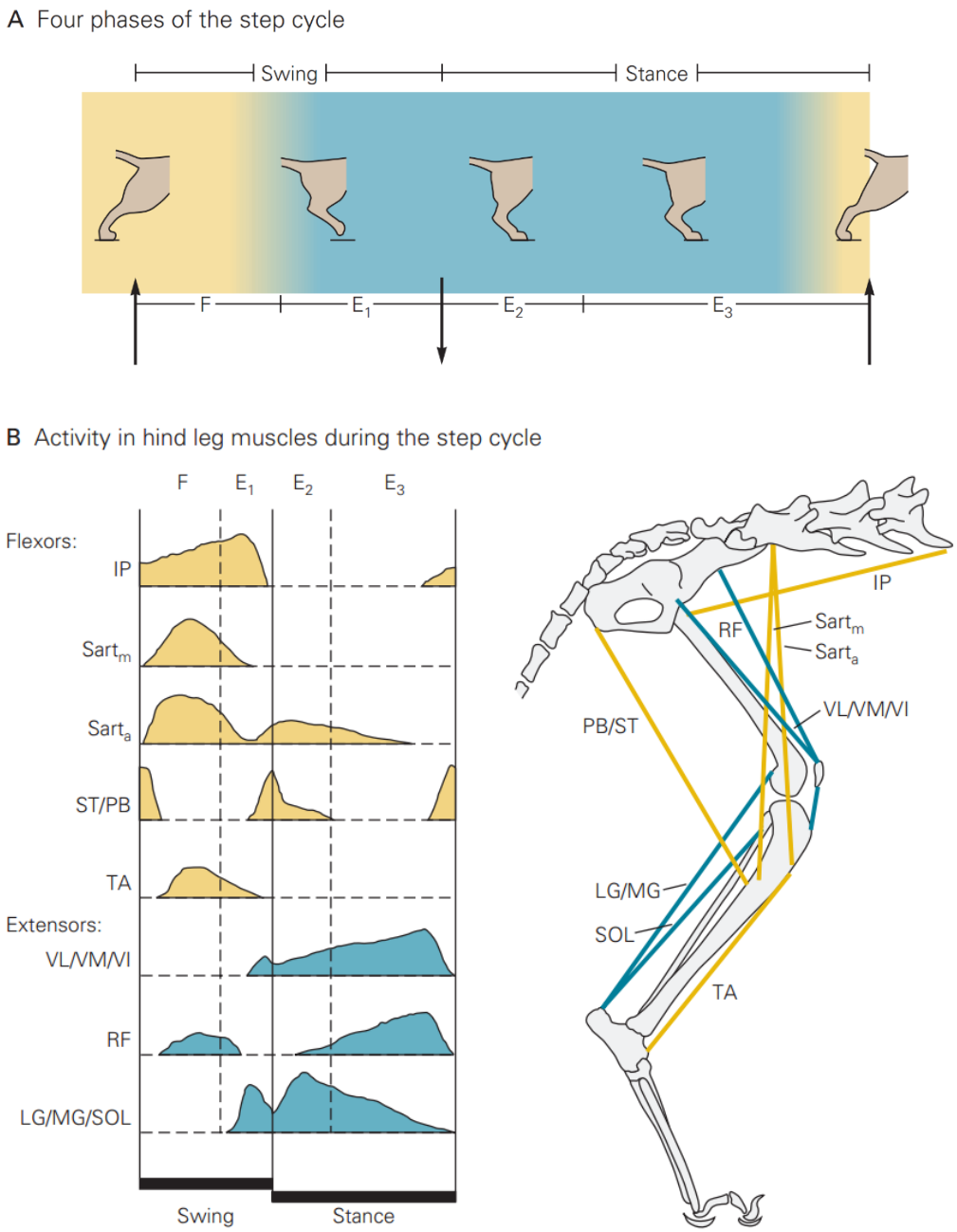

Figure 1: Stepping, its subdivisions and muscles involved (adapted from Engberg and Lundberg, 1969).
A. The step cycle is divided into four phases: the flexion (F) and first extension (E1) phases occur during swing, when the foot is off the ground, whereas second extension (E2) and third extension (E3) occur during stance. **B.** Profiles of electrical activity in some of the hind leg flexor and extensor muscles in the cat during stepping. (IP, iliopsoas; LG and MG, lateral and medial gastrocnemius; PB, posterior biceps; RF, rectus femoris; Sartm and Sarta, medial and anterior sartorius; SOL, soleus; ST, semitendinosus; TA, tibialis anterior; VL, VM, and VI, vastus lateralis, medialis, and intermedialis.)

1.1.1 Spinal interneuronal networks

The presence of a network inside the spinal cord that could generate a locomotor pattern on its own was hinted by a number of studies using spinal or brainstem transections. Dating a century, works by Sherrington and Brown showed that removing cerebral hemispheres did not hinder locomotion (Sherrington, 1906; Brown, 1911). Decerebrated cats can still spontaneously walk or at least walk on a treadmill depending on the transection location (Whelan, 1996). Furthermore, spinally transected cats are not only able to adapt to different speeds on a normal treadmill (Barbeau and Rossignol, 1987) but also on a split-treadmill belt where limbs on opposite sides are set to different speeds (Forssberg et al., 1980). Spinal cord neurons can, therefore produce a rhythmic output that is adapted to the treadmill speed without any supraspinal input. Still, decerebration causes the excursion of hindlimb joints to be reduced and the limbs tend to drag on the treadmill and spinally transected animals need weight support and electrical, chemical or perineal stimulation in order to walk. Therefore, locomotor pattern and rhythm can be generated by a neuronal network in the spinal cord. Yet, in order to obtain real locomotion adapted to the environment, supraspinal inputs and afference from the periphery are necessary.

1.1.2 Sensory and proprioceptive afferences

Although they are not essential for the coupling between limbs (Brown, 1911; Miller et al., 1975b) inputs from the periphery are crucial for motor neurons to adapt their output to produce the precisely timed phases of locomotion. Information from the periphery relay both the position of the limb (proprioceptive) and its cutaneous sensory perception. Cutaneous afferents carry the mechanical, painful, and thermal sensation from the skin to the dorsal horn of the spinal cord. They are responsible for the spinal flexion reflex (Eccles and Sherrington, 1930). Although transection of cutaneous afferents does not impair the ability of cats to walk, it impairs the kinematic of the leg movement and their ability to walk on a ladder (Bouyer and Rossignol, 2003). Stimulation experiments showed that cutaneous afference could be involved in stumbling correction after contact with an obstacle (Zehr et al., 1997). Cutaneous afference therefore plays a crucial role in mediating normal motor function by adapting motor behavior to the environment.

Muscles' state of contraction is detected by muscle spindles (Ia and II afferents) and Golgi tendon organs that depolarize Ib afferents. It has been demonstrated that proprioceptive afferents have a synergistic effect, activating extensors when extensor muscles are contracted (Conway et al., 1987; McCrea et al., 1995). Flexor tension, indicating that the stance phase is over and that the swing phase needs to be initiated, leads to flexor discharge (Hiebert and Pearson, 1999). When muscle spindle feedback is silenced, locomotion on a treadmill is abnormal and on a ladder is clearly impaired (Takeoka et al., 2014).

Therefore, the spinal cord neuronal network is able to produce locomotor rhythm and pattern, and afference from the periphery improves the timing of muscle contraction to get a stable walk on the ground and on complex terrain. Nevertheless, a supraspinal drive is necessary to initiate, control and adapt locomotor behavior to the context. However, in the absence of supraspinal input, a rhythmic coordination is possible between limbs. The spinal circuits that control homologous limb alternation are connected to long spinal interneurons that render limb coordination possible. This interconnection between limbs and its outcome in behaving animals will be the focus of the next section.

1.2 Locomotor gaits

1.2.1 A short history of gait analysis

How animals and humans move has been the subject of research for a very long time. Indeed, Aristotle was the first in recorded history to write about animal gaits (Nussbaum, 1976). Almost 150 years ago, the invention of photography simultaneously allowed Eadweard Muybridge and Etienne-Jules Marey to get detailed access to the timing of footfall by photographing animals with a short delay between photographs (Fig 3A). This technique allowed Muybridge to define seven different types of locomotor gaits. Almost a century later, Milton Hildebrand studied and created a framework to study gaits. He replaced footfall formula (Fig 3. B) with gait diagrams that take timing into consideration (Fig 3. C) (Hildebrand, 1976). He also helped to classify gaits, referring to homologous coupling of either fore- or hindlimbs. He separated gaits into two categories: symmetrical or asymmetrical. In the past 30 years, many researchers have studied the gaits

of a variety of animals and discovered a lot on gaits and how they are produced. The most recent advances will be discussed in the following section.

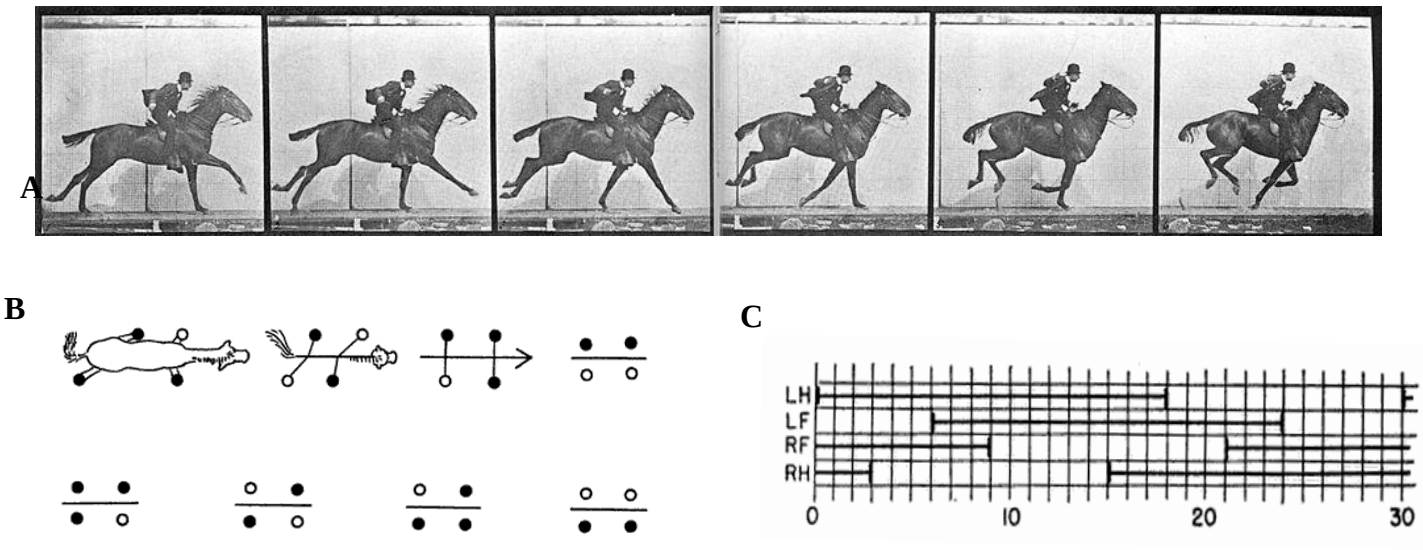

Figure 2: History of gait analysis.

A: Sequence of horse galloping (‘daisy’) by Eadweard Muybridge (Muybridge, 1957). **B**: Footfall formula: the animal is seen from above and goes from left to right. **C**: Gait diagram. Vertical lines represent the number of frames, and each line shows when the limb is in stance (in contact with the ground) or in swing (off the ground) between the lines. LH: Left Hindlimb, LF: Left Forelimb, RF: Right Forelimb and RH: Right Hindlimb (Hildebrand, 1976).

1.2.2 General terminology

Uncommon words or expressions will be used in the next paragraphs. For the sake of clarity and readers' comfort we will start by giving a concise definition for each one of them.

A **stride**, or **step cycle**, is a complete cycle of limb movement.

The **stance**, filled strokes in Fig.3, is the duration of time spent with the foot touching the ground. The **swing,** gaps in Fig. 3, is the duration of time spent with the foot off the ground.

The **duty factor** or **duty cycle** is the fraction of the duration of the stride spent in stance.

The **hind**-, **fore**- and **diagonal-lag** (Fig. 3A) represent the delay between hindlimbs, forelimbs and between one forelimb and hindlimb in diagonal opposition.

The **phase** refers to the fraction of the stride it will take for an event to happen after a reference event. It is the lag divided by the stride. For example, if we choose that the moment the left hindlimb touches the ground is our reference, the phase of the right hindlimb will be the hindlag divided by the stride. If it takes 50% of the stride, there is perfect alternation between the left and right hindlimbs (Fig. 3B) because it takes half a step cycle for the right hindlimb to touch the ground after the left hindlimb (the value of the phase will be 0.5). If the right hindlimb touches the ground at the same time, the phase value will be 0.

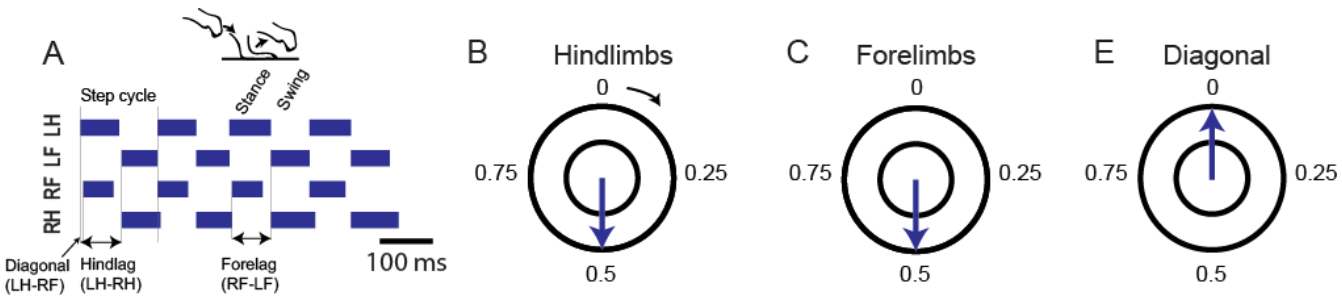

Figure 3: Locomotor gait analysis.

A: Gait diagram showing the swing and stance and the lags. **B,C,D**: polar plot showing the mean phase coupling between limbs for a trot gait (LH: Left Hindlimb, LF: Left Forelimb, RF: Right Forelimb and RH: Right Hindlimb).

A **locomotor gait** is the pattern of cyclic limb movements that appears during locomotion in all terrestrial animals. It is represented by the way animals coordinate movement between left and right sides of the body and between hind- and forelimbs. Keep in mind that the broad term of **gait** is used in reference to a multitude of locomotor parameters that generate the way animals walk but that this manuscript will focus primarily on locomotor gaits.

A **walking gait** has a duty factor superior to 0.5 because most of the stride will be spent in stance, when a **running gait** will have a duty factor inferior to 0.5.

Symmetrical gaits have a 0.5 phase value between hindlimbs and between forelimbs when **asymmetrical gaits** don't.

1.2.3 Locomotor gaits

1.2.3.1 Bipedal and quadrupedal locomotor gaits

Bipedal locomotion is, by definition, characterized by the use of only two limbs to produce locomotion. Therefore, the only three bipedal natural gaits are walking, characterized by limb alternation at low speed, running, with a limb alternation at high speed and hopping where limbs are synchronized (Mann and Hagy, 1980; Diedrich and Warren, 1995). A last bipedal gait that does not occur naturally in bipeds is called skipping, characterized by asymmetry between limbs. Coordination also exists between arms and legs in humans (Wannier et al., 2001). However, the rationale behind the study of locomotor gaits is to better understand the complex control of coordination between left and right but also between the cervical and lumbar spinal cord segments that control the forelimbs and hindlimbs respectively (Figure 4). Therefore, quadrupedal locomotion gives us a perfect window to look into this complex circuitry.

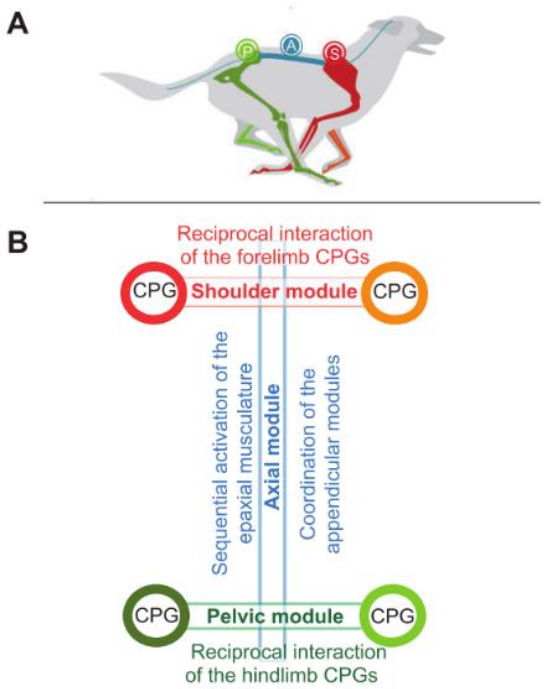

Figure 4: The modular organization of the locomotor coordination in quadrupeds.

A: Three modules interact to coordinate movements. The shoulder module (S) coordinates the movements of the forelimbs, the pelvic module (P) coordinates the movements of the hindlimbs and the axial module (A) coordinates the movement of the trunk. **B:** At the girdle modules, the reciprocal interaction between the central pattern generators (CPGs) coordinates the rhythms of the two limbs. Depending on the coordination of the muscular activity, the command gives rise to lateral bending, sagittal bending and stabilization of the trunk (Maes and Abourachid, 2013).

Quadrupedal gaits were first classified as being symmetrical or asymmetrical (Hildebrand, 1976, 1977a). In symmetrical gaits, the left hindlimb to right hindlimb phase value or hindlag is 0.5, meaning that the right hindlimb touched ground half a stride after the left hindlimb. The gaits fitting that description are walks, characterized by a slow locomotion with three feet on the ground. Two walks are the lateral walk and the diagonal walk (a special case of lateral walk with a slightly different sequence of limb on the ground) (Abourachid, 2003, Fig. 5C&D). The pace is characterized by synchronization between hindlimb and forelimb on the same side of the body. It is mostly found in animals with long limbs (Fig. 5A). When animals trot, diagonal limbs are synchronized (Fig. 5B).

Asymmetrical gaits are defined as gaits having anything else than perfect alternation between hindlimbs or forelimbs. The transverse and rotary gallops still have alternating hindlimbs and forelimbs but the hindlimb phase is neither 0 nor 0.5 (Fig. 5E&F). When hindlimbs start synchronizing but forelimbs still alternate, the gait is called a half-bound (Fig. 5G). Finally, if the hindlimbs and forelimbs synchronize in pairs, the step is classified as a bound. A gait that is not represented here is the pronk, used by deer, where all limbs are synchronized (Fig.5H). Looking at the range of gaits that are available in quadrupeds, one can't help but wonder how such timed coordination between limbs is possible. Many recent studies have tried to uncover the underlying processes responsible for gait selection and transition; they will be reviewed in the next sections.

1.2.3.2 Origin of locomotor gaits

As mentioned previously, locomotor gaits are the result of an extremely precise coordination between limbs. Owing to the intensive use of isolated lumbar spinal cord to study locomotor circuitry, one of the most studied alternations is the one between hindlimbs and the neurons that orchestrate this alternation (Kjaerulff and Kiehn, 1997; Akay et al., 2006; Crone et al., 2008; Zhang et al., 2008).

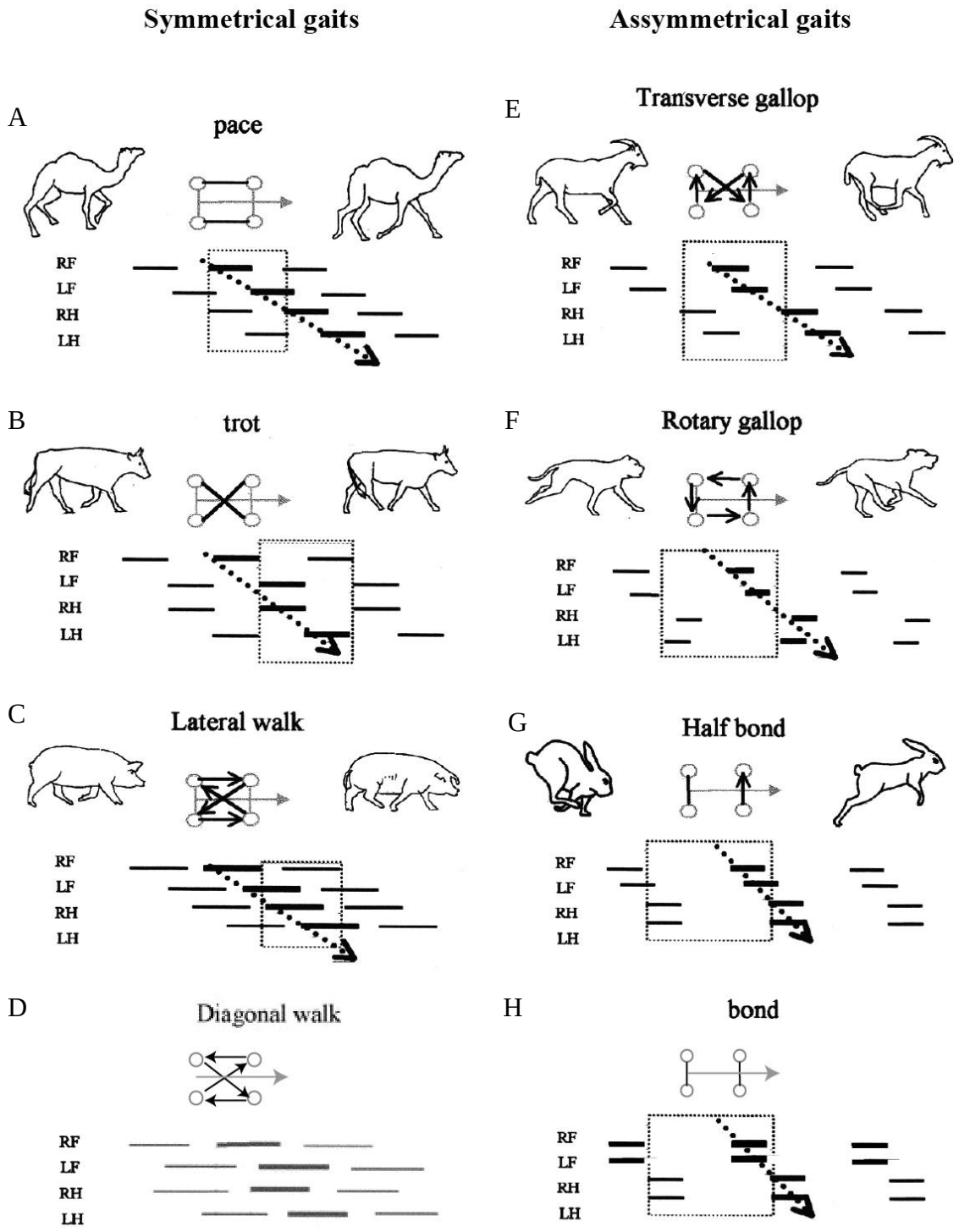

Figure 5: Symmetrical and asymmetrical locomotor gaits in quadrupeds.

The four feet are plotted on successive lines, the time when a foot is on the ground is symbolised by a continuous line. RF: Right Forelimb, LF: Left Forelimb; RH: Right Hindlimb; LH: Left Hindlimb. The grey arrow represents the head, the circles represent the feet. The black lines linking the circles represent simultaneous footfalls and the black arrows the order of succession of the footfalls during a stride (adapted with permission from Abourachid, 2003).

However, locomotor gaits depend on coordination between all four limbs. The precise and rhythmic coordination between forelimb and hindlimbs in quadrupedal locomotion hints towards a connection between limb CPGs that could go through intersegmental propriospinal relays (modeled by Danner et al., 2017, Figure 6).

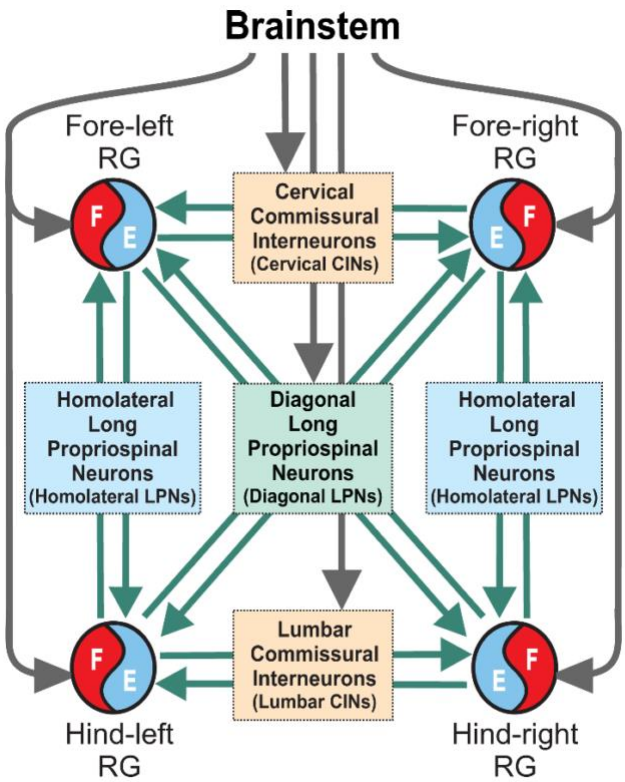

Figure 6: Model concept of the circuitry controlling locomotor gaits.

Each limb is controlled by a separate rhythm generator (RG). The local commissural neurons (CINs) as well as homolaterally and diagonally projecting (descending and ascending) long propriospinal neurons (LPNs) couple the four RGs. Brainstem drive acts on the RGs to control locomotor speed and on CINs and diagonal LPNs to control gaits (Danner et al., 2017).

Anatomical studies were the first to point out a bidirectional propriospinal connection between cervical and lumbar segments of the spinal cord in rats, cats and even humans (Miller et al., 1975b; Matsushita et al., 1979; Nathan et al., 1996; Dutton et al., 2006). Using a whole isolated spinal cord including cervical and lumbar segments, a French team of scientists showed that the spinal cord naturally produced rhythmic output with an alternation between cervical and lumbar motoneuronal extensor bursts corresponding to a walking gait (Juvin et al., 2005). Transection and inhibition experiments showed that there was indeed a direct ipsilateral excitatory and contralateral inhibitory influence from the

lumbar segment onto the cervical segment that is stronger than the descending influence from the cervical to the lumbar. Interestingly, cervico-lumbar projection neurons receive major supraspinal inputs from motor-related regions (Alstermark et al., 1987; Ruder et al., 2016) but also from sensory afferents (Miller et al., 1973). In regard to locomotor gaits, it has been shown that cervico-lumbar propriospinal neuron ablation leads to postural instability and to a greater synchronization between hindlimbs at a fast treadmill speed that was unfortunately not studied in the perspective of locomotor gaits (Ruder et al., 2016). However, these data do suggest that long descending neurons play a role in shaping the transition between symmetrical and asymmetrical gaits. In summary, propriospinal descending and ascending neurons modulate and allow the alternation between hindlimbs and forelimbs, a dynamic system that is most likely crucial for gait initiation, stabilization and transition.

1.2.3.3 Transition between locomotor gaits

It is critical to understand why there is a need for gait transition to explain why there are multiple gaits. In humans, the trigger to start running seems to come from mechanical constraints rather than energy efficiency considerations (Kung et al., 2018). It is more efficient to use a certain gait when a certain speed needs to be attained. Therefore, some gaits can be considered as attractors and increasing speed will lead to changing from one attractor to another (Diedrich and Warren, 1998). In order to get a transition, a break from coordination is necessary (Vilensky et al., 1991). In dogs, coordination analysis showed that mechanical constraints drive the stance phase when coordination is modified during the swing phase (Maes and Abourachid, 2013). Gait transition analysis, therefore is a window on a very specific time when the spinal networks need to break the coordination that is in place and install a new one that is more adapted to the new locomotor speed.

In summary, at least nine different gaits have been clearly identified and research is starting to point towards a role for long propriospinal projecting neurons in regulating the complex synergy between all limbs. Some locomotor gaits are more stable than others at a

certain speed and can be seen as attractors. However, a simple method to classify gaits accepted and used by everyone is still lacking, making results between studies difficult to combine. Still, the amount of scientific data gathered on locomotor gaits and propriospinal neurons allowed computational models of interlimb coordination that can produce simulations that closely fit reality (Danner et al., 2016, 2017). In a broader view, locomotor gait analysis reaches far beyond the study of interlimb coordination and can be applied to studying spinal cord injury (Thibaudier et al., 2017), to design robots (Owaki and Ishiguro, 2017) and to study coupling between respiratory and locomotor rhythms (Kawahara et al., 1989).

While the spinal control of locomotion has been described intensively up to this point, supraspinal inputs are vital to getting a real locomotion that is aware and adapted to the environment. The way brain centers control locomotion and its initiation will be detailed in the next section.

1.3 Supraspinal Control of locomotion

The supraspinal connectivity involved in selecting and initiating locomotor behavior is detailed in Figure 7 (Kiehn, 2016). The basal ganglia (BG) is responsible for choosing behavior. It either projects to the thalamus that will, in turn, project to the motor cortex, or to the mesencephalic locomotor region (MLR), a brainstem center for initiation of locomotion probably formed by the cuneiform nucleus and pedunculopontine nucleus (Jordan et al., 2008). The MLR projects to the medullary reticular formation (RF) that, through the reticulospinal tract, will contact spinal cord locomotor networks controlling locomotion. Brainstem nuclei (BSN), through the vestibulospinal and rubrospinal pathways have a role in posture and modulation of motor output (Sharples et al., 2014). The cerebellum integrates inputs from the spinal cord and adapts the locomotor command accordingly. Visual information will be processed by the visual cortex (VCtx), which projects to the posterior parietal cortex (pPCtx), which will, in turn, modulate pyramidal neurons of the motor cortex. Regions essential to locomotor control will be further detailed in the next paragraphs.

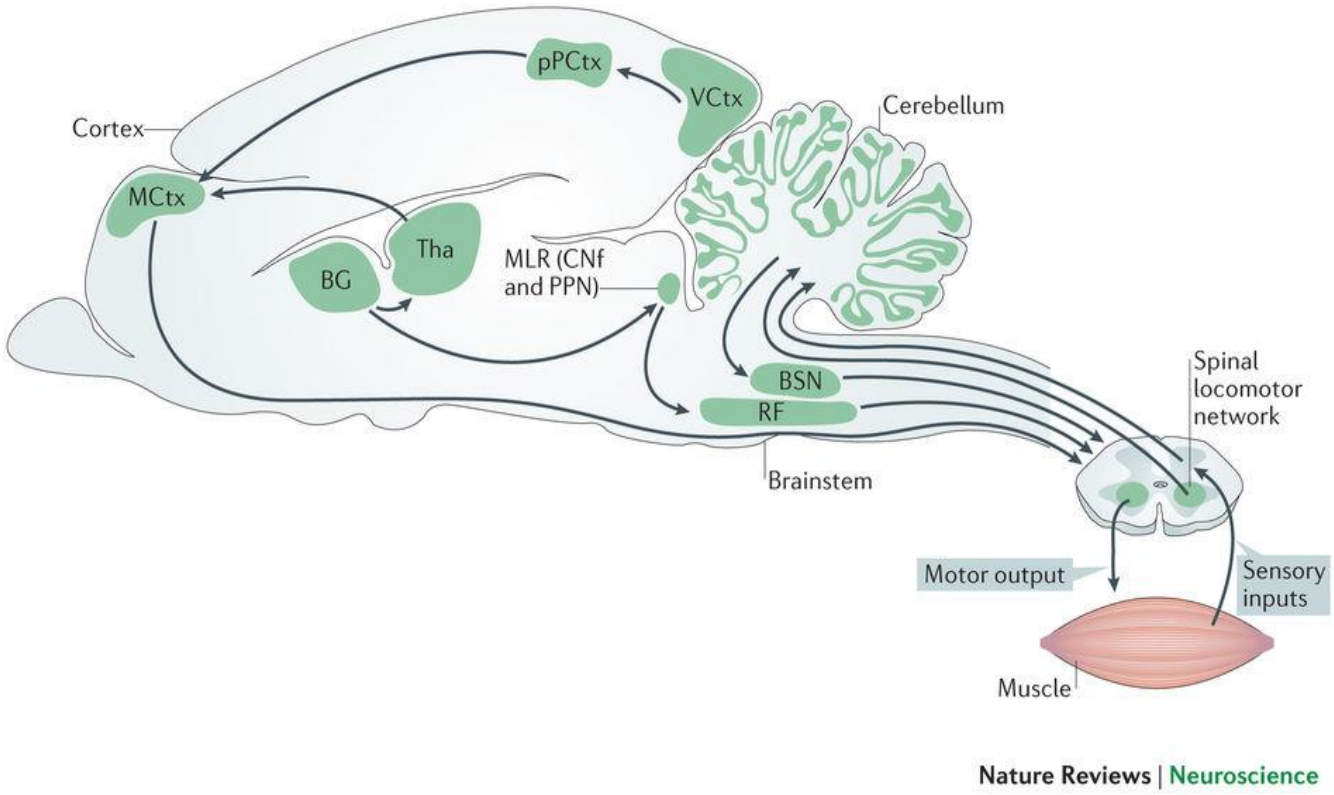

Figure 7: Organization of neuronal control of locomotion in vertebrates.

MCtx: Motor Cortex, pPCtx: posterior parietal cortex, VCtx: visual cortex, BG: Basal ganglia, Tha: Thalamus, MLR: mesencephalic locomotor region, CnF: Cuneiform nucleus, PPN: pedunculopontine nucleus, BSN: Brainstem nuclei, RF: Reticular formation (Kiehn, 2016).

1.3.1 The basal ganglia

The basal ganglia (BG) consist of multiple interconnected nuclei located deep in the brain: the striatum, globus pallidus (GP), substantia nigra (SN), and subthalamic nucleus (STN). They play a crucial role in the control of motion and decision making. Indeed, a dopamine deregulation in BG can lead to pathologies that disrupt motor control, such as Parkinson's or Huntington's disease. The striatum integrates inputs from the cortex and thalamus (Doig et al., 2010) while the globus pallidus interna (GPi) and substantia nigra pars reticulata (SNr) are responsible for sending inhibitory outputs to the thalamus and brainstem locomotor centers such as the MLR (Hikosaka, 2007). The basal ganglia is known to project to the pedunculopontine nucleus. When a motor action needs to be initiated, the striatum will inhibit the SNr and Gpi leading to a disinhibition of brainstem motor centers (Freeze et al., 2013) and, thus, movement.

1.3.2 The motor cortex

While the role of the motor cortex in voluntary movement has been extensively described, its role in locomotor control remained uncertain for a prolonged period. Transection of the pyramidal tract, originating in the motor cortex and crossing to the contralateral side of the spinal cord, or decortication in animal models only had a transient effect on locomotion (Eidelberg and Yu, 1981). These observations imply the motor cortex might not have such a vital role in controlling locomotion. Nevertheless, studies have shown that stimulating the motor cortex could reset the locomotor rhythm (Orlovsky, 1972; Bretzner and Drew, 2005) and that pyramidal neurons in the cortex discharge in synchrony with stepping movements (Armstrong and Drew, 1984). Electrical stimulation of those neurons can also produce changes in the limb trajectory (Armstrong and Drew, 1985). Corticospinal activity is also linked with visually guided gait adaptations, as, for example, in the presence of an obstacle (Drew et al., 1996; DiGiovanna et al., 2016). Microstimulations of the motor cortex during locomotion showed a clear bias towards flexor muscle activity during unobstructed locomotion (Bretzner and Drew, 2005). The motor cortex therefore seems to act as a visual and somatosensory relay adapting locomotion to the exterior world. To obtain initiation of locomotion, good posture, and smooth movements, other regions in the brainstem and cerebellum need to play their part.

1.3.3 The cerebellum

The cerebellum is located dorsal to the brainstem and tucked underneath the cerebral hemispheres. Its role is to properly coordinate smooth and efficient movement. Damage or degeneration of the cerebellum causes ataxia (De Zeeuw et al., 2011), which is characterized by a loss of order and coordination of movement. Focal lesion studies showed that medial parts of the cerebellum are involved in regulating posture and balance (Mori et al., 1999), intermediate zones are more relevant to trajectory, timing and amplitude (Yu and Eidelberg, 1983). Finally the lateral zones are important in the adaptation to complex circumstances (Aoki et al., 2013). As it has such a preeminent role in motor coordination, the cerebellum is largely interconnected with other motor regions of the brain. Its main

locomotor downstream projections are to the red nucleus, the vestibular nuclei and the medullary reticular formation (Tang and Zhang, 1987; Teune et al., 1995).

1.3.4 The red nucleus

The red nucleus (BSN in Fig 7.) gives rise to the flexor-facilitatory rubrospinal tract, projecting to the contralateral spinal cord. In early vertebrates, the red nucleus was involved in controlling limbs, although it is important to note that from lower mammals to primates, the rubrospinal pathway has progressively declined (Massion, 1967) probably because fine motor skills have been taken over by the pyramidal system (ten Donkelaar, 1988) and bipedalism led to a loss of locomotor function in the upper limbs (Massion, 1988). Nevertheless, the red nucleus receives afferents mainly from the contralateral cerebellum and, in humans, the red nucleus mainly relays information from the cortex to the cerebellum. In mice, rubrospinal fibers terminate in hand- and foot- controlling motor neurons of the spinal cord (Liang et al., 2012a), and in cats, neural activity in the red nucleus is correlated with fine motor skills such as grasping (Horn et al., 2002). Therefore, while it does not project to the spinal cord in primates, where the corticospinal tract is preponderant, in rodents and lower mammals, the red nucleus seems to adapt locomotion to the environment, closely mirroring the motor cortex's effects on motor control.

1.3.5 Vestibular nuclei

Vestibular nuclei (BSN in Fig 7.) are the source of the extensor-facilitatory ipsilateral vestibulospinal tract. There are four subnuclei: the medial, lateral, inferior and superior vestibular nuclei. Their main function is the maintenance of equilibrium and posture along with head position and acceleration perception. They work in close cooperation with the cerebellum (Angelaki and Cullen, 2008). In order to adapt to movement, the vestibular nuclei will control gaze stabilization, estimate self-motion and control posture and balance through its outputs to the spinal cord networks, the cerebellum and the thalamus. In mice, the vestibulospinal tract terminates in the medial parts of the gray matter (Liang et al., 2014). They therefore do not contact motor neurons directly but

regulate spinal networks. To summarize, vestibular nuclei's role in locomotor control is to maintain equilibrium and posture by the modulation of spinal networks.

1.3.6 The medullary reticular formation

The medullary reticular formation (RF in Fig 7.) is a complex network of nuclei located in the core of the brainstem that project ipsilaterally to the spinal cord via the lateral and medial reticulospinal tract (Liang et al., 2016). The RF extends from the rostral midbrain to the caudal medulla and has a multitude of roles ranging from respiratory (Onimaru et al., 1995), to cardiovascular (Heidel et al., 2002), to arousal (via the reticular activating system, Skinner et al. 2004) and attention (Kinomura et al., 1996), to motor control. The RF maintains muscle tone (Mori, 1987), activates the CPGs (Grillner, 1981), and is also active during reaching movements (Luccarini et al., 1990). On the other hand, some reticulospinal neurons will display higher activity during REM sleep, exerting an inhibitory effect on brainstem and spinal cord neurons, resulting in atonia, a general decrease of muscle tone (Takakusaki et al., 2001).

The glutamatergic and serotoninergic neurons are the main populations residing in the RF (Hägglund et al., 2010; Cabaj et al., 2017). They both have a major role in locomotor control. Serotoninergic neurons of the medulla oblongata (containing the raphe nuclei) projects mainly to the spinal cord (Bowker and Abbott, 1990). The mainly serotoninergic parapyramidal region (PPR) seems to be a relay between the MLR and the spinal cord. Cooling it down with a probe inhibits MLR's effects on locomotion (Noga et al., 2003) and stimulating it induces locomotion in neonatal rats (Liu and Jordan, 2005). Curiously, the use of serotonin agonists or selective serotonin reuptake inhibitors (SSRI) has a contradictory effect on locomotion. This can be explained by the fact that low concentrations of serotonin have excitatory effects via the 5-HT2/7 receptors and that high concentrations have an inhibitory effect via 5-HT1 receptors (Dunbar et al., 2010). The other major neurotransmitter produced by the medullary reticular formation is glutamate. Glutamatergic neurons in these regions have an increased neuronal activity after locomotion on a treadmill (Bretzner and Brownstone, 2013). However, glutamatergic neurons of the RF do not necessarily increase locomotor drive. Recently, stimulation of

V2a expressing glutamatergic neurons has been shown to stop ongoing locomotion (Bouvier et al., 2015). Another large nucleus whose role has been thoroughly described recently is the ventral part of the medullary reticular formation (MdV). It is connected to forelimb motor neurons and skilled motor tasks (Esposito et al., 2014). Many other nuclei reside in the RF and still need to be functionally and anatomically dissected. To conclude, the medullary reticular formation and the reticulospinal tract are clearly a major component in locomotor control, regulating posture and gait, but uncertainties concerning its anatomy and exact role in locomotion remain to be deciphered.

There is a lot left to be resolved about the spinal and supraspinal control of locomotion. For example, even if considerable progress has been made in recent years, the interneuronal network located in the spinal cord known as the central pattern generator is still a concept that needs to be thoroughly decoded at the cellular level (reviewed in Goulding 2009). Moreover, although the study of each supraspinal region that has a role in locomotor control has been extensive, there are still areas, such as the medullary reticular formation or the mesencephalic locomotor region which remain elusive. Using newly available elegant tools like viral tracing and optogenetic stimulation, the connectivity between these regions and the spinal cord is now a great research topic (Esposito et al., 2014; Han et al., 2017; Zingg et al., 2017). Despite the work that is left to be done, we do know a lot about locomotor control. Research has shown that when combined, all of the supraspinal and spinal neurons that we described control muscle tone, skilled and smooth motor tasks, posture, rhythmic locomotion and adaptation to the environment. Yet, an important issue that was left out up to this point is the functional areas that can initiate locomotion. They will be the focus of the next section.

1.3.7 Supraspinal locomotor centers that initiate locomotion

In lamprey and salamander, extensive work has been done to identify centers that could generate movement in response to stimulation (Cabelguen et al., 2003; Dubuc et al., 2008; Smetana et al., 2010; Ryczko and Dubuc, 2017). Many regions can initiate locomotion but only a few can produce a graded output that is in correlation with the intensity of stimulation such as the MLR (Brocard and Dubuc 2003, Figure 7). The MLR

will be thoroughly described in the next section: however, other less-studied regions fit this definition. They will be briefly detailed here.

1.3.7.1 The diencephalic locomotor region

The diencephalic locomotor region (DLR in lamprey and SLR in Figure 8) has been discovered in lamprey (El Manira et al., 1997; Ménard and Grillner, 2008). It is located in the ventral thalamus in lamprey. Yet, some discrepancies appeared when it was stimulated in mammals. The DLR corresponds either to the SLR (subthalamic locomotor region) in cats (Grossman, 1958; Armstrong, 1986) or lateral hypothalamus in rats (Milner and Mogenson, 1988; Sinnamon, 1993). It projects to reticulospinal cells located in the medullary reticular formation and induces motoneuronal activity upon stimulation (Mori et al., 1989; El Manira et al., 1997). Decerebration experiments showed that spontaneous locomotion was only displayed when the SLR and its downstream projections were left intact (Whelan, 1996). Its connectivity indicates that the SLR will initiate locomotion when basal ganglia's inhibition is lifted.

1.3.7.2 The cerebellar locomotor region

The cerebellar locomotor region, CLR in Figure 8, was discovered when stimulating decerebrated cats (Mori et al., 1998; Takakusaki et al., 2016). In cats, stimulation of a restricted region in the medial cerebellum white matter evokes an increase in muscle tone on a stationary surface and locomotion on a moving treadmill. Anatomical reconstruction showed the stimulated fibers were fastigiofugal and lead to the activation of pontomedullary reticulospinal neurons. The CLR has also been found in humans using fMRI and imagination of gait (Jahn et al., 2008) and could possibly be linked with freezing of gait in parkinsonian patients (Fasano et al., 2017).

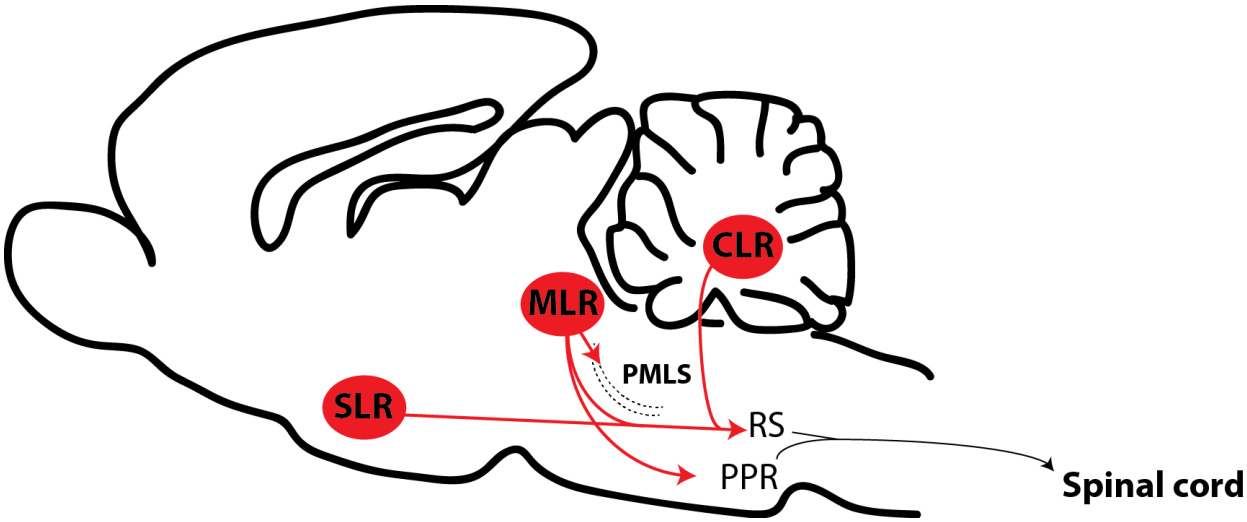

Figure 8: Supraspinal locomotor centers.

SLR (DLR in lamprey): subthalamic locomotor region, MLR: mesencephalic locomotor region, PMLS: pontomedullary locomotor strip, CLR: cerebellar locomotor region, RS: reticulospinal neurons, PPR (including the LPGi and RVM): parapyramidal region.

1.3.7.3 Locomotor regions intermediaries

While the CLR and SLR both project to reticulospinal neurons located in the medullary reticular formation, the MLR has multiple potential relays to attain its effect on locomotion. As previously mentioned, the caudal and ventral brainstem host locomotion initiating regions and the main relays between the MLR and the spinal cord networks are likely to be located in the gigantocellular and magnocellular nuclei of the RF (Shefchyk et al., 1984). Stimulation of the medioventral medulla induces locomotion (Kinjo et al., 1990). As does the stimulation of the parapyramidal region, PPR, located next to the pyramidal tract, in neonatal rats (Jordan et al., 2008). Interestingly, it was abolished by the use of serotonergic inhibitors. However, recent studies have shown that stimulation of the glutamatergic lateral paragigantocellular nucleus, LPGi, located right next to the serotonergic PPR initiated locomotion (Capelli et al., 2017) and that optogenetic stimulation of glutamatergic neurons in this region induced fictive locomotion in an isolated mouse spinal cord preparation when serotonergic stimulation did not (Hsu and Kiehn, 2017). Despite debates over neurotransmitter phenotype, the consensus is that this region is necessary for MLR stimulation to effectively induce movement (Jordan et al., 2008; Capelli et al., 2017).

The pontomedullary locomotor strip, PMLS, seems to be another relay between the MLR and spinal cord networks (Shefchyk et al., 1984; Armstrong, 1986). Its chemical and electrical stimulation leads to decerebrated locomotion (Mori et al., 1977; Steeves et al., 1987) and it projects to the cervical spinal cord (Matsushita et al., 1981). However, after a great surge of publications, mainly with cats, it has mysteriously disappeared from the scientific literature since 1990, thus leaving us with many unanswered questions on its anatomy and physiology in other species.

To sum up, there are three main supraspinal initiating locomotor centers and it is important to note that the CLR has never been stimulated in awake and freely behaving animals. It is, therefore, difficult to ascertain its role in the initiation of locomotion. On the other hand, the SLR has been stimulated in freely behaving animals (Mori et al., 1989) and it is interesting to note that the MLR stimulation had a stronger effect than SLR stimulation in the same implanted cats. This indicates that those two regions may induce different types of locomotion: a slow goal-directed exploratory one with the SLR, which may be the result of a multitude of inputs and pure locomotor escape-like initiation of locomotion with the MLR (Shik and Orlovsky, 1976).

However, owing to a strong debate on its anatomical substrates, the MLR's definition was kept functional. The next and last section will try to untangle the scientific research that led to a better understanding of the topographical and physiological constitution of the nuclei constituting the MLR.

1.4 The mesencephalic locomotor region (MLR)

1.4.1 Brief history: Discovery and debate

Shik and colleagues were the first to describe the MLR in 1966 (Shik et al., 1966). They showed that when stimulated, a specific region of the midbrain could induce locomotion in a precollicular–postmamillary transected, weight-suspended cat. Increasing the intensity of the stimulation led to an increase in speed and to a transition from walk to trot to gallop during locomotion. Since then, many studies have shown that the MLR was indeed conserved throughout the phylogeny and that electrical stimulation had the same effects on locomotor activity in, for example monkeys, rats, lampreys and even Atlantic stingrays (Eidelberg et al., 1981; Skinner and Garcia-Rill, 1984; Bernau et al., 1991; Dubuc et al., 2008). In recent years, advances in mouse genetics have opened the way for optogenetics. Using light-triggered membrane channels, it is now possible to specifically stimulate neurons based on their genetic expression, i.e., their subtype. Very recently, two studies have used optogenetics to study the MLR (Lee et al., 2014; Roseberry et al., 2016). Only when stimulating the glutamatergic MLR did they obtain initiation of locomotion and speed increase usually attained through electrical stimulation. Yet, the MLR is a functionally defined region, which means that while the physiological effects of its stimulation have been widely studied, its precise location and constitution remains debated to this day (Garcia-Rill et al., 1987; Takakusaki et al., 2003; Ryczko and Dubuc, 2013; Sherman et al., 2015).

1.4.2 General topography

The MLR is a functional region. Therefore the only way to know which region of the brain is part of the MLR is to do a precise mapping by either stimulating or recording activity in an awake subject. In 2016, Roseberry et al. used electrical stimulations of the putative MLR (Figure 9A) to map the site that elicited locomotion (green dots) and the sites that did not (red crosses). Their results show that the MLR does not reside in only one nucleus. In the mouse, it overlaps between the cuneiform nucleus (CnF), the pedunculopontine nucleus (PPN or PPTg), the midbrain reticular nucleus (MRN), and scarcely in the parabrachial nucleus (PB) and the inferior colliculus (IC). In humans, the

MLR's topography was acquired through functional imagery techniques. In Figure 9B, the results obtained by Karachi et al. in 2012, show that an imagined walk is enough to activate the MLR and that its location closely fits the one obtained in the mouse, being centered on the CnF and PPN.

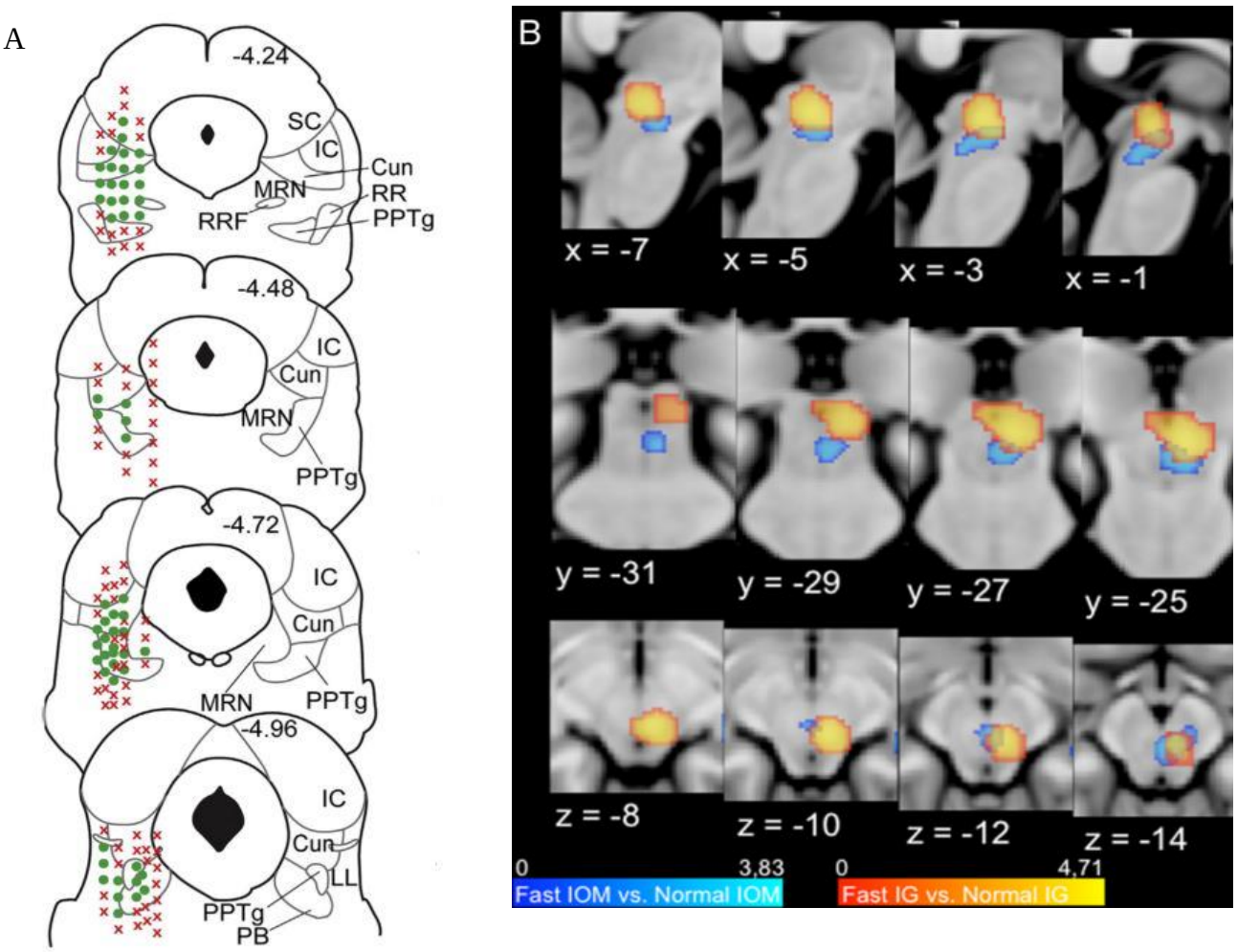

Figure 9: Localization of the MLR in mice and humans.

A: Electrical stimulation sites that elicited locomotion (green dots) or did not (red crosses). IC, inferior colliculus; RRF, retrorubral field; RR, retrorubral nucleus; LL, lateral lemniscus; PB, parabrachial nucleus. **B**: Subcortical contrasts (Fast IG vs Normal IG in orange and Fast IOM vs Normal IOM in blue) are superimposed on series of sagittal, frontal, and axial cross-sections of the MLR region, taken every 2 mm. IG: Imagery of gait, IOM:Imagery of object moving (Karachi et al., 2012; Roseberry et al., 2016).

1.4.3 The Cuneiform nucleus (CnF)

1.4.3.1 Anatomy and connectivity

The CnF is located in the dorsolateral part of the mesencephalic tegmentum, intercalated between the inferior colliculus and the periaqueductal gray (PAG). Laterally, the CnF is bordered by the lateral lemniscus and ventrally by either the PPN in its rostral part or the subcuneiform nucleus in its caudal portion (Fig. 10) (Crosby and Woodburne 1943; Edwards and de Olmos 1976; Olszewski and Baxter 1982). The subcuneiform nucleus has only been identified in humans, cats, and rats and, interestingly, the neuronal population located in the subCnF bears a close resemblance to the PPN's (Taber, 1961). It's important to mention that there is no clear anatomical boundary between the CnF and its ventrally located nuclei (PPN or subCnF) and that they can only be differentiated by cytoarchitectural differences (Olszewski and Baxter, 1982). This lack of clear distinction is probably one of the factors that led to the still ongoing debate about MLR's location.

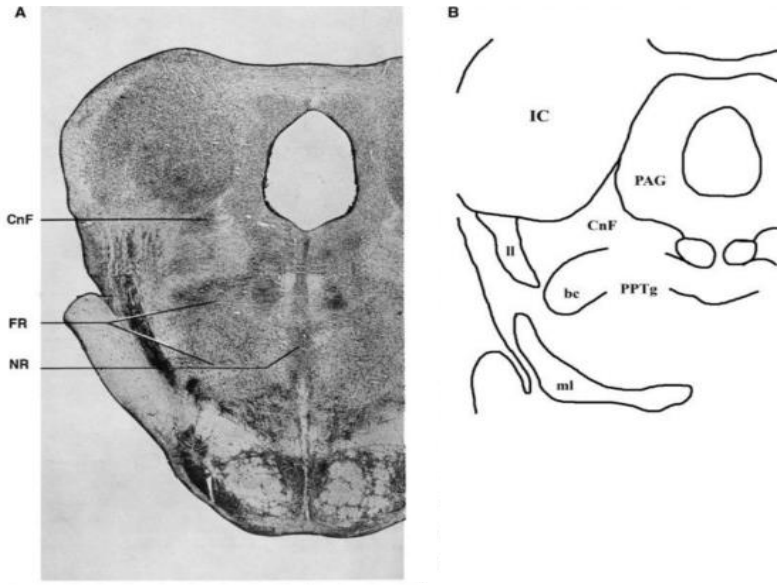

Figure 10: Anatomical location of the cuneiform nucleus.

A: Transversal section of a cat brainstem, pointing to the reticular formation (FR) and raphe nuclei (NR). **B**: sketch of A showing the location of the inferior colliculus (IC), periaqueductal gray matter (PAG), cuneiform nucleus (CnF), pedunculopontine nucleus (PPTg), lateral lemniscus (II), medial lemniscus (ml), brachium conjunctivum (bc) (Alam et al., 2011).

Neurons of the cuneiform nucleus are glutamatergic (Heise and Mitrofanis, 2006), GABAergic in its most rostral portion (Appell and Behan, 1990), sparsely cholinergic ventrally (Spann and Grofova, 1992) and, even more rarely, they express nitric oxidase synthase (Pose et al., 2000). They receive inputs from the periaqueductal gray matter (PAG) (Han et al., 2017), the contralateral cuneiform nucleus and substantia nigra pars lateralis (Bernard et al., 1989), the superior colliculus (Zingg et al., 2017) and from dopaminergic cells probably located in the A13 region (Rolland et al., 2009; Whelan, 2017, Fig. 11). This combination of inputs puts the cuneiform nucleus at the center of a defensive system that will then send downstream outputs to regulate the necessary responses to painful or threatening stimuli.

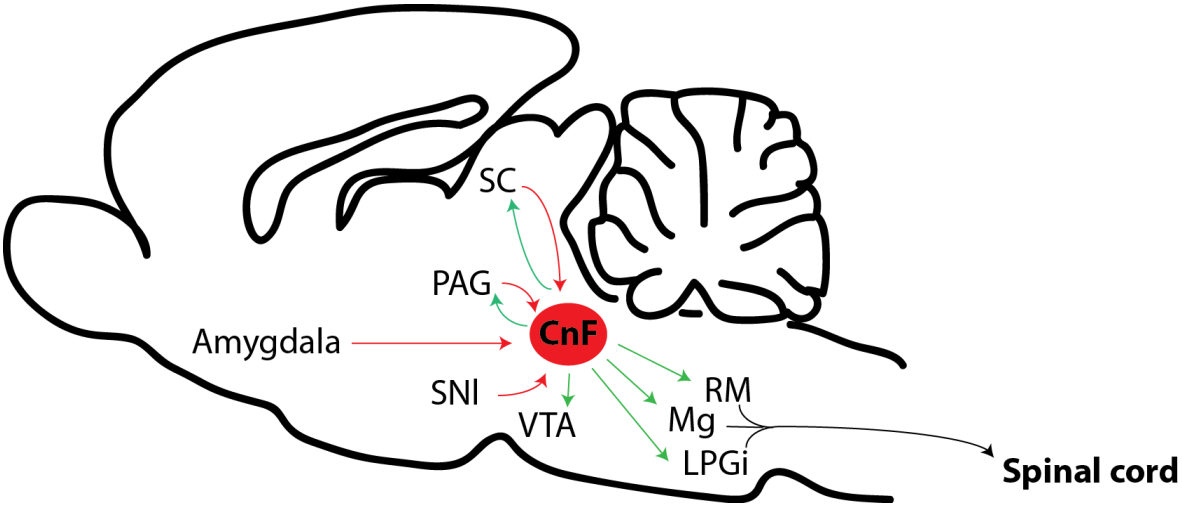

Figure 11: The cuneiform nucleus's connectivity.

The CnF receives inputs from the nuclei located mostly rostrally (red arrows) and projects mostly to caudally located motor regions (green arrows) that will in turn project to the spinal cord through the reticulospinal tract. SC: superior colliculus, PAG: periaqueductal gray matter, SNl: Substantia nigra pars lateralis, VTA: ventral tegmental area, RM: Raphe magnus, Mg: Magnocellular nuclei, LPGi: lateral paragigantocellular nucleus

The CnF sends bilateral descending projections that predominantly end in the medullary reticular formation (Castiglioni et al., 1978) and chiefly, in the raphe magnus (Chung et al., 1983), the lateral paragigantocellular nucleus (LPGi) (Xiang et al., 2013; Capelli et al., 2017), the magnocellular nucleus (Abols and Basbaum, 1981) and the gigantocellular nucleus (Korte et al., 1992) (Fig. 11). Some studies also found that the cuneiform nucleus has a direct connection to the spinal cord (Castiglioni et al., 1978; Liang et al., 2012b). Ascending projections from the CnF are sparse and directed towards the superior colliculus, the periaqueductal gray matter, the hypothalamus and ventral tegmental area (Korte et al., 1992). Being a central hub for inputs from stress and fear integrating regions and giving rise to major outputs in downstream locomotor centers, the cuneiform nucleus therefore understandably plays a crucial role in motor control and especially in the control of escape behaviors that will be detailed in the next section.

1.4.3.2 Physiology and pathophysiology

In monkeys and humans, the CnF fires during locomotion (Piallat et al., 2009; Goetz et al., 2016) and a marker for cellular activity, c-Fos, has also been shown to be increased in rats after locomotor activity (Jordan, 1998). Electric and chemical stimulation of the cuneiform nucleus mostly results in an increase in locomotor drive. Glutamate injection in rats initiates running (Mitchell et al., 1988) and electrical stimulation increased locomotor frequency with a change in locomotor gaits in many species (Eidelberg and Yu, 1981; Kawahara et al., 1989; Mori et al., 1989; Marlinsky and Voitenko, 1991; Musienko et al., 2008). However, it can also lead to mixed effects. For example, in rats, electrical stimulation led to darting but also freezing behavior (Depoortere et al., 1990). This last effect closely mirrors the one recently observed when photostimulating the ventrolateral periaqueductal gray matter (vlPAG) (Tovote et al., 2016), indicating that stimulation may have possibly been medial to the cuneiform nucleus or too strong. In pathologies, the CnF has been considerably less studied than the PPN. Nonetheless, in 6OHDA rats, a model of Parkinson’s disease, the CnF is hyperactive. This could be leading to the dyskinesia observed in parkinsonian patients (Heise and Mitrofanis, 2006).

In acutely decerebrated cats, when comparing CnF and PPN stimulation, activation of the CnF resulted in an increase in posture and locomotion when a PPN stimulation produced atonia (Takakusaki et al., 2003, Figure 12), However, those results are subject to debate and will be discussed after an introduction and thorough description of the PPN.

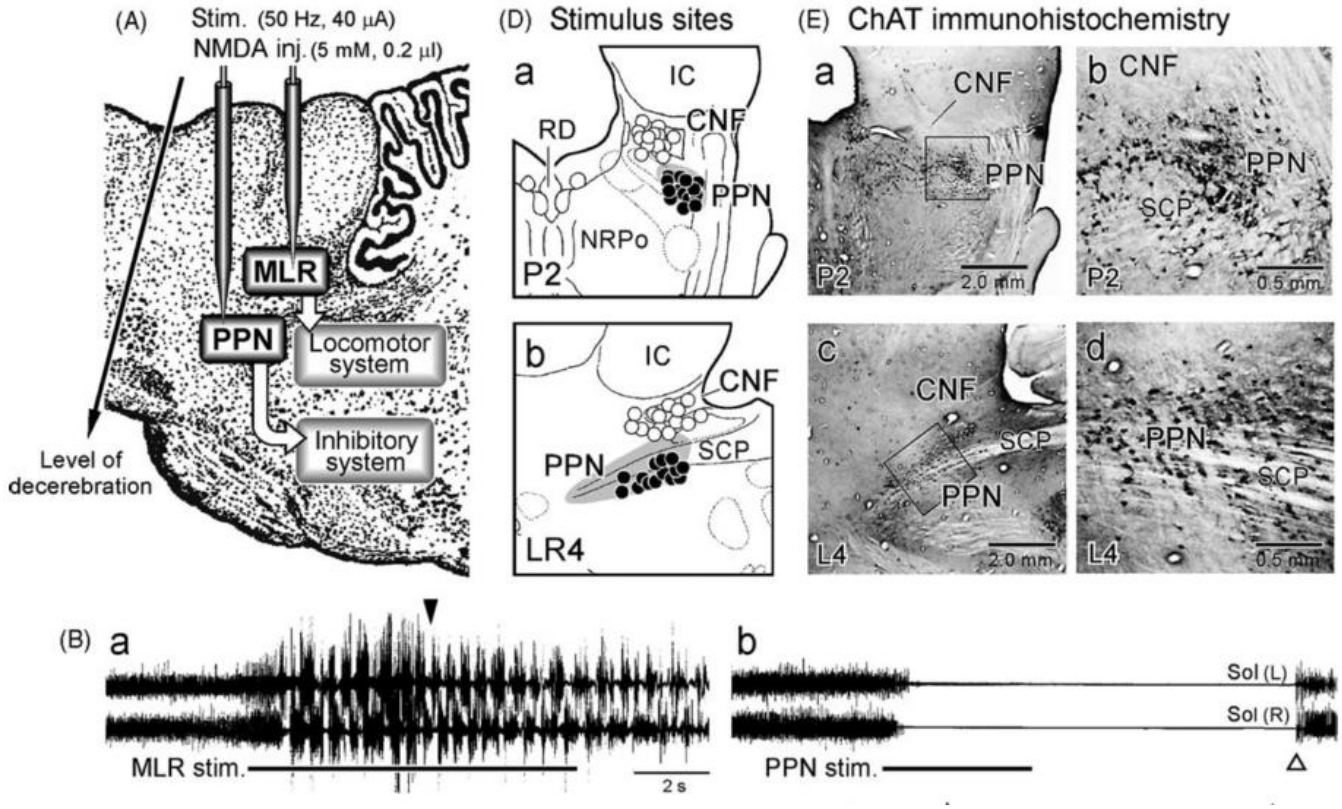

Figure 12: Mesopontine stimulation in the acutely decerebrated cats.

A: Experimental diagram. Either electrical or chemical stimulation were used. **B:** Effects on muscle activities following stimulation of the CnF (a) and the PPN (b). Each trace was obtained from Soleus muscles. An arrowhead indicates the onset of the treadmill. An open triangle indicates stimulation applied by pinching the scapha. **D**: Effective sites on coronal (a) and parasagittal (b) planes for evoking muscular atonia (filled circles) and locomotion (open circles). Shaded area in both planes indicates the PPN. **E**: Distribution of cholinergic neurons stained by choline acetyltransferase (ChAT) immunohistochemistry. Light microscopic photographs of coronal (a and b) and parasagittal (c and d) planes. Lower (a and c) and higher (b and d) magnification are shown in the right and left columns, respectively. Abbreviations: IC, inferior colliculus; CNF, cuneiform nucleus; SCP, superior cerebellar peduncle; PPN, pedunculopontine tegmental nucleus; NRPo, nucleus reticularis pontis oralis; RD, raphe dorsalis (Takakusaki et al., 2004a).

1.4.4 The Pedunculopontine nucleus (PPN)

1.4.4.1 Anatomy and connectivity

Like the cuneiform nucleus, the pedunculopontine nucleus is mainly composed by GABAergic and glutamatergic neurons. The difference comes from the large cholinergic population residing in this nucleus (Wang and Morales, 2009). It is located in the upper brainstem just below the CnF and its boundaries are not clear. The main consensus is that the PPN's location is defined by its cholinergic population. The distribution of neuronal subtypes inside the PPN is represented in Figure 13. To summarize, GABAergic neurons are largely localized rostrally in the pars dissipata when glutamatergic neurons reside caudally in the pars compacta (Mena-Segovia et al., 2009; Martinez-Gonzalez et al., 2011, 2012). Interestingly, cholinergic and non-cholinergic neurons seem to share the same targets (Mena-segovia et al., 2008; Martinez-Gonzalez et al., 2014), the PPN's connectivity is summarized in Figure 14. The rostral PPN is interconnected mainly to the basal ganglia (Jackson and Crossman, 1981; Semba and Fibiger, 1992; Morita et al., 2014) but also with the SLR (Ménard and Grillner, 2008) while the caudal PPN receives input from the motor cortex (Monakow et al., 1979; Aravamuthan et al., 2007) and all neuronal phenotypes project to the reticular formation (Nakamura et al., 1990) when only non-cholinergic neurons scarcely project to the spinal cord (Skinner et al., 1990). The PPN therefore clearly seems to be a relay between cognitive locomotor areas of the brain and reticular formation and other downstream locomotor centers but its subdivisions are not recognized by all, generating literature on its physiology that is not as straightforward as its connectivity.

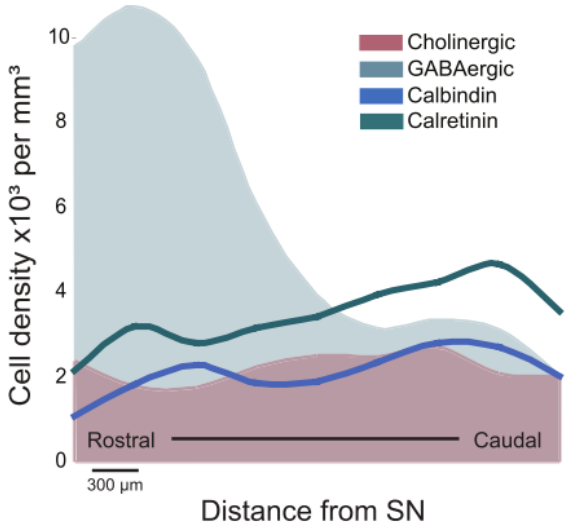

Figure 13: Schematic representation of the neuronal populations in the PPN.

GABAergic neurons are highly concentrated in the rostral PPN, whereas cholinergic, glutamatergic (not shown), calbindin- and calretinin-expressing neurons are more abundant in the caudal PPN. The difference in the rostro-caudal distribution of GABAergic neurons correlates with the differences in cytoarchitecture of the cholinergic neurons traditionally used to identify PPN regions (i.e., pars dissipata and pars compacta). SN, substantia nigra (Martinez-Gonzalez et al., 2012).

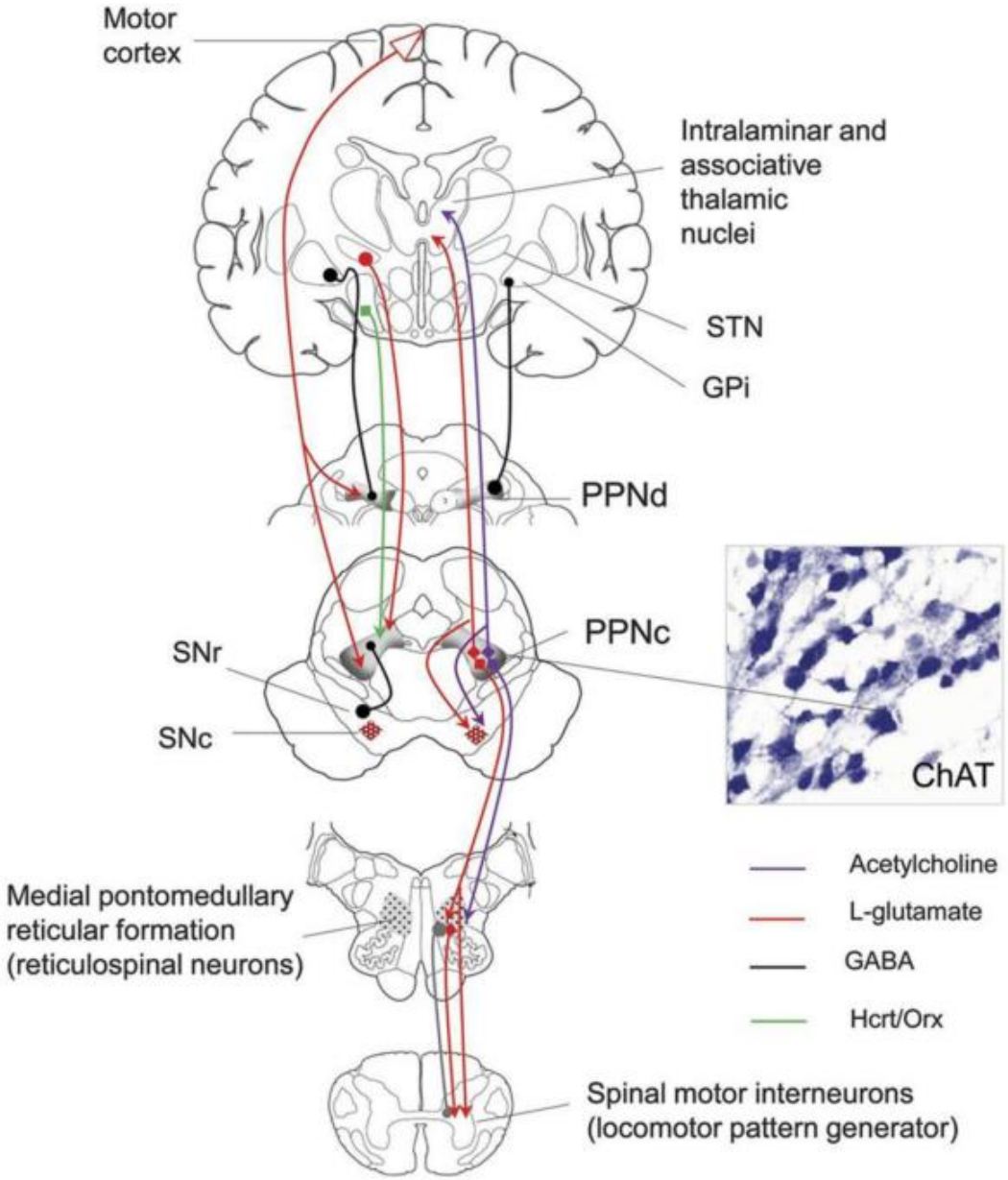

Figure 14: the pedunculopontine nucleus' anatomical connectivity.

SNr, substantia nigra; SNc, substantia nigra pars compacta; STN, subthalamic nucleus; GPi, globus pallidus internal segment; PPNc, pedunculopontine nucleus pars compacta; PPNd, pedunculopontine nucleus pars dissipatus; ChAT, choline acetyltransferase. Blue lines: cholinergic, red lines: glutamatergic, black lines: GABAergic and green lines: orexinergic transmission (Morita et al., 2014)

1.4.4.2 Physiology in health and disease

In monkeys, PPN neurons seem to discharge when the animal is walking (Goetz et al., 2016) and neuronal activity is increased by locomotor activity in the dorsal PPN (Jordan, 1998). However, specific lesions of the PPN in rats do not affect the motor behavior (Keating and Winn, 2002; Winn, 2006) but they do impair the ability to learn food reward tasks (Wilson et al., 2009).

Although experiments by Kaoru Takakusaki and his team, summarized in Figure 12, indicate a clear decrease in muscle tone upon stimulation of the PPN (Takakusaki et al., 2003, 2004a, 2016), they contradict results obtained by Edgar Garcia-Rill and his team (Garcia-Rill et al., 1987; Garcia-Rill and Skinner, 1988, Figure 15) that showed an increase in postural tone, initiation of locomotion and increase in speed when stimulating the PPN. Those results led to the idea that cholinergic neurons of the PPN could be part of the MLR. However, systemic and PPN-specific cholinergic inhibition did not result in any alteration of the MLR induction of locomotion in rats (Jordan et al., 2014; MacLaren et al., 2016). As of now, probably because the boundaries of the PPN are blurry, the available data suggest a functional diversity for the PPN in locomotor control (Ryczko and Dubuc, 2013).

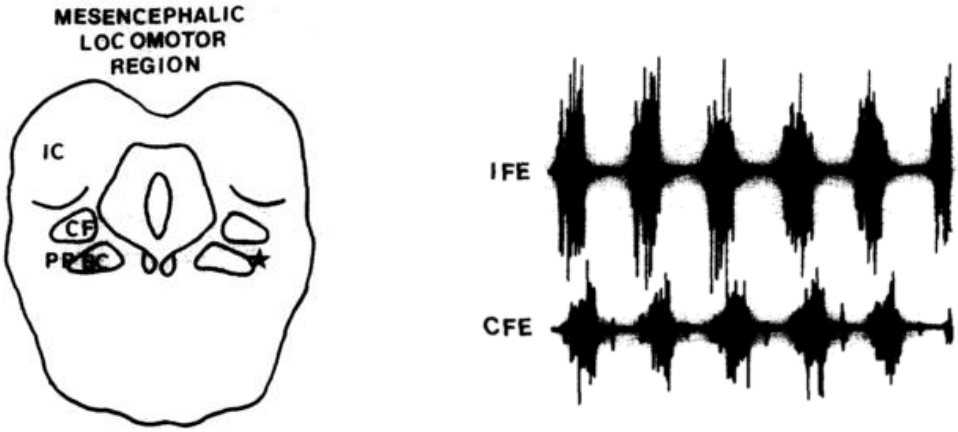

Figure 15: Locomotion initiating site in the vicinity of the cholinergic PPN.

IC: inferior colliculus, CF: cuneiform nucleus, PPT; pedunculopontine nucleus, IFE & CFE: Ipsilateral and Contralateral flexor muscle activity (Garcia-Rill et al., 1987).

Adding to the complexity, the PPN also bears many roles through its ascending projections that seem to have little to do with locomotor control. Rapid eye movement, or REM, sleep is induced by electrical stimulation of the PPN in humans and cats (Takakusaki et al., 2004b; Arnulf et al., 2010). It is also induced by optogenetic activation of the cholinergic neurons of the PPN in rats (Dort et al., 2015). Quite interestingly, REM sleep is characterized by a lowering of the muscle tone throughout the body linking back the PPN to motor control. The PPN could also take a part in the regulation of skeletal muscle activity through melanocortin sympathetic pathways (He et al., 2017). Decision making and reward-associated tasks also activate the PPN (Wilson et al., 2009; Thompson and Felsen, 2013; Gut and Winn, 2016; Xiao et al., 2016). The PPN, therefore, is a multifunctional nucleus with many roles. Its main role might be to integrate all of these inputs and turn them into planned action (Tattersall et al., 2014).

Turning to pathologies, the PPN has been at the center of attention in recent years by reason of its implication in Parkinson's disease. Indeed, a cholinergic loss in the PPN was correlated with an increase in falling and freezing of gait episodes in rats, monkeys and humans (Rinne et al., 2008; Karachi et al., 2010; Xiao et al., 2017). Despite promising results (Mazzone et al., 2009; Thevathasan et al., 2012; de Oliveira Souza et al., 2016), deep brain stimulation of the pedunculopontine nucleus had mixed results in parkinsonian patients (Stefani et al., 2007; Ferraye et al., 2010). The multifunctional nucleus described in previous paragraphs understandably has mixed effect when stimulated in patients. Functional and topographical studies in animal models will be crucial to target the neurons that will most efficiently target parkinsonian symptomatology. The case has also been made that since the PPN is deficient in epileptic patients (Nolte et al., 2006; Cho et al., 2016) and since REM sleep has antiepileptic effects (Jaseja, 2004), the PPN could be an interesting potential DBS target for the treatment of epilepsy (Jaseja, 2014).

To conclude, the pedunculopontine nucleus, the main cholinergic center in the brain, is at a crossroad between many pathways controlling many functions of the brain. Although it might come in the near future, a unifying theory for its complex role in decision making, sleep and locomotor control is still lacking.

1.4.5 Other presumptive nuclei of the MLR

Despite their imperfections, anatomical reconstruction of locomotion initiating sites in the mouse MLR, as shown in Figure 16C, indicate that some nuclei located around the cuneiform and pedunculopontine nuclei can indeed initiate locomotion. Although the CnF and PPN are the main proposed MLR-constituting nuclei, some neighboring regions were found in the scientific literature to be good candidates. They will be reviewed in the following paragraphs.

1.4.5.1 The median MLR

First off, it must be stated that this region is not clearly identified and widely accepted as is. It is situated ventromedial to the cuneiform, outside of the periaqueductal gray matter and above the superior cerebellar peduncle. From left to right in Figure 16, it either has been named medial MLR (Garcia-Rill et al., 1983; Armstrong, 1986), has no name in the Paxinos brain atlas (Paxinos and Watson, 2006), corresponds to the caudal tip of the midbrain reticular nucleus (Allen Mouse Brain Atlas, 2004; Roseberry et al., 2016) or has been called dorsal MLR by (Sherman et al., 2015).

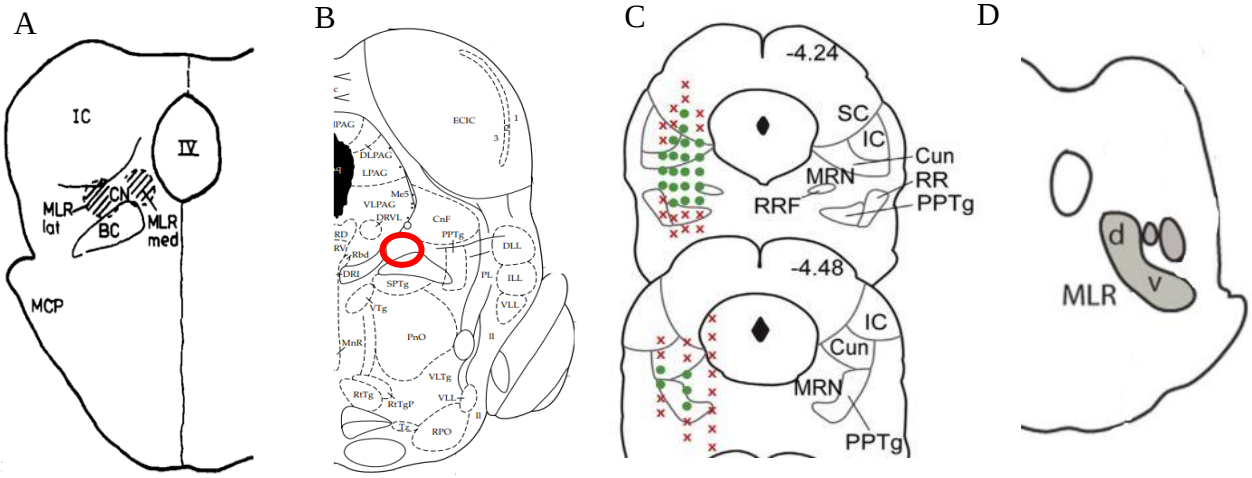

Figure 16: Location of the median MLR.

A: Lateral and medial MLR location in the cat brainstem (Armstrong, 1986). **B**: The red circle indicates the void where the median MLR should be in the paxinos rat brain atlas. **C**: Sites evoking locomotion with electrical stimulation (Roseberry et al., 2016). **D**: Location of the dorsal MLR (Sherman et al., 2015).

The medial MLR seems to project directly to the spinal cord (Liang et al., 2011; Sherman et al., 2015) and some of its neurons express c-Fos, a marker of neuronal activity,

after treadmill exercise (Jordan, 1998). Its ability to initiate locomotion and cooling experiments showed that this effect was mediated by the pontomedullary locomotor strip (Shefchyk et al., 1984). However, data concerning this region are scarce and thorough study of its stimulation in awake and behaving animals would be necessary to be able to draw any conclusion concerning its inclusion in the MLR.

1.4.5.2 The laterodorsal tegmentum

Neurons immunoreactive to ChAT were classified in the brain. The Ch5 group is located in the PPN when the Ch6 is located in the laterodorsal tegmentum, or LDT (Mesulam, 2013). Figure 17 shows that these two regions are in continuity, with the PPN being rostral to the LDTg.

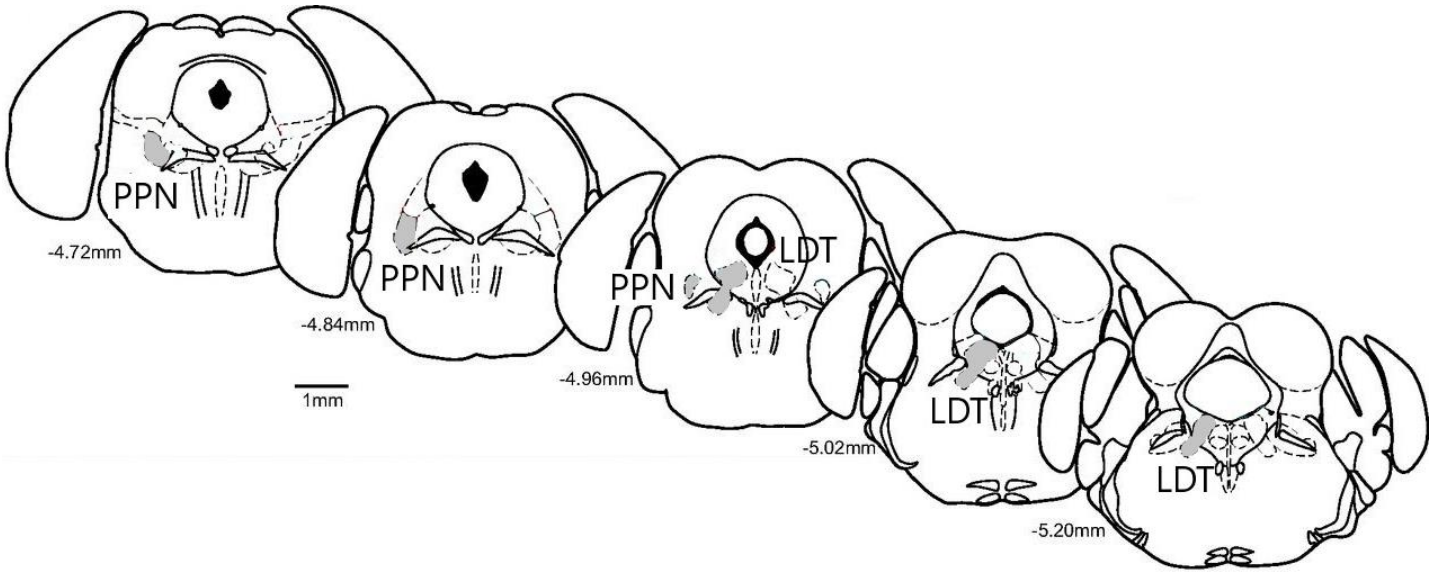

Figure 17: Anatomical location of the PPN and LDT in the mouse brain.

PPN and LDT are the regions in grey in coronal sections modified from the mouse brain atlas (Van Dort et al., 2015).

In lampreys, a denser group of cholinergic cells has been proposed to be the equivalent of the LDT (Le Ray et al., 2003) and stimulation of the cholinergic cells in this region induced locomotion. In lampreys but also in mammals, the LDT projects to reticular

formation (Woolf and Butcher, 1986; Shiromani et al., 1988; Lai et al., 1999). The presence of a predator increased c-Fos activity in the entire periaqueductal gray matter including the LDT (Comoli et al., 2003) leading to the idea that, like the PAG, the LDT could be involved in escaping behaviors. However, when ascending projections were tested, the LDT seemed to have opposite effects when stimulating its ventral tegmental area terminals (Dobbs and Mark, 2012; Xiao et al., 2016). Stimulation and recording data is still lacking in mammals in the context of locomotor initiation and would be crucial to understanding LDT's role in locomotion.

Many regions in the past and present literature have been claimed to be part of the mesencephalic locomotor region. However, only anatomical characterization and functional reproducibility will help us know the exact role of each of these nuclei. Despite the many inconsistencies and doubts on the location of the MLR and its constituents, studies have started looking at its possible use as a therapeutic target of neural stimulation in motor pathologies. In Parkinson's disease, the outcomes were disappointing (Wang et al., 2017) and with a clinical trial stimulating the MLR after a spinal cord injury currently on the way (ClinicalTrials.gov NCT03053791), the need for better understanding of the MLR is more than ever urgent.

1.5 Questions that remain and goal of the thesis

Although there are of course an infinite number of questions that can be asked on any given subject, we will try to narrow our focus onto those that seem the most pertinent and that could presumably be resolved with the techniques available today. For each chapter, the goals will then be stated.

1.5.1 Gaits

Many studies that use rodents to quantify locomotor parameters rely on the broad term of gait to present their results. However, studying locomotor gaits is a gateway to studying the entire spinal networks regulating them and, for now, it has only been extremely rarely done. While locomotor gaits have been characterized in many species (Hildebrand, 1976; Abourachid, 2003), a unified framework adopted by all to classify gaits

is still lacking. In addition, although a lot has been discovered on the role of propriospinal neurons in generating and maintaining locomotor gaits, their identity and precise organization is still a mystery.

The goal of this thesis will be to describe and study the entire range of locomotor gaits in mice. In doing so, we will set a new framework to study and classify locomotor gaits and their transitions in quadrupeds.

1.5.2 MLR

A great deal of uncertainty surrounds the MLR. It is, firstly, an anatomical one. Although many studies point towards the cuneiform and dorsal pedunculopontine nuclei as being the anatomical substrate for the MLR, it is still a disputed fact. Second, the neurotransmitter responsible for initiation of locomotion seems to be glutamate (Roseberry et al., 2016) : yet, a lot of work remains to be done to determine the role of the cholinergic neurons of the PPN and LDT in initiating and maintaining locomotion. Thirdly, projections of the CnF and PPN are multidirectional and projecting neurons to diverse targets are intermingled. A role for each subtype of neuron classified by its projections is still an enigma. Lastly, and more broadly, the MLR needs to be placed into the locomotor circuitry in a way that fits its many diverse roles in locomotion.

The goal of this thesis will be to understand the distinct contributions of the glutamatergic neurons of the cuneiform and pedunculopontine nuclei in freely behaving mice and quantify their role in the initiation of locomotion, muscle activity and locomotor gait transition.

Chapter 2: Speed-Dependent Modulation of the Locomotor Behavior in Adult Mice Reveals Attractor and Transitional Gaits

Speed-Dependent Modulation of the Locomotor Behavior in Adult Mice Reveals Attractor and Transitional Gaits

Nicolas Josset[1†], Maxime Lemieux[1†], Marie Roussel[1], Sébastien Couraud[1] and Frédéric Bretzner[1,2*]

1. Centre de Recherche du CHU de Québec, CHUL-Neurosciences, Québec, QC, Canada,

2. Department of Psychiatry and Neurosciences, Faculty of Medicine, Université Laval, Québec, QC, Canada.

[†] These authors contributed equally to this work

2.1 Résumé

La locomotion est le résultat d'une interaction entre les contraintes biomécaniques des muscles attachés au squelette et les circuits neuronaux contrôlant et coordonnant les activités musculaires. Les quadrupèdes présentent une large gamme d'allures locomotrices. Compte tenu des progrès effectués dans l'identification génétique des circuits spinaux et supraspinaux ayant un rôle dans la locomotion chez la souris, il est maintenant important de mieux comprendre le répertoire complet des allures chez la souris qui marche librement. Pour évaluer les allures de marche chez les souris C57BL / 6J, de jeunes adultes ont été entraînées à marcher et à courir sur un tapis roulant à différentes vitesses. Au lieu d'utiliser le paradigme classique définissant les allures en fonction de leur séquence de pas sur le sol, nous avons combiné le couplage inter-membres et le duty cycle de la phase d'appui, identifiant ainsi plusieurs types d'allures : la marche latérale, le trot, la marche hors phase, le galop rotatoire, le galop transverse, le saut, le demi-bond et le bond. La marche hors phase, le trot et le bond étaient exprimés de manière robuste et semble être des allures attractrices (c'est-à-dire un état vers lequel le réseau va se diriger et se stabiliser) à des vitesses basse, intermédiaire et élevée respectivement. En revanche, la marche latérale, le saut, le galop transverse, le galop rotatoire et le demi bond étaient plus transitoires et donc considérés comme des allures de transition (c'est-à-dire un état labile du réseau d'où il va circule vers une allure attractrice). Étonnamment, la marche latérale a été moins fréquemment observée. En utilisant l'analyse graphique, nous avons démontré que les transitions entre les allures étaient prévisibles et non aléatoires. En résumé, la souris de type sauvage présente un répertoire plus large d'allures locomotrices que prévu. Les études locomotrices futures devraient bénéficier de ce paradigme pour évaluer les souris transgéniques ou les souris de sauvage présentant une lésion neurotraumatique ou une maladie neurodégénérative affectant la démarche.

2.2 Abstract

Locomotion results from an interplay between biomechanical constraints of the muscles attached to the skeleton and the neuronal circuits controlling and coordinating muscle activities. Quadrupeds exhibit a wide range of locomotor gaits. Given our advances in the genetic identification of spinal and supraspinal circuits important to locomotion in the mouse, it is now important to get a better understanding of the full repertoire of gaits in the freely walking mouse. To assess this range, young adult C57BL/6J mice were trained to walk and run on a treadmill at different locomotor speeds. Instead of using the classical paradigm defining gaits according to their footfall pattern, we combined the inter-limb coupling and the duty cycle of the stance phase, thus identifying several types of gaits: lateral walk, trot, out-of-phase walk, rotary gallop, transverse gallop, hop, half-bound, and full-bound. Out-of-phase walk, trot, and full-bound were robust and appeared to function as attractor gaits (i.e., a state to which the network flows and stabilizes) at low, intermediate, and high speeds respectively. In contrast, lateral walk, hop, transverse gallop, rotary gallop, and half-bound were more transient and therefore considered transitional gaits (i.e., a labile state of the network from which it flows to the attractor state). Surprisingly, lateral walk was less frequently observed. Using graph analysis, we demonstrated that transitions between gaits were predictable, not random. In summary, the wild-type mouse exhibits a wider repertoire of locomotor gaits than expected. Future locomotor studies should benefit from this paradigm in assessing transgenic mice or wild-type mice with neurotraumatic injury or neurodegenerative disease affecting gait.

2.3 Introduction

Locomotion results from an interplay between biomechanical constraints of the muscles attached to the axial and appendicular skeleton and the neuronal circuit that controls these muscles. Over the last decade, advances in mouse genetics have allowed us to identify the spinal interneuronal circuits controlling muscles underlying motor and locomotor functions. Neonatal in vitro and adult in vivo locomotor studies using genetic manipulations (e.g., signaling cues involved in neural circuit formation or ablations of genetically identified neuronal populations) have revealed important information about the neural control of locomotion, especially the left-right alternation of the hindlimbs (Kullander et al., 2001a, 2001b; Kullander, 2003; Lanuza et al., 2004; Zhang et al., 2008; Crone et al., 2008; Rabe et al., 2009; Andersson et al., 2012; Rabe Bernhardt et al., 2012; Talpalar et al., 2013; Borgius et al., 2014). However, less is known about the forelimbs and even less about locomotor gaits. Historically, locomotor gaits were identified as symmetrical vs. asymmetrical according to their footfall pattern (Hildebrand, 1976). A gait was defined as symmetrical when it could be described by only half the step cycle, the other half being symmetrical to the first half. Conversely, asymmetrical gaits could not be described by half the cycle. Using this paradigm, it has been shown that most quadrupeds, such as monkeys, horses, dogs, cats, and rats, display a large repertoire of locomotor gaits from walk, to pace, to trot, to gallop (Cohen and Gans, 1975; Grillner, 1975; Miller et al., 1975a; Hildebrand, 1976; Dunbar, 2004; Abourachid et al., 2007; Maes and Abourachid, 2013). The full range of the locomotor repertoire of the mouse has not yet been established. Nevertheless, these different gaits, displaying distinct locomotor rhythms and patterns, are likely generated by the same neuronal circuit across the vertebrate phylogeny (Orlovsky et al., 1999). Previously, in vivo locomotor studies have shown that if some mutant mice can synchronize their hindlimb (i.e., hop, gallop, or bound) at various speeds, their wild-type littermates systematically alternate their hindlimb (i.e., walk or trot) at locomotor speeds up to 8Hz and above (Talpalar et al., 2013; Borgius et al., 2014). Although gallop and bound occur in wild- type mice during brief acceleration phases on a treadmill (Herbin et al., 2004, 2006, 2007), on a catwalk (Bellardita and Kiehn, 2015), and on a catwalk following noxious stimulations (Serradj and Jamon, 2009), these gaits only occur over a few strides, thus raising some concerns as to whether mice can sustain galloping and bounding. Since

most quadruped mammals can sustain galloping at high speed, we therefore hypothesized that wild-type mice should be able to maintain galloping and bounding at high speed. Our experimental approach has been to assess locomotor gaits in young adult C57BL/6Jmice during treadmill locomotion over a wide range of speeds. The advantage of treadmill locomotion over catwalk over-ground locomotion is that by controlling the speed it allows one to analyze slight accelerations or decelerations of the mouse while walking or running at a steady speed. To identify and objectively characterize locomotor gaits, we combined the inter-limb coupling and the duty cycle of the stance phase of individual steps according to the treadmill speed. Assuming that locomotion is a dynamic process, we hypothesized that certain locomotor gaits, by their occurrence, their robustness, and their stability, should emerge as preferential gaits (i.e., attractor gaits), while others would occur as transitional gaits (e.g., during transitions from walking to running or during initiation of locomotion). Here we show that wild-type mice can sustain gallops and bounds at high running speed. Moreover, we identified attractor gaits occurring over a wide range of speeds and transitional gaits over a narrower range of speeds. Using graph analysis, a mathematical approach to describing the elements and interactions within a complex network (Strogatz, 2001; Bullmore and Sporns, 2009), we demonstrated that transitions between gaits are not random, but predictable. Using this new paradigm to better identify and characterize locomotor gaits, our study should help future locomotor studies of transgenic mice or wild-type mice impaired by neurotraumatic injury or neurodegenerative disease.

2.4 Material and methods

Six adult C57BL/6J mice (>3 weeks old) of either sex were used in this study. All procedures were performed according to the guidelines of the Canadian Council on Animal Care and were approved by the local committee of Université Laval (CPAUL and CPAC).

Kinematic Recording

Mice were trained to walk on a commercially available single-lane mouse treadmill (LE 8700 Series, Panlab). The inner dimensions of the lane were 32 × 5 cm. Speed could be adjusted from 5 to 150 cm/s. The electrified grid at the rear of the lane was set at the minimal intensity (0.1mA) to motivate locomotion of mice on the belt. First, mice were allowed to acclimate quietly on the lane for 20–30min. They were then introduced to walk at 10– 15 cm/s for 5min. At that stage, the mice kept walking on the treadmill belt to avoid the electrified grid. Among the group of nine mice used during the training phase, six learned to avoid the electrified grid. The three remaining mice were excluded from the study. Mice were walked at increasing speed. Once they reached 100 cm/s, they were tested 3 times at each speed to obtain at least 10 contiguous strides (bouts of 10–60 s depending on the speed). All mice were filmed on the left and right sides by high-frequency (200 frames/s) cameras (Genie HM640, Dalsa Teledyne) during treadmill locomotion. To study inter-limb coordination over a wide range of locomotor speeds, mice were tested at treadmill belt speeds of 5, 10, 15, 30, 45, 60, 75, 90, 105, 120, 135, and 150 cm/s. To investigate the limb trajectory, mice walked at low (15 cm/s), intermediate (45 cm/s), and high speeds (90 cm/s) with reflective markers. Under isoflurane anesthesia (2–3%), limbs were shaved and reflective markers (2mm diameter) were glued on the iliac crest, hip, knee, ankle, and metatarsophalangeal (MTP) joints and toe for the hindlimb, and on the scapula, shoulder, elbow, and metacarpophalangeal joints and toe for the forelimb. Films were digitized with StreamPix 6.0 (Norpix) and analyzed offline.

Kinematic Analysis

For our kinematic studies, videos were analyzed by using custom- designed software (graciously provided by Drs. S. Rossignol and T. Drew, Université de Montréal) during steady-state treadmill locomotion, thus avoiding the acceleration and deceleration

phases observed with a catwalk setup. The timing of foot lifts and contacts for all four limbs, as well as the two-dimensional spatial coordinates of joints, were manually extracted at a resolution of 5ms (200 samples/s). Temporal and spatial data were exported and processed with custom-written routines in Matlab (MathWorks). We first evaluated basic locomotor parameters. The step cycle was defined by two successive foot contacts from the reference limb (here, the left hindlimb) to determine the instantaneous step frequency. The step cycle was divided in two phases: the stance phase initiated when the foot of a limb made contact with the ground, thus supporting a part of the body weight, and terminated when the foot was lifted at the onset of the swing phase. The duty cycle of the stance phase was computed as the stance duration divided by the cycle duration and expressed as a percentage. The phase value corresponded to the time of foot contact (HL coupling in Figure 19, out-of-phase walk gait diagram) relative to the reference limb step cycle. Phase values range from 0 to 1. Phase values of 0 or 1 indicate a perfect in-phase coupling (i.e., synchrony), while a phase value of 0.5 indicates a perfect anti-phase coupling (i.e., strict alternation). Based on previous studies comparing several quadruped species (Hildebrand, 1968, 1977b; Heglund and Taylor, 1988; Abourachid et al., 2007) or focusing on dogs (Maes and Abourachid, 2013) or mice (Herbin et al., 2004), we identified and classified eight gaits: lateral walk, trot, rotary gallop, transverse gallop, half-bound, full-bound, hop, and out-of-phase walk (see procedure in Figure 18). This last gait has not been previously described. To assign a step cycle in a particular gait, we used as criteria the phase values of homologous limbs and ipsilateral limbs and the duty cycle of the hindlimb stance (Table 1). Once all step cycles were identified, we computed the mean phase and vector length (r) of hind-, fore-, ipsi-, and diagonal couplings of each gait. Coupling was identified as in-phase (phase = 0 ± 0.125), anti-phase (0.5 ± 0.125) or out-of-phase (low coupling: 0.125–0.375, high coupling: 0.625–0.875). We chose ± 0.125 (or 45°) to equally distribute coupling values among quadrants. For the intra-limb coordination, we analyzed the spatial and temporal data of reflective markers placed on fore- and hindlimb joints of 6mice at 3 treadmill speeds (15, 45, and 90 cm/s). We calculated the stride length and height of fore- and hindfoot, as well as the maximal speed and acceleration of the limb trajectory. The product of the speed of the treadmill belt and the duration of the swing phase were added to the apparent stride length to get the real stride length.

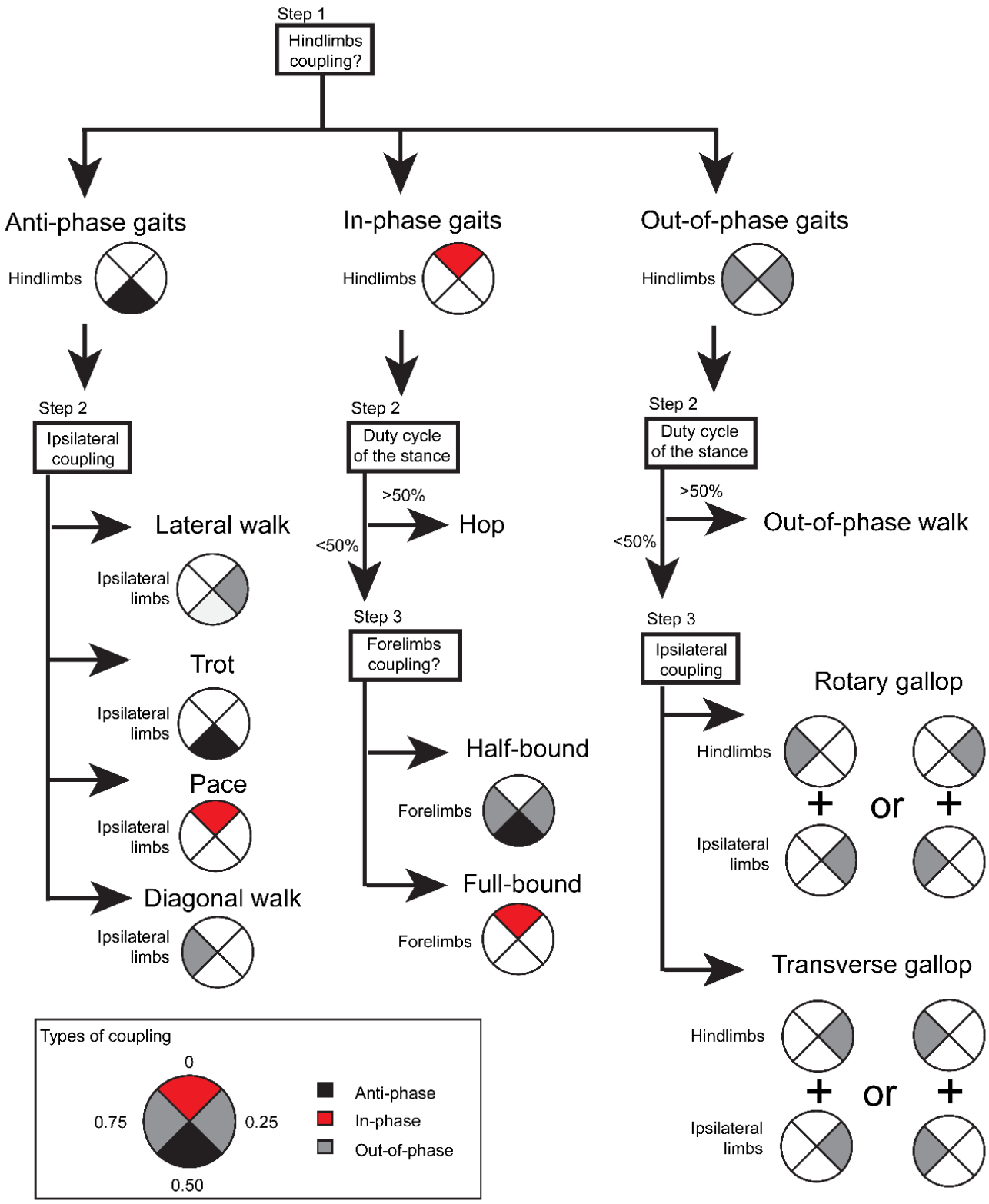

Figure 18: Gait identification.

The procedure depicts the architecture of the automated routine identifying the gait. Step 1 is based on the hindlimbs coupling (left side as reference). Gait may be anti-phase (black), in-phase (red), or out-of-phase (gray). If the step cycle corresponded to a hindlimb anti-phase gait, step 2 used the ipsilateral limbs coupling (hindlimb as reference) to identify the gait: lateral walk (low out-of-phase coupling), trot (anti-phase), pace (in-phase), or diagonal walk (high out-of-phase coupling). If the step cycle corresponded to a hindlimbs anti-phase or in-phase coupling, step 2 differentiated walking (duty cycle of the stance <50%) from running gaits (duty cycle of the stance >50%). For running gaits, a third step was required to differentiate half-bound from full-bound and rotary gallop from transverse gallop. The box presents the definition for the types of coupling

TABLE 1 | Basic locomotor parameters for each gait.

	OPW-lo OPW-hi	Hop-lo Hop-hi	LW	T	RG TG	HB FB
Step frequency (Hz)	1.6 ± 0.8 8.2 ± 1.0	1.8 ± 1.4 10.1 ± 2.5	2.6 ± 0.8	4.8 ± 2.0	8.5 ± 1.1 9.3 ± 1.6	9.6 ± 1.2 10.1 ± 1.5
Stance duration (ms)	664 ± 440 62 ± 21	1040 ± 958 70 ± 12	326 ± 180	176 ± 156	49 ± 11 48 ± 13	40 ± 7 35 ± 6
Swing duration (ms)	128 ± 41 54 ± 10	88 ± 36 43 ± 10	121 ± 58	95 ± 32	71 ± 12 63 ± 10	66 ± 13 66 ± 15
Duty cycle of the stance phase (%)	80.6 ± 10.7 56.2 ± 6.0	86.8 ± 7.5 58.3 ± 6.8	72.3 ± 12.1	60.1 ± 15.6	40.6 ± 5.9 42.7 ± 6.3	38.0 ± 6.7 34.9 ± 6.5

Data are presented as mean ± SD. Gaits: OPW-lo, out-of-phase walk at low step frequency; OPW-hi, out-of-phase walk at high step frequency; Hop-lo, hop at low step frequency; Hop-hi, hop at high step frequency; LW, lateral walk; T, trot; RG, rotary gallop; TG, transverse gallop; HB, half-bound; FB, full-bound.

Graph Analysis

Graph analysis is a technique often applied to the study of complex network (Strogatz, 2001; Mason and Verwoerd, 2007; Bullmore and Sporns, 2009; Ma'ayan, 2009). Networks are represented as nodes (or vertices) connected by links (or edges). Gaits were defined as nodes, and transitions between gaits as edges. Graphs were constructed at each speed. The weight of a transition from one node to another (e.g., from node A to node B) was calculated as the ratio of this path occurrence on all transitions from the node of origin (node A). In the context of our study, we investigated for all speeds: (1) the probability that a gait remains the same from cycle to cycle (stability), (2) the probability that other gaits converge toward a specific gait (attractiveness), and (3) the probability that when a mouse breaks away from a given gait, it tends to move toward another gait (predictability of transition). For all speeds, we calculated the probability of stability of a gait as the ratio of

consecutive step cycles corresponding to the same gait on the total number of step cycles. The attractiveness of a gait corresponded to probability that a step cycle of any other gait changed to this gait. The predictability of transition was computed as the probability of observing a transition from one gait to another. Somewhat similar to the measure of attractiveness, the predictability also included the probability of transition between gaits separated by 2-4 edges (the probability was then calculated as the product of all edges).

Statistics

Circular statistics were used to evaluate the phase values of forelimbs, hindlimbs, homolateral left limbs, and diagonal limbs (opposite left hindlimb and right forelimb) (Drew and Doucet, 1991; Kiehn and Kjkerulff, 1996; Zar, 1996). The significance of step frequencies, stride length, and height was evaluated with Kruskal-Wallis (due to unequal variance of data as evaluated by the Bartlett test) with post-hoc paired comparison with the Tukey's Honestly Significant Difference (HSD) test.

2.5 Results

Locomotor Gaits: A Revised Paradigm

Figure 19A shows typical examples of different gaits in a mouse with left hindlimb, left forelimb, right forelimb, and right hindlimb contacts representing the stance phase, while gaps represent the swing phase. The locomotion of six mice was assessed during steady-state locomotion (at least 10 contiguous steps) at treadmill speeds ranging from 5 to 150 cm/s. Because gaits might change from cycle to cycle, we analyzed the locomotor gait based on individual steps using the phase of the interlimb coupling and the duty cycle of the stance phase. Instead of using a definition based on the symmetry/asymmetry of the footfall of all four limbs across the step cycle (Hildebrand, 1976), we opted to use terms referring directly to the phase of the interlimb coupling. Based on the type of coupling between hindlimbs, forelimbs, and ipsilateral limbs, we identified 8 gaits: 2 gaits with an anti-phase hindlimb coupling, shown in black; 3 gaits with an in-phase hindlimb coupling, shown in red; and 3 gaits with an out-of-phase hindlimb coupling, shown in gray (Figure 19).

Gaits with an Anti-phase Hindlimb Coupling

As shown by the polar plots adjacent to their gait diagrams (Figure 19B–E), anti-phase gaits, such as the lateral walk and the trot, were identified by a robust anti-phase coupling of their left- right hindlimbs and forelimbs. The fore-hindlimb coupling was out-of-phase during lateral walk (phase < 0.5, Supplementary Video 1, the file was added separately), while it was in anti-phase during trot (Figure 19D, Supplementary Video 2, the file was added separately). The two other anti-phase gaits, the pace and the diagonal walk (Hildebrand, 1976; Abourachid et al., 2007), were never observed in C57BL/6Jmice.

Gaits with an In-phase Hindlimb Coupling

These gaits corresponded to half-bound, full-bound, and hop (Grillner, 1975; Hildebrand, 1976). The full-bound was distinguished from the half-bound by a robust in-phase coupling of the left-right forelimbs (Supplementary Videos 3, 4, the files were added separately). The duty cycle of the stance phase was inferior to 50%, which was indicative

of running gaits (Figure 18; see also Figures 4, 8 from Hildebrand, 1976). The hop was observed in 4 out of 6mice and was characterized by a looser in-phase hindlimbs coupling. The couplings of fore-, ipsilateral, or diagonal limbs was quite variable from mouse to mouse, thus identifying it as a distinct gait from half-bound and full-bound but also as a loosely organized gait (Supplementary Video 5, the file was added separately).

Gaits with an Out-of-Phase Hindlimb Coupling

Based on the duty cycle, we were able to identify and characterize two more running gaits, the transverse and the rotary gallop, for which the hindlimb coupling was out-of-phase (Supplementary Video 6, the file was added separately). While the out-of-phase coupling of hindlimbs was more variable in the transverse gallop than in rotary gallop, the anti-phase coupling of forelimbs was more robust. In addition, we also found another gait with an out-of-phase coupling of hindlimbs but with a duty cycle of the stance phase superior to 50% (walking gait). The direction and robustness of coupling between limbs was variable across mice, thus suggesting a less stable coordination of left-right activities at the cervical level and between cervical and lumbar half-centers. To distinguish it from lateral walk, we named this gait “out-of-phase walk” (Supplementary Video 7, the file was added separately).

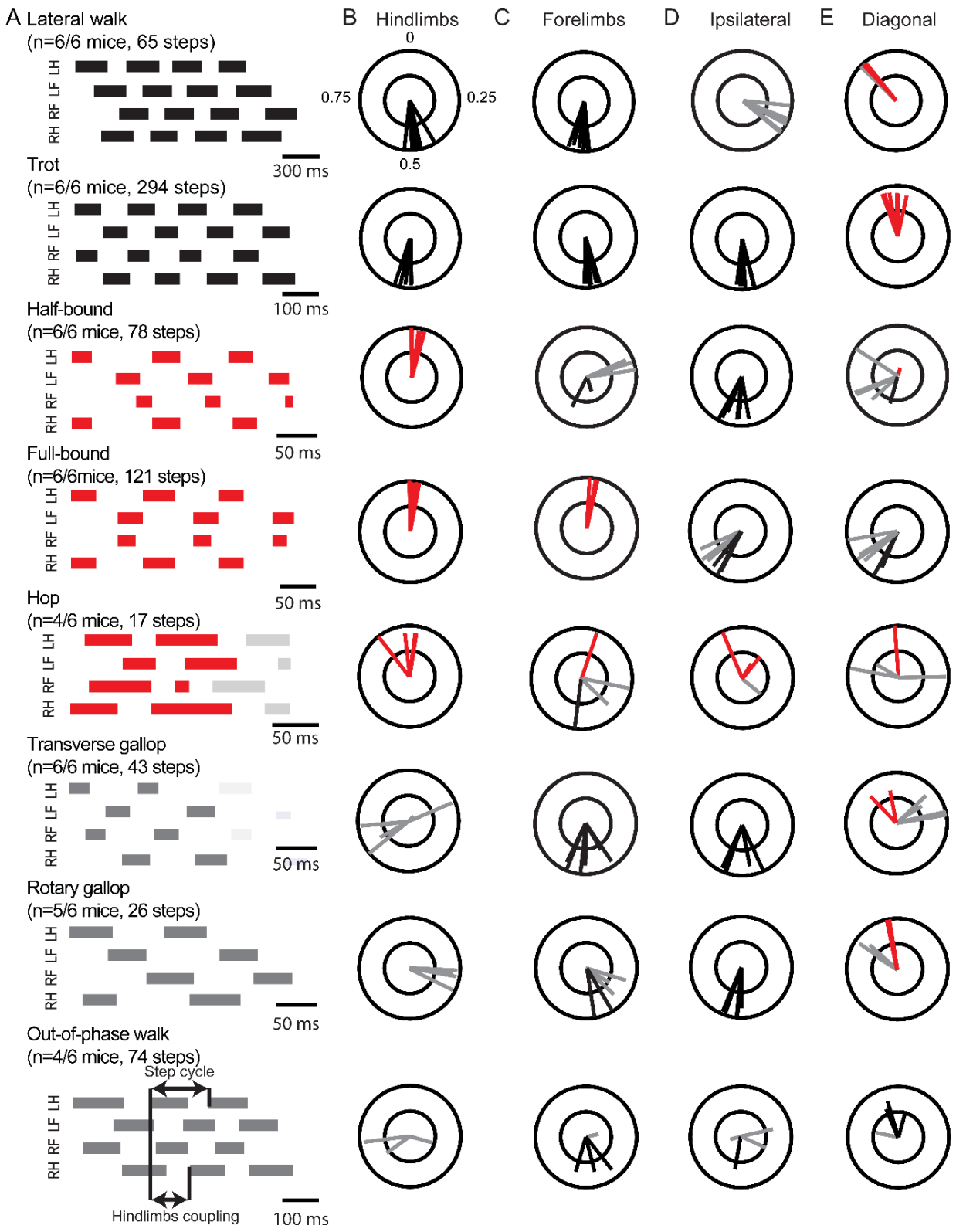

Figure 19: Gait identification and interlimb coordination.

(A) Gait diagrams of locomotor patterns identified in mouse locomotion. Stance phases are represented by thick lines, swing phases correspond to the gaps between them. Gait diagrams and polar plots are color-coded according to the interlimb coupling (anti-phase in black, in-phase in red, and out-of-phase in gray). Limbs are in rows, from top to bottom: the left hindlimb (LH), left forelimb (LF), right forelimb (RF), and right hindlimb (RH). As shown during the out-of-phase walk, phase coupling is the ratio between the lag (i.e., time between a limb contact and its opposite limb contact on the belt) and the step cycle duration. In this case, there is a lag of the right side in relation to the left side. Polar plots in (B–E) show the mean phase coupling of all mice for each gait for (B) the left-right hindlimbs (left hindlimb as reference), (C) the left-right forelimbs (left forelimb as reference), (D) the left forelimb–left hindlimb (ipsilateral, left hindlimb as reference) and (E) right forelimb–left hindlimb (diagonal, left hindlimb as reference). Each vector indicates the mean phase (direction) and robustness (radius) of the coupling. The color of the vector indicates whether the mean coupling is in-phase (red), anti-phase (black), or out-of-phase (gray).

Attractor vs. Transitional Gaits

We next hypothesized that, given their high occurrence, preferential gaits could be considered as attractor gaits and should occur over a wide range of speeds, whereas the others would emerge as transitional gaits, occurring less often and over a narrower range of speeds. All mice could run up to 105 cm/s, and the number of mice running decreased beyond that speed (Figure 20A). As illustrated by the color-coded matrix in Figure 20B, two attractor gaits emerged: trot at walking speed (30 cm/s) and full-bound at running speed (>120 cm/s). The out- of-phase walk was the dominant gait at speeds below 15 cm/s, but never at the extent observed for trot and full-bound. A somewhat similar phenomenon occurred at high speeds with half-bound. Although never dominant over the full-bound, half- bound occurred in similar proportion to full-bound at 90 and 105 cm/s. Mice running at 120–150 cm/s had a clear preference for full-bound. Although we cannot exclude the possibility that full-bound might have been over-represented at the expense of half-bound due to the decreasing number of mice running at and beyond 120 cm/s (Figure 20A), these results suggest that full- bound is a prerequisite to achieving a greater velocity. Overall, these results highlight the existence of two attractor gaits: trot and full-bound.

The other gaits barely exceeded an occurrence of 30% at any speed. Surprisingly, lateral walk was found only at speeds below 30 cm/s and in lower proportion than out-of-phase walk or trot. Hop was the least frequent gait, and was mainly found at the lowest

speeds (5–10 cm/s) and at the transition between walk and run (60–75 cm/s), which could explain its high occurrence in several mutant mice (Kullander, 2003; Beg et al., 2007; Fawcett et al., 2007; Shi et al., 2007; Serradj and Jamon, 2009; Asante et al., 2010). Also less frequent, transverse and rotary gallops occurred between 60 and 105 cm/s. Interestingly, we found that all gaits, except lateral walk, were equally adopted by mice at 75 cm/s, thus suggesting a state of instability in the neuronal networks generating and organizing locomotor gaits at that speed. In summary, our analysis demonstrates the existence of attractor and transitional gaits occurring over a wide or discrete range of speeds, respectively.

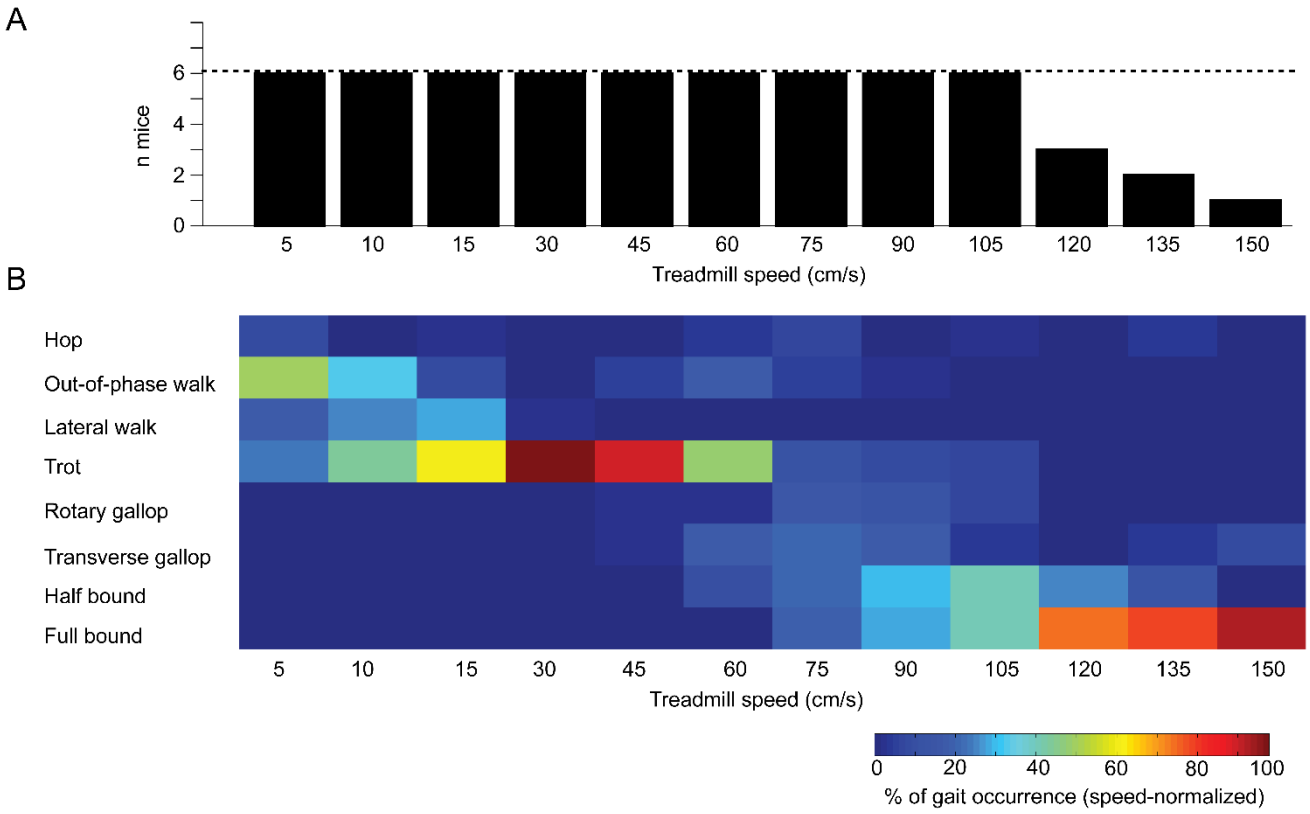

Figure 20: Occurrence of gaits at different treadmill speeds.

(A) Bar graph illustrating the number of mice walking or running for more than 10 consecutive steps at a given speed. Dashed line indicates the number of tested mice (n = 6) (B) Color-coded matrix of the percentage of occurrence of a gait (row) at each speed (column). The sum of a column equals 100%

Outcomes of Locomotor Programs

We next asked whether intra-limb coordination could condition the emergence of one gait over another one. Locomotion is under temporal and spatial constraints conditioned by the step frequency and stride length of individual limbs. Under that premise, we wondered if the selection of one gait over others would provide a beneficial increase of one or more locomotor parameter(s) in the mouse's speed.

Step Frequency

We first analyzed the step frequency of the left hindlimb according to the treadmill speed (Figure 21A) and found that the step frequency increased linearly from 5 cm/s before reaching a plateau (no more significant increase) at 60–75 cm/s ($p < 0.001$, Kruskal-Wallis test and post-hoc Tukey's HSD test). Interestingly, as illustrated in Figure 21B, there were no predominant gaits at 60–75 cm/s, which might reflect a transient state that could preclude the neural locomotor networks from setting a particular locomotor gait. However, half-bound and full-bound emerged as dominant gaits at high treadmill speeds above 75 cm/s (Figure 21), therefore suggesting that other parameters might contribute to overcoming the temporal limitation of the step frequency beyond that speed.

Studying the step frequency as a function of locomotor gaits (Figure 21B and Table 1), we found that hop and out-of-phase walk displayed a clear bimodal distribution at low and high frequency. Although the lateral walk, trot, and half-bound also displayed an apparent bimodal distribution, this was likely due to the discrete sampling of our data (at given treadmill speeds). Therefore, except for hop and out-of-phase walk, all other gaits were treated as unimodal. Lateral walk displayed the narrowest range of step frequencies (1–4Hz, peak at 2.6Hz), while trot covered the widest range of step frequency (1–10Hz with a peak below and above 5Hz). Rotary and transverse gallops were present above 5Hz and were similar in terms of step frequency. Half-bound and full-bound showed the highest mean step frequency. As expected, there was an effect of gait on the step frequency (statistical comparison of distributions from Figure 21B, $p < 0.001$, Kruskal-Wallis test, paired comparison by Tukey HSD test). The step frequency during trot was significantly different from that during other gaits, with the exception of hop at low step frequency. Conversely, the step frequency during half-bound was different from that during walking

gaits (out-of-phase walk and hop at low frequency, lateral walk and trot), but not different from that during half-bound, rotary gallop, and transverse gallop, as well as out-of-phase walk and hop at high frequency. Although trot provided an advantage over slow gaits with a faster step frequency, opting for full-bound over other running gaits could not be explained by an increase in step frequency.

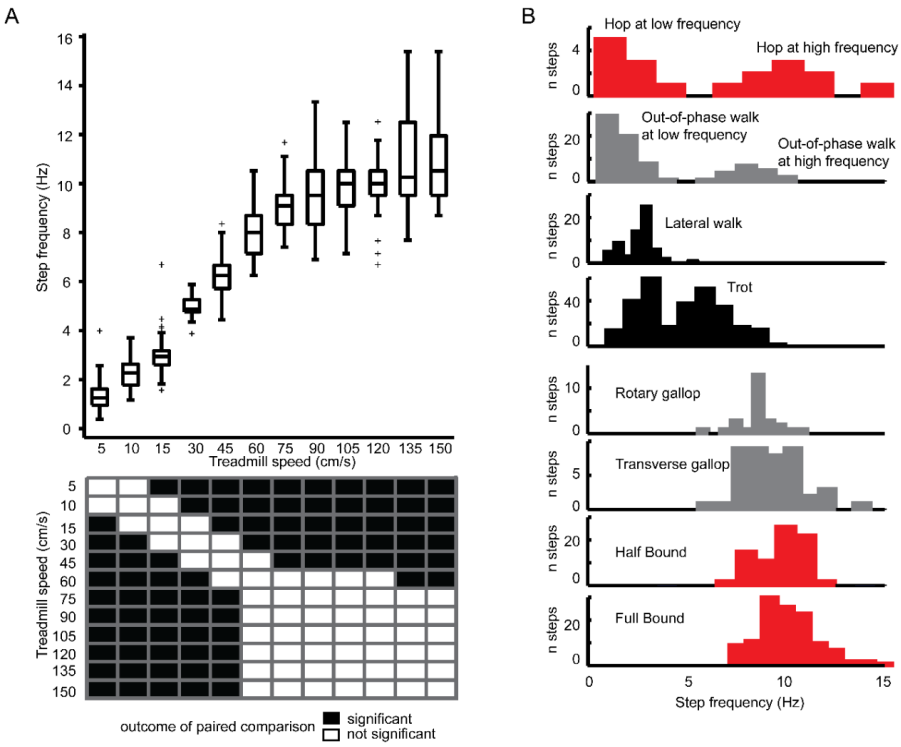

Figure 21: Step frequencies in relation to speed and gait.

(A) Boxplot of step frequencies at different treadmill speeds. The upper and lower limits of the box correspond to the percentiles 75 and 25. The line within the box corresponds to percentile 50 (the median). Whiskers (vertical lines) indicate the maximal and minimal 1.5 interquartile ranges, crosses, and outliers. Outcome of statistical comparison (Kruskal-Wallis and post-hoc Tukey's honest HSD test) is shown in a black and white matrix at the bottom. (B) Color-coded histograms of step frequencies for each gait (anti-phase in black, in-phase in red, and out-of-phase in gray). Note clear bimodality for the hop and the out-of-phase walk.

Limb Trajectory

Figure 22A illustrates typical examples of hindlimb trajectories at three representative treadmill speeds: slow walking (15 cm/s), fast walking (45 cm/s), and running speed (90 cm/s). The maximal length and height of individual hindlimb strides were analyzed according to the gait (Figure 22B). There was an increase in stride length when the mouse switched from lateral or out-of-phase walk to the trot (from less than 4 cm to about 6–7 cm), and another increase when the animal adopted either transverse gallop or rotary gallop. The stride length reached a maximum of 11–12 cm for both half-bound and full-bound.

Because the difference between half-bound and full-bound may lie in the entire trajectory of the limb, we then quantified the maximal stride height for each gait (Figure 22C). The stride height was similar (about 0.6 cm) for the out-of-phase walk, lateral walk, trot, and rotary gallop. Similarly to the stride length, the stride height was significantly higher (twice the height) for both half- bound and full-bound than for any other gaits, but both types of bound still showed similar values. However, there were some differences in the limb trajectory of the forelimb: the stride height but not the stride length was higher during full-bound than half-bound (data not shown). The enhanced stride height of the forelimb during full-bound over half-bound might result from a reduced lateral oscillation of the scapular belt due to forelimb synchronization.

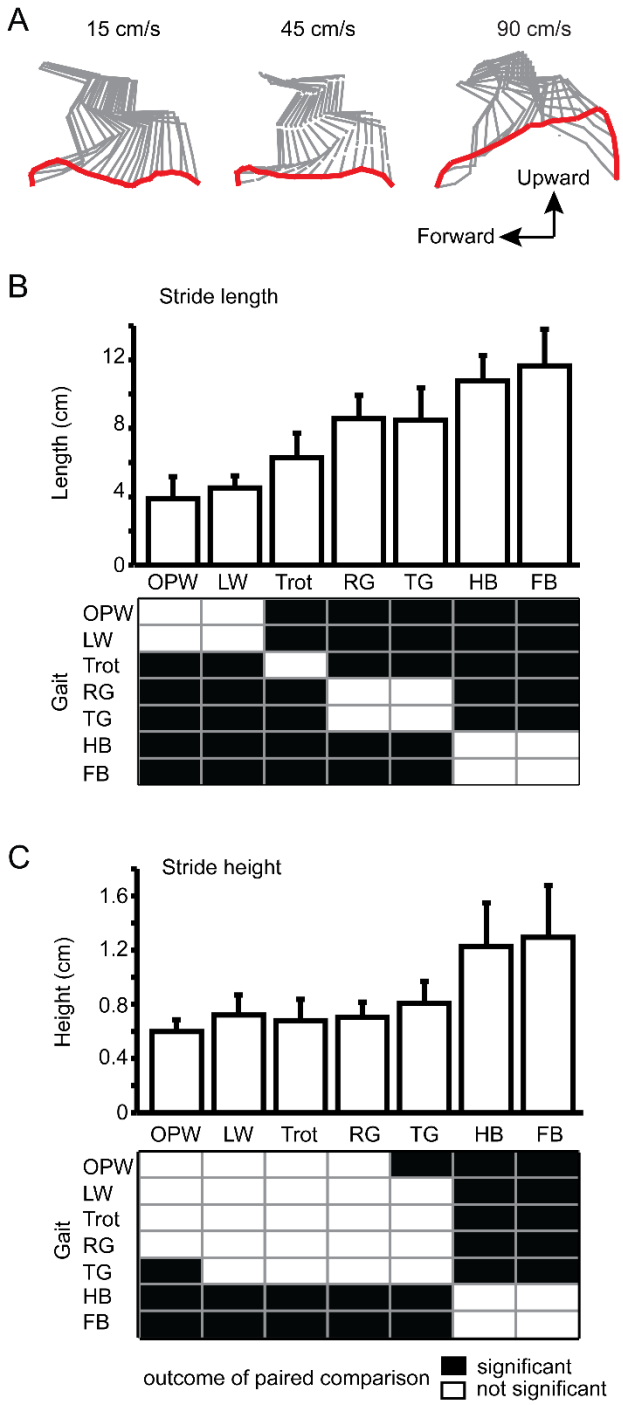

Figure 22: Stride length and height for each gait.

(A) Stick diagrams of the left hindlimb during the swing phase at 15, 45, and 90cm/s. Mean and standard deviation of (B) the stride length and (C) the stride height for each gait. Outcome of statistical comparisons (Kruskal-Wallis and post-hoc Tukey's HSD test) is shown in a black and white matrix at the bottom of each graph. OPW, out-of-phase walk; LW, lateral walk; RG, rotary gallop; TG, transverse gallop; HB, half-bound; FB, full-bound.

Seeking Postural Stability: Distribution of Supporting Limbs

Figure 23A shows the percentage of the step cycle duration spent per individual gait on a given number of limb(s). During lateral walk, hop, and out-of-phase walk at low step frequency, mice were mainly supported on three limbs. During faster gaits (trot, hop, and out-of-phase walk at high speed, gallops, and bounds), mice were supported for more than 50% of the step cycle on two limbs. Although a two-limb support was predominant during gallops and bounds, about a quarter of the step cycle was characterized by a single-limb support. This distribution was especially more frequent during rotary gallop. Because supporting the body weight on a single limb would be more hazardous for a quadruped, the larger occurrence of this support during rotary and transverse gallops might explain, in part, why these gaits were transitional rather than attractors. Similarly, a larger proportion of single-limb support during half-bound caused by an anti-phase coupling of forelimbs concomitant to an in-phase coupling of hindlimbs might explain why full- bound would emerge as an attractor gait over half-bound at the highest velocity. During a period of two-limb support, the mouse stood on the diagonal, lateral, fore-, or hindlimbs (Figure 23B). It is obvious that the impact on postural stability of these four types of support is not equivalent for a mouse. The diagonal support (characteristic of the trot) would be the most stable solution by keeping the center of mass close to the midline along the rostro caudal axis, whereas a lateral support would be the least stable by shifting the center of mass away from the midline (typical of the pace). We indeed found that a diagonal support was the most frequent type of support and was more prominent during trot. It was also more frequent during out- of-phase walk at high step frequency, transverse gallop, and to a lesser extent during rotary gallop. As expected, mice were not found to stand on ipsilateral limbs (no pace was identified in this study), while they mainly contacted the ground with either the forelimbs or the hindlimbs during half-bound, full- bound, and hop, which is consistent with the dynamic of such gaits.

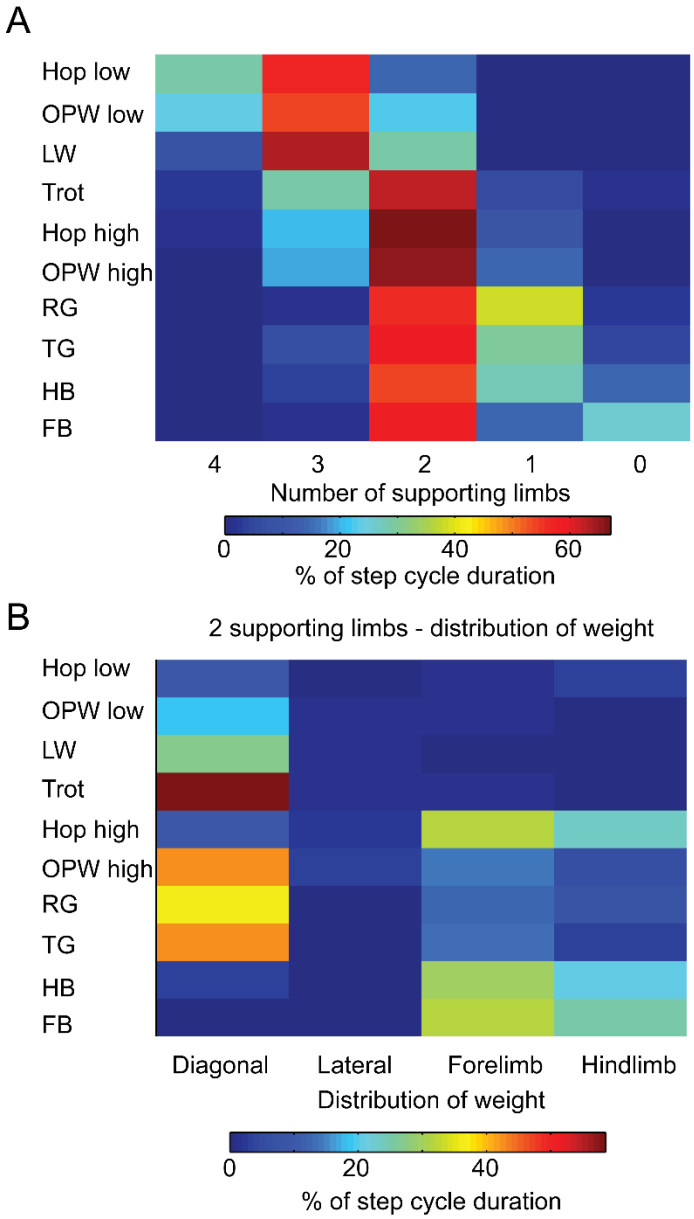

Figure 23: Distribution of weight for each gait.

A: Color-coded matrix of the percentage of the step cycle duration when mice are supported by four to no limbs (columns). Data are presented for each gait (rows). **B**: Color-coded matrix of the percentage of the step cycle duration when mice were supported on two limbs in one of the following configurations (columns): diagonal limbs, ipsilateral limbs, forelimbs, or hindlimbs. Data are presented for each gait (rows).

Gait Transitions

Gait Stability and Attractiveness

Based on the data presented in Figure 20, we have assumed that trot and full-bound were attractor gaits and the remainder were transitional gaits. To assess this assumption and potentially identify a directionality of transition, we represented the relationship between gaits using graph analysis. Figure 24A shows an example of the probability of transition as a color-coded probability matrix of gait transitions during locomotion at 5 cm/s. The

corresponding graph is presented in Figure 24B. The probability of transition is represented as color-coded links and the stability of gait as color-coded nodes. At 5 cm/s, the most stable gait was the out-of-phase walk, thus supporting this gait is an attractor. Lateral walk and trot were much less stable than out-of-phase walk at that speed, and hop was never stabilized. Mice could break away from out-of-phase walk, but it occurred very rarely.

At 15 cm/s, trot was the most stable and considered as an attractor gait (Figure 24C). Out-of-phase and lateral walk had a preferred direction toward trot but could sometimes lead to one another. The link between out-of-phase walk and hop was broken at that speed, hop being either stable or strongly biased toward trot. At 30 cm/s (Figure 24D), trot was the only gait adopted by mice. When lateral walk appeared, it was unstable and led to trot. At 75 cm/s, there was no attractor gait, but rather a diversity of stable gaits (Figure 24E). The probability of transition was low in every direction except from the trot to the transverse gallop or from the hop to the full-bound. When leaving trot (an anti-phase gait) for in-phase gaits, rotary gallop was the only direct access to half-bound, and half-bound the only one to full-bound or hop at high step frequency. At 135 cm/s (Figure 24F), full-bound was the most stable, thus supporting this gait as an attractor gait. Hop and half-bound were unstable and invariably led to full-bound.

The stability and attractiveness of each gait across all speeds is summarized in Figures 25G, H, respectively. Except for the hop, all gaits displayed stability at least over a discrete treadmill speed (Figure 2G). As expected, trot and full-bound presented the widest range of speeds with a strong stability, demonstrating that these gaits were attractors. Out-of-phase walk and half-bound showed strong to moderate stability across a wide range of speeds, but the stability was generally less than for trot or half-bound.

Lateral walk was stable at 10 and 15 cm/s, and both gallops between 75 and 105 cm/s. Regarding the attractiveness of gaits (Figure 24H), the trot and full-bound displayed the widest range of strong probability of transition, further supporting that these gaits are attractors. The other gaits were associated with weaker probability of transition, confirming their role as transitional gaits.

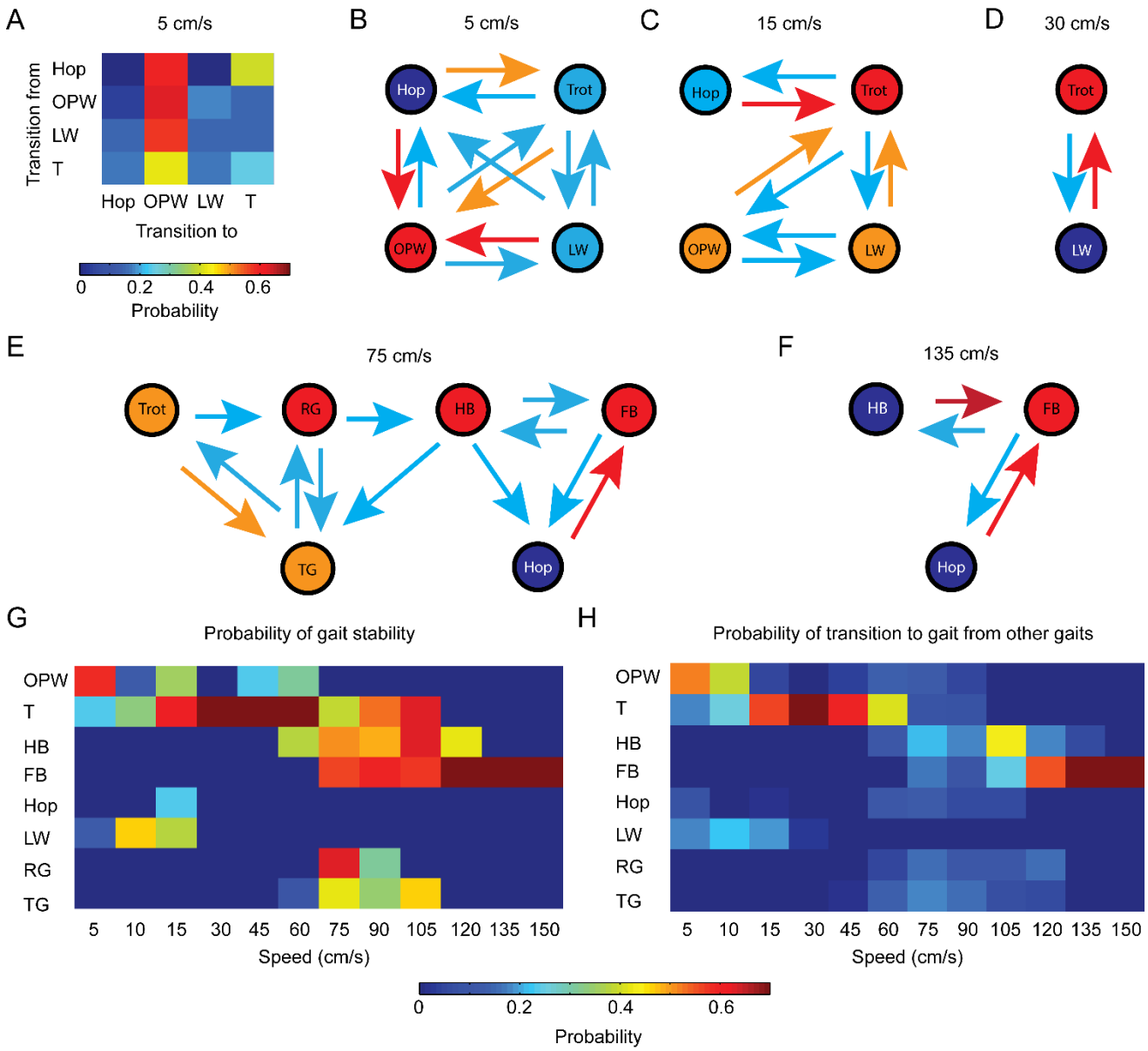

Figure 24: Stability and attractiveness of gaits.

(A) Color-coded matrix of transition probability between gaits. Stability refers to a similar gait between two successive step cycles. Data correspond to a steady-state locomotion at 5cm/s. (B) Graph analysis of the matrix presented in (A). Gaits are represented by nodes (or vertices) and transitions by links (or edges). For sake of clarity, the diversity of color has been reduced: red = all shades of red, orange = green to orange, light blue = most shades of blue (except for deep blue, which denotes absence of link). The color of a circle indicates the stability of a gait. Similar graphs are presented at (C) 15cm/s, (D) 30cm/s, (E) 75cm/s, and (F) 135cm/s. (G) Color-coded matrix of the probability of stability of gaits at all investigated speeds. (H) Color-coded matrix of the probability that any gait will make a transition to another gait.

Are Transitions Toward Gaits Predictable or Random?

To evaluate whether transitions between gaits are predictable or occurred randomly, we analyzed the probability of transition from each gait to any other gait including those separated by 2– 4 links. An example of the calculation is shown in Figure 25A. Out-of-phase walk was clearly biased toward trot, even when it reappeared at 60 cm/s, and to a lesser extent to lateral walk (Figure 25B). Although stable, mice could break away from trot and did toward out-of-phase walk at low speed and gallops at high speed (Figure 25C). As expected, half-bound was drawn toward full-bound, except at 75 cm/s where it mainly led to transverse gallop (Figure 25D). Full-bound presented the lowest values of transition probability. Transitions from full-bound mainly occurred toward half-bound, but could also lead to transverse gallop, out-of-phase walk, or hop (Figure 25E). These results suggest that out-of-phase walk is an initiation gait for locomotion and tends to lead toward walking trot. Our data also suggest that half-bound is the gateway to full-bound, which is the attractor gait at the highest running speeds. Regarding purely transitional gaits, we found that hop was biased toward out-of-phase walk at the lowest speed and toward trot as it became the attractor (Figure 25F). We found a similar phenomenon for lateral walk (Figure 25G). Transverse gallop occurred over a wider range of speeds than rotary gallop. The transition to trot was favored at 75 cm/s and below and to rotary gallop above that speed (Figure 25H). The transition probability to half-bound was moderate at 105 cm/s. The main access to half- bound was via rotary gallop, which could also lead to full-bound. There were some transitions to transverse gallop, especially at 90 cm/s (Figure 25I). Overall, these results show that transitions do not occur in random directions but are rather biased, and thus predictable.

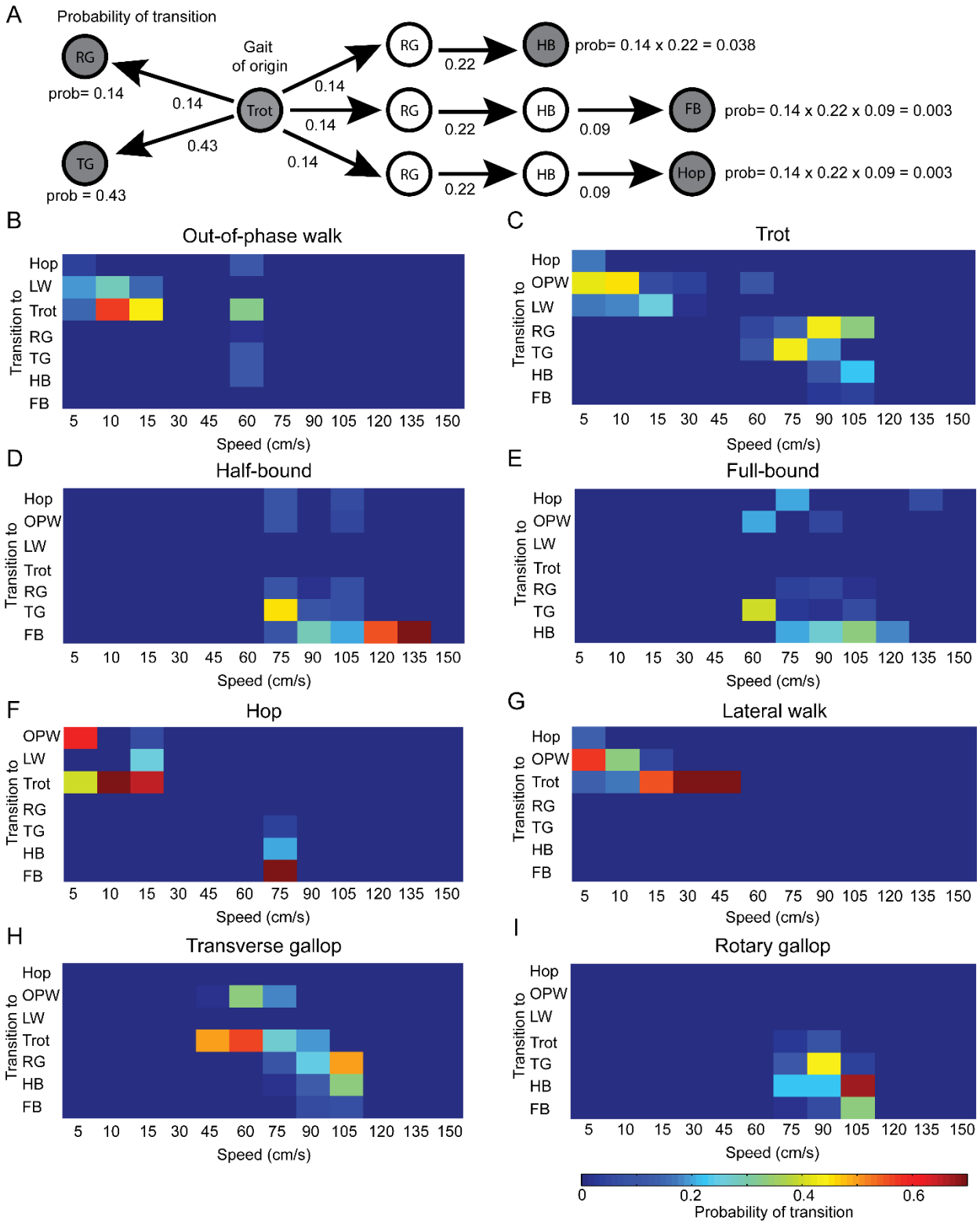

Figure 25: Probability of transition for all gaits.

(A) Example of probability calculation. Probability of transition is straightforward for neighbors (path length of 1 link) but requires multiplication of probability for longer path length (up to 4 links). We used graph analysis to find the shortest path (highest probability) between two gaits. (B–I) Color-coded matrix of the transition probability for all speeds.

2.6 Discussion

Using kinematic analysis on individual step cycles during treadmill locomotion at steady speed, we showed that themouse displays a wide repertoire of locomotor gaits. We identified trot and full-bound as attractor gaits at walking and running speeds, respectively. Moreover, these gaits were preceded by semi-attractor gaits: out-of-phase walk and half-bound. We use the term “semi-attractor” because these gaits were more stable (several contiguous step cycle) than transitional gaits, but appeared as the attractor only at a given speed. By contrast, lateral walk, hop, and rotary and transverse gallops were less robust and less stable, emerging as transitional gaits between these attractor gaits.

Methodological Considerations

To study locomotor gaits at steady speed, we used a treadmill belt, which offers some advantages over other systems (e.g., the catwalk). Although both approaches share similar behavioral outcomes, they also exhibit contextual discrepancies, leading animals to adopt different locomotor gaits (Wetzel et al., 1975; Blaszczyk and Loeb, 1993; Herbin et al., 2007). The catwalk likely has an advantage in exploring a more natural locomotor behavior, with acceleration and deceleration phases (Bellardita and Kiehn, 2015). Nevertheless, the limited length of the catwalk (usually 1 m) limits the number of contiguous steps, in contrast to treadmill locomotion. Using the catwalk or treadmill, the challenge still remains to motivate walking or running in the mouse. Running gaits in the catwalk likely reflect a flight reaction to escape the experimenter at the gateway of the catwalk (Bellardita and Kiehn, 2015) or a noxious stimulation by pinching the tail of the mouse (Serradj and Jamon, 2009). Similarly, mice learn to walk and run on a treadmill to avoid the electrified grid or the hand of the experimenter during initial training. Although treadmill locomotion might not be less stressful during subsequent testing than the catwalk, the treadmill locomotion allows ones to study locomotor gaits over a wide range of speeds and at steady speed.

A Dynamic System with Attractor, Semi-Attractor, and Transient Gaits

Locomotion is a dynamic process, which depends on intrinsic and extrinsic properties. The intrinsic properties reflect the current status and the history of the system and its sub-systems, which are embedded in the anatomy and physiology of spinal cervical and lumbar locomotor circuits, and its supraspinal descending inputs.

Using neonatal locomotor studies, mouse genetics have previously shown that manipulating genes can reorganize the spinal locomotor circuit. This neural rewiring consequently can reduce or increase the diversity of locomotor patterns, thus leading to a unique and strong left-right synchronization or an increased variability in left-right coordination (Kullander et al., 2001a, 2001b; Beg et al., 2007; Fawcett et al., 2007; Iwasato et al., 2007; Rabe et al., 2009; Rabe Bernhardt et al., 2012).

Moreover, the neural circuit undergoes massive changes during development, thus giving rise to functional changes at the cellular, systemic, and behavioral levels. This translates into the acquisition of new locomotor gaits, as illustrated by crawling or rolling in the infant, which eventually switches to a walking then running pattern in the toddler (Forssberg, 1999; Lacquaniti et al., 2012). Similarly, gallop does not emerge prior to the 2nd postnatal week in the rat (Iwahara et al., 1991), and likely in the mouse as well. New locomotor patterns can also emerge to ensure functional compensation or recovery in patients or animal models following spinal cord injury (Barrière et al., 2008; Tester et al., 2011, 2012), neurodegenerative diseases such as Parkinson's (Morris et al., 1996, 2001; Amende et al., 2005) and Down syndrome (Parker and Bronks, 1980; Hampton et al., 2004), or even environmental manipulations (split-belt treadmill) (Thibaudier et al., 2013; Thibaudier and Frigon, 2014).

In addition, the dynamic of locomotor gaits also depends on extrinsic properties, such as the environment and the context in which the mouse evolved. Laboratory mice were fed ad libitum and kept in small cages are not exposed to a rich and life- threatening environment; there is hence no need to seek food and water or to escape potential predators, except occasionally the mouse's own littermates and the experimenter. In the artificial and controlled settings of our laboratory, there is therefore no reason or need for the mouse to experience and adopt a wide range of locomotor gaits, thus explaining the predominance of certain gaits at walking and running speeds in previous locomotor studies in the mouse

(Herbin et al., 2004, 2006, 2007; Serradj and Jamon, 2009; Talpalar et al., 2013; Borgius et al., 2014) and in larger animals, such as the cat (Wetzel et al., 1975; Blaszczyk and Loeb, 1993; Frigon et al., 2014). Therefore, by their high probability of occurrence (Figure 20), their stability (Figure 24G), and finally their attractiveness over other gaits (Figure 24H), preferential gaits were defined as attractor gaits over other ones, which were consequently considered as transitional gaits.

Attractor Gait: Trot and Full-Bound

As previously reported during over-ground and catwalk locomotion (Serradj and Jamon, 2009; Talpalar et al., 2013; Borgius et al., 2014; Bellardita and Kiehn, 2015), we identified the trot as a preferential or attractor gait during treadmill locomotion. Its large spectrum of stride frequency over a wide range of treadmill speeds allowed us to confirm its preferential use at walking and moderate running speeds. Trot was characterized by a robust alternation of hind-, fore-, and ipsilateral limbs (i.e., anti-phase coupling) and consequently a robust synchronization of diagonal fore- hindlimbs (i.e., in-phase coupling), likely resulting from a well-orchestrated and coordinated reciprocal inhibition between spinal locomotor circuits working in concert with sensory feedback and supraspinal descending control. This fore-hindlimb synchronization likely contributes to a better distribution of the mouse body weight support on its diagonal limbs during stance, thus keeping the animal's center of mass along its midline. In addition, this synchronization of diagonal limb in conjunction with a larger stride length than during out-of-phase walk and lateral walk also likely prevents ipsilateral limbs to get in the way of each other during the swing, therefore ensuring an optimal postural stability. At the highest running speeds, we identified full-bound as an attractor gait. Surprisingly, there has been little evidence in the literature until recently that wild-type mice were capable of galloping or bounding. Indeed, previous kinematic studies showed that C57BL/6J mice tended to fast trot rather than gallop at the highest treadmill speeds (Herbin et al., 2004). Although gallops and bounds have been reported during brief acceleration phases on a treadmill (Herbin et al., 2004, 2006, 2007), in a catwalk (Bellardita and Kiehn, 2015), and in a catwalk following noxious stimulations (Serradj and Jamon, 2009), they were observed only for a few strides. Full-bound, as a high-speed running gait, is highly demanding on energy, and calls for a high

motivational state (Heglund and Taylor, 1988), as suggested by the importance of the reward circuitry and especially the maturation of the nucleus accumbens and the neurotransmitter dopamine in high voluntary running rats over more sedentary rats (Garland et al., 2011; Roberts et al., 2014). Moreover, as mentioned in the previous section, the environment and the context can shape the emergence of gaits. Full-bound is necessary in a normal environment for seeking a moving prey or escaping a predator. Not surprisingly, our initial attempts to evoke gallops and bounds during locomotion at steady speed failed with 2- to 3-month-old mice (data not shown). It will therefore be important in the future to determine whether locomotor training can maintain running gaits in aging mice.

Semi-Attractor Gaits: Out-of-Phase Walk at Low Step Frequency and Half-Bound

Semi-attractor gaits were defined as more stable than transitional gaits but over a narrower range of speeds than attractor gaits. Our analysis of locomotor gaits as a function of inter-limb coupling allowed us to identify a new gait: the out-of phase walk, which predominated over other gaits at very low speed. This gait was characterized by an out-of-phase coupling of hindlimbs, a loose anti-phase coupling of ipsilateral forelimb- hindlimb, and a relatively more robust anti-phase coupling of forelimbs. In that sense, out-of-phase walk was an attractor over a very narrow speed range and was therefore considered as a default gait emerging while the mouse was initiating locomotion, exploring its environment, or slowing down its speed. Indeed, when trot was generated at very low speed, it tended to lead back to an out-of-phase walk (Figure 25C). As such, the emergence of alternation in forelimbs, then to forelimb-hindlimb, and eventually to hindlimbs suggests that supraspinal descending inputs recruit primarily the cervical spinal locomotor circuit prior to the lumbar one, thus likely ensuring a postural stability on four limbs prior to movement initiation with forelimbs.

We also identified half-bound as a semi-attractor gait. Like out-of phase walk at slow speed, most locomotor gaits tended to lead to half-bound at low running speed over a narrow speed range, thus justifying the term of semi-attractor over attractor for half-bound. During half-bound, hindlimbs were in-phase, while forelimbs were out-of-phase.

Interestingly, half- bound with its out-of-phase forelimbs appeared to emerge from rotary and transverse gallops with their anti- and out- of-phase forelimbs, but seemed to precede full-bound with its synchronized forelimbs. Therefore, there was a gradual switch from an anti-, to an out-, and then in-phase coupling of left- right forelimbs with increasing speed. Notably, this shift in the coupling of left-right forelimbs occurred at higher speeds in comparison to that of the hindlimbs. From a biomechanical viewpoint, the hindlimbs with stronger and larger extensor muscles than forelimbs are likely more efficient at propelling the animal body forward.

Transitional Gait: Hop, Lateral Walk, Out-of Phase Walk at High Frequency and Gallops

Hop was found at low and high step frequency. At low step frequency, hindlimb synchronization occurred rarely and always led to out-of-phase walk. It is reminiscent of the hop reported in frogs and toads at slow speed (Reilly and Jorgensen, 2011). At high step frequency, the hop resembled the jump or the leap in the frog and was intercalated with half-bound and full-bound in the mouse. Hop differed from bound by its longer duty cycle of the stance phase, thus suggesting a slight deceleration at high locomotor frequency.

Lateral walk was present up to 30 cm/s but never occurred as a dominant gait. Surprisingly, lateral walk is largely adopted by other rodents, such as the guinea pig and the rat (Hildebrand, 1976), while it was clearly less frequent in the mouse (this study). Out-of-phase walk reappeared at fast walking (and slow running) speeds and usually led to trot and rarely to gallops or bounds, suggesting it acted as a transitional gait during a decelerating phase. Gallops arose directly from trot and bridged the transition between trot and both half-bound and full-bound. The postural instability of the gallop was probably due to the larger occurrence of body weight support on a single limb, increasing the likelihood of falling, therefore requiring a rapid transition toward a locomotor gait enhancing postural stability at high running speed.

Functional Implication: What do Mouse Genetics Reveal about Gaits?

Although there is an abundant literature on genetically identified spinal interneurons important to left-right coordination, less is known about flexor-extensor alternation (Zhang et al., 2014), and even less about forelimb-hindlimb coordination. Using genetic ablation

and mutant studies, 4 classes of spinal commissural interneurons: dI6, V0D, V0V, and V3, have been identified as important units to bilateral coordination, based on their transcription factor expression, their Netrin-1-DCC sensitivity, and their neurotransmitter phenotype.

Indirect evidence from Netrin-1 and DCC mutants suggests that V3 spinal interneurons are involved in hindlimb synchronization (Rabe et al., 2009; Rabe Bernhardt et al., 2012), thus likely contributing to hops, gallops, and bounds. Unfortunately, genetic silencing and c-fos studies of V3 interneurons have been performed only at walking speeds (Zhang et al., 2008; Borowska et al., 2013).

Regarding V0 spinal interneurons, genetic ablations of both V0D and V0V lead to a bilateral synchronization of fore- and hindlimbs (as during full-bound) at all locomotor frequencies in neonatal isolated spinal cords as well as in freely walking mice (Talpalar et al., 2013; Bellardita and Kiehn, 2015). The absence of walk, trot, and gallop in these mutant mice suggests that V0 interneurons are likely involved in these locomotor gaits. More specifically, ablation of V0V interneurons abolishes trot (Bellardita and Kiehn, 2015), suggesting a role for V0D in walk and gallop. Although mice lacking inhibitory V0D interneurons do not survive at birth, neonatal isolated spinal cord studies revealed a gradual stabilization in left-right alternation with speed (Talpalar et al., 2013) that appears to corroborate the variability we found in the left-right hindlimb coupling of wild-type mice at locomotor frequencies ≤ 2Hz (Figure 19A), thus suggesting that V0D would initiate and stabilize left-right alternation at very slow walking speeds. Because V0D cannot be specifically ablated in adult mice, it remains uncertain whether V0D interneurons are necessary for gallops, and by extension, in the transition from walking to running gaits.

In absence of mice lacking dI6 interneurons or their Dmrt3 and WT1 interneuronal sub-populations, we can only speculate about their functional contribution. DI6 interneurons display an altered neuronal fate in mice lacking Dmrt3, with a decreased number of inhibitory Dmrt3 commissural interneurons at the expense of an increased number of inhibitory WT1 neurons (Andersson et al., 2012; Vallstedt and Kullander, 2013). Adult mutant mice and Icelandic horses lacking Dmrt3 alternate their left-right hindlimbs with an increased stride length and duration, resulting in a slow locomotor frequency. While pace does not appear to be part of the locomotor repertoire of C57BL/6J mice, it will

be interesting to see whether pace is used by Dmrt3 mutant mice, since Icelandic horses lacking Dmrt3 do not trot or gallop but preferentially pace.

Mouse genetics studies suggest a sequential and topographical recruitment of spinal interneurons as function of the locomotor speed: from V0D during walk, V0V and dI6 during trot, and finally V0V, dI6, and V3 during hops, gallops, and bounds. In that regard, attractor and semi-attractor gaits would rely on the robustness of activity of these interneurons and transitional gaits would emerge when dominant activity shifts from one population to another.

Future Directions

Mouse genetics have been relying on the extensive use of neonatal decerebrated or isolated spinal cord preparations in order to record ENG activities from ventral roots during fictive locomotion. Although this approach has been very informative for studying the intrinsic and extrinsic properties of spinal interneuronal circuits, the diversity of locomotor gaits we found in the adult mouse has never been reported so far in these in vitro studies, thus raising some concerns about neonatal and/or isolated approaches. Unfortunately, attempts to record motor activity from adult isolated spinal cords have failed up to now (Jiang et al., 1999), presumably due to hypoxia (Wilson et al., 2003). Nevertheless, we cannot exclude that the lack of diversity might reside in the developmental stage of these isolated neonatal preparations. Indeed, gallop is not evoked prior the 2nd postnatal week in juvenile rats (Iwahara et al., 1991), and it is likely also the case in the mouse. Moreover, as shown by semi-attached or decerebrated neonatal preparations (Juvin et al., 2005, 2007, 2012), the lack of locomotor diversity in isolated neonatal mouse studies could also result from a lack of convergent inputs from supraspinal descending, cervical, as well as peripheral sensory inputs.

Still technically challenging, adult decerebrated and decerebrated-spinalized mouse preparations have allowed EMG and ENG recordings during treadmill and fictive locomotion (Meehan et al., 2012; Nakanishi and Whelan, 2012). Although there is still very little information about their gaits, it will be important in the future to study supraspinal locomotor centers important in setting these various locomotor gaits.

Alternatively to these reduced preparations, kinematic and EMG recordings in the free-walking mouse are still the best way to study spinal circuits and supraspinal

descending inputs important to locomotion. Although these recordings have already been performed in the mouse at walking speed (Leblond et al., 2003; Pearson et al., 2005; Tysseling et al., 2013), little is known about their locomotor gaits. Besides, EMG implants, by preventing a normal angular excursion of locomotor movements (Pearson et al., 2005), can reduce the spectrum of locomotor gaits and speed (Lemieux et al., unpublished data). With the miniaturization of EMG implants, it will be important in the future to extend the analysis of locomotor output according to the locomotor gait at walking and running speeds.

Conclusion

In summary, the present study shows that the adult mouse displays a wide repertoire of attractor gaits as a function of speed (from out-of-phase walk to trot, to half-bound and full- bound), but can also exhibit transitional gaits (hop, lateral walk, transverse, and rotary gallops). The choice of gait depends on locomotor outcomes: the step frequency, stride length and height, and postural stability. With advances in mouse genetics, our study highlights the importance of using more objective criteria (i.e., the interlimb coupling and the duty cycle of the stance phase) to investigate the functional contribution of genetically identified spinal, propriospinal, and supraspinal neurons to locomotor gaits over a wide range of speeds in freely walking mice.

Acknowledgments

We thank Mr Philippe Drapeau for his technical help. We thank Drs Tuan Bui and Trevor Drew for their insightful comments and suggestions on the first draft of the manuscript.

Supplementary Material

The Supplementary Material for this article can be found online at: http://journal.frontiersin.org/article/10.3389/fnins. 2016.00042

2.7 References

Abourachid, A., Herbin, M., Hackert, R., Maes, L., and Martin, V. (2007). Experimental study of coordination patterns during unsteady locomotion in mammals. J. Exp. Biol. 210, 366–372. doi: 10.1242/jeb.02632

Amende, I., Kale, A., McCue, S., Glazier, S., Morgan, J. P., and Hampton, T. G. (2005). Gait dynamics in mouse models of Parkinson's disease and Huntington's disease. J. Neuroeng. Rehabil. 2:20. doi: 10.1186/1743-0003-2-20

Andersson, L. S., Larhammar, M., Memic, F.,Wootz, H., Schwochow, D., Rubin, C.-J., et al. (2012).Mutations inDMRT3 affect locomotion in horses and spinal circuit function in mice. Nature 488, 642–646. doi: 10.1038/nature11399

Asante, C. O., Chu, A., Fisher, M., Benson, L., Beg, A., Scheiffele, P., et al. (2010). Cortical control of adaptive locomotion in wild-type mice and mutant mice lacking the ephrin-Eph effector protein α2-chimaerin. J. Neurophysiol. 104, 3189–3202. doi: 10.1152/jn.00671.2010

Barrière, G., Leblond, H., Provencher, J., and Rossignol, S. (2008). Prominent role of the spinal central pattern generator in the recovery of locomotion after partial spinal cord injuries. J. Neurosci. 28, 3976–3987. doi: 10.1523/JNEUROSCI.5692-07.2008

Beg, A. A., Sommer, J. E., Martin, J. H., and Scheiffele, P. (2007). α2-chimaerin is an essential EphA4 effector in the assembly of neuronal locomotor circuits. Neuron 55, 768–778. doi: 10.1016/j.neuron.2007.07.036

Bellardita, C., and Kiehn, O. (2015). Phenotypic characterization of speed-associated gait changes in mice reveals modular organization of locomotor networks. Curr. Biol. 25, 1426–1436. doi: 10.1016/j.cub.2015.04.005

Bernhardt,N. R.,Memic, F.,Gezelius, H., Thiebes, A.,Vallstedt, A., and Kullander, K. (2012). DCC mediated axon guidance of spinal interneurons is essential for normal locomotor central pattern generator function. Dev. Biol. 366, 279–289. doi: 10.1016/j.ydbio.2012.03.017

Blaszczyk, J., and Loeb,G. E. (1993).Why cats pace on the treadmill. Physiol. Behav. 53, 501–507. doi: 10.1016/0031-9384(93)90144-5

Borgius, L., Nishimaru, H., Caldeira, V., Kunugise, Y., Low, P., Reig, R., et al. (2014). Spinal glutamatergic neurons defined by EphA4 signaling are essential components of normal locomotor circuits. J. Neurosci. 34, 3841–3853. doi: 10.1523/JNEUROSCI.4992-13.2014

Borowska, J., Jones, C. T., Zhang, H., Blacklaws, J., Goulding, M., and Zhang, Y. (2013). Functional subpopulations of V3 interneurons in the mature mouse spinal cord. J. Neurosci. 33, 18553–18565. doi: 10.1523/JNEUROSCI.2005- 13.2013

Bullmore, E., and Sporns, O. (2009). Complex brain networks: graph theoretical analysis of structural and functional systems. Nat. Rev. Neurosci. 10, 186–198. doi: 10.1038/nrn2575

Cohen, A. H., and Gans, C. (1975). Muscle activity in rat locomotion: movement analysis and electromyography of the flexors and extensors of the elbow. J.Morphol. 146, 177–196. doi: 10.1002/jmor.1051460202

Crone, S. A., Quinlan, K. A., Zagoraiou, L., Droho, S., Restrepo, C. E., Lundfald, L., et al. (2008). Genetic ablation of V2a ipsilateral interneurons disrupts left- right locomotor coordination in mammalian spinal cord. Neuron 60, 70–83. doi: 10.1016/j.neuron.2008.08.009

Drew, T., and Doucet, S. (1991). Application of circular statistics to the study of neuronal discharge during locomotion. J. Neurosci. Methods 38, 171–181. doi: 10.1016/0165-0270(91)90167-X

Dunbar, D. C. (2004). Stabilization and mobility of the head and trunk in vervet monkeys (Cercopithecus aethiops) during treadmill walks and gallops. J. Exp. Biol. 207, 4427–4438. doi: 10.1242/jeb.01282

Fawcett, J. P., Georgiou, J., Ruston, J., Bladt, F., Sherman, A., Warner, N., et al. (2007). Nck adaptor proteins control the organization of neuronal circuits important for walking. Proc. Natl. Acad. Sci. U.S.A. 104, 20973–20978. doi: 10.1073/pnas.0710316105

Forssberg, H. (1999). Neural control of human motor development. Curr. Opin. Neurobiol. 9, 676–682. doi: 10.1016/S0959-4388(99)00037-9

Frigon, A., D'Angelo, G., Thibaudier, Y., Hurteau, M.-F., Telonio, A., Kuczynski, V., et al. (2014). Speed-dependent modulation of phase variations on a step-by- step basis and its impact on the consistency of interlimb coordination during quadrupedal locomotion in intact adult cats. J. Neurophysiol. 111, 1885–1902. doi: 10.1152/jn.00524.2013

Garland, T., Schutz, H., Chappell, M. A., Keeney, B. K., Meek, T. H., Copes, L. E., et al. (2011). The biological control of voluntary exercise, spontaneous physical activity and daily energy expenditure in relation to obesity: human and rodent perspectives. J. Exp. Biol. 214, 206–229. doi: 10.1242/jeb. 048397

Grillner, S. (1975). Locomotion in vertebrates: central mechanisms and reflex interaction. Physiol. Rev. 55, 247–304.

Hampton, T.G., Stasko,M.R.,Kale,A.,Amende, I., andCosta,A.C. S. (2004).Gait dynamics in trisomic mice: quantitative neurological traits ofDown syndrome. Physiol. Behav. 82, 381–389. doi: 10.1016/j.physbeh.2004.04.006

Heglund, N. C., and Taylor, C. R. (1988). Speed, stride frequency and energy cost per stride: how do they change with body size and gait? J. Exp. Biol. 138, 301–318.

Herbin,M.,Gasc, J. P., and Renous, S. (2004). Symmetrical and asymmetrical gaits in the mouse: patterns to increase velocity. J. Comp. Physiol. 190, 895–906. doi: 10.1007/s00359-004-0545-0

Herbin, M., Gasc, J.-P., and Renous, S. (2006). How does a mouse increase its velocity? A model for investigation in the control of locomotion. Comptes Rendus Palevol 5, 531–540. doi: 10.1016/j.crpv.2005.12.012

Herbin, M., Hackert, R., Gasc, J. P., and Renous, S. (2007). Gait parameters of treadmill versus overground locomotion in mouse. Behav. Brain Res. 181, 173–179. doi: 10.1016/j.bbr.2007.04.001

Hildebrand, M. (1968). Symmetrical gaits of dogs in relation to body build. J.Morphol. 124, 353–360. doi: 10.1002/jmor.1051240308

Hildebrand, M. (1976). "Analysis of tetrapod gaits: general considerations and symmetrical gaits," in Neural Control ofMovement, eds R. Herman, S. Grillner, P. S. Stein, and D. G. Stuart (New York, NY: PlenumPress), 203–236.

Hildebrand, M. (1977). Analysis of Asymmetrical gaits. J. Mammal. 58, 131–155. doi: 10.2307/1379571

Iwahara, T.,VanHartesveldt, C.,Garcia-Rill, E., and Skinner, R.D. (1991). L-dopa-induced air-stepping in decerebrate developing rats. Brain Res. Dev. Brain Res. 58, 257–264. doi: 10.1016/0165-3806(91)90013-9

Iwasato, T., Katoh, H., Nishimaru, H., Ishikawa, Y., Inoue, H., Saito, Y. M., et al. (2007). Rac-GAP α-chimerin regulates motor-circuit formation as a key mediator of EphrinB3/EphA4 forward signaling. Cell 130, 742–753. doi: 10.1016/j.cell.2007.07.022

Jiang, Z., Carlin, K. P., and Brownstone, R. M. (1999). An in vitro functionally mature mouse spinal cord preparation for the study of spinal motor networks. Brain Res. 816, 493–499. doi: 10.1016/S0006-8993(98)01199-8

Juvin, L., Le Gal, J.-P., Simmers, J., and Morin, D. (2012). Cervicolumbar coordination in mammalian quadrupedal locomotion: role of spinal thoracic circuitry and limb sensory inputs. J. Neurosci. 32, 953–965. doi: 10.1523/JNEUROSCI.4640-11.2012

Juvin, L., Simmers, J., and Morin, D. (2005). Propriospinal circuitry underlying interlimbcoordination inmammalian quadrupedal locomotion. J.Neurosci. 25, 6025–6035. doi: 10.1523/JNEUROSCI.0696-05.2005

Juvin, L., Simmers, J., and Morin, D. (2007). Locomotor rhythmogenesis in the isolated rat spinal cord: a phase-coupled set of symmetrical flexion extension oscillators. J. Physiol. 583, 115–128. doi: 10.1113/jphysiol.2007.133413

Kiehn, O., and Kjaerulff, O. (1996). Spatiotemporal characteristics of 5-HT and dopamine-induced rythmic hindlimb activity in the in vitro neonatal rat. J. Neurophysiol. 75, 1472–1482.

Kullander, K. (2003). Role of EphA4 and EphrinB3 in local neuronal circuits that control walking. Science 299, 1889–1892. doi: 10.1126/science.1079641

Kullander, K., Croll, S. D., Zimmer, M., Pan, L., McClain, J., Hughes, V., et al. (2001a). Ephrin-B3 is the midline barrier that prevents corticospinal tract axons fromrecrossing, allowing for unilateral motor control. Genes Dev. 15, 877–888. doi: 10.1101/gad.868901

Kullander, K., Mather, N. K., Diella, F., Dottori, M., Boyd, A. W., and Klein, R. (2001b). Kinase-dependent and kinase-independent functions of EphA4 receptors in major axon tract formation in vivo. Neuron 29, 73–84. doi: 10.1016/S0896-6273(01)00181-7

Lacquaniti, F., Ivanenko, Y. P., and Zago, M. (2012). Development of human locomotion. Curr. Opin. Neurobiol. 22, 822–828. doi: 10.1016/j.conb.2012.03.012

Lanuza, G. M., Gosgnach, S., Pierani, A., Jessell, T. M., and Goulding, M. (2004). Genetic identification of spinal interneurons that coordinate left-right locomotor activity necessary for walking movements. Neuron 42, 375–386. doi: 10.1016/S0896-6273(04)00249-1

Leblond, H., L'Esperance, M., Orsal, D., and Rossignol, S. (2003). Treadmill locomotion in the intact and spinal mouse. J. Neurosci. 23, 11411–11419.

Ma'Ayan, A. (2009). Insights into the organization of biochemical regulatory networks using graph theory analyses. J. Biol. Chem. 284, 5451–5455. doi: 10.1074/jbc.R800056200

Maes, L., and Abourachid, A. (2013).Gait transitions and modular organization of mammal locomotion. J. Exp. Biol. 216, 2257–2265. doi: 10.1242/jeb.082149

Mason, O., and Verwoerd,M. (2007). Graph theory and networks in Biology. IET Syst. Biol. 1, 89–119. doi: 10.1049/iet-syb:20060038

Meehan, C. F., Grondahl, L., Nielsen, J. B., and Hultborn, H. (2012). Fictive locomotion in the adult decerebrate and spinal mouse in vivo. J. Physiol. 590, 289–300. doi: 10.1113/jphysiol.2011.214643

Miller, S., Van Der Burg, J., and Van DerMechı, F. (1975). Locomotion in the cat: basic programmes of movement. Brain Res. 91, 239–253. doi: 10.1016/0006-8993(75)90545-4

Morris, M. E., Huxham, F. E., McGinley, J., and Iansek, R. (2001). Gait disorders and gait rehabilitation in Parkinson's disease. Adv. Neurol. 87, 347–361.

Morris, M. E., Iansek, R., Matyas, T. A., and Summers, J. J. (1996). Stride length regulation in Parkinson's disease. Normalization strategies and underlying mechanisms. Brain 119(Pt 2), 551–568. doi: 10.1093/brain/119.2.551

Nakanishi, S. T., and Whelan, P. J. (2012). A decerebrate adult mouse model for examining the sensorimotor control of locomotion. J. Neurophysiol. 107, 500–515. doi: 10.1152/jn.00699.2011

Orlovsky, G. N., Deliagina, T. G., and Grillner, S. (1999). Neural Control of Locomotion, fromMollusc toMan. New York, NY: Oxford University Press.

Parker, A.W., and Bronks, R. (1980). Gait of children withDown syndrome. Arch. Phys.Med. Rehabil. 61, 345–351.

Pearson, K. G., Acharya, H., and Fouad, K. (2005). A new electrode configuration for recording electromyographic activity in behaving mice. J.Neurosci.Methods 148, 36–42. doi: 10.1016/j.jneumeth.2005.04.006

Rabe, N., Gezelius, H., Vallstedt, A.,Memic, F., and Kullander, K. (2009). Netrin-1-dependent spinal interneuron subtypes are required for the formation of left-right alternating locomotor circuitry. J. Neurosci. 29, 15642–15649. doi: 10.1523/JNEUROSCI.5096-09.2009

Rabe Bernhardt, N., Memic, F., Gezelius, H., Thiebes, A. L., Vallstedt, A., and Kullander, K. (2012). DCC mediated axon guidance of spinal interneurons is essential for normal locomotor central pattern generator function. Dev. Biol. 366, 279–289. doi: 10.1016/j.ydbio.2012.03.017

Reilly, S. M., and Jorgensen, M. E. (2011). The evolution of jumping in frogs: morphological evidence for the basal anuran locomotor condition and the radiation of locomotor systems in crown group anurans. J. Morphol. 272, 149–168. doi: 10.1002/jmor.10902

Roberts, M. D., Toedebusch, R. G., Wells, K. D., Company, J. M., Brown, J. D., Cruthirds, C. L., et al. (2014). Nucleus accumbens neuronal maturation differences in young rats bred for low versus high voluntary running behavior.

J. Physiol. 10, 1–48. doi: 10.1113/jphysiol.2013.

268805

Serradj,N., and Jamon,M. (2009). The adaptation of limb kinematics to increasing walking speeds in freely moving mice 129/Sv and C57BL/6. Behav. Brain Res. 201, 59–65. doi: 10.1016/j.bbr.2009.01.030

Shi, L., Fu,W.-Y., Hung, K.-W., Porchetta, C., Hall, C., Fu, A. K. Y., et al. (2007). Alpha2-chimaerin interacts with EphA4 and regulates EphA4-dependent growth cone collapse. Proc. Natl. Acad. Sci. U.S.A. 104, 16347–16352. doi: 10.1073/pnas.0706626104

Strogatz, S. H. (2001). Exploring complex networks. Nature 410, 268–276. doi: 10.1038/35065725

Talpalar, A. E., Bouvier, J., Borgius, L., Fortin,G., Pierani, A., and Kiehn,O. (2013). Dual-mode operation of neuronal networks involved in left-right alternation. Nature 500, 85–88. doi: 10.1038/nature12286

Tester,N. J., Barbeau, H., Howland,D. R., Cantrell, A., and Behrman, A. L. (2012). Arm and leg coordination during treadmill walking in individuals with motor incomplete spinal cord injury: a preliminary study. Gait Posture 36, 49–55. doi: 10.1016/j.gaitpost.2012.01.004

Tester, N. J., Howland, D. R., Day, K. V., Suter, S. P., Cantrell, A., and Behrman, A. L. (2011). Device use, locomotor training and the presence of arm swing during treadmill walking after spinal cord injury. Spinal Cord 49, 451–456. doi: 10.1038/sc.2010.128

Thibaudier, Y., and Frigon, A. (2014). Spatiotemporal control of interlimb coordination during transverse split-belt locomotion with 1:1 or 2:1 coupling patterns in intact adult cats. J. Neurophysiol. 112, 2006–2018. doi: 10.1152/jn.00236.2014

Thibaudier, Y., Hurteau, M. F., Telonio, A., and Frigon, A. (2013). Coordination between the fore- and hindlimbs is bidirectional, asymmetrically organized, and flexible during quadrupedal locomotion in the intact adult cat. Neuroscience 240, 13–26. doi: 10.1016/j.neuroscience.2013.02.028

Tysseling, V. M., Janes, L., Imhoff, R., Quinlan, K. A., Lookabaugh, B., Ramalingam, S., et al. (2013). Design and evaluation of a chronic EMG multichannel

detection system for long-term recordings of hindlimb muscles in behaving mice. J. Electromyogr. Kinesiol. 23, 531–539. doi: 10.1016/j.jelekin.2012.11.014

Vallstedt, A., and Kullander, K. (2013). Dorsally derived spinal interneurons in locomotor circuits. Ann. N.Y. Acad. Sci. 1279, 32–42. doi: 10.1111/j.1749-6632.2012.06801.x

Wetzel, M. C., Atwater, A. E., Wait, J. V., and Stuart, D. C. (1975). Neural implications of different profiles between treadmill and overground locomotion timings in cats. J. Neurophysiol. 38, 492–501.

Wilson, R. J. A., Chersa, T., andWhelan, P. J. (2003). Tissue PO2 and the effects of hypoxia on the generation of locomotor-like activity in the in vitro spinal cord of the neonatal mouse. Neuroscience 117, 183–196. doi: 10.1016/S0306- 4522(02)00831-X

Zar, J. (1996). Biostatistical Analysis, 3rd Edn. ed S. Snavely (Englewood Cliffs, NJ: Prentice-Hall).

Zhang, J., Lanuza, G. M., Britz, O., Wang, Z., Siembab, V. C., Zhang, Y., et al. (2014). V1 and V2b interneurons secure the alternating flexor-extensor motor activity mice require for limbed locomotion. Neuron 82, 138–150. doi: 10.1016/j.neuron.2014.02.013

Zhang, Y., Narayan, S., Geiman, E., Lanuza, G.M., Velasquez, T., Shanks, B., et al. (2008). V3 spinal neurons establish a robust and balanced locomotor rhythm during walking. Neuron 60, 84–96. doi: 10.1016/j.neuron.2008.09.027

Chapter 3: Distinct contributions of mesencephalic locomotor region nuclei to locomotor control in the freely behaving mouse

Distinct contributions of mesencephalic locomotor region nuclei to locomotor control in the freely behaving mouse

Authors: Nicolas Josset[1*], Marie Roussel[1*], Maxime Lemieux[1], David Lafrance-Zoubga[1], Ali Rastqar[1], Frederic Bretzner[1,2]

[1] Centre de Recherche du CHU de Québec, CHUL-Neurosciences, 2705 boul. Laurier, Québec (QC), Canada, G1V 4G2

[2] Faculty of Medicine, Department of Psychiatry and Neurosciences, Université Laval, Québec (QC), Canada, G1V 4G2

[*] Equivalent contribution

Corresponding author: Dr. Frederic Bretzner

Email: frederic.bretzner.1@ulaval.ca

3.1 Résumé

La région mésencéphalique locomotrice (MLR) a été initialement identifiée comme un centre supraspinal capable d'initier et de moduler la locomotion. Alors que sa contribution fonctionnelle à la locomotion a été largement documentée tout au long de la phylogénie de la lamproie à l'homme, il existe encore un débat sur son organisation exacte. Combinant des enregistrements cinématiques et électrophysiologiques chez des souris modifiées génétiquements, notre étude montre que les neurones glutamatergiques du noyau cunéiforme initient la locomotion et induisent des allures de course, tandis que les neurones glutamatergiques et cholinergiques du noyau pédonculopontin modulent le rythme locomoteur, contribuant aux allures de marche lente et à un arrêt locomoteur. En initiant, en modulant et en accélérant la locomotion, notre étude identifie et caractérise des populations neuronales distinctes de cette région fonctionnelle importante pour le contrôle locomoteur.

3.2 Abstract

The mesencephalic locomotor region (MLR) has been initially identified as a supraspinal center capable of initiating and modulating locomotion. While its functional contribution to locomotion has been widely documented throughout the phylogeny from the lamprey to humans, there is still debate about its exact organization. Combining kinematic and electrophysiological recordings in mouse genetics, our study reveals that glutamatergic neurons of the cuneiform nucleus initiate locomotion and induce running gaits, whereas glutamatergic and cholinergic neurons of the pedunculopontine nucleus modulate locomotor pattern and rhythm, contributing to slow-walking gaits. By initiating, modulating, and accelerating locomotion, our study identifies and characterizes distinct neuronal populations of this functional region important to locomotor command.

3.3 Introduction

Locomotor gait results from the interplay between peripheral inputs relaying sensory afferents and supraspinal inputs descending from the brain within the spinal locomotor circuit [1]. While recent advances in mouse genetics have prompted a better understanding of the neural mechanisms in the spinal interneuronal circuits pertaining to locomotion, less is known about the descending motor command from the brain. In 1966, Shik and Orlovskii discovered that electrical stimulation of a region in the posterior midbrain can induce locomotion [2, 3]. Stimulation of this functional area, also called the Mesencephalic Locomotor Region (MLR), was found to elicit locomotion and fine-tune locomotor rhythm, just like a rheostat. Increasing stimulation of this region increases locomotor rhythm, changes the locomotor pattern, and switches gaits from a slow-walking gait to a running gait. Although this structure is well conserved throughout the phylogeny from lower vertebrates to humans [4], there is still debate about its exact organization.

Using decerebrated preparations, the pedunculopontine nucleus (PPN) was initially identified as an anatomical correlate of the mesencephalic locomotor region based on electrical stimulations and postmortem reconstruction [5-7]. Nevertheless, the inclusion of the PPN to this functional region has been challenged since then. Indeed, stimulation within the cuneiform nucleus (CnF), a nucleus dorsal to the PPN, generates locomotion, whereas the PPN hyperpolarizes spinal motoneurons, inducing motor atonia and tonic inhibition in decerebrated animal models [8-13]. This suggests that the CnF will be a more efficient site for evoking locomotion than the PPN.

Regarding the neurotransmitter phenotype of the mesencephalic locomotor region, both the CnF and PPN contain intermixed but separate populations of peptidergic, GABAergic, and excitatory cholinergic and glutamatergic neurons [7, 14-16]. Pharmacological studies in semi-intact lower vertebrates have shown that this functional region generates locomotion through an excitatory glutamatergic pathway [17] and boosts locomotor rhythm through an excitatory cholinergic pathway [18]. Recently, using optogenetic tools in the head-restrained mouse, it has been shown that activation of glutamatergic neurons across the midbrain, including the CnF and PPN, initiates locomotion and increases locomotor speed, thus suggesting that the glutamatergic PPN

might initiate locomotion. On the other hand, photostimulation of cholinergic neurons fails to initiate locomotion but increases locomotor speed [19, 20], which is in sharp contrast with locomotor arrests reported upon injections of cholinergic agonists in the PPN in freely behaving animals [21, 22]. Taken together, these findings raise questions about the functional contribution of these distinct neuronal populations in freely behaving animals.

With current clinical trials investigating the potential of Deep Brain Stimulations in the midbrain of patients suffering from neurodegenerative disease or neurotraumatic spinal cord injury affecting gait, it is becoming urgent to identify and characterize the most appropriate neuronal population for improving locomotor recovery. Combining kinematic and electrophysiological recordings with discrete optogenetic manipulations in the freely behaving mouse, we investigated the distinct excitatory neuronal populations circumscribed within the midbrain region pertaining to locomotion. Our results identify the glutamatergic CnF as a locomotor center that initiates and accelerates locomotion, thus giving rise to running gaits likely involved during flight reaction, whereas the glutamatergic and cholinergic PPN would regulate slow-walking gaits likely involved during exploratory behavior. Some of this work was previously published in abstract form [23].

3.4 Methods

Experimental Model and Subject Details

Mice

VGluT2-IRES-Cre (RRID: IMSR_JAX:016963), ChAT-IRES-Cre (RRID: IMSR_JAX:006410), Ai32 (RCL-ChR2(H134R)/EYFP, RRID: IMSR_JAX:024109), Ai39 (RCL-eNpHR3.0/EYFP, RRID: IMSR_JAX:014539) mouse strains were maintained on a mixed genetic background (129/C57Bl6). Adult (≥60 days) weighing approximately 30 grams were used randomly in this study regardless of their sex. Before experiments, mice were housed in groups of maximum 5 per cage. After surgery, they were housed alone to avoid implant damaging. AAV2/9 EF1-DIO-hChR2(H134R)-mcherry [50] was injected in VGluT2-IRES-Cre or ChAT-IRES-Cre mice to induce a restricted cre-lox recombination. Housing, surgery, behavioral experiments, and euthanasia were performed in compliance with the guidelines of the Canadian Council on Animal Care and approved by the local committee of Université Laval (CPAC-CHUL).

Method Details

Surgery

Under isoflurane (1,5-2% O_2) anesthesia, the mouse was installed in a stereotaxic frame, a craniotomy was performed for chronic implantation of an unilateral optical fiber (diameter: 200µm) above the nucleus of interest: the cuneiform nucleus (CnF; anteroposterior from the Bregma (AP), -4.6 to -4.9 mm; mediolateral (ML), 1.2 to 1.4 mm; depth, 2.2 to 2.7 mm), the pedunculopontine nucleus (PPN; AP, -4.3 to -4.8 mm; ML, 1 to 1.5 mm; depth, 3.1 to 4.3 mm), or the mesencephalic reticular nucleus (MRN; AP, -4.6 mm; ML, 0.8 mm; depth, 2.6 mm). The fiber was held in place with dental acrylic and machine screw (cat#19010-10, FST, North Vancouver, Canada).

For AAV-injected mice, 100nL AAV2/9 (titer 1,2E13 GC/mL) was injected in a nucleus of interest prior to chronic implantation of an optical fiber during the same surgery under isoflurane (1,5-2% O_2) anesthesia. A glass micropipette (WPI, ID: 0.53 and OD: 1.19 mm) was backfilled with mineral oil and fixed on a micro-injector (Nanoliter 2010 Injector,

WPI). The pipette was lowered slowly into the nucleus of interest. After a 5-min period, the AAV was injected at a slow pace of 50nL/min. To avoid any leaking of the AAV, the glass pipette was held in place for 5 min following the injection before being slowly retracted.

For chronic electromyographic EMG recordings in AAV-injected mice during isoflurane (1,5-2% O_2) anesthesia, local block (lidocaine: 7.5 mg/kg) was injected subcutaneously prior to surgical openings. Stainless steel wires were implanted into hindlimb muscles (tibialis anterior (TA), gastrocnemius lateralis (GL), Semitendinosus (ST), Vastus Lateralis (VL)). Stainless steel wires were run under the skin up to a connector attached to the back of the mouse.

For all surgical procedures, analgesics (Buprenorphine hydrochloride SR: 5mg/kg) were provided at the end of the surgery for long-duration release. After a 1-week recovery, mice were tested in the laboratory.

Optogenetic and electrophysiological experiments

Mice were tested during the day in a room dedicated to treadmill experiments. Kinematic and electromyographic (EMG) recordings were performed upon optical manipulations of Channelrhodopsin-2.0 (ChR2) or Halorhodopsin-3.0 (eNpHR3.0) expressing neurons in freely behaving mice at rest and during treadmill locomotion. The pattern and timing of optical manipulations were controlled using a mechanical shutter (Connectorized Mechanical Shutter Adapters; Doric, Canada) and controller (SR470 Laser Shutter Controller; Stanford Research Systems, California, USA) synchronized online during kinematic and EMG recordings. Channelrhodopsin-2.0-expressing neurons (ChR2) were photostimulated by using a blue laser (50mW power, 473nm wavelength, Laserglow Technologies, Ontario, Canada). To determine the laser power threshold, kinematic and EMG signals were recorded upon 10ms pulse photostimulations delivered in the animal at rest (Fig. 27). Locomotor studies were performed at the threshold at a steady speed during treadmill locomotion (Fig. 28-31). Regarding the timing of stimulations, continuous 10 and 50ms pulse duration were delivered every 3 seconds to assess changes in locomotor pattern, rhythm, and gait; trains of 10ms pulses at 20Hz were also used for longer stimulations of 1s every 5s. Since there were no initiation effects and only subtle effects on the locomotor output using ChAT x Ai32-ChR2 mice, the intensity was set at the submaximal laser power

in this mouse model (90% of the laser power). Halorhodopsin-expressing cells (eNpHR3.0) were photoinhibited by using a yellow laser (100mW power, 590nm wavelength, Laserglow Technologies, Ontario, Canada). Kinematic and EMG recordings were performed upon 1s-pulses delivered every 5 seconds at rest and at a comfortable speed for each animal during steady locomotion on a treadmill belt.

Kinematic and electromyographic recordings

Prior to any surgery, mice were trained to walk on a treadmill over a wide range of speeds (LE 8700 Series, Panlab). Reflective markers were painted on the hindlimb joints (iliac crest, hip, knee, ankle, and MTP) for post-hoc kinetic and kinematic analysis. All mice were filmed on the left and right sides with high-frequency cameras (Genie HM640, Dalsa Teledyne; 250 frames/s). Videos were digitized with StreamPix 6.0 (Norpix) and analyzed offline using custom-designed software and MATLAB.

Electromyographic activity of the tibialis anterior (TA, ankle flexor), gastrocnemius lateralis (GL, ankle extensor), semitendinosus (St, knee flexor), and vastus lateralis (VL, knee extensor) muscles were recorded using acute and chronic settings. For acute settings, transgenic Ai32 or Ai39 cre-lox mice were slightly anaesthetized to insert dual core wires into muscles of interest, as previously described elsewhere [28]. Electromyographic signals were amplified (x 1000), band-pass filtered (0.1–10kHz), sampled at 10KHz, and digitally converted (Power 1401; CED, Cambridge, UK) using Spike2 version 8 (CED, Cambridge, UK). Electromyographic signals were high-pass filtered, rectified, and analyzed offline using custom-designed software and MATLAB.

Kinematic analysis

As previously described [28], joint markers of the iliac crest, hip, ankle, and MTP were detected. To avoid skin slippage, the knee was inferred by triangulation using the length of the femur and the tibia. Stick and gait diagrams were generated for locomotor gait analysis. Data collected before, during, and after optical manipulations were averaged and plotted as functions of time. Locomotor gaits were identified based on the inter-limb coupling, the footfall pattern and the duty cycle of the stance phase to delineate running and

walking gaits (hop, lateral walk, diagonal walk, pace, out-of-phase walk, trot, rotatory gallop, transverse gallop, half-bound, and bound). Using 200ms bin width, locomotor gait predominance upon long optical manipulations (100ms, 200ms, or 1s) was illustrated by histograms of frequency as function of time. During photostimulation and photoinhibition experiments, mice walked at a comfortable speed with a stance duration ranging from 100 to about 200ms; therefore a locomotor arrest was considered when the stance phase outlasted 400ms or 200% of the pre-stimulus step cycle duration.

Analysis of motor activity and response

As previously described [79], background EMG activity and evoked EMG responses were synchronized on the onset of a flexor muscle, the right tibialis anterior (TA), ipsilateral to the stimulation site. This muscle was used as a reference to align EMG signals according to the phase of the step cycle and optical stimulations.

For analysis of background EMG activity (Fig. 30 and 32), the onset and offset of EMG activity of each muscle were measured in reference to the right TA. The amplitude, duration, and time of EMG activity of each muscle were calculated before, during, and after optical manipulations.

For stimulus-triggered averaging during locomotion (Fig. 27 at rest and 29 during treadmill locomotion), the step cycle duration of the hindlimb ipsilateral to the stimulation was normalized and divided into 5 equal epochs, corresponding to the swing phase for the first two epochs, and the stance phase for the last three epochs. Stimulus-triggered averaging of rectified EMG responses (blue line) was superimposed on the background EMG activity (black line) according to the step cycle phase as in Figure 29. A similar analysis was performed for stimulus-triggered averaging evoked at rest as in Figure 27. Stimulus-triggered averaging (blue line) was considered significant when responses crossed the 99.5% confidence interval of the background EMG activity (thin black line). Using custom software and scripts written in MATLAB, the latency, duration, and amplitude of motor responses were calculated from the onset and offset of these EMG responses.

The net amplitude of motor responses was used to study motor changes at rest (Figure 27C-D). To assess the phase-dependency of motor responses during treadmill locomotion (Figure 29C-D), the amplitude of motor responses was normalized as function

of the maximal response evoked in each individual muscle. Data were plotted as a percentage of the step cycle duration as in Figure 29C.

For long photostimulation/inhibition studies (pulse duration > 50ms, Figures 31-32), the onset and offset of EMG bursts were quantified for the stimulated step cycle, the three steps before and the four steps after optical manipulation. The net amplitude and duration of EMG activity were normalized to the averaged activity recorded prior to optical manipulation.

Multi-unit activity (MUA) recordings

Under ketamine-xylazine anesthesia, the animal's head was fixed in a stereotaxic frame. A craniotomy was performed to expose the tectum and the cerebellum (anteroposterior -4 to -7 mm from Bregma, mediolateral 1.5 mm on both side). A homemade optrode combining an optical probe (multimode 100um diameter, ThorLabs, Newton, NJ, USA) coupled to a tungsten electrode (0.1MOhms, WPI, Saratosa, FL, USA) was inserted in the cuneiform (depth 2.7 mm) or pedunculopontine (depth 3.3 mm) nucleus. The laser was set to suprathreshold intensity to evoke reliable responses. Signals from tungsten electrodes were amplified (A-M System model 1800, Seqim, WA, USA) and digitally converted (Power 1401; CED, Cambridge, UK). MUA were analyzed offline using Spike2 and MATLAB.

Neuroanatomy

At the end of the experiment, animals were deeply anesthetized and transcardially perfused with 10 mL saline (0,9% NaCl) followed by 20 mL paraformaldehyde (4% PFA). Tissues were harvested and post-fixed overnight in 4% PFA, then in 30% sucrose until saturation. Tissues were frozen in Leica tissue freezing medium, then cut on a Leica cryostat (Leica CM1860, Germany). The following primary antibodies were used: anti-choline acetyltransferase (ChAT) 1:100 (Chemicon-Millipore, AB144P), anti-Cre recombinase (CRE) 1:1000 (EMD Millipore, MAB3120) and anti-cfos (EMD Millipore, PC05). The following secondary antibodies were used: donkey anti-mouse-AF594 1:1000 (Thermofisher Scientific, A-21203), donkey anti-goat-AF488 1:1,000 (Abcam, AB150129)

and donkey anti-rabbit-AF594 (Invitrogen, A21207). Cfos immunostaining was performed on free floating sections while all of the others immunostaining were done on slides.. Images were taken on an Axio Imager M2 microscope connected to an AxioCam camera using ZEN2 software (Zeiss, Germany).

Injection localization was verified on post-mortem tissues. To confirm that the tip of the canula was located in the cholinergic staining for PPN stimulation and above the cholinergic staining for CnF stimulation (Fig. 28B, Kruskal-wallis, $p<0.0001$, and Tukey HSD test showing $p<0.001$ difference between CnF and PPN).

Quantification and Statistical Analysis

Information about mice number, statistical tests and representation can be found in the figure legends. Data are represented as mean ± standard error of mean and statistical difference was indicated by Asterisks (* $P\leq0.005$, ** $P\leq0.001$, *** $P\leq0.0001$). Before every analysis, the normality of the data distribution was assessed using a Shapiro-wilk test. In order to test statistical difference from a specified value we used a one sample t-test if the distribution was normal or a Mann-Whitney test if the distribution was not normal. In order compare groups, a one-way ANOVA was performed with a Bartlett post-test used if the distribution was normal. Otherwise, if the distribution was not normal, a Kruskall-Wallis test was performed with a Dunn's multiple comparison post-test.. In absence of differences between mouse models (transgenic versus virally-transfected mice), neuronal populations (glutamatergic versus cholinergic), or flexor or extensor muscles, data were pooled together.

3.5 Results

The mesencephalic locomotor center is a functional region defined by its capacity to initiate and maintain locomotion upon electrical or pharmacological activation [24]. However, little is known about its anatomical correlates, its neurotransmitter phenotype, and its topography. Given the identification of potentially two distinct anatomical correlates within this region—the Cuneiform Nucleus (CnF) and the Pedunculopontine Nucleus (PPN)—and two excitatory neurotransmitters—glutamatergic and cholinergic—we assessed the functional contribution of these neuronal populations to motor control by using optogenetic tools accessible in the mouse. Channelrhodopsin-2 (ChR2) was conditionally expressed in either glutamatergic or cholinergic neurons by cre-lox recombination in regions of interest using viral transfection or crossing transgenic mice (Fig. 27A-B). Crossed transgenic mice gave us the opportunity to study a recruitment of neuronal tissues, similar to electrical stimulations with a restriction to a specific neurotransmitter phenotype, either glutamatergic or cholinergic. Probe locations for both mouse models and the extent of cre-lox recombination for virally transfected mice were confirmed histologically on postmortem tissue (Fig. 27A; Fig. 34A for virally transfected mice and 27B for crossed transgenic ones). As illustrated in Fig. 27A, we used anatomical landmarks such as the periaqueductal gray, the inferior colliculus, the lateral lemniscus, the superior cerebellar peduncle, and cholinergic staining [25-27] to identify the glutamatergic CnF and PPN, and the cholinergic PPN.

Glutamatergic (VGluT2) or cholinergic (ChAT) neurons were photostimulated upon blue laser illumination (wavelength = 473 nm) delivered through an optical probe chronically implanted above the unilateral right midbrain (1 probe per region and per animal). Short pulses (10ms) of photostimulation evoked optogenetically identified multi-unit activity in glutamatergic and cholinergic CnF and PPN neuronal populations targeted in the anesthetized mouse (Fig. 27C-D). The number of spikes increased as a function of laser power in all three neuronal populations (Fig. 27E). The firing frequency sustained as a function of stimulation frequency (Fig. 27F) up to 40Hz in glutamatergic CnF neurons and up to 20Hz in glutamatergic and cholinergic PPN neurons, prior to decreasing beyond that frequency (Fig. 35), thus supporting a robust spike fidelity up to 20Hz in all populations. Although the number of spikes tended to decrease over time in

response to long trains of photostimulation of cholinergic PPN neurons at 20 Hz and beyond (Fig. 27F and Fig. 35), the total number of spikes and their spike adaptation were not significantly different from glutamatergic CnF or PPN neurons upon long pulses or long trains of photostimulation (Fig. 1G, p=0.679, χ^2=0.77, d.f.=12 upon 200ms activation; Fig. 1H, p=0.0665, χ^2=5.42, d.f.=14 upon 20Hz trains of stimulation; and Fig. 1I, p=0.229, χ^2=2.95, d.f.=14 for spike adaptation). Similar to previous optogenetic studies [19, 20], our results support that 20Hz stimulation would be an ideal frequency for inducing motor movements and locomotion.

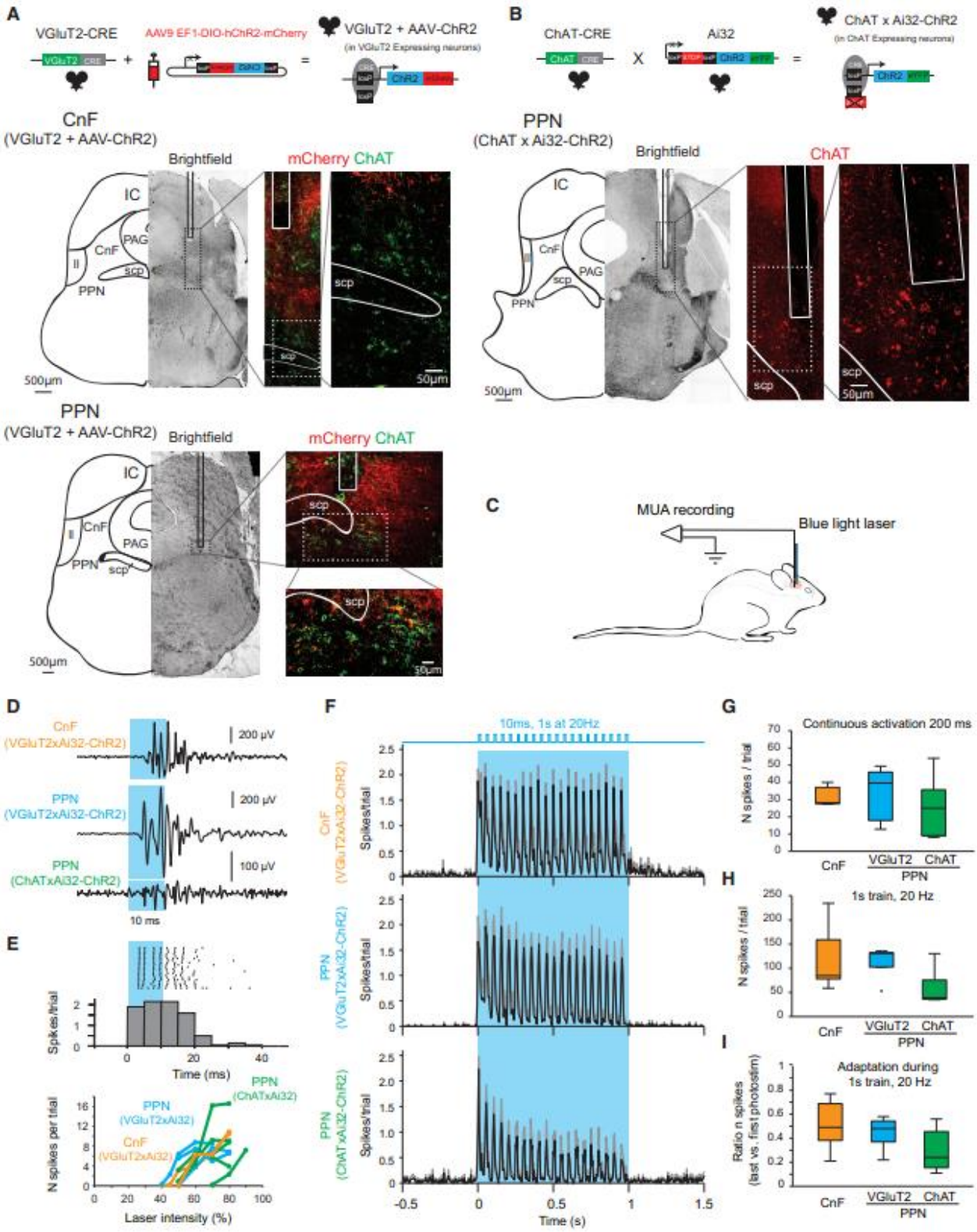

Figure 27: Mouse genetics to assess functional contribution of the midbrain locomotor center.

(A), Genetic construction for VGluT2-CRE mice injected with AAV2.9 EF1-DIO-hChR2-mcherry. (B), Genetic construction for VGluT2-CRE or ChAT-CRE x Ai32-ChR2-YFP mice. (C), Examples of low-magnification image (left), schematic outlines of the section (middle) and high-magnification (right) image of the cre-lox recombination, cholinergic (ChAT) staining, and the optical cannula. Glutamatergic neurons transfected with the virus express the red fluorescent protein (mcherry or red); cholinergic PPN neurons were identified by ChAT immunostaining (green). Outlines show the anatomical landmarks used to delineate the Cuneiform Nucleus (CnF) from the Pedunculopontine Nucleus (PPN), the cholinergic PPN (green area), and the cannula implantation site (white). Bottom right image illustrates C-FOS staining 1-hour after long trains of photostimulations (10ms pulse duration, 20Hz, 1s) in freely behaving crossed transgenic mice. Scale bar: 500µm. (D-E), Multi-unit activity evoked upon a short pulse of photostimulation (10ms pulse duration) of the glutamatergic CnF, PPN, or cholinergic PPN in anesthetized (ketamine-xylazine) crossed transgenic mice. (F), Raster plot (top) and peri-stimulus time histograms (middle) evoked upon stimulation of glutamatergic CnF neurons. Number of spikes evoked as function of the laser power (bottom). (G), Trains of spikes evoked as function of the time in response to long trains of photostimulation (10ms pulse duration, 20Hz, 1s) in the three neuronal populations. Black line is the average; gray line is the standard error. (H), Boxplot of the number of spikes per trial evoked upon photostimulations of 200ms pulse duration. (I) Boxplot of the number of spikes per trial evoked upon 1s trains of stimulation (10ms pulse duration, 20Hz). (J), Boxplot of the ratio of the number of spikes evoked for the 20th (last) versus the first pulse of the train of photostimulation (10ms pulse duration, 20Hz, 1s). Statistical differences for the number of spikes and the ratio of spikes (n= 5 VGluT2-CRExAi32+CnF, 5 VGluT2-CRExAi32+PPN, and 5 ChAT-CRExAi32+PPN) were tested by Kruskall-Wallis with Tukey HSD test.

Abbreviations: CnF: Cuneiform Nucleus, IC: inferior colliculus, LL: Lateral Lemniscus, PAG: Periaqueductal Gray, PPN: Pedunculopontine Nucleus, scp: Superior Cerebellar Peduncle.

Glutamatergic neurons evoked short-latency motor responses, whereas cholinergic neurons evoked long-latency motor responses in the mouse at rest

Motor movements were videotaped with high-speed cameras, and electromyographic (EMG) responses of the ankle flexor tibialis anterior (TA), the knee flexor semitendinosus (ST), the ankle extensor gastrocnemius lateralis (GL), and the knee extensor vastus lateralis (VL) were recorded upon photostimulation in the freely behaving mouse at rest and during locomotion (Fig. 28-31). In virally transfected mice at rest (Fig. $28B_{1-2}$), short photostimulations (10ms pulse duration) of glutamatergic-expressing CnF or PPN neurons evoked short-latency excitatory motor responses in about 15ms in both flexor and extensor muscles (Fig. 28E).

As illustrated by the net integrated amplitude of motor responses evoked in pairs of antagonist flexor versus extensor muscles (Fig. $28C_1$), both glutamatergic CnF and PPN neurons evoked the strongest motor responses in flexor muscles rather than extensors, with the strongest changes in virally transfected mice (Fig. $28C_{1-2}$), thus arguing a fast and strong glutamatergic drive on flexor-related activity. Similarly, glutamatergic neurons also evoked the strongest motor changes in contralateral flexor muscles in comparison to their antagonist extensors (Fig. $28D_{1-2}$). Although our attempts to stimulate virally transfected ChAT+PPN failed, short photostimulations of cholinergic PPN neurons of crossed transgenic mice evoked long-latency motor responses in the range of 80ms (Fig. 28E), with the strongest motor changes in extensor muscles at the expense of flexors (Fig. $28C_2$ and $28D_2$), thus suggesting a slow but strong drive on extensor-related activity.

Concerning pairs of ipsilateral versus contralateral homologous muscles (Fig. 36), glutamatergic CnF neurons induced a strong drive in the ipsilateral flexor in virally transfected mice, whereas the other glutamatergic neuronal populations evoked a slight bias toward the contralateral flexor muscle (Fig. 36 for ipsi- versus contralateral flexor muscles and Fig. 36B for ipsi- versus contralateral extensor muscles). In summary, short photostimulations of the midbrain evoked a strong motor drive in the mouse at rest, with glutamatergic neurons having a stronger and faster drive on flexor muscles and cholinergic neurons having a stronger but slower drive on extensor muscles.

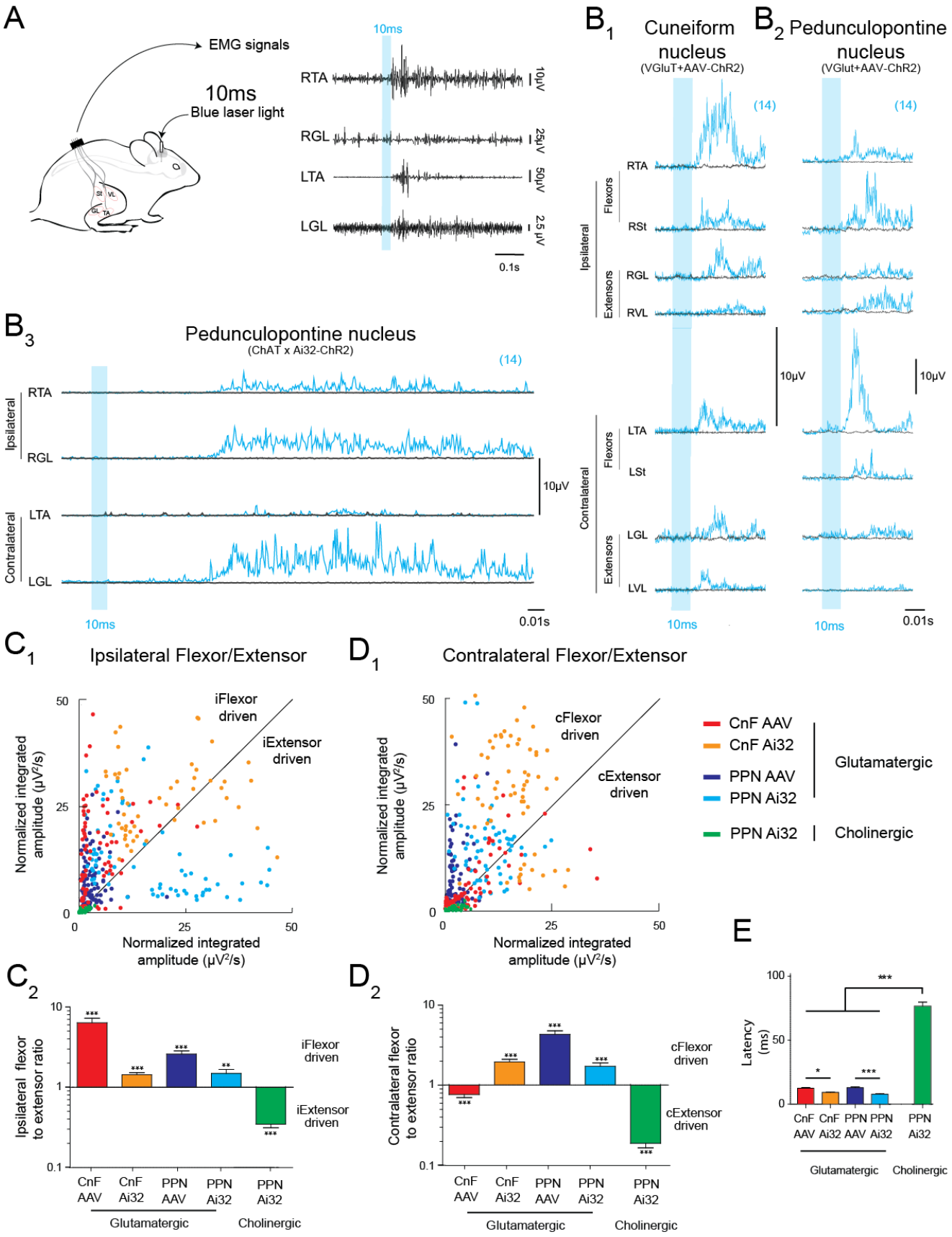

Figure 28: Photoactivations evoke distinct motor responses in the resting mouse.

(A), Short pulses of photostimulation (10ms pulse duration) delivered to the right cuneiform nucleus evoked motor responses in the ankle flexors (right tibialis anterior RTA and left tibialis anterior LTA) and antagonist extensors (right gastrocnemius lateralis RGL and left gastrocnemius lateralis LGL) of the hindlimb in the mouse at rest.

(B), Examples of stimulus-triggered averaging of rectified EMG responses (blue) superimposed on the background EMG activity (mean ± STD in black and grey) in the ankle flexor (RTA), antagonist extensor (RGL), the knee flexor (right semitendinosus RSt) and antagonist extensor (right vastus lateralis RVL) evoked by glutamatergic CnF (B_1), PPN (B_2), or cholinergic PPN (B_3) neurons in freely behaving mice at rest. The number of stimulated sweeps and background EMG activity are in parenthesis in blue.

(C), Amplitude of the integrated motor responses normalized by response duration evoked in the antagonist flexor versus extensor muscle ipsilateral to the stimulation site (C1). Neuronal populations are color-coded. Each dot represents an antagonist flexor versus extensor muscle pair. (C2), Mean and SEM of the ratio of the net integrated amplitude illustrated in C1. Glutamatergic neurons evoked stronger motor responses in flexor muscles than in extensors, whereas cholinergic neurons evoked stronger motor responses in extensor muscles than flexors. (n=7 VGluT2-CRE::AAV-ChR2+CnF, 7 VGluT2-CRE::AAV-ChR2+PPN, and 5 VGluT2-CRExAi32-ChR2+CnF, 5 VGluT2-CRExAi32-ChR2+PPN, and 4 ChAT-CRExAi32-ChR2+PPN; statistical differences were tested with a Wilcoxon signed rank test for a theoretical value of 1).

(D), Amplitude of the integrated motor responses normalized by the response duration evoked in the antagonist flexor versus extensor muscle contralateral to the stimulation site (D1). Neuronal populations are color-coded. Each dot represents an antagonist flexor versus extensor muscle pair. (D2), Mean and SEM of the ratio of the net integrated amplitude illustrated in D1. (n=7 VGluT2-CRE::AAV-ChR2+CnF, 7 VGluT2-CRE::AAV-ChR2+PPN, and 5 VGluT2-CRExAi32-ChR2+CnF, 5 VGluT2-CRExAi32-ChR2+PPN, and 4 ChAT-CRExAi32-ChR2+PPN; statistical differences were tested with a Wilcoxon signed rank test for a theoretical value of 1).

(E), Mean and SEM of the latency of motor responses evoked upon short photostimulations of VGluT2+CnF, +PPN, and ChAT+PPN neurons. (n=7 VGluT2-CRE::AAV-ChR2+CnF, 7 VGluT2-CRE::AAV-ChR2+PPN, and 5 VGluT2-CRExAi32-ChR2+CnF, 5 VGluT2-CRExAi32-ChR2+PPN, and 4 ChAT-CRExAi32-ChR2+PPN; statistical differences were tested by Kruskall-Wallis ($p<0.0001$) with Dunn's multiple comparison post-hoc test, * $P\leq0.005$, ** $P\leq0.001$, *** $P\leq0.0001$).

Glutamatergic CnF initiates locomotion

Given some functional differences in their motor responses in the animal at rest, we further assessed the capacity of these potentially distinct neuronal populations to initiate locomotion using trains of photostimulation in physiological ranges (10ms pulse duration at 20Hz for 1 second). As illustrated by the intralimb coordination, joint movements, EMG traces, and gait diagrams in Fig. 29, glutamatergic CnF stimulation induced locomotion in virally transfected and crossed transgenic mice by increasing the motor and postural tone prior to initiating a short bout of locomotion with a proper alternation between flexor and extensor hindlimb muscles (Fig. 29D$_1$, Supplementary Video 8, Fig. 37 for a high magnification of the Fig. 29D1, and Fig. 39 for VGluT2-Ai32 crossed transgenic mice, , the file was added separately). In line with their phasic motor responses evoked in flexor and extensor muscles upon short pulses of photostimulation in the mouse at rest (Fig. 28B$_2$), glutamatergic PPN neurons evoked a phasic motor activity locked to the stimulation frequency in virally transfected mice (Fig. 29D$_2$, Supplementary Video 8, , the file was added separately), but they failed to initiate locomotion. As with short pulses (Fig. 28B$_3$), long trains of stimulation of cholinergic PPN neurons had little effect, except for increasing the motor tone in hindlimb extensor muscles (Fig. 29D$_3$).

Regarding the histological reconstruction (Fig. 29A-B), all stimulation sites evoking locomotion were restricted within the glutamatergic CnF, whereas most sites located more ventrally within the glutamatergic or cholinergic PPN failed to initiate locomotion. Nevertheless, the most dorsal PPN sites evoked locomotion in crossed transgenic mice (Fig. 29A, 29F, and Fig. 37A$_2$: N= 5 out of 7 PPN sites in VGluT2-cre;Ai32-ChR2 mice). Given the close anatomical proximity between the CnF and the dorsal PPN and the light scattering from the tip of the optical probe, an indirect activation of ChR2-expressing CnF neurons while targeting the PPN could explain, in part, this effect in crossed transgenic mice, thus recapitulating to some extent the locomotor initiation previously reported upon electrical stimulations of the dorsal PPN in decerebrated animals [9].

Assuming a potential depolarizing block of the PPN, we also tested whether modulating the laser power could induce locomotor initiation in virally transfected mice. Again both glutamatergic and cholinergic PPN neurons failed to initiate or evoke episodes

of locomotion, whereas increasing the laser power in glutamatergic CnF neurons increased the maximal locomotor speed (Fig. 29E, data not shown for ChAT-CRExAi32-ChR2). Therefore, in contrast to all other neuronal populations and recent optogenetic studies [19, 20], our results argue that solely the glutamatergic CnF was capable of enhancing motor and postural tone, and of initiating locomotion.

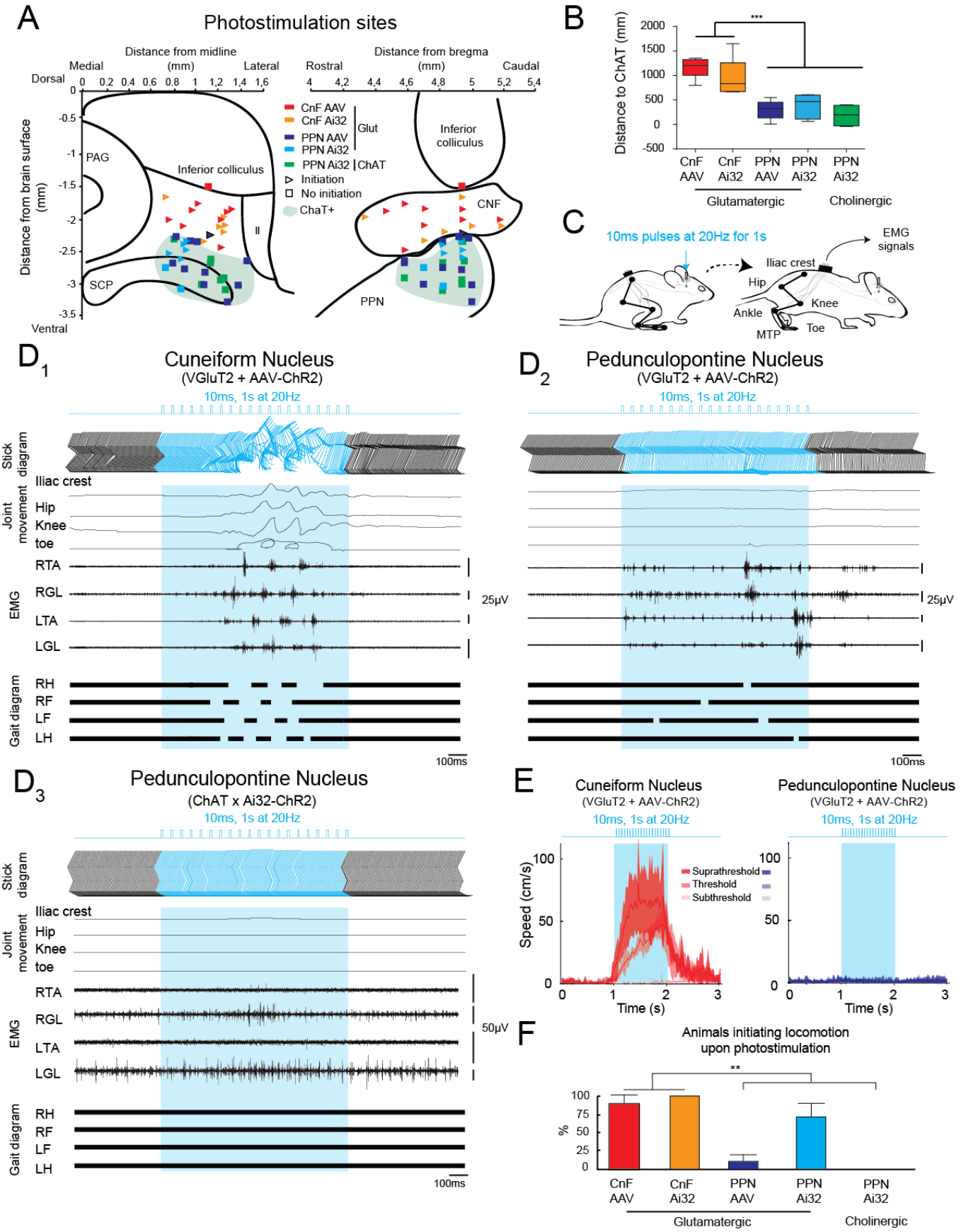

Figure 29: Long trains of photostimulation of glutamatergic CnF neurons initiate locomotion.

(A), Schematic representation of histological identification of stimulated sites evoking locomotion (triangle) or not (square) in virally transfected and crossed transgenic mice. Right, coronal representation; Left, sagittal representation.

(B), Boxplot of the distance of the tip of the cannula from the cholinergic expressing PPN region (Kruskal-wallis, $p<0.0001$, and Tukey HSD test, $p<0.01$).

(C), Experimental design for long trains of photostimulation (10ms pulse duration, 20Hz, 1s) evoking motor, postural, and locomotor changes in the freely behaving mouse initially at rest.

(D), Stick diagram illustrating hindlimb joints, joint movements, toe trajectory, EMG activity, and gait diagram showing the stance (black bar) and swing (gap) phases evoked upon long trains of photostimulation of the glutamatergic CnF (D1), PPN (D2), or cholinergic PPN neurons (D3). The stimulation parameters and period are indicated in blue on top of each example. Note the increase in the height of the iliac crest and the alternation of swing and stance phases in response to photostimulations of the glutamatergic CnF, absent in the two other neuronal populations stimulated.

(E), Plot of instantaneous locomotor speed as a function of time in response to long trains of photostimulation (10ms pulse duration, 20Hz, 1s) delivered at various laser powers (n=4 VGluT2+AAV-ChR2+CnF and 4 VGluT2+AAV-ChR2+PPN).

(F), Bar graph of the proportion of mice initiating locomotion upon long trains of photostimulation, using virally transfected and crossed transgenic mice. Statistical differences between groups (n=9 VGluT2-CRE::AAV-ChR2+CnF, 11 VGluT2-CRE::AAV-ChR2+PPN, and 7 VGluT2-CRExAi32-ChR2+CnF, 7 VGluT2-CRExAi32-ChR2+PPN, and 7 ChAT-CRExAi32-ChR2+PPN; Kruskall-Wallis ($p<0.0001$) with Dunn's multiple comparison post test, * $P\leq0.005$, ** $P\leq0.001$, *** $P\leq0.0001$).

Short photostimulations of midbrain neurons modify the locomotor pattern

We next assessed the functional contribution of these neuronal populations to the locomotor pattern during locomotion at a steady speed. Short photostimulations (10ms pulse duration) were delivered during treadmill locomotion at the threshold laser intensity in virally transfected and crossed transgenic mice (Fig. 30). To assess changes in motor efficacy relative to the level of muscle activity, the step cycle was divided into five equal epochs, synchronized on the ipsilateral right tibialis anterior (RTA), as a proxy of the hindlimb's swing phase (Fig. 30A). Short photostimulations of glutamatergic PPN neurons evoked short-latency excitatory motor responses in the ipsilateral flexor muscle during the swing and stance phases (Fig. $30B_2$, RTA), but inhibitory ones in the ipsilateral extensor (Fig. $30B_2$, RGL). To quantify changes in the motor efficacy according to the locomotor phase, the amplitude of motor responses was normalized on the absolute value of the maximal motor response of each individual muscle throughout the step cycle (Fig. 30C). Upon short photostimulation of the glutamatergic PPN (Fig. 30C-D), excitatory motor responses were overall the highest in flexors during the stance phase when the muscle was relaxed (+100% in red) and minimal during the swing phase when the muscle was active (0% in green), whereas inhibitory motor responses were the lowest in extensors when they were active (-100% in blue).

In contrast, although short photostimulations of glutamatergic CnF neurons evoked short-latency excitatory motor responses in ipsilateral flexor muscles throughout the step cycle and especially during the swing phase (Fig. $30B_1$, 30C), they also evoked short-latency excitatory motor responses in ipsilateral extensor muscles with the highest increases during the stance phase when these muscles were active (Fig. 30D).

As shown in examples (Fig. 30B), short photostimulations also evoked robust motor responses in contralateral hindlimb muscles according to neuronal populations targeted, with similar latencies to ipsilateral ones during their contraction phase (data not shown), thus demonstrating a descending bilateral facilitation of glutamatergic CnF and PPN populations. Such a phase dependency of motor responses throughout the step cycle argues for a gating of descending supraspinal inputs by the spinal locomotor circuit.

Interestingly, short photostimulations of either glutamatergic CnF or PPN neurons evoked a similar and more stereotyped locomotor pattern in crossed transgenic mice, although the CnF evoked weaker motor decreases in extensors than the PPN (Fig. 29C-D), in line with a less specific recruitment of neuronal populations.

In contrast, short photostimulations of cholinergic PPN neurons failed to evoke short-latency motor responses (Fig. 30B_3 and 30C), but increased the duration of the extensor burst (as well as the stimulated step cycle duration) by 15 to 30% in crossed transgenic mice (Fig. 38; see next section about their effects on the locomotor rhythm). This is consistent with long-latency motor responses evoked in bilateral extensor muscles in the resting mouse (Fig. 28C_2-D_2), advancing the hypothesis that cholinergic PPN neurons modulate locomotor pattern by prolonging the extension phase. In summary, whereas glutamatergic CnF neurons increased excitatory drive on bilateral flexor and extensor muscles, and glutamatergic PPN neurons evoked a bilateral facilitation in flexors and a robust inhibition in extensors during locomotion, cholinergic PPN neurons appear to prolong the stance phase. Thus, our results suggest distinct locomotor commands onto the spinal locomotor circuit originating from these different neuronal midbrain populations.

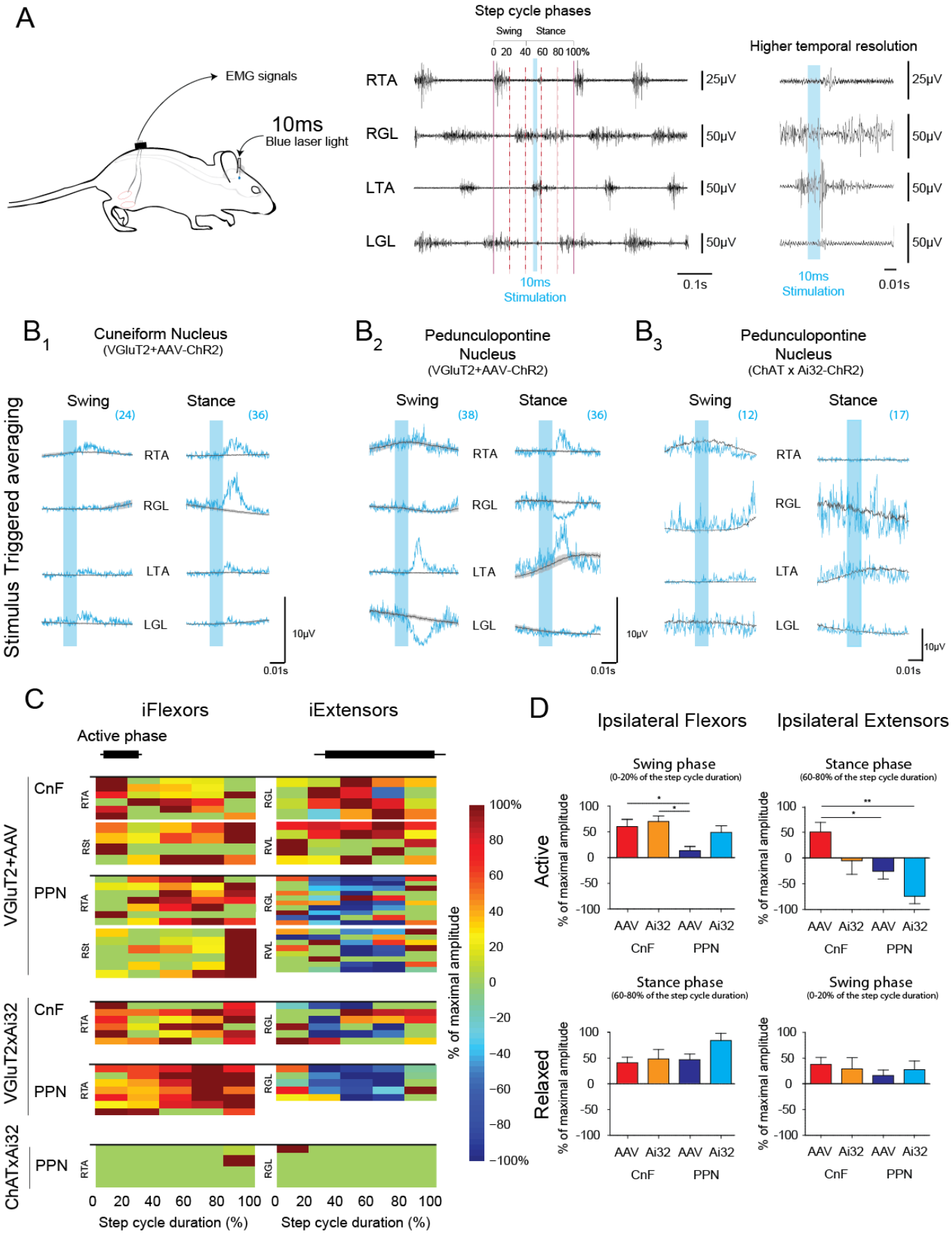

Figure 30: Synaptic changes in the locomotor pattern.

(A), Short pulses of photostimulation (10ms pulse duration) evoked motor responses in flexor (tibialis anterior) and extensor (gastrocnemius lateralis) hindlimb muscles during treadmill locomotion. The step cycle was divided into five equal epochs, synchronized on the onset of the flexor tibialis anterior to investigate phase-dependent motor responses.

(B), Examples of stimulus-triggered averaging of rectified motor responses (blue) superimposed on the background EMG activity (mean ± standard deviation in black and grey) evoked by glutamatergic CnF (B1), PPN (B2), or cholinergic PPN (B3) neurons during the swing and stance phase (0-20% and 60-80% of the step cycle respectively). The number of stimulated sweeps and background EMG activity are in parentheses in blue, respectively.

(C), Color-coded matrix of the amplitude of motor responses of the ipsilateral hindlimb flexor and extensor muscles normalized on the maximal response of each muscle at different phases of the step cycle using virally transfected (AAV-ChR2) and crossed transgenic (Ai32-ChR2) mice. Each line represents a mouse.

(D), Mean and SEM of the normalized amplitude of motor responses evoked by short photostimulations of VGluT2+CnF, PPN, and ChAT+PPN neurons during the swing and stance phase of the right hindlimb ipsilateral to the stimulation site. (n=9 VGluT2-CRE::AAV-ChR2+CnF, 10 VGluT2-CRE::AAV-ChR2+PPN, 6 VGluT2-CRExAi32-ChR2+CnF, 7 VGluT2-CRExAi32-ChR2+PPN, and 6 ChATxAi32-ChR2+PPN; Kruskal-wallis followed by a Dunn's multiple comparison post-test, $p=0.0048$ for the active flexor and $p=0.25$ for the relaxed flexor, $p=0.0038$ for the active extensor, and $p=0.6629$ for the relaxed extensor, * $P\leq0.005$, ** $P\leq0.001$, *** $P\leq0.0001$).

Long photostimulations reset the locomotor rhythm during locomotion

Using long pulses of photostimulation, we next assessed whether these distinct neuronal populations can reset locomotor rhythm during treadmill locomotion. Given that stride duration ranges from 200 to 330ms at a treadmill speed of 15 to 25cm/s, we set the duration of long photostimulations to 50ms to alter about 25-30% of the ongoing step cycle duration, without directly affecting the subsequent step cycles (Fig. 31A). We also used a similar laser intensity to the one used for short photostimulations at rest and during locomotion (Fig. 28-30), in order to activate the same neuronal pool in each individual mouse. As shown by their EMG activity (Fig. $31B_1$) and normalized data for an individual mouse (Fig. $31C_1$) and averaging from each mouse (Fig. $31C_2$ and 31D), 50ms photostimulations of glutamatergic CnF neurons decreased the stimulated and subsequent step cycles by shortening the duration of the ongoing extensor burst and advancing the onset of the next flexor burst in a smooth and rhythmic way, thus resetting and accelerating the locomotor rhythm. In comparison, long photostimulations of glutamatergic PPN neurons increased step cycle duration by prolonging the duration of the extensor burst and by delaying the onset of the next flexor burst (Fig. $31B_2$, $31C_2$ and 31D), thus resetting and slowing down the locomotor rhythm. Similar to the glutamatergic PPN, and in agreement with their long-latency motor responses in the resting mouse (Fig. $28B_3$), long photostimulations of cholinergic PPN neurons also increased extensor burst duration (Fig. $31C_2$ and 31D). In summary, our study shows that the glutamatergic CnF accelerates locomotor rhythm, whereas the glutamatergic PPN, and to a lesser extent the cholinergic PPN, slow down locomotion.

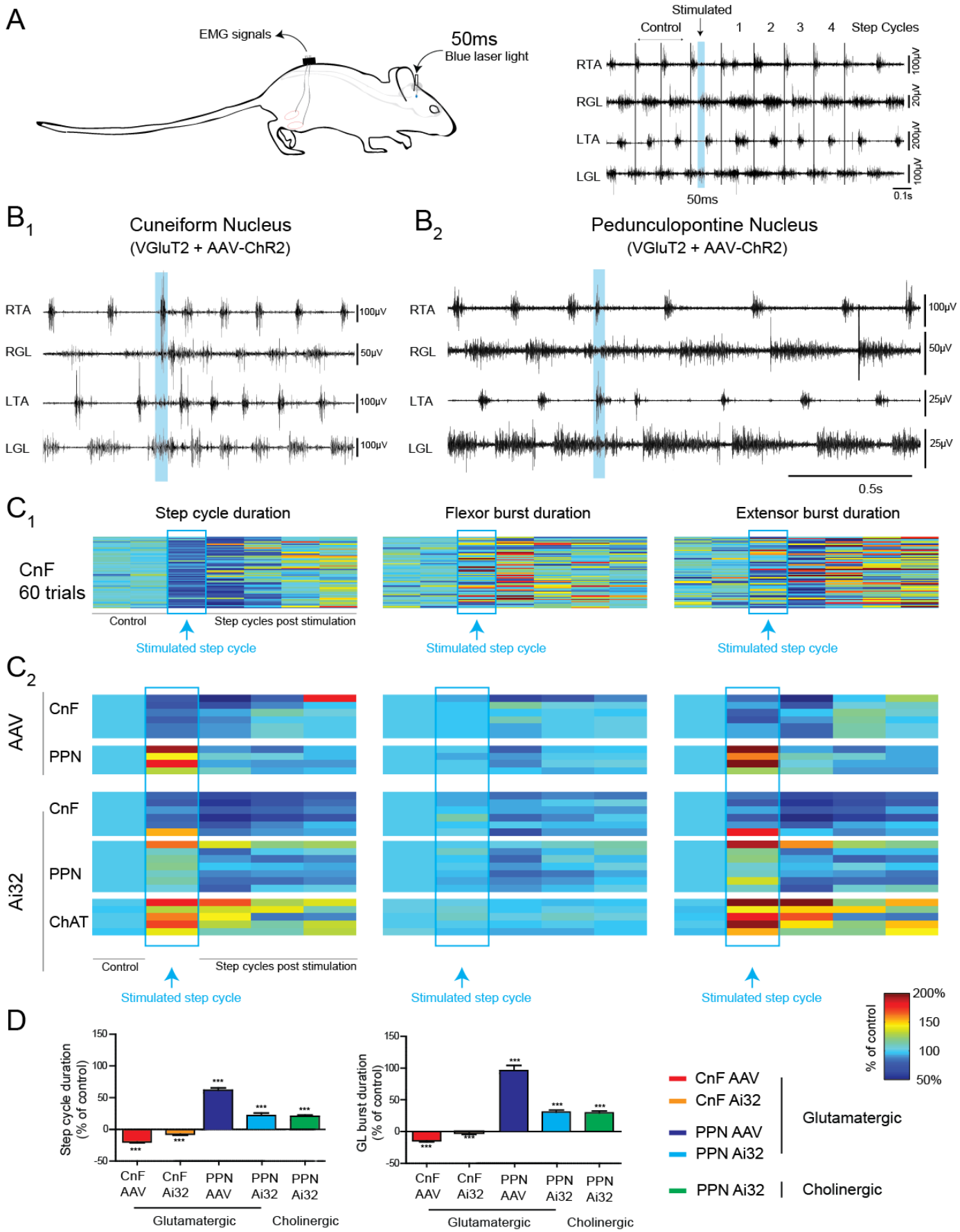

Figure 31: Glutamatergic CnF neurons increase locomotor rhythm.

(A), Left, experimental design. Right, raw EMG traces during locomotion. Photostimulation (50ms in duration) evoked changes in locomotor rhythm.

(B), Examples of raw EMG activity evoked upon 50ms photostimulations of either glutamatergic CnF (B1) or PPN (B2) neurons.

(C), Example of step cycle duration, flexor and extensor burst duration normalized on the pre-stimulus values following long photostimulations of the glutamatergic CnF using a virally transfected mouse (C1). Color-coded matrices of the step cycle duration and flexor and extensor burst duration normalized on the pre-stimulus values following long photostimulations of the glutamatergic CnF, PPN, or cholinergic PPN using virally transfected (AAV-ChR2) and crossed transgenic (Ai32-ChR2) mice (C2).

(D), Mean and SEM of the normalized step cycle duration and extensor burst duration of virally transfected (AAV-ChR2) and crossed transgenic (Ai32-ChR2) mice. Statistical differences between groups (n=5 VGluT2-CRE::AAV-ChR2+CnF, 4 VGluT2-CRE::AAV-ChR2+PPN, 6 VGluT2-CRExAi32-ChR2+CnF, 7 VGluT2-CRExAi32-ChR2+PPN, and 5 ChAT-CRExAi32-ChR2+PPN; statistical differences were tested with a Wilcoxon signed rank test for a theoretical value of 0. (* $P \leq 0.005$, ** $P \leq 0.001$, *** $P \leq 0.0001$).

Long photostimulations modify locomotor gait and speed

Given photostimulation's effect on locomotor rhythm, we next hypothesized that these distinct neuronal populations should be able to modulate locomotor speed and to induce transitions toward running, walking, or stopping gaits. As illustrated by the stick diagram of the hindlimb and EMG recordings ipsilateral to the stimulation site (Fig. 32A-B_1, Supplementary Video 9, the file was added separately), long photostimulations (long trains of 10ms pulse duration at 20Hz for 1 second) of glutamatergic CnF neurons increased motor and postural tone, the angular excursion of the hindlimbs' joints, the height of the iliac crest, as well as the stride height and length. As previously shown [28, 29], using the interlimb coupling, the footfall pattern, and the duty cycle of the stance phase, it is possible to identify and characterize locomotor gaits. In addition to changing the intra-limb kinematics (bottom panel of Fig. 32B_1), long photostimulations of glutamatergic CnF neurons also changed inter-limb coordination from a trot (color-coded in blue in Fig. 32B_1) to a transverse gallop (color-coded in yellow in Fig. 32B_1). The color-coded stacked histogram of gait occurrence shows that the trot, the most comfortable gait used by mice at a treadmill speed of 30 cm/s (Fig. 32C_1), dropped from 80% to 40% upon photostimulation of the glutamatergic CnF in favor of running gaits such as rotary gallop (orange), transverse gallop (yellow), half-bound (orange), and full-bound (red), the fastest running gait in quadrupeds. Note that the occurrence of running gaits was consistent and robust from trial to trial and between mice (Fig. 39 for individual gait analysis). As with electrical stimulations [30], increasing the laser power increased locomotor speed (Fig. 32D_1, Fig. 32E_3, and Fig. 42) and increased the occurrence of running gaits (Fig. 32E_4).

In contrast to glutamatergic CnF, long trains of photostimulations of glutamatergic PPN neurons induced a deceleration of the locomotor speed (Fig. 32B_2, Supplementary Video 9, the file was added separately) with a phasic response in flexor muscles but no effects in extensors, translating into an increase in the stance phase duration, a decrease in the height of the iliac crest, and in the angular excursion of the hindlimb's joints (Fig. 32B_2). Increasing the laser power decreased the locomotor speed (Fig. 32D_2 and 32E) and induced transition of gaits, such as an out-of-phase walk and eventually locomotor arrests (Fig. 32C_2, 32E).

In comparison to these glutamatergic neuronal populations, long trains of photostimulations of cholinergic PPN neurons had very little effect on the transition of gaits (Fig. 32C_3 and 32E): although they reduced locomotor speed, this did not reach significance (Fig. 32D_3). Taken together, our results argue that glutamatergic CnF neurons increased locomotor speed and induced running gaits, whereas glutamatergic PPN neurons decreased locomotor speed, thus contributing to slow-walking gaits and eventually locomotor arrests.

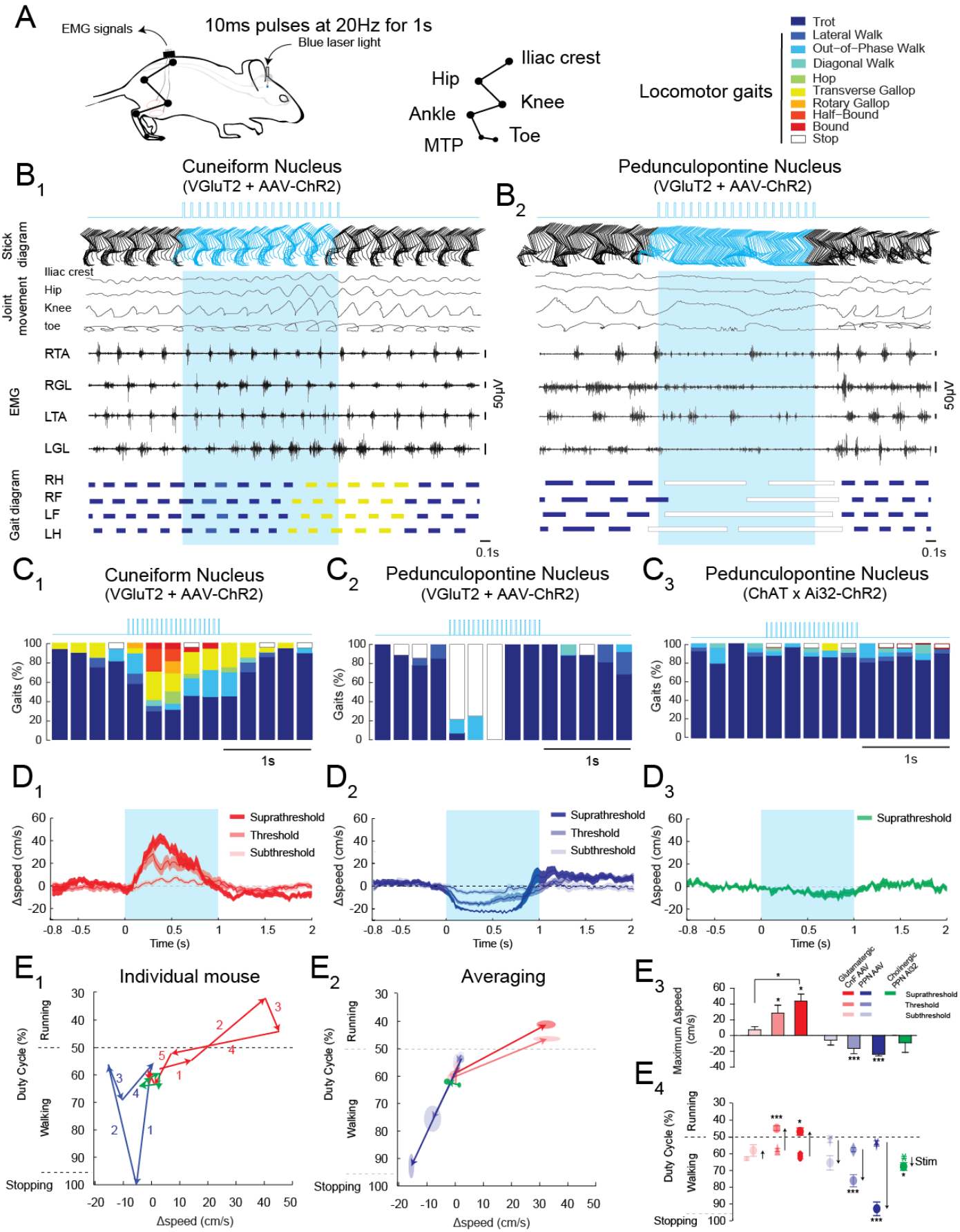

Figure 32: Glutamatergic CnF neurons induce running gaits.

(A) Left, experimental design for kinematic and EMG recordings during long trains of photostimulation (10ms pulse duration, 20Hz, 1s) in the freely behaving mouse during treadmill locomotion at steady speed. Middle, representation of analyzed joints. Right, color codes of gaits.

(B), Stick diagram illustrating hindlimb joints, joint movements, toe trajectory, EMG activity, gait diagrams showing the stance (filled bar) and swing (gap) phases evoked upon long trains of photostimulation applied to the glutamatergic CnF (B1) or PPN (B2). Gait diagrams are color-coded.

(C), Color-coded stacked histograms of gaits occurrence computed in bins of 200 ms before, during, and after long trains of photostimulation (1s) of the glutamatergic CnF (C1), PPN (C2), or cholinergic (C3) PPN neurons at threshold. (n= 3 VGluT2-CRE::AAV-ChR2+CnF, N=5 VGluT2-CRE::AAV-ChR2+PPN, and 6 ChATxAi32-ChR2+PPN).

(D) Plot of instantaneous Δ locomotor speed as a function of time upon long trains of photostimulation of the glutamatergic CnF (D1), PPN (D2), or cholinergic (D3) PPN neurons evoked at different laser power. (n= 4, 6, and 4 VGluT2-CRE::AAV-ChR2+CnF stimulated at subthreshold, threshold, and suprathreshold laser power; n= 4, 7, and 4 VGluT2-CRE::AAV-ChR2+PPN stimulated at subthreshold, threshold, and suprathreshold laser power; n= 4 ChATxAi32-ChR2+PPN at suprathreshold).

(E) Plot of the duty cycle as a function of the Δ locomotor speed. (E1), Examples of step-by-step changes in the duty cycle of the stance phase (delineating running versus walking gaits) as function of the Δ locomotor speed evoked upon long trains of photostimulation of glutamatergic CnF (red), PPN (blue), or cholinergic (green) PPN sites at threshold. The number attached to the vector indicates the step number from the beginning of the stimulation.

(E2), Averaged vectors illustrating maximal changes in the duty cycle of the stance phase (delineating running versus walking gaits) as function of the Δ locomotor speed evoked upon long trains of photostimulation of glutamatergic CnF (red), PPN (blue), or cholinergic (green) PPN as function of the laser power. Areas represent the mean and SEM of the data before and at the maximal changes during the photostimulation period.

(E3), Mean and SEM of locomotor speeds and duty cycle of the stance phase (E4) evoked upon long trains of photostimulation at different laser powers. (One sample t-test, VGluT2-CRE::AAV-ChR2+CnF at subthreshold (n=4, p=0.1619), at threshold (n=6, p=0.016), at suprathreshold (n=4, p=0.148), for VGluT2-CRE::AAV-ChR2+PPN at subthreshold (n=4, p=0.1418), at threshold (n=7, p=0.0005), at suprathreshold (n=4, p=0.0002), and ChATxAi32-ChR2+PPN (n=4, p=0.2348), and one-way ANOVA ($p<0.0001$)).

(E4), Mean and SEM of the duty cycle of the stance phase evoked upon long trains of photostimulation at different laser powers. (Mann-Whitney test, VGluT2-CRE::AAV-ChR2+CnF at subthreshold (n=4, p=0.1179), at threshold (n=6, $p<0.0001$), and at suprathreshold (n=4, p=0.0216), VGluT2-CRE::AAV-ChR2+PPN at subthreshold (n=4, p=0.0578), at threshold (n=7, $p<0.0001$), and at suprathreshold (n=4, p=0.0003), ChATxAi32-ChR2+PPN (n=4, p=0.0216)). (* $P\leq0.005$, ** $P\leq0.001$, *** $P\leq0.0001$).

Long photoinhibitions of the glutamatergic PPN stop locomotion

Having demonstrated the ability of these neuronal midbrain populations to modulate locomotor pattern, rhythm, and gait in different ways, we next wanted to determine their necessity using Halorhodospin-3.0, a yellow-driven chloride pump (Fig. 33A) [31]. All photoinhibited sites were confirmed histologically (Fig. 33B and Fig. 43). Given that the effects were not immediate, we focused on the second step post-inhibition, corresponding to the first step cycle inhibited for its entire duration. As illustrated by our kinematic and motor analysis (Fig. 33C, Supplementary Video 10, the file was added separately), long photoinhibitions of glutamatergic PPN neurons robustly increased the duration of the step cycle and the extensor burst, thus contributing to slowing down and locomotor arrests (Fig. $33C_2$ and 33D). Although photoinhibitions of glutamatergic CnF neurons or cholinergic PPN neurons also increased the step cycle and extensor burst duration, they rarely stopped locomotion (Fig. $33C_1$, $33D_2$, and 33E). Interestingly, among all glutamatergic neuronal populations, the glutamatergic PPN evoked the strongest inhibitory effects on the locomotor step cycle and the extensor burst duration, reaching 150 to 200% increases in the pre-stimulus value following photoinhibition, and could even stop locomotion in up to 45% of trials (Fig. 33E). Nevertheless, all neuronal populations increased the duty cycle of the stance phase (Fig. 33G), thus suggesting that they are all necessary for maintaining locomotion at least at slow and moderate walking speed.

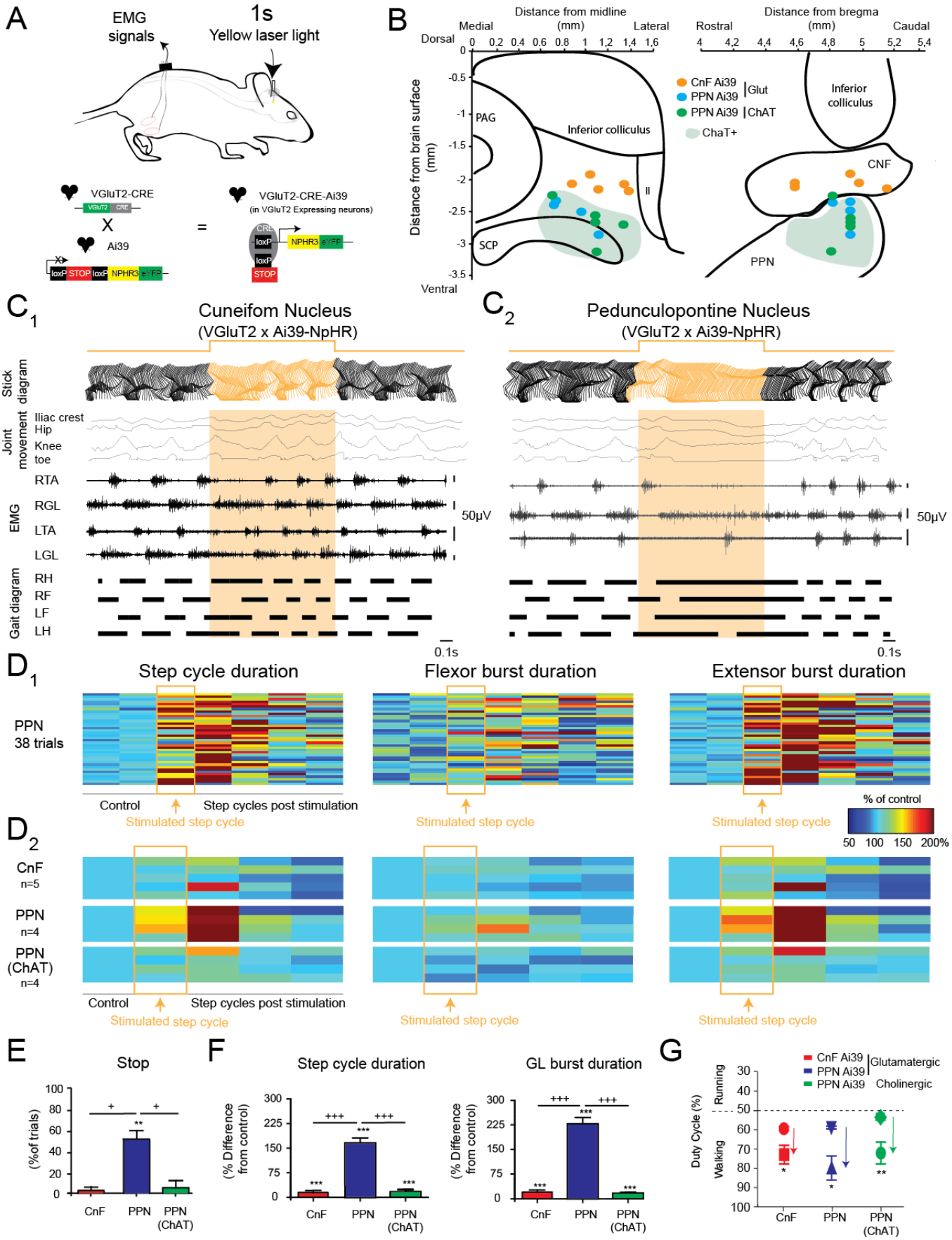

Figure 33: Photoinhibition reveals the contribution of the glutamatergic PPN to slow-waking gait.

(A), Schematic of the experimental design and genetic construct for photoinhibition.

(B), Schematic representation of histologically verified stimulated sites from crossed transgenic mice.

(C), Stick diagram, joint movements, toe trajectory, and gait diagram evoked upon long photoinhibition (1s) of glutamatergic CnF (C1) or PPN (C2) neurons during treadmill locomotion.

(D), Durations of the step cycle, flexor burst, and extensor burst are normalized as a function of pre-stimulus data for the mouse illustrated in C2 (PPN, D1). Color-coded matrices of step cycle duration and flexor and extensor burst duration normalized on the pre-stimulus values following long photoinhibitions of the glutamatergic CnF, PPN, or cholinergic PPN (D2).

(E-F), Bar graph of percentage of stops (mean and SEM) evoked upon long photoinhibitions. Note the significant percentage of stops evoked by inhibition of glutamatergic PPN neurons. (n= 5 VGluT2-CRExAi39-NpHR3.0+CnF, 4 VGluT2-CRExAi39-NpHR3.0+PPN, and 4 ChAT-CRExAi39-NpHR3.0+PPN, Kruskal-wallis (p=0.0103) followed by Dunn's multiple comparison).

(F), Mean and SEM of the normalized step cycle and extensor burst duration of crossed transgenic (Ai39-NpHR3) mice at the maximal change (corresponding to the first step cycle fully inhibited). Group difference from a theoretical value of 100 was tested with a Wilcoxon signed rank test. Step cycle duration: VGluT2-CRExAi39-NpHR3.0+CnF (n= 5, p=0.006), VGluT2-CRExAi39-NpHR3.0+PPN (n= 4, p<0.0001) and ChAT-CRExAi39-NpHR3.0+PPN (n= 4, p=0.0007). Extensor burst duration: VGluT2-CRExAi39-NpHR3.0+CnF (n= 5, p=0.0011), VGluT2-CRExAi39-NpHR3.0+PPN (n= 4, p<0.0001) and ChAT-CRExAi39-NpHR3.0+PPN (n= 4, p=0.0044)).

(G), Mean and SEM of the duty cycle of the stance phase evoked upon long pulses of photoinhibition. Statistical differences from the pre-stimulus control baseline and between groups were tested by Mann-Whitney test for VGluT2-CRExAi39-NpHR3.0+CnF (n= 3, p=0.0406), VGluT2-CRExAi39-NpHR3.0+PPN (n=2, p=0.0268), and ChAT-CRExAi39-NpHR3.0+PPN (n=3, p=0.0048). (* P≤0.005, ** P≤0.001, *** P≤0.0001).

3.6 Discussion

Given its position at the interface of the cortex and spinal cord circuits, the midbrain locomotor region can play a key role by integrating and processing sensory, cognitive, and limbic inputs and translating this information into a motor command adapted to our current environment [32]. However, while electrical stimulations of this functional region can initiate and modulate locomotion, less is known about its presumed anatomical correlates, the Cuneiform Nucleus (CnF) and the Pedunculopontine Nucleus (PPN), and its excitatory neurotransmitter phenotypes, glutamatergic and cholinergic. We aimed here to investigate the functional contribution of these distinct neuronal populations to the motor and locomotor command. Combining kinematic analysis and electrophysiological recordings with discrete optical manipulations, our study reveals that the glutamatergic CnF initiates locomotion, increases the descending drive onto flexor and extensor muscles, and accelerates locomotor rhythm, thus giving rise to running gaits. In contrast, the glutamatergic PPN, and to some extent its cholinergic population, exhibit a different effect on locomotor pattern and rhythm, contributing to slow-walking gaits and locomotor arrests. Our findings show that these supraspinal pathways originating from the mesencephalic locomotor region contribute differently to motor and locomotor command.

Methodological considerations

One of the main challenges in the identification of the anatomical correlates of the mesencephalic locomotor region is to delineate properly the CnF from the PPN. According to previous anatomical studies and the Paxinos atlas [25-27], while the PPN can be easily identified by its cholinergic expression, we identified the CnF as the region circumscribed by the inferior colliculus dorsally, the periaqueductal gray medially, the lateral lemniscus laterally and the cholinergic expressing PPN ventrally.

Although our functional study was limited to one site per animal, our kinematic and EMG recordings allowed us to monitor functional changes in several hindlimb muscles in freely behaving mice upon discrete optical manipulations circumscribed within either the glutamatergic CnF, cholinergic or glutamatergic PPN. These EMG recordings enabled us to

monitor at a high spatiotemporal resolution motor changes that could not have been addressed with a sole kinematic analysis, while photostimulations were set at the minimum laser irradiance to evoke motor transients in most of our experiments, thus preventing any gross changes in behavior or locomotor gait.

Some PPN neurons have been reported to co-express and release glutamate and acetylcholine [14]. Although this population is very small with only a few cells per nucleus, suggesting a main cholinergic drive upon optical stimulation of the cholinergic PPN, it will be important to further assess the functional contribution of this subpopulation using intersectional and subtractive genetic strategies [33].

Calculations derived from brain measurements [34] suggest that irradiance at 1 mm depth has already decreased by 99%. Although we cannot exclude a potential recruitment of the surrounding tissue, photostimulation (or photoinhibition) was likely restricted to the area around the tip of the optical probe. Supporting this conclusion, we found very distinct locomotor effects upon photostimulation of either the glutamatergic CnF or the PPN, but also between the glutamatergic and the cholinergic PPN. And although these functional effects changed as a function of the stimulation frequency and laser power, they were still specific to the site stimulated in both virally transfected and crossed transgenic mice. Furthermore, we also found that increasing the laser power delivered to the glutamatergic CnF invariably increased locomotor speed and induced running gaits, whereas varying the laser power delivered around the threshold to either the glutamatergic or cholinergic PPN invariably slowed down the locomotor rhythm and stopped locomotion without any post-stimulation rebound. Therefore, this excludes the possibility of a depolarizing block or an increasing stimulation efficacy and rather argues the existence of distinct functional dynamics associated with these neuronal populations.

Initiation of locomotion

Standing is a prerequisite to locomotor initiation. In the resting mouse, short photostimulations of all glutamatergic CnF or PPN neurons evoked short-latency motor responses, especially strong in flexor muscles, whereas cholinergic PPN neurons evoked long-latency motor responses preferentially in extensor muscles, thus contributing to motor movements by increasing the motor and likely postural tone. Similar to findings from previous electrical stimulations [9] or optogenetic studies targeting the midbrain region with large volume of AAV-ChR2 (300-500nL) [19, 20], our kinematic and motor analysis showed that long trains of photostimulations at 20Hz delivered above the dorsal glutamatergic PPN, but not the cholinergic PPN, initiated locomotion in crossed transgenic mice. However, using smaller volume injections of AAV-ChR2 (100nL) in virally transfected mice, our results revealed that solely the glutamatergic CnF enhanced motor and postural tone, and initiated locomotion, thus supporting the conclusion that the glutamatergic CnF is the primary supraspinal locomotor center to initiate locomotion.

Modulation of the locomotor pattern and rhythm

Our different patterns of photostimulations and –inhibitions revealed some discrepancy in the descending motor drive, locomotor rhythm, and transitions of gaits, suggesting a fine-tuning of the locomotor command according to neuronal populations targeted.

Long photostimulations of the glutamatergic CnF increased locomotor rhythm, leading predominantly to running gaits, such as gallops and bounds; conversely long photoinhibitions decelerated locomotor rhythm by lengthening the duration of the extensor motor activity, giving rise to slow-walking gaits. Given that short photostimulations of the glutamatergic CnF increased the descending excitatory drive onto both flexor and extensor muscles during ongoing locomotion, it is tempting to hypothesize that this synergistic co-activation of antagonist muscles could contribute to propelling the animal forward by enhancing its muscle tone. Such a behavioral response has been previously reported upon chemical or electrical stimulations in the vicinity of the CnF in freely behaving animals [21,

35, 36], inducing frantic locomotion, explosive jumps, and escape reactions [37], thus supporting the idea that the glutamatergic CnF could be involved in flight reaction to escape unexpected perturbations or predators in a wild environment [38, 39].

In contrast, long pulses of photostimulation of either glutamatergic or cholinergic PPN neurons decelerated locomotor rhythm by increasing the duration of the extensor activity without significantly affecting the flexor motor output. Indeed, short pulses of photostimulation delivered above the glutamatergic PPN also induced an antagonist activation between flexor and extensor muscles. Moreover, long trains of photostimulation delivered at 20 Hz triggered a stereotyped motor pattern following the stimulation, with a short latency increase in flexor muscles followed by a long latency increase in extensor muscles, which never translated into a higher locomotor frequency in contrast to previous electrical and optogenetic studies [19, 20, 40].

Similar to photostimulations, but counterintuitively, long photoinhibitions applied to the glutamatergic PPN also decelerated the locomotor rhythm by increasing the step cycle duration and the extensor burst duration during treadmill locomotion, leading eventually to locomotor arrests at the suprathreshold. Given their short distance, it is possible that our photoinhibition studies in targeting the glutamatergic PPN might have also inhibited a portion of the medial nucleus reticularis pontis oralis, which relays PPN inputs and contributes to the postural tone [9, 41], though inhibition of both glutamatergic and cholinergic PPN failed to decrease the postural tone.

Alternatively, and more likely, it is also possible that the simultaneous recruitment of ascending and descending collaterals of the PPN might impair locomotion [16, 42-44]. In support of that possibility, PPN neurons discharge with a tonic and phasic pattern during goal-directed locomotion in non-human primates [45] and freely behaving mice [46], and stimulation of ascending PPN collaterals to the dopaminergic ventral tegmental area or substantia nigra increases locomotor activity in open field [47-49]. Although there are no studies regarding descending PPN collaterals, there is indirect evidence from their postsynaptic brainstem circuits, which inhibit locomotion in response to their neural activation in freely behaving mice [50, 51] and in decerebrated animal preparations [52]. Therefore, photostimulation of the PPN might slow down locomotion by recruiting

brainstem circuits decreasing locomotor functions, while long photoinhibitions could prevent goal-directed locomotion by shutting down the tonic drive of ascending collaterals of the PPN on the dopaminergic striatum. Further electrophysiological studies will be necessary to decipher how the rostral and caudal parts of the PPN act precisely on these downstream circuits during basic and goal-directed locomotion.

In sharp contrast with a recent study reporting locomotor acceleration upon photoactivation of cholinergic PPN neurons in head-restrained mice [19], we found that activation of the cholinergic PPN had little effect on locomotor speed and gait. Nevertheless, short photostimulations (50ms) reset the locomotor rhythm and long photoinhibitions slowed down walking gait. In line with our findings, blocking the synaptic transmission of cholinergic PPN and laterodorsal tegmentum neurons impairs posture and balance, and increases step frequency during rotarod and catwalk locomotion [53], therefore supporting the functional contribution of cholinergic PPN neurons to slow-walking gaits.

Potential postsynaptic brainstem targets of the mesencephalic locomotor region

Although there is an abundant literature on the postsynaptic brainstem targets recruited by electrical stimulation of the midbrain (for review see [54]), less is known about their neurotransmitter phenotype. As recently reported, genetically identified glutamatergic Chx10 neurons of the gigantocellular reticular nucleus (GRN) express C-FOS (a cell activity marker) following an episode of locomotion [55], and long photostimulations (80 to 500ms) of either Chx10 or glutamatergic GRN neurons can induce a pause during overground or treadmill locomotion [50, 51], thus suggesting that the glutamatergic PPN could slow down and stop locomotion through recruitment of the glutamatergic GRN.

Furthermore, electrical, pharmacological, and optical stimulations, as well as cooling and lesion studies have clearly identified the importance of the ventral aspect of the medullary reticular formation to locomotion [21, 35-37, 56-58]; nevertheless, it is only recently that the serotonergic parapyramidal region and the glutamatergic lateral paragigantocellular nucleus have been identified as important brainstem relays of the

mesencephalic locomotor region for initiating and accelerating locomotion [59-61]. Further studies using intersectional and subtractive genetics will be necessary to uncover the neuronal populations of the pontomedullary reticular formation integrating midbrain inputs pertaining to motor control and locomotion [33].

Clinical implication

Over the last decade, the PPN has been proposed as an alternative Deep Brain Stimulation (DBS) target for people with Parkinson's disease who are refractory to pharmacological treatments. Although PPN stimulation improves gait and postural adjustments in some advanced Parkinson's disease patients, the functional outcomes have been extremely variable across clinical studies [62-64]. Such variability, also reported in 6-OHDA-treated rodents [65], suggests that the PPN might not be the best target for improving locomotor functions in these patients. Although the most effective site for inducing locomotion was found to be the CnF and the dorsal part of the PPN [5, 8, 9, 21, 40], our results argue that the glutamatergic CnF might be a better therapeutic target for initiating locomotion and potentially treating akinesia in Parkinson's disease**.**

In addition, co-contraction is one of the hallmarks of Parkinson's disease [66-69], and dopaminergic treatment decreases the activity in flexor muscles and consequently the rigidity in Parkinson's patients [70]. Interestingly, our results show that glutamatergic CnF neurons have a preferential access onto both flexor and extensor locomotor circuits in comparison to glutamatergic and cholinergic PPN neurons. Given the increased number of activated neurons in the CnF in a mouse model of Parkinson's disease [71], cell atrophy and death in the cholinergic PPN in Parkinson's disease patients [72-75], and the fact that cholinergic denervation seems to predict gait impairment more accurately than dopaminergic denervation alone (Bohnen et al. 2013), our results suggest that the co-contraction and rigidity in Parkinson's disease might be due to an unbalanced activity between the CnF and PPN.

More recently, electrical stimulation of the midbrain locomotor region has been reported to improve functional locomotor recovery in rodent models of spinal cord injury,

even with very limited spared white matter [76, 77]. With current and ongoing clinical trials assessing the midbrain locomotor region as a brain target for improving locomotor gait in Parkinson's disease and incomplete spinal cord injury patients [78], our study stresses the importance of carefully choosing neuronal targets according to the expected functional locomotor outcome.

Conclusion

In summary, our locomotor study reveals distinct neuronal populations in the midbrain, which by their specific phasic or tonic effects can adapt postural adjustments and locomotor commands in the freely behaving mouse. By their subtle motor control, both glutamatergic and cholinergic PPN could modulate slow-walking gait, whereas the glutamatergic CnF would more likely contribute to flight reaction to escape predators by triggering running gaits.

Acknowledgments

Resources, Mr. Philippe Drapeau for software development; Mr. Hugo Delivet-Mongrain and Ms. Cloé Brindamour for technical help, and Dr. Karl Deisseroth for his kind gift of AAV-DiO-mCherry-ChR2.

Declaration of Interests

The authors declare no competing interests.

3.7 References

1. Rossignol, S., Frigon, A., Barriere, G., Martinez, M., Barthelemy, D., Bouyer, L., Belanger, M., Provencher, J., Chau, C., Brustein, E., et al. (2011). Chapter 16--spinal plasticity in the recovery of locomotion. Progress in brain research *188*, 229-241.
2. Shik, M.L., Severin, F.V., and Orlovsky, G.N. (1969). Control of walking and running by means of electrical stimulation of the mesencephalon. Electroencephalography and clinical neurophysiology *26*, 549.
3. Mori, S., Nishimura, H., Kurakami, C., Yamamura, T., and Aoki, M. (1978). Controlled locomotion in the mesencephalic cat: distribution of facilitatory and inhibitory regions within pontine tegmentum. J Neurophysiol *41*, 1580-1591.
4. Ryczko, D., and Dubuc, R. (2013). The multifunctional mesencephalic locomotor region. Curr Pharm Des *19*, 4448-4470.
5. Garcia-Rill, E., Skinner, R.D., and Fitzgerald, J.A. (1985). Chemical activation of the mesencephalic locomotor region. Brain research *330*, 43-54.
6. Skinner, R.D., Kinjo, N., Ishikawa, Y., Biedermann, J.A., and Garcia-Rill, E. (1990). Locomotor projections from the pedunculopontine nucleus to the medioventral medulla. Neuroreport *1*, 207-210.
7. Garcia-Rill, E., and Skinner, R.D. (1987). The mesencephalic locomotor region. I. Activation of a medullary projection site. Brain research *411*, 1-12.
8. Takakusaki, K., Kohyama, J., and Matsuyama, K. (2003). Medullary reticulospinal tract mediating a generalized motor inhibition in cats: III. Functional organization of spinal interneurons in the lower lumbar segments. Neuroscience *121*, 731-746.
9. Takakusaki, K., Habaguchi, T., Ohtinata-Sugimoto, J., Saitoh, K., and Sakamoto, T. (2003). Basal ganglia efferents to the brainstem centers controlling postural muscle tone and locomotion: a new concept for understanding motor disorders in basal ganglia dysfunction. Neuroscience *119*, 293-308.
10. Habaguchi, T., Takakusaki, K., Saitoh, K., Sugimoto, J., and Sakamoto, T. (2002). Medullary reticulospinal tract mediating the generalized motor inhibition in cats: II. Functional organization within the medullary reticular formation with respect to postsynaptic inhibition of forelimb and hindlimb motoneurons. Neuroscience *113*, 65-77.
11. Iwakiri, H., Oka, T., Takakusaki, K., and Mori, S. (1995). Stimulus effects of the medial pontine reticular formation and the mesencephalic locomotor region upon medullary reticulospinal neurons in acute decerebrate cats. Neuroscience research *23*, 47-53.
12. Kelland, M.D., and Asdourian, D. (1989). Pedunculopontine tegmental nucleus-induced inhibition of muscle activity in the rat. Behavioural brain research *34*, 213-234.

13. Lai, Y.Y., and Siegel, J.M. (1990). Muscle tone suppression and stepping produced by stimulation of midbrain and rostral pontine reticular formation. J Neurosci *10*, 2727-2734.
14. Wang, H.-L., and Morales, M. (2009). Pedunculopontine and laterodorsal tegmental nuclei contain distinct populations of cholinergic, glutamatergic and GABAergic neurons in the rat. In Eur. J. Neurosci., Volume 29. pp. 340-358.
15. Mena-Segovia, J., Micklem, B.R., Nair-Roberts, R.G., Ungless, M.A., and Bolam, J.P. (2009). GABAergic neuron distribution in the pedunculopontine nucleus defines functional subterritories. In J. Comp. Neurol., Volume 515. pp. 397-408.
16. Martinez-Gonzalez, C., Wang, H.-L., Micklem, B.R., Bolam, J.P., and Mena-Segovia, J. (2012). Subpopulations of cholinergic, GABAergic and glutamatergic neurons in the pedunculopontine nucleus contain calcium-binding proteins and are heterogeneously distributed. In Eur. J. Neurosci., Volume 35. pp. 723-734.
17. Brocard, F., and Dubuc, R. (2003). Differential contribution of reticulospinal cells to the control of locomotion induced by the mesencephalic locomotor region. J Neurophysiol *90*, 1714-1727.
18. Le Ray, D., Brocard, F., Bourcier-Lucas, C., Auclair, F., Lafaille, P., and Dubuc, R. (2003). Nicotinic activation of reticulospinal cells involved in the control of swimming in lampreys. Eur J Neurosci *17*, 137-148.
19. Roseberry, T.K., Lee, A.M., Lalive, A.L., Wilbrecht, L., Bonci, A., and Kreitzer, A.C. (2016). Cell-Type-Specific Control of Brainstem Locomotor Circuits by Basal Ganglia. Cell *164*, 526-537.
20. Lee, A.M., Hoy, J.L., Bonci, A., Wilbrecht, L., Stryker, M.P., and Niell, C.M. (2014). Identification of a brainstem circuit regulating visual cortical state in parallel with locomotion. Neuron *83*, 455-466.
21. Milner, K.L., and Mogenson, G.J. (1988). Electrical and chemical activation of the mesencephalic and subthalamic locomotor regions in freely moving rats. Brain research *452*, 273-285.
22. Brudzynski, S.M., Wu, M., and Mogenson, G.J. (1988). Modulation of locomotor activity induced by injections of carbachol into the tegmental pedunculopontine nucleus and adjacent areas in the rat. Brain research *451*, 119-125.
23. Josset, N., Roussel, M., Lemieux, M., and Bretzner, F. (2016). Functional contribution of the mesencephalic locomotor region to locomotor control. In Session 808 - Gait: Muscle Activity, Exercise, and Biomechanics. (Society for Neuroscience).
24. Jordan, L.M. (1998). Initiation of locomotion in mammals. Annals of the New York Academy of Sciences *860*, 83-93.
25. Kroeger, D., Ferrari, L.L., Petit, G., Mahoney, C.E., Fuller, P.M., Arrigoni, E., and Scammell, T.E. (2017). Cholinergic, Glutamatergic, and GABAergic Neurons of the Pedunculopontine Tegmental Nucleus Have Distinct Effects on Sleep/Wake Behavior in Mice. In J. Neurosci., Volume 37. pp. 1352-1366.

26. VanderHorst, V.G., and Ulfhake, B. (2006). The organization of the brainstem and spinal cord of the mouse: relationships between monoaminergic, cholinergic, and spinal projection systems. Journal of chemical neuroanatomy *31*, 2-36.
27. Paxinos, G., and Franklin, K.B.J. (2003). The Mouse Brain in Stereotaxic Coordinates, Compact Second Edition Edition, (Academic Press).
28. Lemieux, M., Josset, N., Roussel, M., Couraud, S., and Bretzner, F. (2016). Speed-Dependent Modulation of the Locomotor Behavior in Adult Mice Reveals Attractor and Transitional Gaits. Front Neurosci *10*, 42.
29. Thiry, L., Lemieux, M., and Bretzner, F. (2017). Age- and Speed-Dependent Modulation of Locomotor Gaits in Dscam2j Mutant Mice. J Neurophysiol, jn 00471 02017.
30. Garcia-Rill, E., Houser, C.R., Skinner, R.D., Smith, W., and Woodward, D.J. (1987). Locomotion-inducing sites in the vicinity of the pedunculopontine nucleus. Brain research bulletin *18*, 731-738.
31. Madisen, L., Mao, T., Koch, H., Zhuo, J.M., Berenyi, A., Fujisawa, S., Hsu, Y.W., Garcia, A.J., 3rd, Gu, X., Zanella, S., et al. (2012). A toolbox of Cre-dependent optogenetic transgenic mice for light-induced activation and silencing. Nature neuroscience *15*, 793-802.
32. Mena-Segovia, J., and Bolam, J.P. (2017). Rethinking the Pedunculopontine Nucleus: From Cellular Organization to Function. In Neuron, Volume 94. pp. 7-18.
33. Zeng, H., and Madisen, L. (2012). Mouse transgenic approaches in optogenetics. Progress in brain research *196*, 193-213.
34. Yizhar, O., Fenno, L.E., Davidson, T.J., Mogri, M., and Deisseroth, K. (2011). Optogenetics in neural systems. Neuron *71*, 9-34.
35. Coles, S.K., Iles, J.F., and Nicolopoulos-Stournaras, S. (1989). The mesencephalic centre controlling locomotion in the rat. Neuroscience *28*, 149-157.
36. Mori, S., Sakamoto, T., Ohta, Y., Takakusaki, K., and Matsuyama, K. (1989). Site-specific postural and locomotor changes evoked in awake, freely moving intact cats by stimulating the brainstem. Brain research *505*, 66-74.
37. Depoortere, R., Di Scala, G., and Sandner, G. (1990). Treadmill locomotion and aversive effects induced by electrical stimulation of the mesencephalic locomotor region in the rat. Brain research bulletin *25*, 723-727.
38. Han, W., Tellez, L.A., Rangel, M.J., Jr., Motta, S.C., Zhang, X., Perez, I.O., Canteras, N.S., Shammah-Lagnado, S.J., van den Pol, A.N., and de Araujo, I.E. (2017). Integrated Control of Predatory Hunting by the Central Nucleus of the Amygdala. Cell *168*, 311-324 e318.
39. Zingg, B., Chou, X.L., Zhang, Z.G., Mesik, L., Liang, F., Tao, H.W., and Zhang, L.I. (2017). AAV-Mediated Anterograde Transsynaptic Tagging: Mapping Corticocollicular Input-Defined Neural Pathways for Defense Behaviors. Neuron *93*, 33-47.

40. Garcia-Rill, E., Kinjo, N., Atsuta, Y., Ishikawa, Y., Webber, M., and Skinner, R.D. (1990). Posterior midbrain-induced locomotion. Brain research bulletin *24*, 499-508.
41. Sherman, D., Fuller, P.M., Marcus, J., Yu, J., Zhang, P., Chamberlin, N.L., Saper, C.B., and Lu, J. (2015). Anatomical Location of the Mesencephalic Locomotor Region and Its Possible Role in Locomotion, Posture, Cataplexy, and Parkinsonism. Frontiers in neurology *6*, 140.
42. Ros, H., Magill, P.J., Moss, J., Bolam, J.P., and Mena-Segovia, J. (2010). Distinct types of non-cholinergic pedunculopontine neurons are differentially modulated during global brain states. In Neuroscience, Volume 170. pp. 78-91.
43. Martinez-Gonzalez, C., van Andel, J., Bolam, J.P., and Mena-Segovia, J. (2014). Divergent motor projections from the pedunculopontine nucleus are differentially regulated in Parkinsonism. In Brain Struct Funct, Volume 219. pp. 1451-1462.
44. Martinez-Gonzalez, C., Bolam, J.P., and Mena-Segovia, J. (2011). Topographical organization of the pedunculopontine nucleus. Frontiers in neuroanatomy *5*, 22.
45. Goetz, L., Piallat, B., Bhattacharjee, M., Mathieu, H., David, O., and Chabardes, S. (2016). On the Role of the Pedunculopontine Nucleus and Mesencephalic Reticular Formation in Locomotion in Nonhuman Primates. In J. Neurosci., Volume 36. (Society for Neuroscience), pp. 4917-4929.
46. Thompson, J.A., and Felsen, G. (2013). Activity in mouse pedunculopontine tegmental nucleus reflects action and outcome in a decision-making task. In J. Neurophysiol., Volume 110. pp. 2817-2829.
47. Estakhr, J., Abazari, D., Frisby, K., McIntosh, J.M., and Nashmi, R. (2017). Differential Control of Dopaminergic Excitability and Locomotion by Cholinergic Inputs in Mouse Substantia Nigra. In Curr. Biol., Volume 27. pp. 1900-1914.e1904.
48. Dautan, D., Souza, A.S., Huerta-Ocampo, I., Valencia, M., Assous, M., Witten, I.B., Deisseroth, K., Tepper, J.M., Bolam, J.P., Gerdjikov, T.V., et al. (2016). Segregated cholinergic transmission modulates dopamine neurons integrated in distinct functional circuits. In Nat. Neurosci.
49. Xiao, C., Cho, J.R., Zhou, C., Treweek, J.B., Chan, K., McKinney, S.L., Yang, B., and Gradinaru, V. (2016). Cholinergic Mesopontine Signals Govern Locomotion and Reward through Dissociable Midbrain Pathways. In Neuron, Volume 90. pp. 333-347.
50. Bouvier, J., Caggiano, V., Leiras, R., Caldeira, V., Bellardita, C., Balueva, K., Fuchs, A., and Kiehn, O. (2015). Descending Command Neurons in the Brainstem that Halt Locomotion. Cell *163*, 1191-1203.
51. Lemieux, M., and Bretzner, F. (2016). Functional contribution of glutamatergic neurons of the medullary reticular formation to the motor control in mice. Volume 536.04 / CCC14. (San Diego, CA: Society for Neuroscience).
52. Takakusaki, K., Kohyama, J., Matsuyama, K., and Mori, S. (2001). Medullary reticulospinal tract mediating the generalized motor inhibition in cats: parallel

inhibitory mechanisms acting on motoneurons and on interneuronal transmission in reflex pathways. Neuroscience *103*, 511-527.

53. Janickova, H., Rosborough, K., and Al Onaizi, M. (2017). Deletion of the vesicular acetylcholine transporter from pedunculopontine/laterodorsal tegmental neurons modifies gait - Janickova - 2017 - Journal of Neurochemistry - Wiley Online Library. In Journal of ….
54. Takakusaki, K., Chiba, R., Nozu, T., and Okumura, T. (2016). Brainstem control of locomotion and muscle tone with special reference to the role of the mesopontine tegmentum and medullary reticulospinal systems. In J Neural Transm, Volume 123. pp. 695-729.
55. Bretzner, F., and Brownstone, R.M. (2013). Lhx3-Chx10 reticulospinal neurons in locomotor circuits. J Neurosci *33*, 14681-14692.
56. Noga, B.R., Kriellaars, D.J., and Jordan, L.M. (1991). The effect of selective brainstem or spinal cord lesions on treadmill locomotion evoked by stimulation of the mesencephalic or pontomedullary locomotor regions. J Neurosci *11*, 1691-1700.
57. Noga, B.R., Kriellaars, D.J., Brownstone, R.M., and Jordan, L.M. (2003). Mechanism for activation of locomotor centers in the spinal cord by stimulation of the mesencephalic locomotor region. J Neurophysiol *90*, 1464-1478.
58. Hagglund, M., Borgius, L., Dougherty, K.J., and Kiehn, O. (2010). Activation of groups of excitatory neurons in the mammalian spinal cord or hindbrain evokes locomotion. Nature neuroscience *13*, 246-252.
59. Jordan, L.M., Liu, J., Hedlund, P.B., Akay, T., and Pearson, K.G. (2008). Descending command systems for the initiation of locomotion in mammals. Brain Res Rev *57*, 183-191.
60. Liu, J., and Jordan, L.M. (2005). Stimulation of the parapyramidal region of the neonatal rat brain stem produces locomotor-like activity involving spinal 5-HT7 and 5-HT2A receptors. J Neurophysiol *94*, 1392-1404.
61. Capelli, P., Pivetta, C., Soledad Esposito, M., and Arber, S. (2017). Locomotor speed control circuits in the caudal brainstem. In Nature.
62. Mazzone, P., Insola, A., Lozano, A., Galati, S., Scarnati, E., Peppe, A., Stanzione, P., and Stefani, A. (2007). Peripeduncular and pedunculopontine nuclei: a dispute on a clinically relevant target. Neuroreport *18*, 1407-1408.
63. Mazzone, P., Lozano, A., Stanzione, P., Galati, S., Scarnati, E., Peppe, A., and Stefani, A. (2005). Implantation of human pedunculopontine nucleus: a safe and clinically relevant target in Parkinson's disease. Neuroreport *16*, 1877-1881.
64. Stefani, A., Lozano, A.M., Peppe, A., Stanzione, P., Galati, S., Tropepi, D., Pierantozzi, M., Brusa, L., Scarnati, E., and Mazzone, P. (2007). Bilateral deep brain stimulation of the pedunculopontine and subthalamic nuclei in severe Parkinson's disease. Brain *130*, 1596-1607.

65. Rauch, F., Schwabe, K., and Krauss, J.K. (2010). Effect of deep brain stimulation in the pedunculopontine nucleus on motor function in the rat 6-hydroxydopamine Parkinson model. Behavioural brain research *210*, 46-53.
66. Andrews, C.J., Burke, D., and Lance, J.W. (1972). The response to muscle stretch and shortening in Parkinsonian rigidity. Brain *95*, 795-812.
67. Tatton, W.G., and Lee, R.G. (1975). Evidence for abnormal long-loop reflexes in rigid Parkinsonian patients. Brain research *100*, 671-676.
68. Berardelli, A., Sabra, A.F., and Hallett, M. (1983). Physiological mechanisms of rigidity in Parkinson's disease. Journal of neurology, neurosurgery, and psychiatry *46*, 45-53.
69. Xia, R., Powell, D., Rymer, W.Z., Hanson, N., Fang, X., and Threlkeld, A.J. (2011). Differentiation between the contributions of shortening reaction and stretch-induced inhibition to rigidity in Parkinson's disease. Experimental brain research. Experimentelle Hirnforschung *209*, 609-618.
70. Selionov, V.A., Solopova, I.A., Zhvansky, D.S., Karabanov, A.V., Chernikova, L.A., Gurfinkel, V.S., and Ivanenko, Y.P. (2013). Lack of non-voluntary stepping responses in Parkinson's disease. Neuroscience *235*, 96-108.
71. Heise, C.E., and Mitrofanis, J. (2006). Fos immunoreactivity in some locomotor neural centres of 6OHDA-lesioned rats. Anatomy and embryology *211*, 659-671.
72. Hirsch, E.C., Graybiel, A.M., Duyckaerts, C., and Javoy-Agid, F. (1987). Neuronal loss in the pedunculopontine tegmental nucleus in Parkinson disease and in progressive supranuclear palsy. Proceedings of the National Academy of Sciences of the United States of America *84*, 5976-5980.
73. Jellinger, K. (1988). The pedunculopontine nucleus in Parkinson's disease, progressive supranuclear palsy and Alzheimer's disease. Journal of neurology, neurosurgery, and psychiatry *51*, 540-543.
74. Zweig, R.M., Jankel, W.R., Hedreen, J.C., Mayeux, R., and Price, D.L. (1989). The pedunculopontine nucleus in Parkinson's disease. Ann Neurol *26*, 41-46.
75. Karachi, C., Grabli, D., Bernard, F.A., Tande, D., Wattiez, N., Belaid, H., Bardinet, E., Prigent, A., Nothacker, H.P., Hunot, S., et al. (2010). Cholinergic mesencephalic neurons are involved in gait and postural disorders in Parkinson disease. The Journal of clinical investigation *120*, 2745-2754.
76. Bachmann, L.C., Matis, A., Lindau, N.T., Felder, P., Gullo, M., and Schwab, M.E. (2013). Deep brain stimulation of the midbrain locomotor region improves paretic hindlimb function after spinal cord injury in rats. Science translational medicine *5*, 208ra146.
77. Zorner, B., Bachmann, L.C., Filli, L., Kapitza, S., Gullo, M., Bolliger, M., Starkey, M.L., Rothlisberger, M., Gonzenbach, R.R., and Schwab, M.E. (2014). Chasing central nervous system plasticity: the brainstem's contribution to locomotor recovery in rats with spinal cord injury. Brain *137*, 1716-1732.

78. Stieglitz, L.H., and Prusse, A. (2017). Deep Brain Stimulation in Patients With Incomplete Spinal Cord Injury for Improvement of Gait (DBS-SCI). p. Clinical trial.
79. Bretzner, F., and Drew, T. (2005). Contribution of the motor cortex to the structure and the timing of hindlimb locomotion in the cat: a microstimulation study. J Neurophysiol *94*, 657-672.

3.8 Supplementary figures

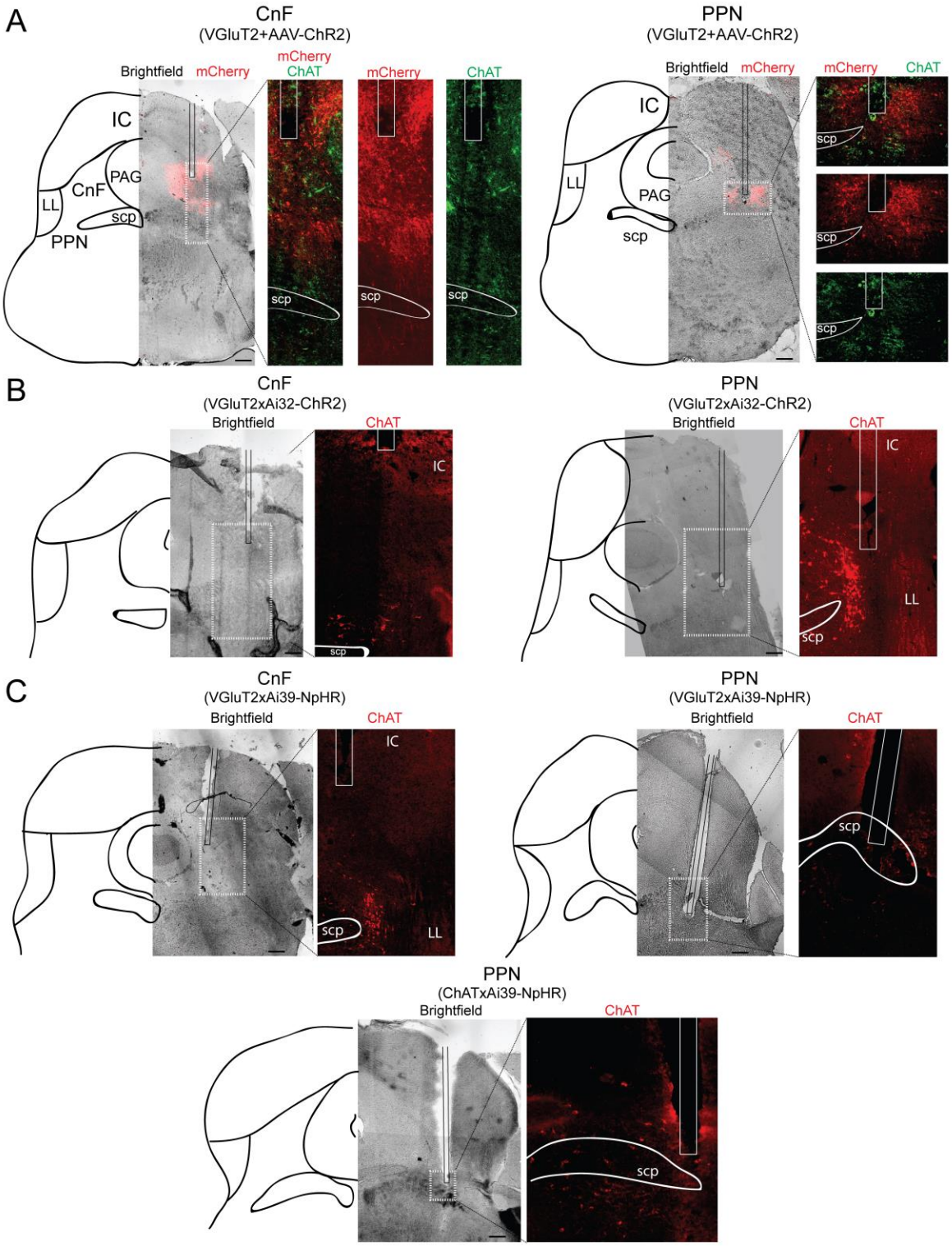

Figure 34: Histological identification of stimulated sites in virally transfected (VGluT2-CRE + AAV-ChR2) and crossed transgenic (VGluT2-CRE or ChAT-CRE x Ai32-ChR2/Ai39-NpHR3.0) mice

(A), Left, low-magnification images illustrating the extent of the cre-lox recombination (mCherry in red) and the position of the cannula in bright field. Right, high-magnification images illustrating the cre-lox recombination (mCherry in red) and the cholinergic staining (green) at the level of the tip of the optical cannula located within the CnF or PPN of virally transfected (VGluT2-CRE + AAV-ChR2) mice.
(B), left, low-magnification images illustrating the position of the cannula in bright field. Right, high-magnification images illustrating cholinergic staining (red) at the level of the optical cannula located within the CnF or PPN of crossed transgenic (VGluT2-CRE or ChAT-CRE x Ai32-ChR2) mice.
(C), Low- and high-magnification images illustrating the extent of the cholinergic staining (red) at the level of the tip of the optical cannula located within the CnF or PPN of crossed transgenic (VGluT2-CRE or ChAT-CRE x Ai39-NpHR3.0) mice.
Abbreviations: CnF: Cuneiform Nucleus, IC: Inferior Colliculus, LL: Lateral Lemniscus, PAG: Periaqueductal Gray, PPN: Pedunculopontine Nucleus, scp: Superior Cerebellar Peduncle. Scale bar: 500µm.

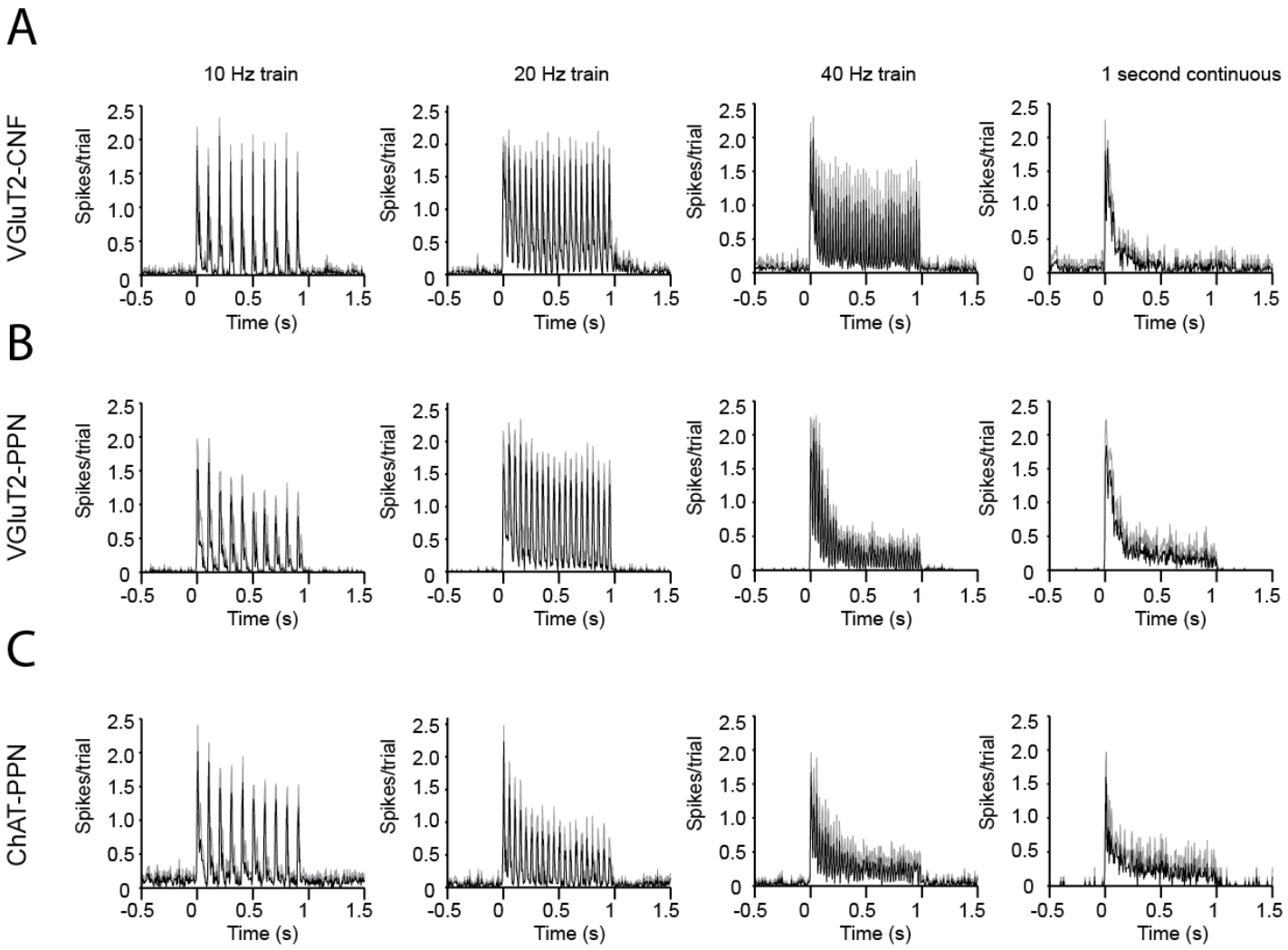

Figure 35: Firing pattern upon long photostimulations.

(A-C), Firing patterns of VGluT2+CnF (A), VGluT2+PPN (B) or ChAT+PPN (C) neurons upon long trains of photostimulations (10ms pulse duration) at 10, 20, 40Hz and upon a continuous pulse for 1 second in crossed transgenic mice (VGluT2-CRE or ChAT-CRE x Ai32-ChR2). Note the sustained firing frequency as function of the stimulation frequency up to 20Hz in all neuronal populations targeted.

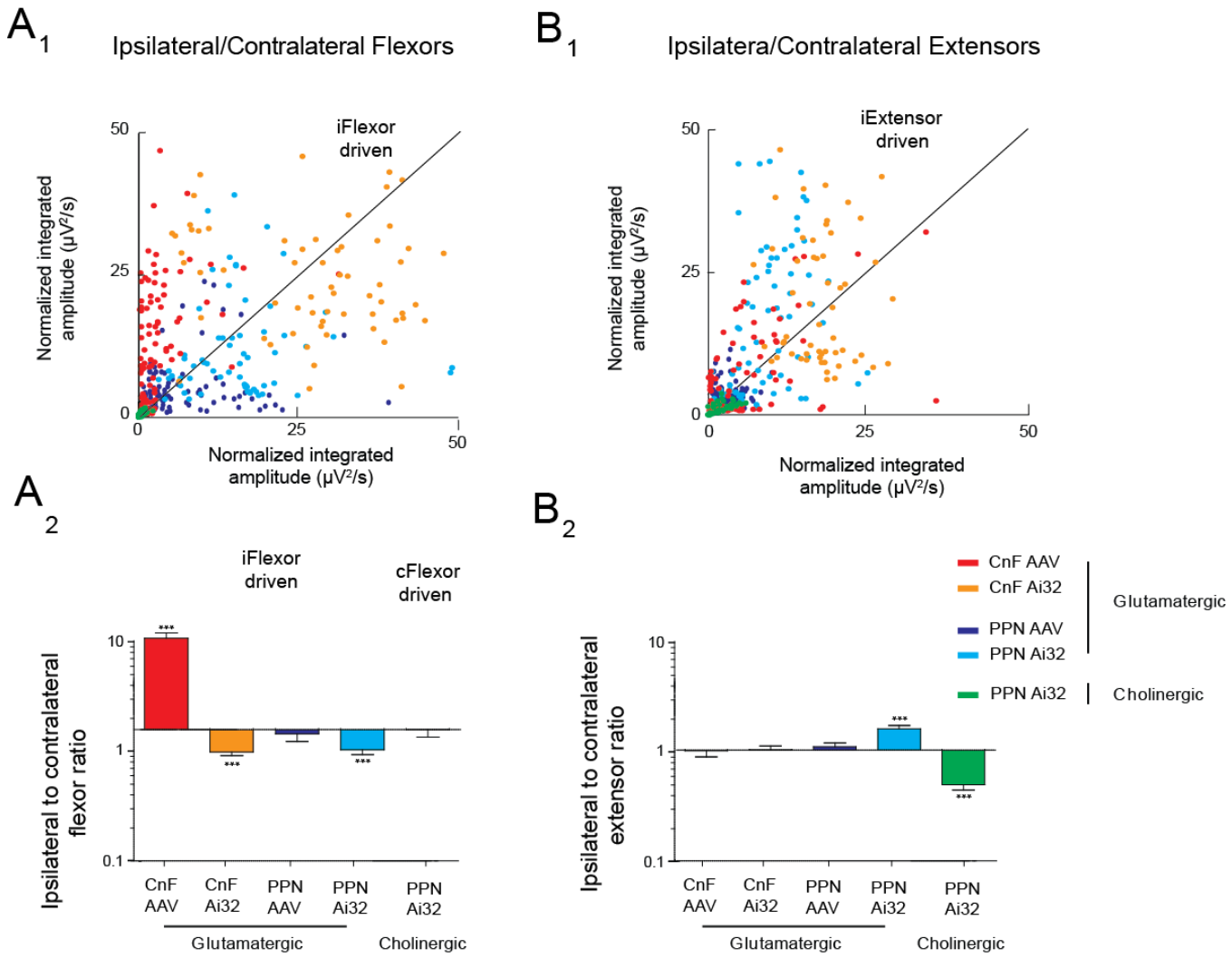

Figure 36: Short stimulations of glutamatergic CnF or PPN neurons evoke motor responses ipsilateral to the stimulation site in the resting mouse.

(A), Amplitude of the net integrated motor responses evoked in flexor muscles ipsilateral versus contralateral to the stimulation site (A1). Neuronal populations are color-coded. Each dot represents an antagonist flexor versus extensor muscle pair. (A2), Mean and SEM of the ratio of the net integrated amplitude illustrated in A1).

(B), Amplitude of the net integrated motor responses evoked in flexor muscles ipsilateral versus contralateral to the stimulation site (A1). Neuronal populations are color-coded. Each dot represents an antagonist flexor versus extensor muscle pair. (B2), Mean and SEM of the ratio of the net integrated amplitude illustrated in B1.

(A-B) Statistical differences between groups (N=7 VGluT2-CRE::AAV-ChR2+CnF, 7 VGluT2-CRE::AAV-ChR2+PPN, and 5 VGluT2-CRExAi32-ChR2+CnF, 5 VGluT2-CRExAi32-ChR2+PPN, and 4 ChAT-CRExAi32-ChR2+PPN) was tested with a Wilcoxon signed rank test from 1.

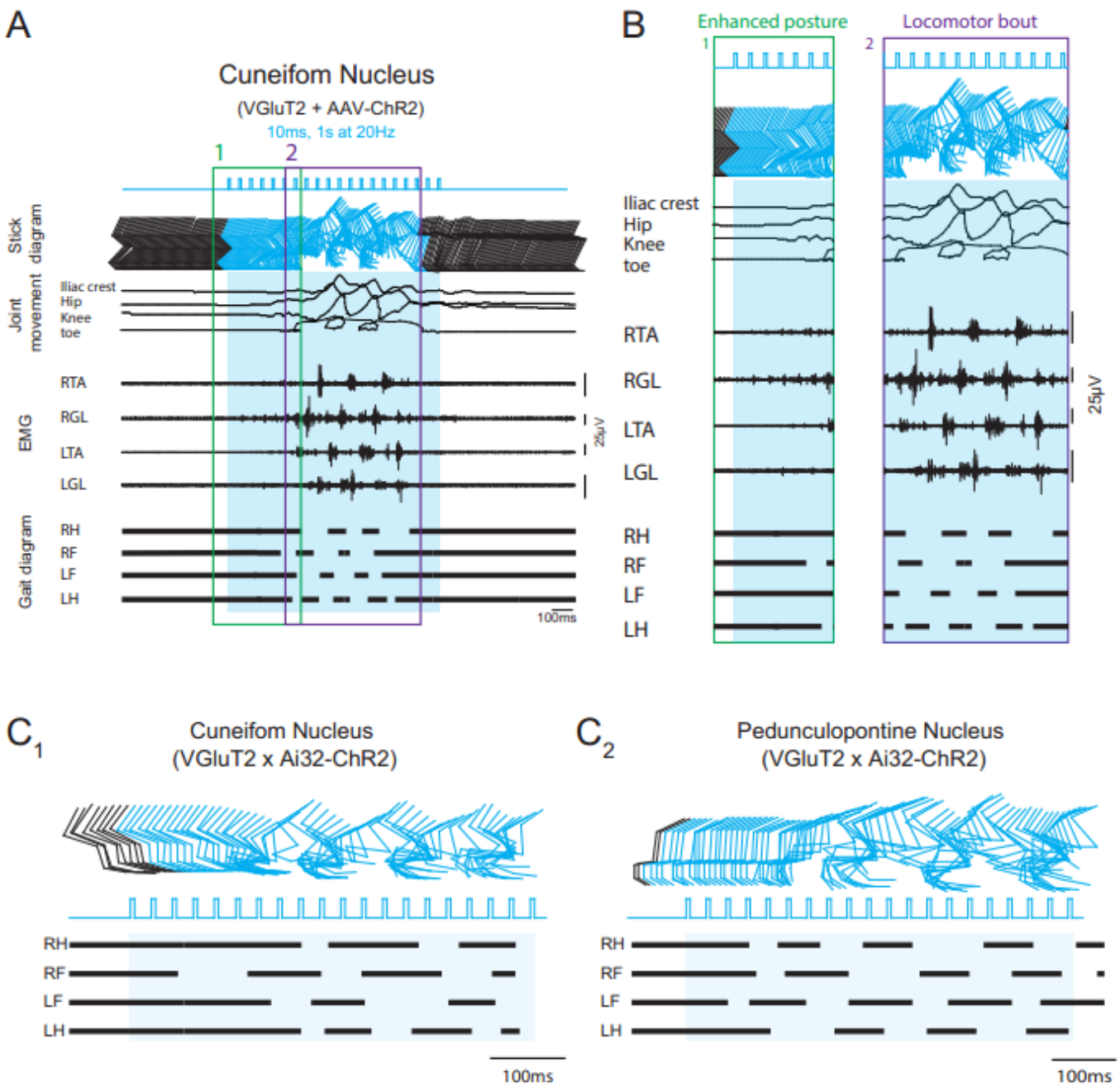

Figure 37: Long trains of photostimulation of glutamatergic CnF neurons enhance the postural tone and initiate locomotion.

Only long trains of photostimulation of glutamatergic CnF neurons enhance postural tone and initiate locomotion in virally transfected (VGluT2-CRE + AAV- ChR2) mice, whereas long trains of photostimulation of either glutamatergic CnF or PPN neurons

initiate locomotion in crossed transgenic (VGl uT2 -CRE x Ai32-ChR2) mice, related to Figure 3. (A), Example of stick diagram illustrating hindlimb joints, joint trajectory, EMG ctivity, and gait diagram showing the stance (black bar) and swing (gap) phases evoked upon long trains of photostimulation of the glutamatergic CnF illustrated in Figure 3D1. Periods delimitated by colored boxes are enlarged in B. (B), High er temporal resolution at the onset of the stimulation illustrating enhanced motor and postural tone (B1), and high resolution at the onset of locomotion (B2). (C), Stick diagram illustrating hindlimb joints and gait diagrams showing the stance (black bar) and swing (gap) phases evoked upon long trains of photostimulation of the gl utamatergic CnF (C1) or PPN (C2) neurons. P hotostimulation pulses are indicated in blue on top of each example. Photostimulated period is highlighted in light blue (N= 7 VGluT2-CRExAi32 -ChR2+CnF and 7 +PPN).

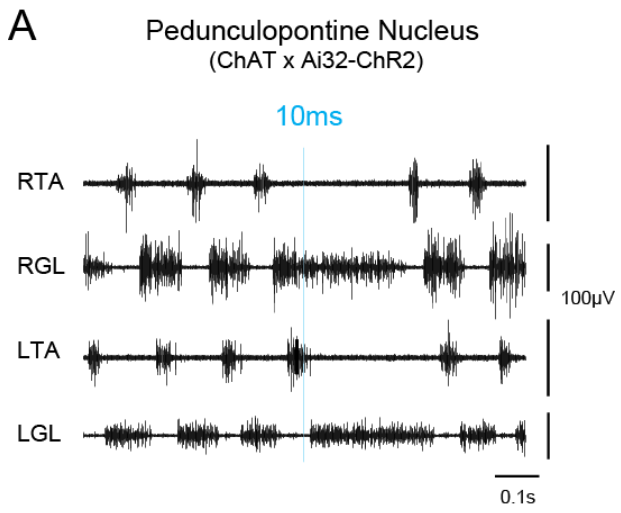

Figure 38: Short pulses of photostimulation of glutamatergic PPN neurons lengthen the step cycle.

EMG activity evoked upon a short pulse of photostimulation delivered above the glutamatergic PPN increased the duration of the extensor phase. (N=1 ChAT-CRExAi32-ChR2+PPN mice).

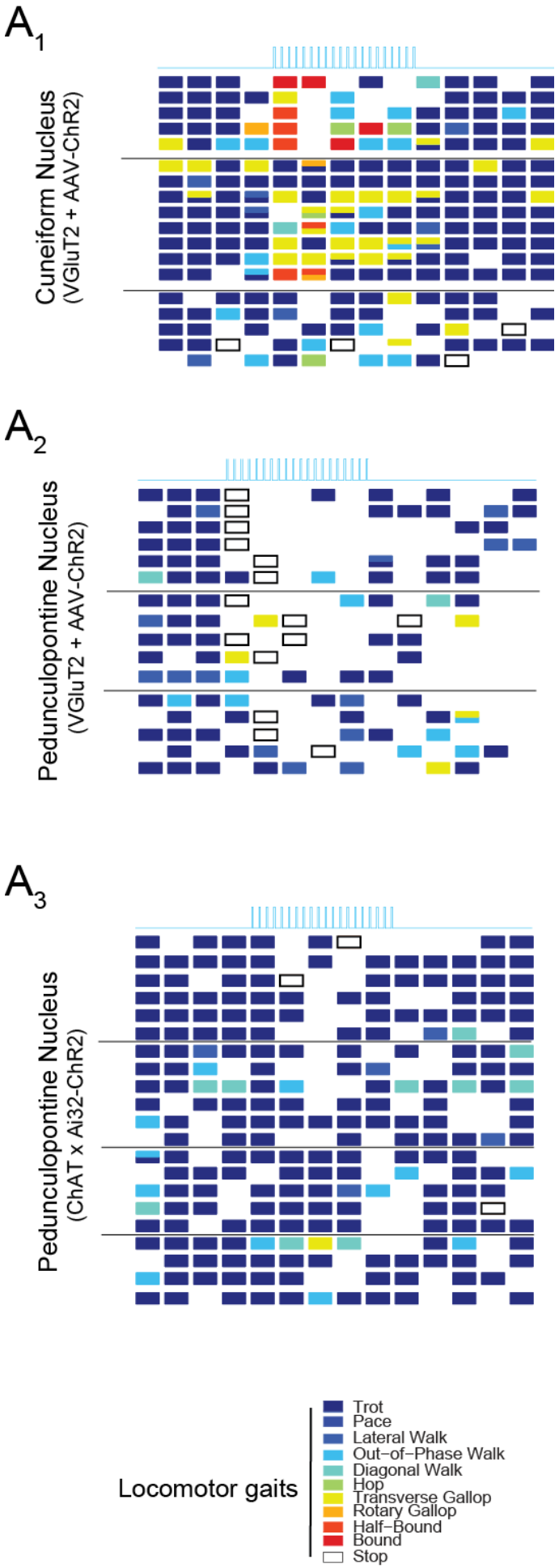

Figure 39: Individual locomotor gaits upon photostimulation.

Locomotor gait as function of the time before, during and after a long pulse of photostimulation applied to the glutamatergic CnF (A1), PPN (A2), or cholinergic (A3) PPN neurons. (N=3 VGluT2-CRE::AAV-ChR2+CnF,3 VGluT2-CRE::AAV-ChR2+PPN, and 3 ChAT-CRE xAi32-ChR2+PPN).

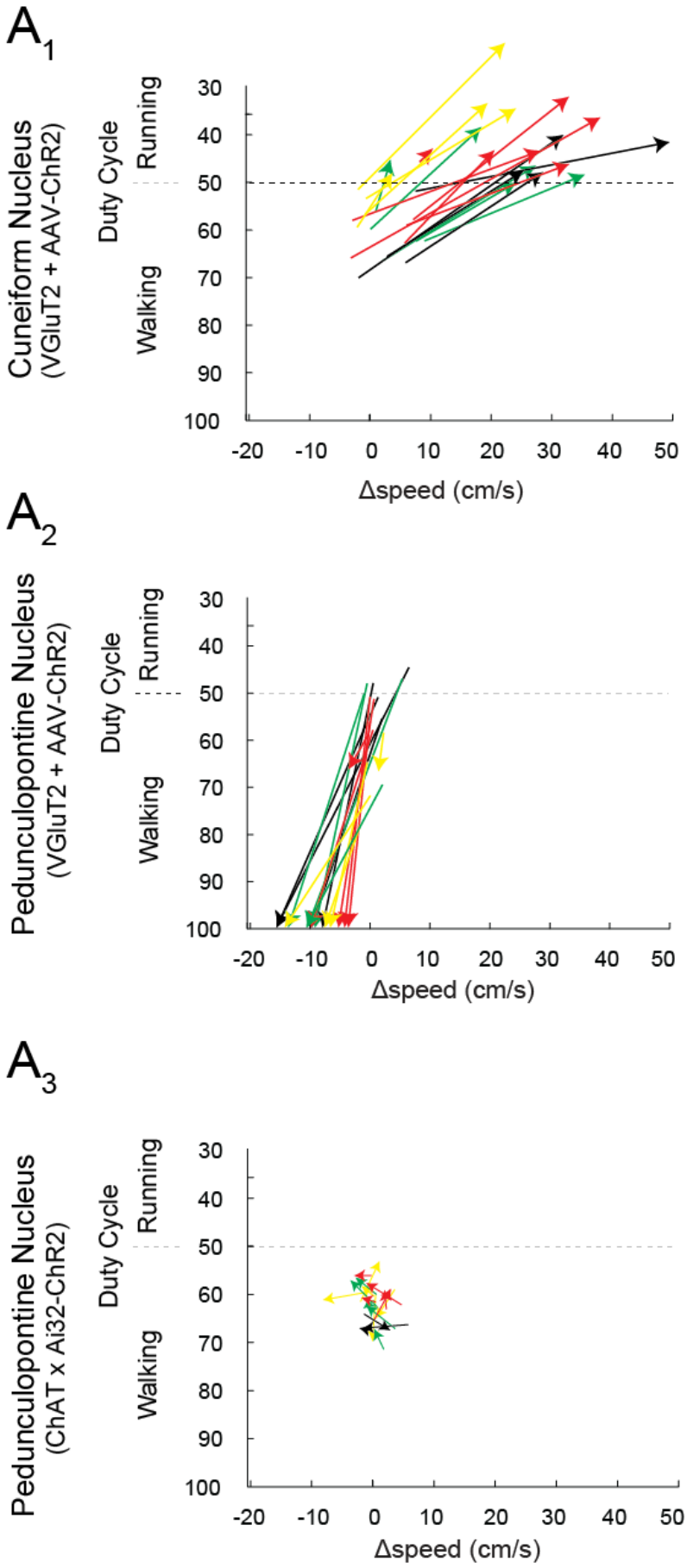

Figure 40: Individual locomotor gaits upon photostimulation.

Vectors illustrating maximal changes in the duty cycle of the stance phase (delineating running versus walking gaits) as function of the Δ locomotor speed evoked upon long trains of photostimulation of glutamatergic CnF (A1), PPN (A2), or cholinergic (A3) PPN. Each color represents a mouse. (N=5 VGluT2-CRE::AAV-ChR2+CnF, 6 VGluT2-CRE::AAV-ChR2+PPN and 4 ChAT-CRE xAi32-ChR2+PPN).

Chapter 4: General Discussion

4.1 Discussion

Each chapter has its own discussion that can be found at the end of chapters 2 and 3. In this section, broader perspectives will be added to the work that has been done and some questions and ideas on the paths that could be taken to move forward will be discussed.

4.1.1 Gaits

To fully comprehend the role of the mesencephalic locomotor region in the control of locomotion, we decided to use optogenetics. As it is, for now, mainly restricted to mice and because we discovered that there was no classification of locomotor gaits in mice, our first study undertook the task of characterizing the entire range of locomotor gaits available in the wild-type mouse.

Although there is an existing taxonomy for gaits that has been established in quadrupeds (Hildebrand, 1989), it is somehow outdated and not as intelligible as it could be. For example, locomotor gaits' "symmetry" is defined as the perfect alternation between hindlimbs, when what understandably comes to mind when we refer to symmetry would be synchronization between limbs. Moreover, this classification puts all gaits that do not have a perfect alternation between homologous limbs (gallops and bounds) in the same category when they are clearly different and represented in different conditions. Our study tried to mitigate these problems by setting an unbiased, clear and reproducible framework for the classification of gaits that can be used in all quadrupeds.

Although we have set a framework to study locomotor gaits in quadrupeds, it can be used and improved in any number of ways. An issue that needs to be addressed in the future is double stepping. Mice will sometimes produce two steps with a limb within a reference limb step cycle. For this study, those steps were not analyzed. Although extremely rare, quantifying those gait defects in pathologies and transgenic mice will help us understand the spinal locomotor networks involved in those particular cases. Another flaw that could lead to misinterpretation could be found in the fact that some gaits can occur both at low and high speeds. While the hop is clearly transitional at all speeds, the out-of-phase walk is a semi-attractor at low speed while it is a transitional gait at high speed. For the sake of

clarity, the point could be made that those two gaits are different and should have different names.

We used this analysis paradigm to assess the range of gaits available to the C57Bl6 mouse background and we hope that it will be applied in many other animals and conditions. Improvement will hopefully come with usage and adaptation of this model over time. In the laboratory, for example, it was used to quantify gaits in another mouse strain and in a mouse model lacking DSCAM (Down Syndrome Cell Adhesion Molecule) (Lemieux et al., 2016; Thiry et al., 2017, Fig. 41). Many differences appear in locomotor gait occurrence when comparing between strains (C57 vs C3H) and between mutant and control (DSCAM^{2J} vs C3H), leading to the conclusion that this protein is necessary for a good coordination between limbs: its absence resulting in an impaired locomotion.

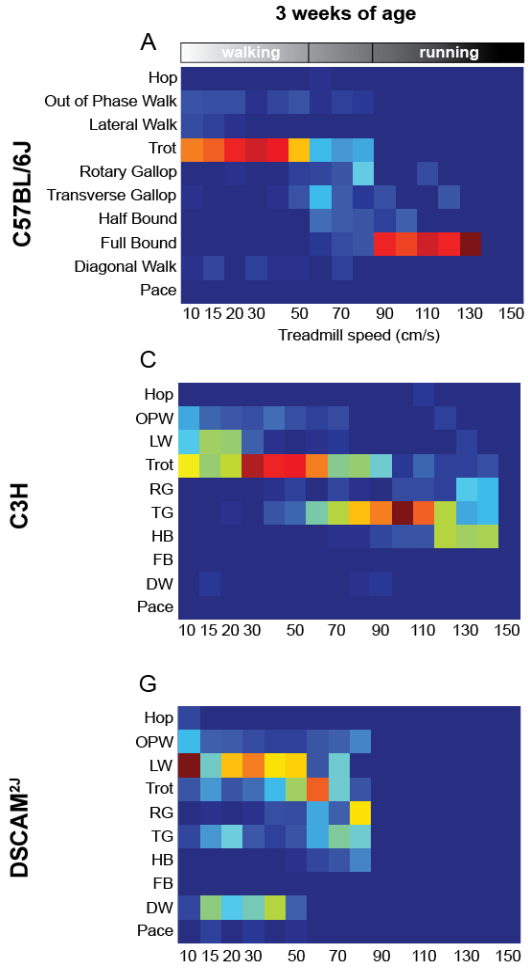

Figure 41: Gait occurrence for C57BL/6J, C3H and DSCAM^{2J} mice at different treadmill speeds.

Color-coded matrices of the percentage of occurrence of a gait (row) at each speed (column) for C57BL/6J (A), C3H (C) and DSCAM2^{J} mutant (G) mice at 3 weeks of age. The sum of a column equals 100%.

OPW=out-of-phase walk, LW=lateral walk, RG=rotary gallop, TG=transverse gallop, HB=half-bound, FB=full-bound, DW=diagonal walk (Thiry et al., 2017).

The impact of aging in health and pathology on locomotion is of great interest to the scientific community. The first results obtained in the lab show that old mice are not able to run at high speeds and age leads to locomotor gait modifications that still need to be analyzed thoroughly (Fig.42). Looking at the impact of aging in mouse models of neurodegenerative disorders could help us understand the biomechanical and neural defects that appear with age.

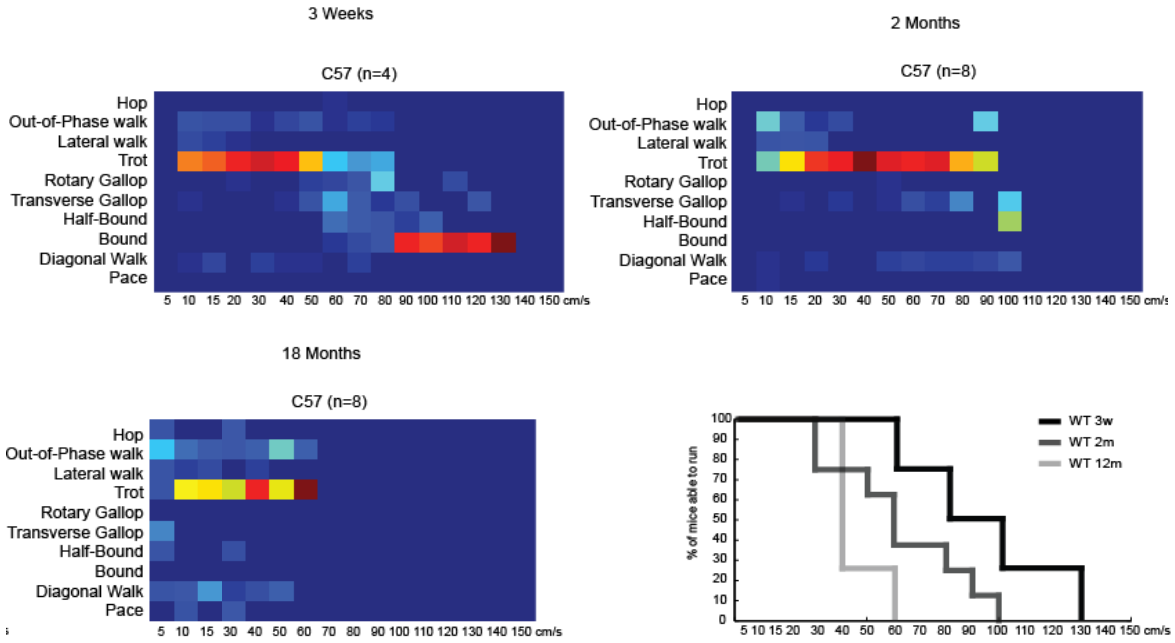

Figure 42: Aging affects gait occurrence in C57BL/6J mice.
Color-coded matrices of the percentage of occurrence of a gait (row) at each speed (column) for C57BL/6J) mice at 3 weeks, 2 months and 18 months of age. The sum of a column equals 100%. Bottom right panel shows the percentage of mice that are able to walk at a certain treadmill speed. OPW=out-of-phase walk, LW=lateral walk, RG=rotary gallop, TG=transverse gallop, HB=half-bound, FB=full-bound, DW=diagonal walk.

Many mutants with silenced local and propriospinal interneurons could also be used with this paradigm. Some are already known and could be easily tested like the dI6, V3, V2a, V0v or V0d interneurons silencing (Zhang et al., 2008; Talpalar et al., 2013; Vallstedt and Kullander, 2013). In addition, although there are no progenitor markers for propriospinal neurons yet, silencing those neurons is feasible using conditional targeting via the use of the diphtheria toxin receptor and a combination of anterograde and retrograde CRE protein carrying viruses (as for example in Crone et al., 2008; Ruder et al., 2016; Capelli et al., 2017). Quantifying gaits after recovery from a lateral hemisection of the

spinal cord would also be an elegant way to understand the role of propriospinal neurons in producing gaits.

While little is known about the supraspinal control of locomotor gait transition, it has recently been shown that reticulospinal neurons contact onto cervical propriospinal neurons vastly more than corticospinal neurons (Mitchell et al., 2016) and the MLR has been shown to induce gait transition upon stimulation (Shik et al., 1966). The MLR, via its relays in the medullary reticular formation, could activate cervicolumbar and cervical interneurons in the spinal cord that would, in turn, activate the locomotor gait coordination circuitry.

As we have shown that the cuneiform nucleus is probably the fittest target to increase speed and modulate locomotor gaits, studies should look more precisely into its role. Tracing experiments could link the cervicospinal neurons to the cuneiform nucleus, and conditional silencing could look into the role of the specific propriospinal neurons that are controlled by the CnF. Moreover, looking into the photostimulation of the glutamatergic cuneiform neurons on gait at different speeds would help us understand if the CnF can directly trigger gallops or if the CnF triggers an increase in speed that causes the spinal interneuronal networks to turn to gallops. The MLR, therefore, seems to be a perfect target to study locomotor gaits and their transitions.

4.1.2 MLR

4.1.2.1 Anatomical considerations

The mesencephalic locomotor region is a brainstem locomotor center that has been shown to be able to initiate and change locomotor behavior depending on the frequency of stimulation (Shik et al., 1966). Although the anatomical correlates of the MLR have been initially identified as the cuneiform nucleus (CnF) and the pedunculopontine nucleus (PPN), there is still an ongoing debate about the exact anatomical correlate of this supraspinal locomotor center. Combining kinematic and electromyographic recordings with optogenetic manipulations (ChR2 and NpHR3) in transgenic mice, we investigated the functional contribution of VGluT2 or ChAT neurons of the CnF or PPN to locomotion. By their distinct effects on locomotor pattern and rhythm, glutamatergic CnF neurons contribute to running gaits while glutamatergic and, to some extent, cholinergic PPN

neurons induce walking gaits. While specific limitations of this particular study have been recapitulated already, there is one point that needs further examination. The major goal of this study was to discriminate between the effects obtained when stimulating the CnF to those obtained when stimulating the PPN. While there are some anatomical landmarks delimiting the medial, dorsal, and lateral parts of the CnF (Fig. 43) and, although the PPN is mostly cholinergic, part of it is glutamatergic and is located dorsal to the superior cerebellar peduncle (scp) in the reference atlases used by most scientists (Paxinos et al., 2004; Allen Institute for Brain Science, 2015). Still, there is no clear anatomical distinction between the CnF and the dorsal PPN, in the study presented in chapter 3, we, therefore, decided to only consider we were stimulating the PPN when the tip of the cannula was located close to the ChAT immunostaining. However, a clear distinction between the CnF and dorsal PPN needs to be made when stimulating this region in order to avoid any inconsistencies between studies. One way of sorting neurons that are located between the inferior colliculus and superior cerebellar peduncle could be to identify their progenitor identity. Another way could be to record neurons in awake animals. While the neurons of the PPN have already been studied based on their electrophysiological properties (Takakusaki et al., 1996; Roš et al., 2010; Petzold et al., 2015), the studies focused on the PPN at large and not on its dorsal part or its anatomical boundary with the CnF. Recording in multiple sites across the brainstem in awake animals or in patients implanted with DBS electrodes would help resolve this anatomical conundrum. Recordings in awake animals would also have the advantage of getting a better understanding of the MLR. It is, for now, impossible to record from only a given neuronal population: however, it would still help separate the CnF from the dorsal PPN and answer many questions like. 'Are the PPN and/or CnF active during locomotion? and Are they correlated with the speed the animal is going, or with its initiation of locomotion?'

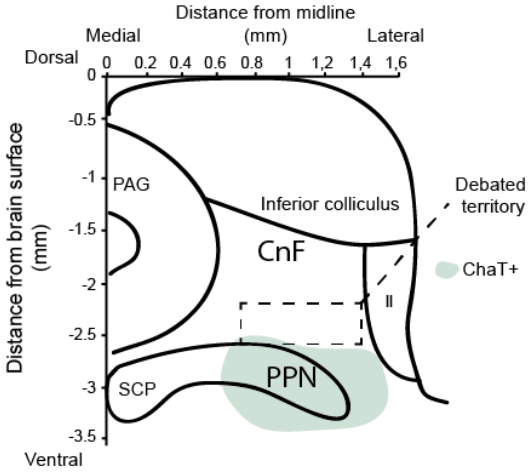

Figure 43: Anatomical landmarks surrounding the MLR.
Schematic representation of a transversal section of a mouse brainstem showing the CnF, the PPN and the anatomical landmarks surrounding them. PAG: periaqueductal gray matter, ll: lateral lemniscus, SCP: superior cerebellar peduncle.

While the cuneiform is a homogeneous nucleus with straightforward inputs and outputs that places it in the center of the escape circuitry, the PPN is quite the opposite. It is composed of intermingled glutamatergic and cholinergic neurons with GABAergic neurons in its rostral portion (Wang and Morales, 2009). As shown in Figure 44A, a single cholinergic neuron can have collateral in almost every PPN target. This pattern of connectivity could explain the PPN's apparently contradictory role in locomotor behavior. The PPN has been shown to have a clear inhibitory role on muscle tone in decerebrated cats (Takakusaki et al., 2016) and in our own experiments. However, it also has been proven to be locomotion inducing when stimulating the cholinergic PPN (Roseberry et al., 2016) and cholinergic terminals in the VTA (Dautan et al., 2016) in intact mice. Altogether, these results suggest that while the cholinergic PPN has a direct inhibitory control of midbrain locomotor centers and motor neurons through its descending projections, it can also have a positive effect on goal-directed locomotion through its ascending projections and subsequent release of dopamine in the striatum. Discrepancies between studies might therefore come from the location of the stimulation.

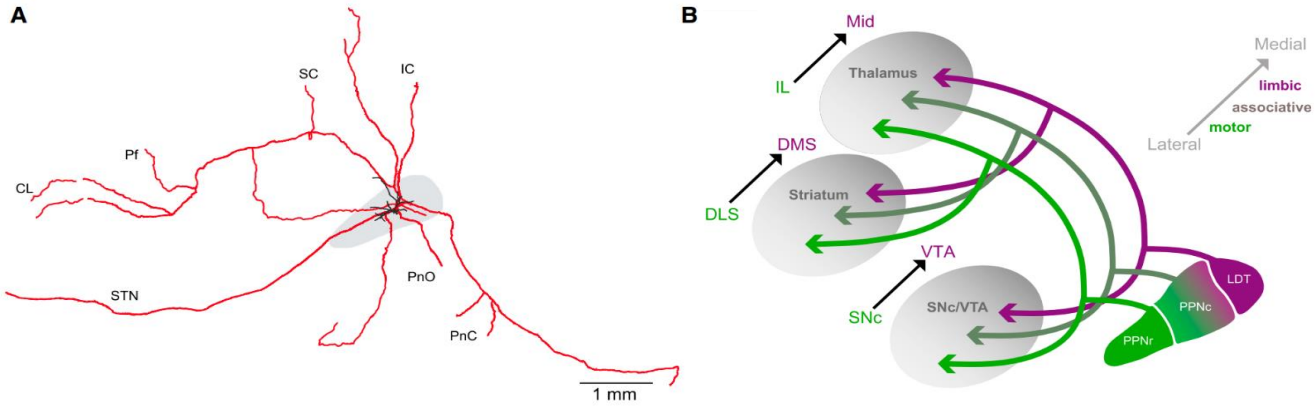

Figure 44: Connectivity of the Cholinergic Brainstem.

A: Single-cell tracing studies have revealed that individual neurons innervate most of the known targets of cholinergic neurons (only one neuron is illustrated). Shaded area represents the PPN outline. **B**: Topographical organization of the cholinergic brainstem. (Mena-Segovia and Bolam, 2017) Abbreviations: IL, intralaminar thalamic nuclei; Mid, midline thalamic nuclei; CL, centrolateral thalamic nucleus; GiN, gigantocellular nucleus; IC, inferior colliculus; PnO, nucleus pontis oralis; PnC, nucleus pontis caudalis; SC, superior colliculus; SNc, substantia nigra pars compacta; STN, subthalamic nucleus; VTA, ventral tegmental area. Topographical Organization of the Cholinergic Brainstem.

Brainstem cholinergic neurons display a distinct organization that is consistent with their respective projections (Fig. 44B). The rostral PPN (PPNr) innervates motor-related circuits, the LDT targets limbic-related circuits, and the caudal PPN (PPNc) projects to both. While we focused our efforts on the most caudal PPN because it had been placed inside the MLR (Skinner and Garcia-Rill, 1984), the effects of cholinergic stimulation on the rostral PPN and LDT on locomotion remains a mystery. The most direct way to resolve this issue would be to replicate our study and photostimulate the rostral PPN and LDT. Yet, many more elaborate options are available today. Some of them will be detailed in the next section.

Two paths of research could resolve some of the issues that were raised in the previous paragraphs. Firstly, anatomical studies using CRE transgenic mice combined with anterograde and retrograde AAVs followed by a stereological analysis of these tracings will answer the questions regarding the neurotransmitter identity of the projecting neurons of the CnF, PPN, and LDT and their location inside each nucleus. An interesting path could be taken using transneuronal circuit tracing with neurotropic viruses (Xiang et al., 2013). Injection in a limb muscle results in the tagging of each neuron in the chain of command involved in its control all the way up to the brain. We would, therefore, be able to discriminate between nuclei that are involved in locomotion and those that are not. Secondly, optogenetic stimulation of the axonal terminals of each neurotransmitter subtype for each nucleus in the brainstem locomotor centers and basal ganglia nuclei at rest and during locomotion would give a detailed and unbiased account of the many roles played by these nuclei in locomotor control.

Getting a better understanding of the neurons located inside the MLR and their activity and connectivity in health and disease is crucial to be able to target the nuclei that will be the best-fitted to helping patients suffering from Parkinson’s disease and spinal cord injury.

4.1.2.2 Stimulating the MLR in Parkinson's disease

As previously stated, PPN DBS to alleviate symptoms of Parkinson's disease has been disconcerting (Wang et al., 2017). DBS of the PPN led to the appearance of side effects such as involuntary miction (Aviles-Olmos et al., 2011), sleep (Arnulf et al., 2010) or monocular oscillopsia (Ferraye et al., 2009). Moreover, the precise effect of the deep brain stimulation on cells neighboring the electrode is also uncertain. Instead of analyzing DBS as being excitatory or inhibitory, it could be interpreted as being disruptive (Chiken and Nambu, 2016). Discrepancies may also appear owing to the natural differences between patients, their disease stage and their treatment history.

Despite many uncertainties, PPN DBS did alleviate motor symptoms in a great number of parkinsonian patients (Hamani et al., 2016). Progress could be made by improving the targeting of the rostral or caudal PPN and reducing variability between DBS techniques and stimulation parameters. Considering that the cuneiform is hyperactive in a model of parkinsonian rats (Heise and Mitrofanis, 2006), an approach could be to try to decrease its activity in patients. It has been shown in a model of Parkinson's disease in rats that cholinergic neurons projecting from the PPN to the STN are hyperactive while those projecting to the gigantocellular nucleus do not appear to show a change in neuronal activity (Martinez-Gonzalez et al., 2014). Using specific tracing with AAVs, we would know if there is plasticity in the projections from the glutamatergic or cholinergic CnF, PPN and LDT to its targets. Stimulating the axon terminals in those models would help identify the best target for deep brain stimulation experiments.

4.1.2.3 Simulating the MLR after a Spinal cord injury

Any damage to the spinal cord, whatever its origin, is labeled a spinal cord injury, or SCI. Depending on the location and extent of the injury, symptoms may include a severe loss of sensory and/or motor functions. Severed axons are not able to regenerate but some compensatory mechanisms exist (Fink and Cafferty, 2016). It has been shown that sprouting in the spinal cord will reconnect the reticulospinal neurons to the affected limb CPGs through the use of pre-existing propriospinal neurons (Courtine et al., 2008; Filli et al., 2014; May et al., 2017). Spinal cord injury also drives plasticity in the brainstem.

Indeed, it has been shown that the MLR will increase its projections to the contralateral medullary reticular formation (Zörner et al., 2014) and to cervical propriospinal neurons (May et al., 2017). However, their location and neurotransmitter phenotype remain unknown. Using the AAV tracing paradigm described in the previous section, we could acquire a more detailed view of the neuronal phenotype and nucleus of origin of the neurons that show plasticity after spinal cord injury.

To this day, many therapeutic strategies have been tried to cure SCI (Figure 46), going from stem cells (Bretzner et al., 2008) to regrowth promoting antibodies (Lindau et al., 2014). New exciting approaches alleviating spinal cord injury symptoms include electrical stimulation of either supraspinal or spinal locomotor centers to obtain recovery of limb movement (Chari et al., 2017). Approaches that are being developed try to either stimulate the entire lumbar locomotor networks directly (Gerasimenko et al., 2015) or to target flexors and extensor motoneurons in the spinal cord in synchrony with flexor or extensor signals recorded from the motor cortex (Capogrosso et al., 2016). Another strategy has been to stimulate the MLR after SCI and results were impressive (Bachmann et al., 2013).

Indeed, stimulation of the MLR after SCI improved rats' ability to walk (Figure 45) and swim. Some animals were even able to move their otherwise paralyzed limbs upon stimulation of the MLR.

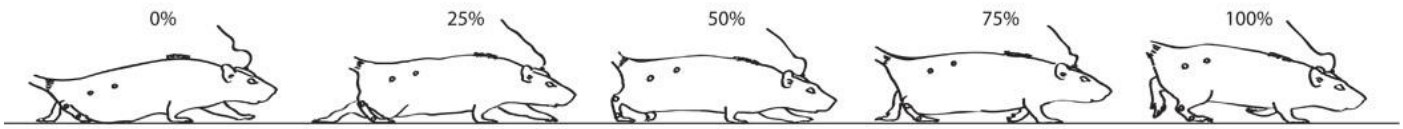

Figure 45: Stimulation of the MLR in rats with SCI.

Percentage of the maximal intensity used to stimulate the MLR is represented above each representation of rats and the effect of the stimulation can be observed in the rat's posture and paw placement.

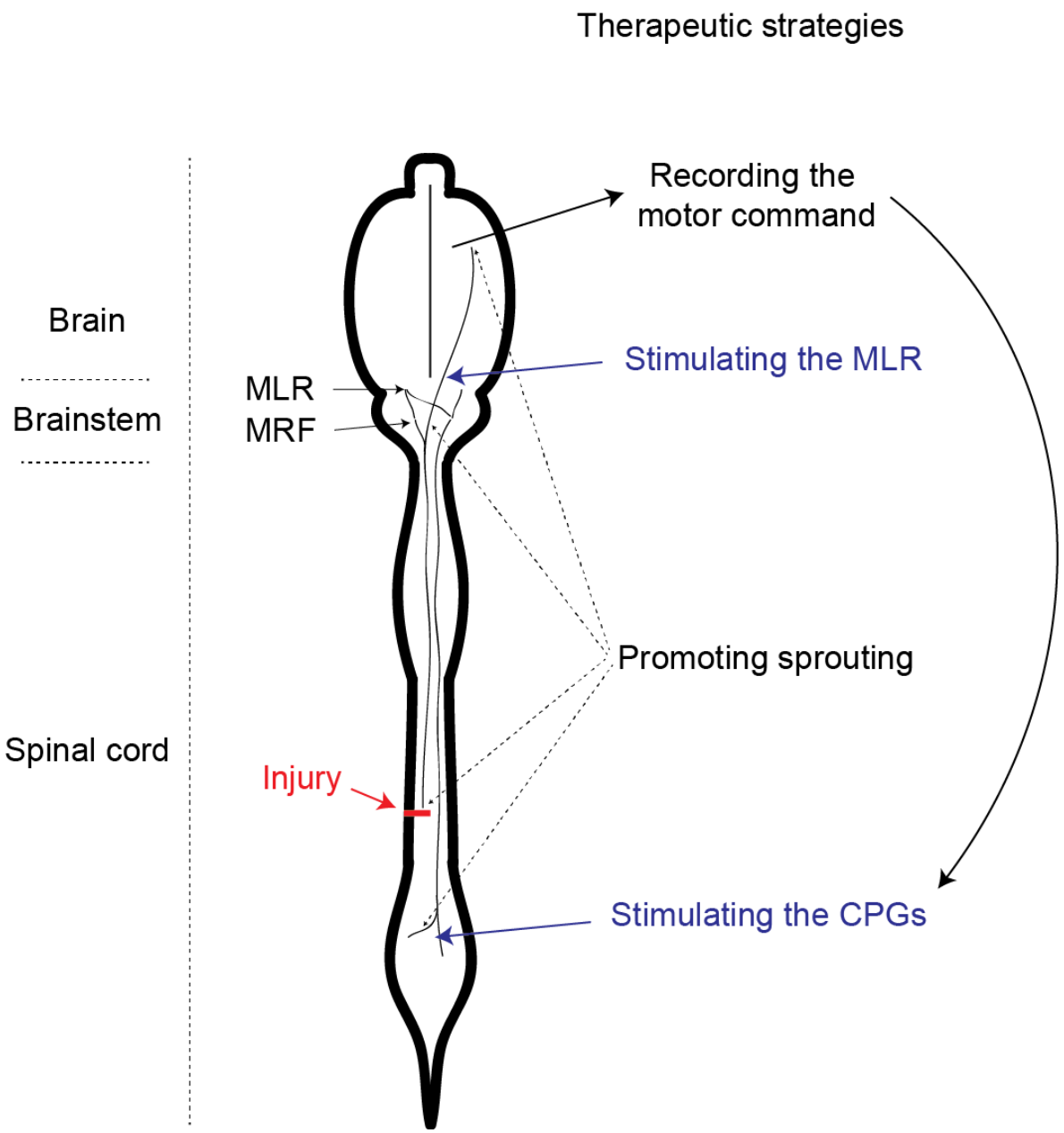

Figure 46: Schematics of a brain and spinal cord showing therapeutic strategies to improve locomotor functions after spinal cord injuries.

MLR: mesencephalic locomotor region, MRF: medullary reticular formation, CPG: central pattern generator. Therapeutic strategies involving stimulation are in blue. Spinal cord injury is in red

However, the stimulation site was chosen because of its ability to induce locomotion, not based on anatomy. Although we assume from our results that the CnF was indeed the site of stimulation, its exact location remains unknown. We therefore decided to pursue our genetic dissection of the MLR and quantified the effects of photostimulation of the glutamatergic CnF and PPN after a lateral hemi-section of the spinal cord. While our results are preliminary regarding spinal efficacy, we do see that stimulating the glutamatergic CnF increases the speed and the muscle burst amplitude while decreasing the extensor burst duration during locomotion on a treadmill (Figure 47). After SCI, photostimulation of the glutamatergic PPN still stopped locomotion.

This study can and will be improved in a number of ways. First, knowledge from tracing experiments could help target the region that is the most actively reorganized after SCI. As the lateral paragigantocellular nucleus is a known target of the CnF, stimulation of the axon terminals in the LPGi but also the LPGi itself could give interesting results. Second, while we are, for now, only stimulating the MLR that is located contralaterally to the spinal cord hemisection, stimulating the ipsilateral side would give insight on the circuitry connecting the MLR to spinal networks below the site of injury. Lastly, of course, stimulating cholinergic neurons of the different portions of the PPN and the LDT after spinal cord injury will clear any doubts remaining concerning the putative role of cholinergic neurons in the recovery after spinal cord injury.

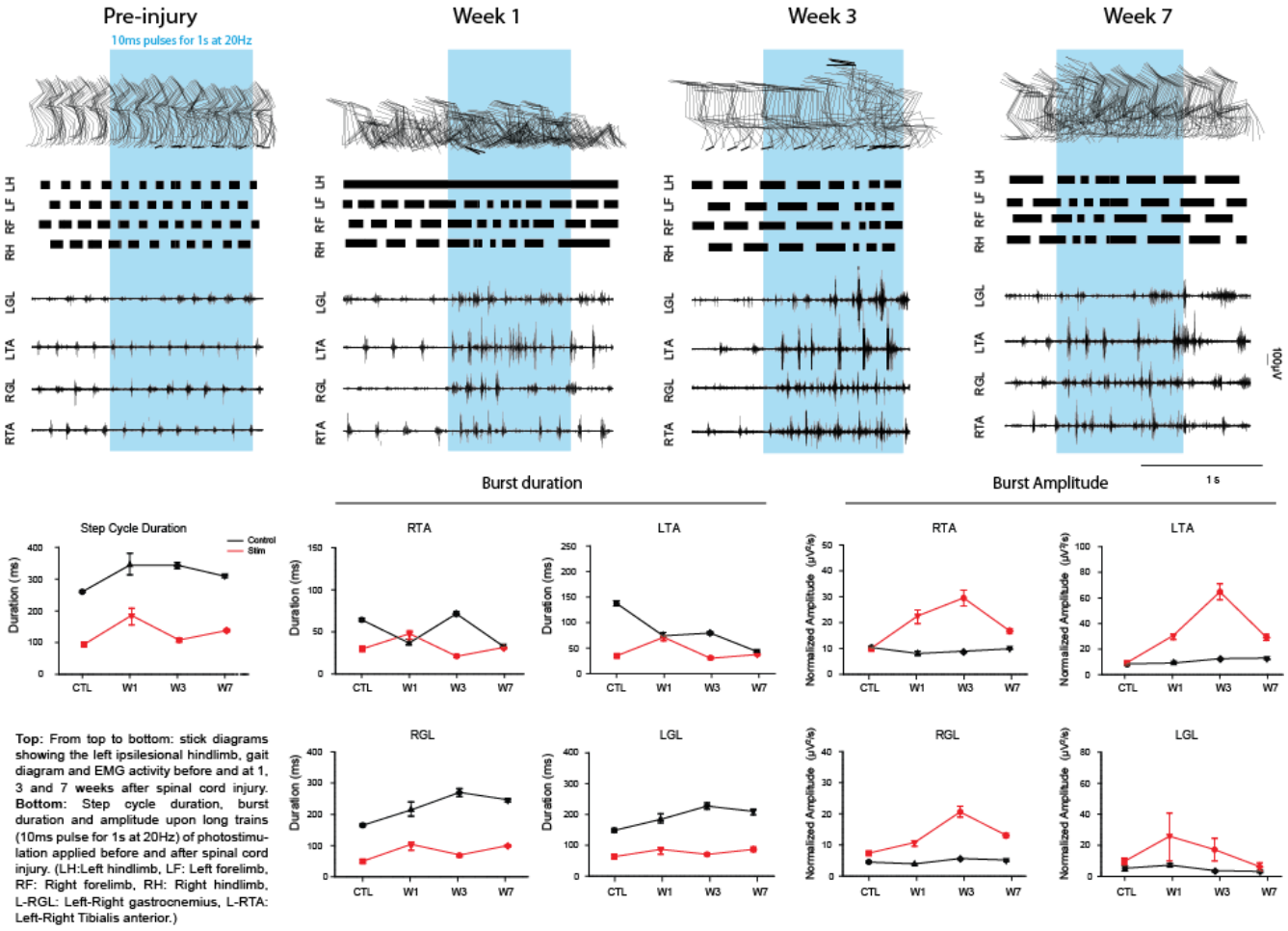

Figure 47: Long photostimulations of the cuneiform nucleus before and after SCI.

From top to bottom: stick diagrams showing the left ipsilesional hindlimb, gait diagram and EMG activity before and at 1, 3 and 7 weeks after spinal cord injury. Bottom: Step cycle duration, burst duration and amplitude upon long trains (10ms pulse for 1s at 20Hz) of photostimulation applied before and after spinal cord injury. (LH:Left Hindlimb, LF: Left Forelimb, RH: Right Hindlimb, L-RGL: Left-Right gastrocnemius lateralis, L-RTA: Left-Right tibialis anterior).

4.2 Conclusion

Although it has already been 50 years since the MLR was discovered, its anatomical substrate remains debated. With current clinical trials investigating the potential of deep brain stimulations in the midbrain of patients suffering from Parkinson's disease, parasupranuclear palsy (PSP) and spinal cord injury it has become urgent to identify and characterize the most appropriate neuronal population that needs to be targeted in order to improve locomotor recovery.

Before starting to study the role of the MLR in gait transition, we had to describe the entire range of locomotor gaits available in mice. We identified and characterized eight different locomotor gaits displayed over various ranges of speed in wild-type mice. Moreover, we identified attractor gaits, like the trot, and transitional gaits, like the gallops. This paradigm will also hopefully be useful to other studies looking into the control of locomotion and the diseases that cause locomotor impairments.

Then, combining kinematic and electrophysiological recordings of optogenetic stimulation and inhibition in the freely behaving mouse, we identified the glutamatergic CnF as a locomotor center that initiates and accelerates locomotion, thus giving rise to running gaits likely involved during flight reaction, whereas the glutamatergic and cholinergic PPN would regulate slow walking gaits and stopping likely involved exploratory behavior.

We, therefore have identified the cuneiform nucleus as the main correlate for the MLR and hope more studies will come to advance the knowledge acquired on the MLR in order to improve treatment for neurodegenerative diseases and traumatic spinal cord injuries.

Bibliography

Abols IA, Basbaum AI (1981) Afferent connections of the rostral medulla of the cat: A neural substrate for midbrain‐medullary interactions in the modulation of pain. J Comp Neurol 201:285–297.

Abourachid A (2003) A new way of analysing symmetrical and asymmetrical gaits in quadrupeds. C R Biol 326:625–630.

Abourachid A, Herbin M, Hackert R, Maes L, Martin V (2007) Experimental study of coordination patterns during unsteady locomotion in mammals. J Exp Biol 210:366–372.

Akay T, Acharya HJ, Fouad K, Pearson KG (2006) Behavioral and electromyographic characterization of mice lacking EphA4 receptors. J Neurophysiol 96:642–651.

Alam M, Schwabe K, Krauss JK (2011) The pedunculopontine nucleus area: Critical evaluation of interspecies differences relevant for its use as a target for deep brain stimulation. Brain 134:11–23.

Allen Institute for Brain Science (2015) Allen Mouse Brain Atlas. Allen Mouse Brain Atlas 2.

Alstermark B, Kümmel H, Tantisira B (1987) Monosynaptic raphespinal and reticulospinal projection to forelimb motoneurones in cats. Neurosci Lett 74:286–290.

Amende I, Kale A, McCue S, Glazier S, Morgan JP, Hampton TG (2005) Gait dynamics in mouse models of Parkinson's disease and Huntington's disease. J Neuroeng Rehabil 2:20.

Andersson LLS et al. (2012) Mutations in DMRT3 affect locomotion in horses and spinal circuit function in mice. Nature 488:642–646.

Angelaki DE, Cullen KE (2008) Vestibular system: the many facets of a multimodal sense. Annu Rev Neurosci 31:125–150.

Aoki S, Sato Y, Yanagihara D (2013) Lesion in the lateral cerebellum specifically produces overshooting of the toe trajectory in leading forelimb during obstacle avoidance in the rat. J Neurophysiol 110:1511–1524.

Appell PP, Behan M (1990) Sources of subcortical GABAergic projections to the superior colliculus in the cat. J Comp Neurol 302:143–158.

Aravamuthan BR, Muthusamy K a., Stein JF, Aziz TZ, Johansen-Berg H (2007) Topography of cortical and subcortical connections of the human pedunculopontine and subthalamic nuclei. Neuroimage 37:694–705.

Armstrong D, Drew T (1985) Forelimb electropyographic responses to motor cortex stimulation during locomotion in the cat. J Physiol 367:327–351.

Armstrong DM (1986) Supraspinal contributions to the initiation and control of locomotion in the cat. Prog Neurobiol 26:273–361.

Armstrong DM, Drew T (1984) Discharges of pyramidal tract and other motor cortical neurones during locomotion in the cat. J Physiol 346:471–495.

Arnulf I, Ferraye M, Fraix V, Benabid AL, Chabardès S, Goetz L, Pollak P, Debû B (2010) Sleep induced by stimulation in the human pedunculopontine nucleus area. Ann Neurol 67:546–549.

Asante CO, Chu a., Fisher M, Benson L, Beg a., Scheiffele P, Martin J (2010) Cortical Control of Adaptive Locomotion in Wild-Type Mice and Mutant Mice Lacking the Ephrin-Eph Effector Protein 2-Chimaerin. J Neurophysiol 104:3189–3202.

Aviles-Olmos I, Foltynie T, Panicker J, Cowie D, Limousin P, Hariz M, Fowler CJ, Zrinzo L (2011) Urinary incontinence following deep brain stimulation of the pedunculopontine nucleus. Acta Neurochir (Wien) 153:2357–2360.

Bachmann LC, Matis a., Lindau NT, Felder P, Gullo M, Schwab ME (2013) Deep Brain Stimulation of the Midbrain Locomotor Region Improves Paretic Hindlimb Function After Spinal Cord Injury in Rats. Sci Transl Med 5:208ra146-208ra146.

Barbeau H, Rossignol S (1987) Recovery of locomotion after chronic spinalization in the adult cat. Brain Res 412:84–95.

Barrière G, Leblond H, Provencher J, Rossignol S (2008) Prominent role of the spinal central pattern generator in the recovery of locomotion after partial spinal cord injuries. J Neurosci 28:3976–3987.

Beg A a., Sommer JE, Martin JH, Scheiffele P (2007) α2-Chimaerin Is an Essential EphA4 Effector in the Assembly of Neuronal Locomotor Circuits. Neuron 55:768–778.

Bellardita C, Kiehn O (2015) Phenotypic Characterization of Speed-Associated Gait Changes in Mice Reveals Modular Organization of Locomotor Networks. Curr Biol 25:1426–1436.

Bernard JF, Peschanski M, Besson JM (1989) Afferents and efferents of the rat cuneiformis nucleus: an anatomical study with reference to pain transmission. Brain Res 490:181–185.

Bernau NA, Puzdrowki RL, Leonard RB (1991) Identification of the midbrain locomotor region and its relation to descending locomotor pathways in the Atlantic stingray,Dasyatis sabina. Brain Res 557:83–94.

Blaszczyk J, Loeb GE (1993) Why cats pace on the treadmill. Physiol Behav 53:501–507.

Borgius L, Nishimaru H, Caldeira V, Kunugise Y, Low P, Reig R, Itohara S, Iwasato T, Kiehn O (2014) Spinal Glutamatergic Neurons Defined by EphA4 Signaling Are Essential Components of Normal Locomotor Circuits. J Neurosci 34:3841–3853.

Borowska J, Jones CT, Zhang H, Blacklaws J, Goulding M, Zhang Y (2013) Functional subpopulations of V3 interneurons in the mature mouse spinal cord. J Neurosci 33:18553–18565.

Bouvier J, Caggiano V, Leiras R, Caldeira V, Bellardita C, Balueva K, Fuchs A, Kiehn O (2015) Descending Command Neurons in the Brainstem that Halt Locomotion. Cell

163:1191–1203.

Bouyer LJG, Rossignol S (2003) Contribution of cutaneous inputs from the hindpaw to the control of locomotion. I. Intact cats. J Neurophysiol 90:3625–3639.

Bowker RM, Abbott LC (1990) Quantitative re-evaluation of descending serotonergic and non-serotonergic projections from the medulla of the rodent: evidence for extensive co-existence of serotonin and peptides in the same spinally projecting neurons, but not from the nucleus raphe ma. Brain Res 512:15–25.

Bretzner F, Brownstone RM (2013) Lhx3-Chx10 reticulospinal neurons in locomotor circuits. J Neurosci 33:14681–14692.

Bretzner F, Drew T (2005) Contribution of the motor cortex to the structure and the timing of hindlimb locomotion in the cat: a microstimulation study. J Neurophysiol 94:657–672.

Bretzner F, Liu J, Currie E, Roskams a. J, Tetzlaff W (2008) Undesired effects of a combinatorial treatment for spinal cord injury - Transplantation of olfactory ensheathing cells and BDNF infusion to the red nucleus. Eur J Neurosci 28:1795–1807.

Brocard F, Dubuc R (2003) Differential contribution of reticulospinal cells to the control of locomotion induced by the mesencephalic locomotor region. J Neurophysiol 90:1714–1727.

Brown TG (1911) The Intrinsic Factors in the Act of Progression in the Mammal. Proc R Soc B Biol Sci 84:308–319.

Bullmore E, Sporns O (2009) Complex brain networks: graph theoretical analysis of structural and functional systems. Nat Rev Neurosci 10:186–198.

Cabaj AM, Majczyński H, Couto E, Gardiner PF, Stecina K, Sławińska U, Jordan LM (2017) Serotonin controls initiation of locomotion and afferent modulation of coordination via 5-HT7 receptors in adult rats. Intergovernmental Panel on Climate Change, ed. J Physiol 595:301–320.

Cabelguen J-M, Bourcier-Lucas C, Dubuc R (2003) Bimodal locomotion elicited by electrical stimulation of the midbrain in the salamander Notophthalmus viridescens. J Neurosci 23:2434–2439.

Capelli P, Pivetta C, Soledad Esposito M, Arber S (2017) Locomotor speed control circuits in the caudal brainstem. Nature 551:373–377.

Capogrosso M et al. (2016) A brain-spine interface alleviating gait deficits after spinal cord injury in primates. Nature 539:284–288.

Castiglioni a J, Gallaway MC, Coulter JD (1978) Spinal projections from the midbrain in monkey. J Comp Neurol 178:329–346.

Chari A, Hentall ID, Papadopoulos MC, Pereira EACC (2017) Surgical neurostimulation for spinal cord injury. Brain Sci 7:1–17.

Chiken S, Nambu A (2016) Mechanism of Deep Brain Stimulation: Inhibition, Excitation, or Disruption? Neuroscientist 22:313–322.

Cho KH, Cho Y-J, Lee BI, Heo K (2016) Atrophy of the pedunculopontine nucleus region in patients with sleep-predominant seizures: A voxel-based morphometry study. Epilepsia 57:e151–e154.

Chung JM, Kevetter G a., Yezierski RP, Haber LH, Martin RF, Willis WD (1983) Midbrain nuclei projecting to the medial medulla oblongata in the monkey. J Comp Neurol 214:93–102.

Cohen a H, Gans C (1975) Muscle activity in rat locomotion: movement analysis and electromyography of the flexors and extensors of the elbow. J Morphol 146:177–196.

Comoli E, Ribeiro-Barbosa ER, Canteras NS (2003) Predatory hunting and exposure to a live predator induce opposite patterns of Fos immunoreactivity in the PAG. Behav Brain Res 138:17–28.

Conway BA, Hultborn H, Kiehn O (1987) Proprioceptive input resets central locomotor rhythm in the spinal cat. Exp brain Res 68:643–656.

Courtine G, Song B, Roy RR, Zhong H, Herrmann JE, Ao Y, Qi J, Edgerton VR, Sofroniew M V (2008) Recovery of supraspinal control of stepping via indirect propriospinal relay connections after spinal cord injury. Nat Med 14:69–74.

Crone S a., Quinlan K a., Zagoraiou L, Droho S, Restrepo CE, Lundfald L, Endo T, Setlak J, Jessell TM, Kiehn O, Sharma K (2008) Genetic Ablation of V2a Ipsilateral Interneurons Disrupts Left-Right Locomotor Coordination in Mammalian Spinal Cord. Neuron 60:70–83.

Crosby EC, Woodburne RT (1943) The nuclear pattern of the non-tectal portions of the midbrain and isthmus in primates. J Comp Neurol 78:441–482.

Danner SM, Shevtsova NA, Frigon A, Rybak IA (2017) Computational modeling of spinal circuits controlling limb coordination and gaits in quadrupeds. Elife 6:1–25.

Danner SM, Wilshin SD, Shevtsova NA, Rybak IA (2016) Central control of interlimb coordination and speed-dependent gait expression in quadrupeds. J Physiol 594:6947–6967.

Dautan D, Souza AS, Huerta-Ocampo I, Valencia M, Assous M, Witten IB, Deisseroth K, Tepper JM, Bolam JP, Gerdjikov T V, Mena-Segovia J (2016) Segregated cholinergic transmission modulates dopamine neurons integrated in distinct functional circuits. Nat Neurosci 19:1–14.

de Oliveira Souza C, de Lima-Pardini AC, Coelho DB, Brant Machado R, Alho EJL, Di Lorenzo Alho AT, Teixeira LA, Teixeira MJ, Barbosa ER, Fonoff ET (2016) Peduncolopontine DBS improves balance in progressive supranuclear palsy: Instrumental analysis. Clin Neurophysiol 127:3470–3471.

De Zeeuw CI, Hoebeek FE, Bosman LWJ, Schonewille M, Witter L, Koekkoek SK (2011) Spatiotemporal firing patterns in the cerebellum. Nat Rev Neurosci 12:327–344.

Depoortere R, Sandner G, Di Scala G (1990) Aversion induced by electrical stimulation of the mesencephalic locomotor region in the intact and freely moving rat. Physiol Behav 47:561–567.

Diedrich FJ, Warren WH (1995) Why change gaits? Dynamics of the walkun transition. J Exp Psychol Hum Percept Perform 21:183–202.

Diedrich FJ, Warren WH (1998) The dynamics of gait transitions: effects of grade and load. J Mot Behav 30:60–78.

DiGiovanna J, Dominici N, Friedli L, Rigosa J, Duis S, Kreider J, Beauparlant J, van den Brand R, Schieppati M, Micera S, Courtine G (2016) Engagement of the Rat Hindlimb Motor Cortex across Natural Locomotor Behaviors. J Neurosci 36:10440–10455.

Dobbs LK, Mark GP (2012) Acetylcholine from the mesopontine tegmental nuclei differentially affects methamphetamine induced locomotor activity and neurotransmitter levels in the mesolimbic pathway. Behav Brain Res 226:224–234.

Doig NM, Moss J, Bolam JP (2010) Cortical and thalamic innervation of direct and indirect pathway medium-sized spiny neurons in mouse striatum. J Neurosci 30:14610–14618.

Drew T, Doucet S (1991) Application of circular statistics to the study of neuronal discharge during locomotion. J Neurosci Methods 38:171–181.

Drew T, Jiang W, Kably B, Lavoie S (1996) Role of the motor cortex in the control of visually triggered gait modifications. Can J Physiol Pharmacol 74:426–442.

Dubuc R, Brocard F, Antri M, Fénelon K, Gariépy JF, Smetana R, Ménard A, Le Ray D, Viana Di Prisco G, Pearlstein É, Sirota MG, Derjean D, St-Pierre M, Zielinski B, Auclair F, Veilleux D (2008) Initiation of locomotion in lampreys. Brain Res Rev 57:172–182.

Dunbar DC (2004) Stabilization and mobility of the head and trunk in vervet monkeys (Cercopithecus aethiops) during treadmill walks and gallops. J Exp Biol 207:4427–4438.

Dunbar MJ, Tran MA, Whelan PJ (2010) Endogenous extracellular serotonin modulates the spinal locomotor network of the neonatal mouse. J Physiol 588:139–156.

Dutton RC, Carstens MI, Antognini JF, Carstens E (2006) Long ascending propriospinal projections from lumbosacral to upper cervical spinal cord in the rat. Brain Res 1119:76–85.

Eccles JC, Sherrington CS (1930) Reflex summation in the ipsilateral spinal flexion reflex. J Physiol 69:1–28.

Edwards SB, de Olmos JS (1976) Autoradiographic studies of the projections of the midbrain reticular formation: Ascending projections of nucleus cuneiformis. J Comp Neurol 165:417–431.

Eidelberg E, Walden JG, Nguyen LH (1981) Locomotor control in macaque monkeys. Brain 104:647–663.

Eidelberg E, Yu J (1981) Effects of corticospinal lesions upon treadmill locomotion by cats. Exp brain Res 43:101–103.

El Manira A, Pombal MA, Grillner S (1997) Diencephalic projection to reticulospinal neurons involved in the initiation of locomotion in adult lampreys Lampetra fluviatilis. J Comp Neurol 389:603–616.

Engberg I, Lundberg A (1969) An electromyographic analysis of muscular activity in the hindlimb of the cat during unrestrained locomotion. Acta Physiol Scand 75:614–630.

Esposito MS, Capelli P, Arber S (2014) Brainstem nucleus MdV mediates skilled forelimb motor tasks. Nature 508:351–356.

Fasano A, Laganiere SE, Lam S, Fox MD (2017) Lesions causing freezing of gait localize to a cerebellar functional network. Ann Neurol 81:129–141.

Fawcett JP, Georgiou J, Ruston J, Bladt F, Sherman A, Warner N, Saab BJ, Scott R, Roder JC, Pawson T (2007) Nck adaptor proteins control the organization of neuronal circuits important for walking. Proc Natl Acad Sci U S A 104:20973–20978.

Ferraye MU, Debû B, Fraix V, Goetz L, Ardouin C, Yelnik J, Henry-Lagrange C, Seigneuret E, Piallat B, Krack P, Le Bas JF, Benabid a. L, Chabards S, Pollak P (2010) Effects of pedunculopontine nucleus area stimulation on gait disorders in Parkinson's disease. Brain 133:205–214.

Ferraye MU, Gerardin P, Debû B, Chabardès S, Fraix V, Seigneuret E, LeBas J-F, Benabid A-L, Tilikete C, Pollak P (2009) Pedunculopontine nucleus stimulation induces monocular oscillopsia. J Neurol Neurosurg Psychiatry 80:228–231.

Filli L, Engmann a. K, Zorner B, Weinmann O, Moraitis T, Gullo M, Kasper H, Schneider R, Schwab ME (2014) Bridging the Gap: A Reticulo-Propriospinal Detour Bypassing an Incomplete Spinal Cord Injury. J Neurosci 34:13399–13410.

Fink KL, Cafferty WBJ (2016) Reorganization of Intact Descending Motor Circuits to Replace Lost Connections After Injury. Neurotherapeutics.

Forssberg H (1999) Neural control of human motor development. Curr Opin Neurobiol 9:676–682.

Forssberg H, Grillner S, Halbertsma J, Rossignol S (1980) The locomotion of the low spinal cat. II. Interlimb coordination. Acta Physiol Scand 108:283–295.

Freeze BS, Kravitz A V., Hammack N, Berke JD, Kreitzer AC (2013) Control of Basal Ganglia Output by Direct and Indirect Pathway Projection Neurons. J Neurosci 33:18531–18539.

Frigon A, D'Angelo G, Thibaudier Y, Hurteau M-F, Telonio A, Kuczynski V, Dambreville C (2014) Speed-dependent modulation of phase variations on a step-by-step basis and its impact on the consistency of interlimb coordination during quadrupedal locomotion in intact adult cats. J Neurophysiol 111:1885–1902.

Garcia-Rill E, Houser CR, Skinner RD, Smith W, Woodward DJ (1987) Locomotion-inducing sites in the vicinity of the pedunculopontine nucleus. Brain Res Bull 18:731–

738.

Garcia-Rill E, Skinner RD (1988) Modulation of rhythmic function in the posterior midbrain. Neuroscience 27:639–654.

Garcia-Rill E, Skinner RD, Gilmore SA, Owings R (1983) Connections of the mesencephalic locomotor region (MLR) II. Afferents and efferents. Brain Res Bull 10:63–71.

Garland T, Schutz H, Chappell M a, Keeney BK, Meek TH, Copes LE, Acosta W, Drenowatz C, Maciel RC, van Dijk G, Kotz CM, Eisenmann JC (2011) The biological control of voluntary exercise, spontaneous physical activity and daily energy expenditure in relation to obesity: human and rodent perspectives. J Exp Biol 214:206–229.

Gerasimenko Y, Gorodnichev R, Moshonkina T, Sayenko D, Gad P, Reggie Edgerton V (2015) Transcutaneous electrical spinal-cord stimulation in humans. Ann Phys Rehabil Med.

Goetz L, Piallat B, Bhattacharjee M, Mathieu H, David O, Chabardes S (2016) On the Role of the Pedunculopontine Nucleus and Mesencephalic Reticular Formation in Locomotion in Nonhuman Primates. J Neurosci 36:4917–4929.

Goulding M (2009) Circuits controlling vertebrate locomotion: moving in a new direction. Nat Rev Neurosci 10:507–518.

Grillner S (1975) Locomotion in vertebrates: central mechanisms and reflex interaction. Physiol Rev 55:247–304.

Grillner S (1981) Control of locomotion in bipeds, tetrapods, and fish. Handb Physiol Nerv Syst II:1179–1236.

Grillner S, Wallén P (1985) Central pattern generators for locomotion, with special reference to vertebrates. Gene 8:233–261.

Grossman RG (1958) Effects of stimulation of non-specific thalamic system on locomotor movements in cat. J Neurophysiol 21:85–93.

Gut NK, Winn P (2016) The pedunculopontine tegmental nucleus-A functional hypothesis from the comparative literature. Mov Disord 0:n/a-n/a.

Hägglund M, Borgius L, Dougherty KJ, Kiehn O (2010) Activation of groups of excitatory neurons in the mammalian spinal cord or hindbrain evokes locomotion. Nat Neurosci 13:246–252.

Hamani C et al. (2016) Pedunculopontine Nucleus Region Deep Brain Stimulation in Parkinson Disease: Surgical Anatomy and Terminology. Stereotact Funct Neurosurg 94:298–306.

Hampton TG, Stasko MR, Kale A, Amende I, Costa a. CS (2004) Gait dynamics in trisomic mice: Quantitative neurological traits of Down syndrome. Physiol Behav 82:381–389.

Han W, Tellez LA, Rangel MJ, Motta SC, Zhang X, Perez IO, Canteras NS, Shammah-Lagnado SJ, van den Pol AN, de Araujo IE (2017) Integrated Control of Predatory Hunting by the Central Nucleus of the Amygdala. Cell 168:311–324.e18.

He Z, Liu B-W, Li Z, Tian X-B, Liu S, Manyande A, Zhang D-Y, Xiang H-B (2017) The caudal pedunculopontine tegmental nucleus may be involved in the regulation of skeletal muscle activity by melanocortinsympathetic pathway: a virally mediated trans-synaptic tracing study in spinally transected transgenic mice. Oncotarget 8:71859–71866.

Heglund NC, Taylor CR (1988) Speed, stride frequency and energy cost per stride: how do they change with body size and gait? J Exp Biol 138:301–318.

Heidel KM, Benarroch EE, Gené R, Klein F, Meli F, Saadia D, Nogués MA (2002) Cardiovascular and respiratory consequences of bilateral involvement of the medullary intermediate reticular formation in syringobulbia. Clin Auton Res 12:450–456.

Heise CE, Mitrofanis J (2006) Fos immunoreactivity in some locomotor neural centres of 6OHDA-lesioned rats. Anat Embryol (Berl) 211:659–671.

Herbin M, Gasc J-P, Renous S (2006) How does a mouse increase its velocity? A model for investigation in the control of locomotion. Comptes Rendus Palevol 5:531–540.

Herbin M, Gasc J-PP, Renous S (2004) Symmetrical and asymmetrical gaits in the mouse: Patterns to increase velocity. J Comp Physiol A Neuroethol Sensory, Neural, Behav Physiol 190:895–906.

Herbin M, Hackert R, Gasc JP, Renous S (2007) Gait parameters of treadmill versus overground locomotion in mouse. Behav Brain Res 181:173–179.

Hiebert GW, Pearson KG (1999) Contribution of sensory feedback to the generation of extensor activity during walking in the decerebrate Cat. J Neurophysiol 81:758–770.

Hikosaka O (2007) GABAergic output of the basal ganglia. Prog Brain Res 160:209–226.

Hildebrand M (1968) Symmetrical gaits of dogs in relation to body build. J Morphol 124:353–360.

Hildebrand M (1976) Analysis of tetrapod gaits: general considerations and symmetrical gaits. In: Neural control of locomotion (Herman R., Grillner S, Stein PS., Stuart DG, eds), pp 203–236. New York: Plenum Press.

Hildebrand M (1977a) Analysis of assymetrical gaits. J Mammal 58:131–155.

Hildebrand M (1977b) Analysis of asymmetrical gaits. J Mammal 58:131–156.

Hildebrand M (1989) The Quadrupedal Gaits of Vertebrates. Bioscience 39:766–775.

Horn KM, Pong M, Batni SR, Levy SM, Gibson a R (2002) Functional specialization within the cat red nucleus. J Neurophysiol 87:469–477.

Hsu L, Kiehn O (2017) Excitatory signal from brainstem neurons that initiates locomotion. In: Program N. 65.16 / GG21 Neuroscience Meeting Planner. Washington, DC:

Society for neuroscience. Online.

Iwahara T, Van Hartesveldt C, Garcia-Rill E, Skinner RD (1991) L-dopa-induced air-stepping in decerebrate developing rats. Brain Res Dev Brain Res 58:257–264.

Iwasato T, Katoh H, Nishimaru H, Ishikawa Y, Inoue H, Saito YM, Ando R, Iwama M, Takahashi R, Negishi M, Itohara S (2007) Rac-GAP α-Chimerin Regulates Motor-Circuit Formation as a Key Mediator of EphrinB3/EphA4 Forward Signaling. Cell 130:742–753.

Jackson A, Crossman AR (1981) Subthalamic projection to nucleus tegmenti pedunculopontinus in the rat. Neurosci Lett 22:17–22.

Jahn K, Deutschländer A, Stephan T, Kalla R, Wiesmann M, Strupp M, Brandt T (2008) Imaging human supraspinal locomotor centers in brainstem and cerebellum. Neuroimage 39:786–792.

Jaseja H (2004) Purpose of REM sleep: endogenous anti-epileptogenesis in man -- a hypothesis. Med Hypotheses 62:546–548.

Jaseja H (2014) Pedunculopontine nucleus (PPN) stimulation in intractable epilepsy: Evidence-related programming. Epilepsy Behav 31:56.

Jiang Z, Carlin KP, Brownstone RM (1999) An in vitro functionally mature mouse spinal cord preparation for the study of spinal motor networks. Brain Res 816:493–499.

Jordan LM (1998) Initiation of locomotion in mammals. Ann N Y Acad Sci 860:83–93.

Jordan LM, Liu J, Hedlund PB, Akay T, Pearson KG (2008) Descending command systems for the initiation of locomotion in mammals. Brain Res Rev 57:183–191.

Jordan LM, McVagh JR, Noga BR, Cabaj a. M, Majczyński H, Sławińska U, Provencher J, Leblond H, Rossignol S (2014) Cholinergic mechanisms in spinal locomotion-potential target for rehabilitation approaches. Front Neural Circuits 8:132.

Juvin L, Le Gal J-P, Simmers J, Morin D (2012) Cervicolumbar Coordination in Mammalian Quadrupedal Locomotion: Role of Spinal Thoracic Circuitry and Limb Sensory Inputs. J Neurosci 32:953–965.

Juvin L, Simmers J, Morin D (2005) Propriospinal circuitry underlying interlimb coordination in mammalian quadrupedal locomotion. J Neurosci 25:6025–6035.

Juvin L, Simmers J, Morin D (2007) Locomotor rhythmogenesis in the isolated rat spinal cord: a phase-coupled set of symmetrical flexion extension oscillators. J Physiol 583:115–128.

Karachi C, Andre a., Bertasi E, Bardinet E, Lehericy S, Bernard F a. (2012) Functional Parcellation of the Lateral Mesencephalus. J Neurosci 32:9396–9401.

Karachi C, Grabli D, Bernard F a., Tandé D, Wattiez N, Belaid H, Bardinet E, Prigent A, Nothacker HP, Hunot S, Hartmann A, Lehéricy S, Hirsch EC, François C (2010) Cholinergic mesencephalic neurons are involved in gait and postural disorders in Parkinson disease. J Clin Invest 120:2745–2754.

Kawahara K, Kumagai S, Nakazono Y, Miyamoto Y (1989) Coupling between respiratory and stepping rhythms during locomotion in decerebrate cats. J Appl Physiol 67:110–115.

Keating GL, Winn P (2002) Examination of the role of the pedunculopontine tegmental nucleus in radial maze tasks with or without a delay. Neuroscience 112:687–696.

Kiehn O (2016) Decoding the organization of spinal circuits that control locomotion. Nat Rev Neurosci 17:224–238.

Kiehn O, Kjkerulff O (1996) Spatiotemporal Characteristics of 5-HT and Dopamine-induced Rythmic Hindlimb Activity in the In Vitro Neonatal Rat. J Neurophysiol 75:1472–1482.

Kinjo N, Atsuta Y, Webber M, Kyle R, Skinner RD, Garcia-Rill E (1990) Medioventral medulla-induced locomotion. Brain Res Bull 24:509–516.

Kinomura S, Larsson J, Gulyás B, Roland PE (1996) Activation by attention of the human reticular formation and thalamic intralaminar nuclei. Science 271:512–515.

Kjaerulff O, Kiehn O (1997) Crossed rhythmic synaptic input to motoneurons during selective activation of the contralateral spinal locomotor network. J Neurosci 17:9433–9447.

Korte SM, Jaarsma D, Luiten PG, Bohus B (1992) Mesencephalic cuneiform nucleus and its ascending and descending projections serve stress-related cardiovascular responses in the rat. J Auton Nerv Syst 41:157–176.

Kullander K (2003) Role of EphA4 and EphrinB3 in Local Neuronal Circuits That Control Walking. Science (80-) 299:1889–1892.

Kullander K, Croll SD, Zimmer M, Pan L, McClain J, Hughes V, Zabski S, DeChiara TM, Klein R, Yancopoulos GD, Gale NW (2001a) Ephrin-B3 is the midline barrier that prevents corticospinal tract axons from recrossing, allowing for unilateral motor control. Genes Dev 15:877–888.

Kullander K, Mather NK, Diella F, Dottori M, Boyd AW, Klein R (2001b) Kinase-dependent and kinase-independent functions of EphA4 receptors in major axon tract formation in vivo. Neuron 29:73–84.

Kung SM, Fink PW, Legg SJ, Ali A, Shultz SP (2018) What factors determine the preferred gait transition speed in humans? A review of the triggering mechanisms. Hum Mov Sci 57:1–12.

Lacquaniti F, Ivanenko YP, Zago M (2012) Development of human locomotion. Curr Opin Neurobiol 22:822–828.

Lai YY, Clements JR, Wu XY, Shalita T, Wu JP, Kuo JS, Siegel JM (1999) Brainstem projections to the ventromedial medulla in cat: Retrograde transport horseradish peroxidase and immunohistochemical studies. J Comp Neurol 408:419–436.

Lanuza GM, Gosgnach S, Pierani A, Jessell TM, Goulding M (2004) Genetic identification of spinal interneurons that coordinate left-right locomotor activity necessary for

walking movements. Neuron 42:375–386.

Le Ray D, Brocard F, Bourcier-Lucas C, Auclair F, Lafaille P, Dubuc R (2003) Nicotinic activation of reticulospinal cells involved in the control of swimming in lampreys. Eur J Neurosci 17:137–148.

Leblond H, L'Esperance M, Orsal D, Rossignol S (2003) Treadmill locomotion in the intact and spinal mouse. J Neurosci 23:11411–11419.

Lee a. M, Hoy JL, Bonci A, Wilbrecht L, Stryker MP, Niell CM (2014) Identification of a brainstem circuit regulating visual cortical state in parallel with locomotion. Neuron 83:455–466.

Lemieux M, D. Laflamme O, Thiry L, Boulanger-Piette A, Frenette J, Bretzner F (2016) Motor hypertonia and lack of locomotor coordination in mutant mice lacking DSCAM. J Neurophysiol 115:1355–1371.

Liang H, Bácskai T, Watson C, Paxinos G (2014) Projections from the lateral vestibular nucleus to the spinal cord in the mouse. Brain Struct Funct 219:805–815.

Liang H, Paxinos G, Watson C (2011) Projections from the brain to the spinal cord in the mouse. Brain Struct Funct 215:159–186.

Liang H, Paxinos G, Watson C (2012a) The red nucleus and the rubrospinal projection in the mouse. Brain Struct Funct 217:221–232.

Liang H, Paxinos G, Watson C (2012b) Spinal projections from the presumptive midbrain locomotor region in the mouse. Brain Struct Funct 217:211–219.

Liang H, Watson C, Paxinos G (2016) Terminations of reticulospinal fibers originating from the gigantocellular reticular formation in the mouse spinal cord. Brain Struct Funct 221:1623–1633.

Lindau NT, Bänninger BJ, Gullo M, Good N a., Bachmann LC, Starkey ML, Schwab ME (2014) Rewiring of the corticospinal tract in the adult rat after unilateral stroke and anti-Nogo-A therapy. Brain 137:739–756.

Liu J, Jordan LM (2005) Stimulation of the parapyramidal region of the neonatal rat brain stem produces locomotor-like activity involving spinal 5-HT7 and 5-HT2A receptors. J Neurophysiol 94:1392–1404.

Luccarini P, Gahery Y, Pompeiano O (1990) Cholinoceptive pontine reticular structures modify the postural adjustments during the limb movements induced by cortical stimulation. Arch Ital Biol 128:19–45.

Ma'ayan A (2009) Insights into the organization of biochemical regulatory networks using graph theory analyses. J Biol Chem 284:5451–5455.

MacLaren DAA, Wilson DIG, Winn P (2016) Selective lesions of the cholinergic neurons within the posterior pedunculopontine do not alter operant learning or nicotine sensitization. Brain Struct Funct 221:1481–1497.

Maes L, Abourachid A (2013) Gait transitions and modular organization of mammal

locomotion. J Exp Biol 216:2257–2265.

Mann RA, Hagy J (1980) Biomechanics of walking, running, and sprinting. Am J Sports Med 8:345–350.

Marlinsky V V., Voitenko LP (1991) The effect of procaine injection into the medullary reticular formation of forelimb muscle activity evoked by mesencephalic locomotor region and vestibular stimulation in the decerebrated guinea-pig. Neuroscience 45:753–759.

Martinez-Gonzalez C, Bolam JP, Mena-Segovia J (2011) Topographical organization of the pedunculopontine nucleus. Front Neuroanat 5:22.

Martinez-Gonzalez C, Van Andel J, Bolam JP, Mena-Segovia J (2014) Divergent motor projections from the pedunculopontine nucleus are differentially regulated in Parkinsonism. Brain Struct Funct 219:1451–1462.

Martinez-Gonzalez C, Wang HL, Micklem BR, Bolam JP, Mena-Segovia J (2012) Subpopulations of cholinergic, GABAergic and glutamatergic neurons in the pedunculopontine nucleus contain calcium-binding proteins and are heterogeneously distributed. Eur J Neurosci 35:723–734.

Mason O, Verwoerd M (2007) Graph theory and networks in Biology. IET Syst Biol 1:89–119.

Massion J (1967) The mammalian red nucleus. 47:383–436.

Massion J (1988) Red nucleus: past and future. Behav Brain Res 28:1–8.

Matsushita M, Ikeda M, Hosoya Y (1979) The location of spinal neurons with long descending axons (long descending propriospinal tract neurons) in the cat: A study with the horseradish peroxidase technique. J Comp Neurol 184:63–79.

Matsushita M, Okado N, Ikeda M, Hosoya Y (1981) Descending projections from the spinal and mesencephalic nuclei of the trigeminal nerve to the spinal cord in the cat. A study with the horseradish peroxidase technique. J Comp Neurol 196:173–187.

May Z, Fenrich KK, Dahlby J, Batty NJ, Torres-Espín A, Fouad K (2017) Following Spinal Cord Injury Transected Reticulospinal Tract Axons Develop New Collateral Inputs to Spinal Interneurons in Parallel with Locomotor Recovery. Neural Plast 2017:1–15.

Mazzone P, Insola A, Sposato S, Scarnati E (2009) The Deep Brain Stimulation of the Pedunculopontine Tegmental Nucleus. 12.

McCrea D a, Shefchyk SJ, Stephens MJ, Pearson KG (1995) Disynaptic group I excitation of synergist ankle extensor motoneurones during fictive locomotion in the cat. J Physiol 487 (Pt 2:527–539.

McCrea DA, Rybak IA (2008) Organization of mammalian locomotor rhythm and pattern generation. Brain Res Rev 57:134–146.

Meehan CF, Grondahl L, Nielsen JB, Hultborn H (2012) Fictive locomotion in the adult decerebrate and spinal mouse in vivo. J Physiol 590:289–300.

Mena-Segovia J, Bolam JP (2017) Rethinking the Pedunculopontine Nucleus: From Cellular Organization to Function. Neuron 94:7–18.

Mena-Segovia J, Micklem BR, Nair-Roberts RG, Ungless MA, Bolam JP (2009) GABAergic neuron distribution in the pedunculopontine nucleus defines functional subterritories. J Comp Neurol 515:397–408.

Mena-segovia J, Sims HM, Magill PJ, Bolam JP (2008) Cholinergic brainstem neurons modulate cortical gamma activity during slow oscillations. J Physiol 586:2947–2960.

Ménard A, Grillner S (2008) Diencephalic locomotor region in the lamprey--afferents and efferent control. J Neurophysiol 100:1343–1353.

Mesulam M-M (2013) Cholinergic circuitry of the human nucleus basalis and its fate in Alzheimer's disease. J Comp Neurol 521:4124–4144.

Miller S, Reitsma DJ, van der Meché FG (1973) Functional organization of long ascending propriospinal pathways linking lumbo-sacral and cervical segments in the cat. Brain Res 62:169–188.

Miller S, Van Der Burg J, Van Der Meché F (1975a) Locomotion in the cat: basic programmes of movement. Brain Res 91:239–253.

Miller S, van der Burg J, van der Meché FGA (1975b) Coordination of movements of the hindlimbs and forelimbs in different forms of locomotion in normal and decerebrate cats. Brain Res 91:217–237.

Milner KL, Mogenson GJ (1988) Electrical and chemical activation of the mesencephalic and subthalamic locomotor regions in freely moving rats. Brain Res 452:273–285.

Mitchell EJ, McCallum S, Dewar D, Maxwell DJ (2016) Corticospinal and Reticulospinal Contacts on Cervical Commissural and Long Descending Propriospinal Neurons in the Adult Rat Spinal Cord; Evidence for Powerful Reticulospinal Connections. PLoS One 11:e0152094.

Mitchell IJ, Dean P, Redgrave P (1988) The projection from superior colliculus to cuneiform area in the rat. Exp Brain Res 72.

Monakow KH, Akert K, Künzle H (1979) Projections of precentral and premotor cortex to the red nucleus and other midbrain areas in Macaca fascicularis. Exp Brain Res 34:91–105.

Mori S (1987) Integration of posture and locomotion in acute decerebrate cats and in awake, freely moving cats. Prog Neurobiol 28:161–195.

Mori S, Matsui T, Kuze B, Asanome M, Nakajima K, Matsuyama K (1998) Cerebellar-induced locomotion: reticulospinal control of spinal rhythm generating mechanism in cats. Ann N Y Acad Sci 860:94–105.

Mori S, Matsui T, Kuze B, Asanome M, Nakajima K, Matsuyama K (1999) Stimulation of a restricted region in the midline cerebellar white matter evokes coordinated quadrupedal locomotion in the decerebrate cat. J Neurophysiol 82:290–300.

Mori S, Sakamoto T, Ohta Y, Takakusaki K, Matsuyama K (1989) Site-specific postural and locomotor changes evoked in awake, freely moving intact cats by stimulating the brainstem. Brain Res 505:66–74.

Mori S, Shik ML, Yagodnitsyn AS (1977) Role of pontine tegmentum for locomotor control in mesencephalic cat. J Neurophysiol 40:284–295.

Morita H, Hass CJ, Moro E, Sudhyadhom A, Kumar R, Okun MS (2014) Pedunculopontine Nucleus Stimulation: Where are We Now and What Needs to be Done to Move the Field Forward? Front Neurol 5.

Morris ME, Huxham FE, McGinley J, Iansek R (2001) Gait disorders and gait rehabilitation in Parkinson's disease. Adv Neurol 87:347–361.

Morris ME, Iansek R, Matyas T a, Summers JJ (1996) Stride length regulation in Parkinson's disease. Normalization strategies and underlying mechanisms. Brain 119 (Pt 2:551–568.

Musienko PE, Zelenin P V, Lyalka VF, Orlovsky GN, Deliagina TG (2008) Postural performance in decerebrated rabbit. Behav Brain Res 190:124–134.

Muybridge E (1957) Animals in Motion. New York Dover Nicodemus, M C Clayton, H C 80:133–142.

Nakamura Y, Kudo M, Tokuno H (1990) Monosynaptic projection from the pedunculopontine tegmental nuclear region to the reticulospinal neurons of the medulla oblongata. An electron microscope study in the cat. Brain Res 524:353–356.

Nakanishi ST, Whelan PJ (2012) A decerebrate adult mouse model for examining the sensorimotor control of locomotion. J Neurophysiol 107:500–515.

Nathan PW, Smith M, Deacon P (1996) Vestibulospinal, reticulospinal and descending propriospinal nerve fibres in man. Brain 119:1809–1833.

Noga BR, Kriellaars DJ, Brownstone RM, Jordan LM (2003) Mechanism for activation of locomotor centers in the spinal cord by stimulation of the mesencephalic locomotor region. J Neurophysiol 90:1464–1478.

Nolte MW, Löscher W, Gernert M (2006) Pedunculopontine neurons are involved in network changes in the kindling model of temporal lobe epilepsy. Neurobiol Dis 23:206–218.

Nussbaum MC (1976) The text of Aristotle's "De motu animalium". Harv Stud Classic Philol 80:111–159.

Olszewski J, Baxter D (1982) Cytoarchitecture of the human brain stem. Karger.

Onimaru H, Arata A, Homma I (1995) Intrinsic burst generation of preinspiratory neurons in the medulla of brainstem-spinal cord preparations isolated from newborn rats. Exp brain Res 106:57–68.

Orlovsky GN (1972) The effect of different descending systems on flexor and extensor activity during locomotion. Brain Res 40:359–372.

Orlovsky GN, Deliagina TG, Grillner S (1999) Neural control of locomotion, from mollusc to man. New York: Oxford University Press.

Owaki D, Ishiguro A (2017) A Quadruped Robot Exhibiting Spontaneous Gait Transitions from Walking to Trotting to Galloping. Sci Rep 7:277.

Paper TW (2012) ALLEN Mouse Brain Connectivity Atlas. Brain:1–11.

Parker AW, Bronks R (1980) Gait of children with Down syndrome. Arch Phys Med Rehabil 61:345–351.

Paxinos G, Franklin KBJ, Paxinos, G and Franklin KBJ, Paxinos G, Franklin KBJ (2004) Mouse Brain in Stereotaxic Coordinates.

Paxinos G, Watson C (2006) The Rat Brain in Stereotaxic Coordinates: Hard Cover Edition.

Pearson KG, Acharya H, Fouad K (2005) A new electrode configuration for recording electromyographic activity in behaving mice. J Neurosci Methods 148:36–42.

Petzold A, Valencia M, Pál B, Mena-Segovia J (2015) Decoding brain state transitions in the pedunculopontine nucleus: cooperative phasic and tonic mechanisms. Front Neural Circuits 9:1–16.

Piallat B, Chabardès S, Torres N, Fraix V, Goetz L, Seigneuret E, Bardinet E, Ferraye M, Debu B, Krack P, Yelnik J, Pollak P, Benabid AL (2009) Gait is associated with an increase in tonic firing of the sub-cuneiform nucleus neurons. Neuroscience 158:1201–1205.

Pose I, Sampogna S, Chase MH, Morales FR (2000) Cuneiform neurons activated during cholinergically induced active sleep in the cat. J Neurosci 20:3319–3327.

Rabe N, Gezelius H, Vallstedt A, Memic F, Kullander K (2009) Netrin-1-dependent spinal interneuron subtypes are required for the formation of left-right alternating locomotor circuitry. J Neurosci 29:15642–15649.

Rabe Bernhardt N, Memic F, Gezelius H, Thiebes AL, Vallstedt A, Kullander K, Bernhardt NR, Memic F, Gezelius H, Thiebes AL, Vallstedt A, Kullander K (2012) DCC mediated axon guidance of spinal interneurons is essential for normal locomotor central pattern generator function. Dev Biol 366:279–289.

Reilly SM, Jorgensen ME (2011) The evolution of jumping in frogs: Morphological evidence for the basal anuran locomotor condition and the radiation of locomotor systems in crown group anurans. J Morphol 272:149–168.

Rinne JO, Ma SY, Lee MS, Collan Y, Röyttä M (2008) Loss of cholinergic neurons in the pedunculopontine nucleus in Parkinson's disease is related to disability of the patients. Parkinsonism Relat Disord 14:553–557.

Roberts MD, Toedebusch RG, Wells KD, Company JM, Brown JD, Cruthirds CL, Heese AJ, Zhu C, Rottinghaus GE, Childs TE, Booth FW (2014) Nucleus accumbens neuronal maturation differences in young rats bred for low versus high voluntary running behavior. J Physiol 10:1–48.

Rolland A-SS, Tandé D, Herrero M-TT, Luquin M-RR, Vazquez-Claverie M, Karachi C, Hirsch EC, François C (2009) Evidence for a dopaminergic innervation of the pedunculopontine nucleus in monkeys, and its drastic reduction after MPTP intoxication. J Neurochem 110:1321–1329.

Roš H, Magill PJ, Moss J, Bolam JP, Mena-Segovia J (2010) Distinct types of non-cholinergic pedunculopontine neurons are differentially modulated during global brain states. Neuroscience 170:78–91.

Roseberry TK, Lee AM, Lalive AL, Wilbrecht L, Bonci A, Kreitzer AC (2016) Cell-Type-Specific Control of Brainstem Locomotor Circuits by Basal Ganglia. Cell 164:526–537.

Ruder L, Takeoka A, Arber S (2016) Long-Distance Descending Spinal Neurons Ensure Quadrupedal Locomotor Stability. Neuron 92:1063–1078.

Rybak IA, Dougherty KJ, Shevtsova NA (2015) Organization of the Mammalian Locomotor CPG: Review of Computational Model and Circuit Architectures Based on Genetically Identified Spinal Interneurons. eNeuro 2.

Ryczko D, Dubuc R (2013) The multifunctional mesencephalic locomotor region. Curr Pharm Des 19:4448–4470.

Ryczko D, Dubuc R (2017) Dopamine and the Brainstem Locomotor Networks: From Lamprey to Human. Front Neurosci 11:295.

Semba K, Fibiger HC (1992) Afferent connections of the laterodorsal and the pedunculopontine tegmental nuclei in the rat: a retro- and antero-grade transport and immunohistochemical study. J Comp Neurol 323:387–410.

Serradj N, Jamon M (2009) The adaptation of limb kinematics to increasing walking speeds in freely moving mice 129/Sv and C57BL/6. Behav Brain Res 201:59–65.

Sharples SA, Koblinger K, Humphreys JM, Whelan PJ (2014) Dopamine: a parallel pathway for the modulation of spinal locomotor networks. Front Neural Circuits 8:55.

Shefchyk SJ, Jell RM, Jordan LM (1984) Reversible cooling of the brainstem reveals areas required for mesencephalic locomotor region evoked treadmill locomotion. Exp Brain Res 56:257–262.

Sherman D, Fuller PM, Marcus J, Yu J, Zhang P, Chamberlin NL, Saper CB, Lu J (2015) Anatomical Location of the Mesencephalic Locomotor Region and Its Possible Role in Locomotion, Posture, Cataplexy, and Parkinsonism. Front Neurol 6:1–13.

Sherrington SC (1906) The Integrative Action of the Nervous System. Classics in psychology.

Shi L, Fu W-Y, Hung K-W, Porchetta C, Hall C, Fu AKY, Ip NY (2007) Alpha2-chimaerin interacts with EphA4 and regulates EphA4-dependent growth cone collapse. Proc Natl Acad Sci U S A 104:16347–16352.

Shik ML, Orlovsky GN (1976) Neurophysiology of locomotor automatism. Physiol Rev 56:465–501.

Shik ML, Severin F V, GN O (1966) Control of walking and running by means of electrical stimulation of mid-brain. BIOPHYSICS-USSR 11:756.

Shiromani PJ, Armstrong DM, Gillin JC (1988) Cholinergic neurons from the dorsolateral pons project to the medial pons: A WGA-HRP and choline acetyltransferase immunohistochemical study. Neurosci Lett 95:19–23.

Sinnamon HM (1993) Preoptic and hypothalamic neurons and the initiation of locomotion in the anesthetized rat. Prog Neurobiol 41:323–344.

Skinner RD, Garcia-Rill E (1984) The mesencephalic locomotor region (MLR) in the rat. Brain Res 323:385–389.

Skinner RD, Homma Y, Garcia-Rill E (2004) Arousal mechanisms related to posture and locomotion: 2. Ascending modulation. Prog Brain Res 143:291–298.

Skinner RD, Kinjo N, Henderson V, Garcia-Rill E (1990) Locomotor projections from the pedunculopontine nucleus to the spinal cord. Neuroreport 1:183–186.

Smetana R, Juvin L, Dubuc R, Alford S (2010) A parallel cholinergic brainstem pathway for enhancing locomotor drive. Nat Neurosci 13:731–738.

Spann BM, Grofova I (1992) Cholinergic and non-cholinergic neurons in the rat pedunculopontine tegmental nucleus. Anat Embryol (Berl) 186:215–227.

Steeves JD, Sholomenko GN, Webster DM (1987) Stimulation of the pontomedullary reticular formation initiates locomotion in decerebrate birds. Brain Res 401:205–212.

Stefani A, Lozano AM, Peppe A, Stanzione P, Galati S, Tropepi D, Pierantozzi M, Brusa L, Scarnati E, Mazzone P (2007) Bilateral deep brain stimulation of the pedunculopontine and subthalamic nuclei in severe Parkinson's disease. Brain 130:1596–1607.

Strogatz SH (2001) Exploring complex networks. Nature 410:268–276.

Taber E (1961) The cytoarchitecture of the brain stem of the cat. I. Brain stem nuclei of cat. J Comp Neurol 116:27–69.

Takakusaki K, Chiba R, Nozu T, Okumura T (2016) Brainstem control of locomotion and muscle tone with special reference to the role of the mesopontine tegmentum and medullary reticulospinal systems. J Neural Transm 123:695–729.

Takakusaki K, Habaguchi T, Ohtinata-Sugimoto J, Saitoh K, Sakamoto T (2003) Basal ganglia efferents to the brainstem centers controlling postural muscle tone and locomotion: A new concept for understanding motor disorders in basal ganglia dysfunction. Neuroscience 119:293–308.

Takakusaki K, Kohyama J, Matsuyama K, Mori S (2001) Medullary reticulospinal tract mediating the generalized motor inhibition in cats: parallel inhibitory mechanisms acting on motoneurons and on interneuronal transmission in reflex pathways. Neuroscience 103:511–527.

Takakusaki K, Saitoh K, Harada H, Kashiwayanagi M (2004a) Role of basal ganglia-

brainstem pathways in the control of motor behaviors. Neurosci Res 50:137–151.

Takakusaki K, Saitoh K, Harada H, Okumura T, Sakamoto T (2004b) Evidence for a role of basal ganglia in the regulation of rapid eye movement sleep by electrical and chemical stimulation for the pedunculopontine tegmental nucleus and the substantia nigra pars reticulata in decerebrate cats. Neuroscience 124:207–220.

Takakusaki K, Shiroyama T, Yamamoto T, Kitai ST (1996) Cholinergic and noncholinergic tegmental pedunculopontine projection neurons in rats revealed by intracellular labeling. J Comp Neurol 371:345–361.

Takeoka A, Vollenweider I, Courtine G, Arber S (2014) Muscle Spindle Feedback Directs Locomotor Recovery and Circuit Reorganization after Spinal Cord Injury. Cell 159:1626–1639.

Talpalar AE, Bouvier J, Borgius L, Fortin G, Pierani A, Kiehn O (2013) Dual-mode operation of neuronal networks involved in left-right alternation. Nature 500:85–88.

Tang ZW, Zhang SQ (1987) The cerebellar projection from the reticular formation of the brain stem in the rabbit. An experimental study using HRP as a retrograde tracer. Anat Embryol (Berl) 175:521–526.

Tattersall TL, Stratton PG, Coyne TJ, Cook R, Silberstein P, Silburn P a, Windels F, Sah P (2014) Imagined gait modulates neuronal network dynamics in the human pedunculopontine nucleus. Nat Neurosci 17:449–454.

ten Donkelaar HJ (1988) Evolution of the red nucleus and rubrospinal tract. Behav Brain Res 28:9–20.

Tester NJ, Barbeau H, Howland DR, Cantrell A, Behrman AL (2012) Arm and leg coordination during treadmill walking in individuals with motor incomplete spinal cord injury: A preliminary study. Gait Posture 36:49–55.

Tester NJ, Howland DR, Day K V, Suter SP, Cantrell A, Behrman a L (2011) Device use, locomotor training and the presence of arm swing during treadmill walking after spinal cord injury. Spinal cord Off J Int Med Soc Paraplegia 49:451–456.

Teune TM, der Burg J, Ruigrok TJH (1995) Cerebellar projections to the red nucleus and inferior olive originate from separate populations of neurons in the rat: a non-fluorescent double labeling study. Brain Res 673:313–319.

Thevathasan W, Cole MH, Graepel CL, Hyam J a., Jenkinson N, Brittain JS, Coyne TJ, Silburn P a., Aziz TZ, Kerr G, Brown P (2012) A spatiotemporal analysis of gait freezing and the impact of pedunculopontine nucleus stimulation. Brain 135:1446–1454.

Thibaudier Y, Frigon A (2014) Spatiotemporal control of interlimb coordination during transverse split-belt locomotion with 1:1 or 2:1 coupling patterns in intact adult cats. J Neurophysiol 112:2006–2018.

Thibaudier Y, Hurteau M-F, Dambreville C, Chraibi A, Goetz L, Frigon A (2017) Interlimb Coordination during Tied-Belt and Transverse Split-Belt Locomotion before and after

an Incomplete Spinal Cord Injury. J Neurotrauma 34:1751–1765.

Thibaudier Y, Hurteau M-F, Telonio A, Frigon A (2013) Coordination between the fore- and hindlimbs is bidirectional, asymmetrically organized, and flexible during quadrupedal locomotion in the intact adult cat. Neuroscience 240:13–26.

Thiry L, Lemieux M, Bretzner F (2017) AGE- AND SPEED-DEPENDENT MODULATION OF LOCOMOTOR GAITS IN DSCAM2J MUTANT MICE. J Neurophysiol:jn.00471.2017.

Thompson JA, Felsen G (2013) Activity in mouse pedunculopontine tegmental nucleus reflects action and outcome in a decision-making task. J Neurophysiol 110:2817–2829.

Tovote P, Esposito MS, Botta P, Chaudun F, Fadok JP, Markovic M, Wolff SBE, Ramakrishnan C, Fenno L, Deisseroth K, Herry C, Arber S, Lüthi A (2016) Midbrain circuits for defensive behaviour. Nature 534:206–212.

Tysseling VM, Janes L, Imhoff R, Quinlan K a., Lookabaugh B, Ramalingam S, Heckman CJ, Tresch MC (2013) Design and evaluation of a chronic EMG multichannel detection system for long-term recordings of hindlimb muscles in behaving mice. J Electromyogr Kinesiol 23:531–539.

Vallstedt A, Kullander K (2013) Dorsally derived spinal interneurons in locomotor circuits. Ann N Y Acad Sci 1279:32–42.

Van Dort CJ, Zachs DP, Kenny JD, Zheng S, Goldblum RR, Gelwan N a, Ramos DM, Nolan MA, Wang K, Weng F-J, Lin Y, Wilson M a, Brown EN (2015) Optogenetic activation of cholinergic neurons in the PPT or LDT induces REM sleep. Proc Natl Acad Sci 112:584–589.

Vilensky J a, Libii JN, Moore a M (1991) Trot-gallop gait transitions in quadrupeds. Physiol Behav 50:835–842.

Wang HL, Morales M (2009) Pedunculopontine and laterodorsal tegmental nuclei contain distinct populations of cholinergic, glutamatergic and GABAergic neurons in the rat. Eur J Neurosci 29:340–358.

Wang J-W, Zhang Y-Q, Zhang X-H, Wang Y-P, Li J-P, Li Y-J (2017) Deep Brain Stimulation of Pedunculopontine Nucleus for Postural Instability and Gait Disorder After Parkinson Disease: A Meta-Analysis of Individual Patient Data. World Neurosurg 102:72–78.

Wannier T, Bastiaanse C, Colombo G, Dietz V (2001) Arm to leg coordination in humans during walking, creeping and swimming activities. Exp Brain Res 141:375–379.

Wetzel MC, Atwater AE, Wait J V, Stuart DC (1975) Neural implications of different profiles between treadmill and overground locomotion timings in cats. J Neurophysiol 38:492–501.

Whelan P (1996) Control of Locomotion in the Decerebrate Cat. Prog Neurobiol 49:481–515.

Whelan PJ (2017) Dopaminergic control of locomotion: Uncovering parallel pathways for movement control. In: Program No. 267.06 . 2017 Neuroscience Meeting Planner., pp 38. Washington, DC: Society for neuroscience. Online.

Wilson DIG, MacLaren DAA, Winn P (2009) Bar pressing for food: Differential consequences of lesions to the anterior versus posterior pedunculopontine. Eur J Neurosci 30:504–513.

Wilson RJ a, Chersa T, Whelan PJ (2003) Tissue PO2 and the effects of hypoxia on the generation of locomotor-like activity in the in vitro spinal cord of the neonatal mouse. Neuroscience 117:183–196.

Winn P (2006) How best to consider the structure and function of the pedunculopontine tegmental nucleus: evidence from animal studies. J Neurol Sci 248:234–250.

Woolf NJ, Butcher LL (1986) Cholinergic systems in the rat brain: III. Projections from the pontomesencephalic tegmentum to the thalamus, tectum, basal ganglia, and basal forebrain. Brain Res Bull 16:603–637.

Xiang H-B, Zhu W-Z, Guan X-H, Ye D-W, Alam M, Schwabe K, Krauss JK (2013) Reply: The cuneiform nucleus may be involved in the regulation of skeletal muscle tone by motor pathway: A virally mediated trans-synaptic tracing study in surgically sympathectomized mice. Brain 136:2011–2014.

Xiao C, Cho JR, Zhou C, Mckinney SL, Yang B, Gradinaru V, Xiao C, Cho JR, Zhou C, Treweek JB, Chan K, Mckinney SL, Yang B (2016) Cholinergic Mesopontine Signals Govern Locomotion and Reward through Dissociable Midbrain Pathways Article Cholinergic Mesopontine Signals Govern Locomotion and Reward through Dissociable Midbrain Pathways. Neuron 90:333–347.

Xiao H, Li M, Cai J, Li N, Zhou M, Wen P, Xie Z, Wang Q, Chang J, Zhang W (2017) Selective cholinergic depletion of pedunculopontine tegmental nucleus aggravates freezing of gait in parkinsonian rats. Neurosci Lett.

Yu J, Eidelberg E (1983) Recovery of locomotor function in cats after localized cerebellar lesions. Brain Res 273:121–131.

Zar J. (1996) Biostatistical analysis (Snavely S., ed)., 3rd Editio. Englewood Cliffs: Prentice-Hall.

Zehr EP, Komiyama T, Stein RB (1997) Cutaneous reflexes during human gait: electromyographic and kinematic responses to electrical stimulation. J Neurophysiol 77:3311–3325.

Zhang J, Lanuza GM, Britz O, Wang Z, Siembab VC, Zhang Y, Velasquez T, Alvarez FJ, Frank E, Goulding M (2014) V1 and v2b interneurons secure the alternating flexor-extensor motor activity mice require for limbed locomotion. Neuron 82:138–150.

Zhang Y, Narayan S, Geiman E, Lanuza GM, Velasquez T, Shanks B, Akay T, Dyck J, Pearson K, Gosgnach S, Fan M, Goulding M, Fan C-M, Goulding M (2008) V3 spinal neurons establish a robust and balanced locomotor rhythm during walking. Neuron 60:84–96.

Zingg B, Chou X, Zhang Z-G, Mesik L, Liang F, Tao HW, Zhang LI (2017) AAV-Mediated Anterograde Transsynaptic Tagging: Mapping Corticocollicular Input-Defined Neural Pathways for Defense Behaviors. Neuron 93:33–47.

Zörner B, Bachmann LC, Filli L, Kapitza S, Gullo M, Bolliger M, Starkey ML, Röthlisberger M, Gonzenbach RR, Schwab ME (2014) Chasing central nervous system plasticity: The brainstem's contribution to locomotor recovery in rats with spinal cord injury. Brain 137:1716–1732.